OTHER PERGAMON TITLES OF INTEREST

BABISTER	Aircraft Dynamic Stability and Response
CHERINGTON	Airline Price Policy
HEARN	Mechanics of Materials
KÜCHEMANN	The Aerodynamic Design of Aircraft
MANN & MILLIGAN	Aircraft Fatigue Design, Operation and Economic Aspects
MARSCHALL & MARINGER	Dimensional Instability
NAPOLITANO	Space Activity, Impact on Science and Technology
	Space Stations, Present and Future
	Space and Energy
	A New Era in Space Transportation
	Using Space - Today and Tomorrow Volume 1 - Space Based Industry Symposium Volume 2 - Communications Satellite Symposium
	Astronautics for Peace and Human Progress
OPPENHEIM	Gasdynamics of Explosive and Reactive Systems
REAY	The History of Man Powered Flight

RELATED JOURNALS PUBLISHED BY PERGAMON

Acta Astronautica

Advances in Earth Oriented Applications of Space Technology

Planetary and Space Science

Progress in Aerospace Sciences

Vertica

SIR FRANK WHITTLE, K.B.E., C.B.

GAS TURBINE AERO-THERMODYNAMICS

With Special Reference to Aircraft Propulsion

SIR FRANK WHITTLE, K.B.E., C.B.,
Air Commodore R.A.F. (ret.), M.A. Sc.D. (h.c.),
F.R.S., F. Eng. Hon. F.I. Mech.E., Hon. F.R.Ac.S., Hon. F.A.I.A.A.

PERGAMON PRESS

OXFORD · NEW YORK · TORONTO · SYDNEY · PARIS · FRANKFURT

U.K.	Pergamon Press Ltd., Headington Hill Hall, Oxford OX3 0BW, England
U.S.A.	Pergamon Press Inc., Maxwell House, Fairview Park, Elmsford, New York 10523, U.S.A.
CANADA	Pergamon Press Canada Ltd., Suite 104, 150 Consumers Road, Willowdale, Ontario M2J 1P9, Canada
AUSTRALIA	Pergamon Press (Aust.) Pty. Ltd., P.O. Box 544, Potts Point, N.S.W. 2011, Australia
FRANCE	Pergamon Press SARL, 24 rue des Ecoles, 75240 Paris, Cedex 05, France
FEDERAL REPUBLIC OF GERMANY	Pergamon Press GmbH, 6242 Kronberg-Taunus, Hammerweg 6, Federal Republic of Germany

First Edition 1981

British Library Cataloguing in Publication Data

Whittle, *Sir* Frank

Gas turbine aero-thermodynamics. - (Pergamon international library).

1. Gas-turbines

I. Title

629.134'353 TJ778 80-41372

ISBN 0-08-026719-X Hardcover

ISBN 0-8-026718-1 Flexicover

Printed in Great Britain by A. Wheaton & Co. Ltd., Exeter

PREFACE

In the early 1930s, when I was deeply involved in the design of Britain's first jet engine, I was regarded as a 'crazy optimist' by the many who found it difficult to believe that a young officer of the Royal Air Force could be successful in the field of gas turbines when this field was littered by a history of failure. Yet, in retrospect, I was a pessimist. I certainly did not foresee that the day would come when (on Sept 4th 1976) I would be a passenger in the Concorde and fly across the Atlantic from London (Heathrow) to Washington DC (Dulles) in exactly 3½ hours. Neither did I foresee that, in less than four decades, engines would be in service having about twenty times the power of the W2/700 (2000 - 2500 lb static thrust at sea level)—the last of the series of engines, designed by the team of Power Jets Ltd. led by me, to be built and flown. Nor did I foresee that time between overhauls would increase to thousands of hours as against the 500 hours or so that I predicted. Also, though my 1936 notebooks contain jet engine performance for speeds of the order of 1500 mph and clearly showed that such supersonic speeds were best suited for high efficiency with this type of engine, it did not seem likely to me that the aerodynamics of supersonic aircraft could be improved to the point where long range SSTs and bombers would become possible. In those days the very few—including myself—who refused to accept that the sound barrier could never be broken, (despite ballistic proof to the contrary), were not optimistic about achieving lift/drag ratios much above about 4:1. It seems that I was a pessimist in all respects except one—the time scale for development. In 1945, since we had found that it was possible to design, build, and test a jet engine in 6 months, I was predicting the advent of jet powered civil aircraft within five years and that the turbofan would take over in quite a short time thereafter. In the event I proved to be over-optimistic on both counts. I still believe that these things could have been done had not there still existed the barrier of skepticism which obstructed them.

Perhaps the thing I least expected was that I would ever attempt to write a textbook on aero-thermodynamic theory of gas turbine design. Especially, as a consequence of the formation of the National Gas Turbine Establishment in 1946, my team and I were denied

the right to continue to design and build engines. As a result, my interest in the work I had pioneered began to wane and virtually disappeared to the extent that, after 1952, when I resigned my post (honorary) as Adviser to British Overseas Airways, I lost touch with the course of development altogether for many years, my interests having turned to other fields, the chief of which was oil well drilling technology. I did not, however, stop thinking about gas turbines in general in a somewhat superficial way, but remained aloof from becoming involved with them in any practical sense, having ceased to believe that anything I could hope to do could possibly compare with my earlier achievements. I did, however, accept a number of lecture engagements over the years, mainly on the subject of the early history.

My involvement with oil well drilling technology from 1953 onwards (as "Mechanical Engineering Specialist" to Bataafsche Petroleum Maatschappij–the main operating company of the Shell Group) included the design and "paper development" of an oil well drilling motor–the Whittle turbo-drill. It was, however, outside the policy of the Shell Group to enter into the drilling equipment business beyond the point of backing innovation to the stage where it could be handed over to specialist firms. So, under the terms of my contract with Shell, all the turbo drill patents were eventually assigned to me and this gave me the opportunity to seek a sponsor for its practical development. Strangely enough this started a chain of events which led to a revival of my interest in aircraft engines.

This came about as follows: In 1959 I succeeded in arousing the interest of Bristol Siddeley Engines–then one of the two largest British aircraft engine companies–in the turbo drill project, largely by virtue of their confidence in me of Sir Arnold Hall, the Chairman and Managing Director, and Sir Stanley Hooker, the Technical Director (Aero). Both these brilliant men were friends of long standing. Arnold Hall had been a fellow undergraduate at Cambridge University taking the Mechanical Sciences Tripos and had assisted me in the design of the compressor impellor of the first experimental jet engine before we both graduated in 1936. Stanley Hooker and I first met in 1940. He was then with Rolls Royce. He became an immediate convert to the jet engine and was successful in enlisting the interest of his Chief Executive, E. W. Hives (later Lord Hives). Thereafter, Power Jets received much assistance from Rolls Royce and vice versa. This resulted in increasing technical collaboration and a ripening of the friendship between Hooker and myself. Eventually under Hooker's leadership Rolls Royce became responsible for the production of jet engines based on Power Jets designs, and began their own vigorous and highly successful development of increasingly powerful jet engines.

After I ceased to be connected with jet engine design and development in 1946 and Stanley Hooker left Rolls Royce to become Chief Engineer of Bristol Siddeley, we rather lost touch with each other for about 13 years until, in 1959, he invited me to visit Bristol "to see what they were up to." On that interesting occasion I received a warm welcome and succeeded in arousing Hooker's interest in the turbo drill. The outcome was that B.S.E. agreed to back the project and, by 1961, practical development began. Thereafter I made frequent visits to B.S.E.'s Patchway factory near Bristol for several years. Hooker and I saw much of each other and the inevitable and frequent contacts with B.S.E.'s other aero engine designers re-aroused my interest in aeronautical engineering, especially as several ambitious projects were "on the boil," including the Concorde and its Olympus 593 engines, the Harrier "jump jet" and its Pegasus vectored thrust turbo fan engine, etc. I played no official role in these projects. I was a 'spectator from my sidelines,' but was often drawn into discussions of technical problems and flatter myself that I made an occasional useful contribution.

At the same time (1961 onwards) I became involved in the patent infringement action Rateau v. Rolls Royce and accepted an invitation from Rolls Royce to act as expert witness and technical advisor. Little did I realise that this was to absorb an increasing amount of my time until the case was decided in favour of Rolls Royce in January, 1967. It did, however, oblige me to brush up on jet engine theory and this stirred my interest to such an extent that I began to explore the possibilities of improving on the Olympus 593 for a second generation SST and did indeed succeed in convincing myself that very considerable improvements were possible in the form of a low bypass ratio turbo fan. Rolls Royce (now merged with B.S.E.) and U.S. firms were also engaged on project work on similar lines. The turbo drill, however, remained my main activity until it went 'on the shelf' as a consequence of the takeover of B.S.E. by Rolls Royce in 1968. At that time it had reached an advanced stage of development and was in limited production and commercial use. But Rolls Royce were already in the financial difficulties which led to bankruptcy and the nationalisation of the aero engine divisions in 1971. This, plus a general lack of interest of the new management in a field of engineering so remote from their main sphere of activity, resulted in a rapid reduction of support for the turbo drill project until it dried up altogether. This unhappy course of events and the failure to find alternative sponsors caused me to lose interest in the drill and to increase my 'private venture' exploration of SST power plant possibilities. A strong desire to see a second generation SST come into service in my own lifetime became almost an obsession.

It was clear that such a venture would be far beyond the means of any single firm or small group of firms without massive support from government and probably beyond the means of any single government, so, in 1974-75 I took it upon myself to attempt to act as a "catalyst" in the promotion of a major cooperative scheme for the development of a second generation SST involving the U.S. and U.K. governments and, possibly, the French government and the major aircraft and engine firms of these nations. I visualised a jointly owned international company at the centre of the web which would be responsible for the project phase of the operation, for development, and for the assembly phase of production and to which the several aircraft and engine firms would contribute personnel and act as subcontractors. This scheme differed from the Anglo-French Concorde joint venture in that in the case of the latter no single central company was ever formed. There were, of course, coordinating committees.

It should be mentioned that the Boeing 7011 had been smothered to death ostensibly by the environmentalist lobby in the U.S.A. (though one may venture the surmise that the vast cost to the U.S. taxpayer was the real cause).

The opportunity for my attempt was furnished by a few invitations to lecture in the U.S. Before leaving the U.K. I had sounded out the views of Rolls Royce (1971) and obtained an encouraging reaction, but refrained from contacting the U.K. Government so as to be able to claim that I was speaking for no one but myself. In Washington D.C. I succeeded in obtaining the 'unofficial blessing' of H. M. Brittanic Ambassador, Sir Peter Ramsbotham, and had a series of encouraging reactions from officials of the F.A.A. and N.A.S.A. from whom I received much help in arranging my schedule of visits to McDonnell Douglas, Lockheed, Boeing, General Electric and Pratt and Whitney with all of whom I discussed my proposals. One of these companies was distinctly 'lukewarm' to the scheme, but, in general, the results were most encouraging and I reported accordingly on my return to the U.K.

I visited the U.S.A. again from April-June 1976 with the intention of further pursuing the matter, but suffered minor injuries in a fall after arrival at J.F.K. airport and so accom-

plished little in furthering the scheme which, in the event (so far as I know) came to nothing. This particular visit, however, marked the beginning of the chain of events which led to the writing of this work. In the course of it I received several important invitations, the chief of which, relevant to this book, was one from Professor A. A. Pouring to lecture at the U.S. Naval Academy in October, 1976.

For personal reasons I was then seriously considering the possibility of becoming a resident in the U.S.A., but it was necessary to return to the U.K. to make preparations for this.

I returned to the U.S.A. on September 4, 1976, as a passenger in the Concorde, to keep the engagements I had accepted, to become a U.S. resident, and, hopefully, to marry an ex-U.S. Navy nurse with whom I had been friendly over many years.

During my visit to the Naval Academy, Annapolis (to lecture) in October, 1976, Dr. Andrew A. Pouring, the then Chairman of the Aero Space Department, on hearing that I was contemplating becoming resident in the U.S., asked if I would consider joining the Faculty of the Academy as a Distinguished Visiting Research Professor. The appointment would be for one year. I indicated that the offer was of interest. This led to a number of visits to the Academy and a formal invitation from the Superintendent to become 'Navair Research Professor.' This I accepted and duly became a member of the Faculty on August 1, 1977.

At this point I must go back in time to the early days of my work on jet engine development. During that period I evolved my own special methods of dealing with the aero-thermodynamics of gas turbine design which were fundamentally far simpler than the then accepted ways of treating aero-thermodynamic problems. Stanley Hooker, for one, often remarked that this theoretical innovation was more important than the original concept of the jet engine itself.

During one of my talks with Dr. Pouring at the Naval Academy I explained my methods of dealing with thermal cycles and was extremely surprised to learn that, after a period of some thirty years, these had not found their way into textbooks and so were not available to students though I knew they had become familiar to aero engine designers. Dr. Pouring urged me to write up the subject in a thesis as part of my duties at the Academy. This I agreed to do. That became the starting point of this work.

My original intention was to do no more than explain my treatment of thermal cycles, but as time passed my so-called 'thesis' began to grow and grow. The main reasons for its expansion was the course of lectures I gave on aircraft propulsion to a class of senior midshipmen who had elected to take this subject as one of their majors. Since much of the content of these lectures was not included in available textbooks I decided it would be necessary to write every lecture in advance and distribute copies to my class. It then seemed logical to expand my thesis to include the subject matter of my lectures which covered much more ground than the treatment of thermal cycles. Moreover, as time passed, I found myself extending my methods into realms of theory beyond those with which I was familiar. This intellectual exploration proved very fruitful and I added quite substantially to my knowledge of the aero-thermodynamics of turbo machinery. The boldest of these ventures was a limited excursion into shock wave theory (Section 4). This was a field of aero-thermodynamics with which I was almost entirely unfamiliar and I was curious to find out whether, if at all, my methods could be applied. I was pleasantly surprised to find that they could. I decided that these (to me) novel results must be included in this work. It now became clear that the original thesis was becoming a book.

This piecemeal expansion has had its drawbacks. It has meant much re-writing and re-arrangement of its sections into a more logical sequence as additional material was included. I hope the reader will be tolerant with any remaining 'patchiness' he may find. I, myself, am far from satisfied with my efforts. I fear that some evidence of over-hastiness (e.g., some inconsistencies in notation) will be apparent because I have had to meet a financial deadline imposed by the fact that the funds which have been allotted for its initial publication will be cut off automatically very soon after these words are written. The completion of the work has been considerably delayed by preoccupation with other very interesting but time consuming projects plus the domestic complications arising out of transplanting myself from the U.K. to the U.S.A. and five moves of home in little more than eighteen months.

As the reader will find, the fundamental basis of my methods was to treat air as a perfect gas of constant specific heat and to deal with thermal cycles by using temperatures and temperature ratios. Also to treat velocities (or kinetic energy) as having a temperature equivalent and vice versa. These assumptions are very accurate for the temperature range 180-400°K where specific heat is, in fact, virtually constant, but become increasingly inaccurate with increase of temperature above 400°K owing to the increase of specific heat. Nevertheless, as will be shown, they give good comparative results, and make it possible to deal with even compound thermal cycles in a matter of minutes. When, in jet engine design, greater accuracy was necessary for detail design, I worked in pressure ratios, used $\gamma = 1.4$ for compression and $\gamma = 1.33$ for expansion and assumed specific heats for combustion and expansion corresponding to the temperature range concerned. I also allowed for the increase of mass flow in expansion due to fuel addition (in the range 1½ - 2%). The results, despite the guesswork involved in many of the assumptions, amply justified these methods to the point where I was once rash enough to declare that "jet engine design has become an exact science." (This statement was inspired by the fact that on the first test of the W2/500 engine every experimental point fell almost exactly on the predicted curves of performance.)

Much of Sections 1 and 2 will be familiar to advanced students, but they have been included for the benefit of students comparatively new to the subject and to provide the foundation for later sections.

I have assumed throughout that the reader will have a knowledge of the rudiments of thermodynamics, aerodynamics and calculus.

As the reader will find, I have made frequent use of numerals instead of such constants as $\frac{\gamma}{\gamma-1}$, $\sqrt{2gK_p}$ etc., thus formulae which would otherwise look most complicated are greatly simplified. I make no apology for this. I feel sure that most readers will welcome it. Any purist who would prefer otherwise can always substitute $\frac{\gamma}{\gamma-1}$ wherever he sees the exponent 3.5 and $\frac{1}{\gamma-1}$ wherever 2.5 appears as an exponent. If he wishes to translate $147.1\sqrt{\theta}$ into $\sqrt{2gK_pT_1\left[1-\left(\frac{P_2}{P_1}\right)^{\frac{\gamma-1}{\gamma}}\right]}$ he should have no trouble in doing so.

A Note on Units. I apologise to those who might have preferred the S.I. system of units. I grew up with the foot-pound-second system (except for chemistry and physics). In my young days the metric system was never used in mechanical engineering in the U.K., and I find it hard to break the habit of a lifetime. Moreover, if I had talked about thrust in kilograms, height in metres, speed in metres/second and so on, it would have been much

harder to convince the skeptics in the U.K. than it was. Talking about thrust instead of horse power, of specific fuel consumption instead of lbs./H.P. hour caused quite a lot of misunderstanding. It was a bit like talking about shekels per cubic ell as a measure of density.

I have, however, always used degrees centigrade (or Celsius) and degrees Kelvin for temperature and pound calories for heat and deplore the continued use of the Fahrenheit scale in the U.S.A. It has caused me considerable trouble in my discussions with American engineers.

No system of units has a logical basis. The metric system has the merit of using multiples of ten, but otherwise its basic units such as metres, kilograms, etc. are no more logical than feet, pounds, etc. Fortunately, certain important quantities such as specific fuel consumption, specific thrust, etc. are numerically the same in both the c.g.s. and f.p.s. systems.

In my opinion any logical system of units should be based on fundamental constants of nature such as the speed of light, the universal constant of gravitation, the mass of a neutron—and so on (though there is no certainty that these constants will maintain their 'fundamentality').

As the reader will find, I have made generous use of non-dimensional methods which, of course, are independent of any system of units.

I cannot end without acknowledging that I owe much to the extensive engineering training I received in the Royal Air Force—3 years as an Aircraft Apprentice in No. 4 Apprentices' Wing, RAF Cranwell, 2 years as a Flight Cadet at the Royal Air Force College, also at Cranwell, 2 years at the Officer's School of Engineering, RAF Henlow, and 2 years at Cambridge University taking the Mechanical Sciences Tripos, followed by a post graduate year for aerodynamic research and jet engine design—a total of 10 years. Also the experience I gained as a fighter pilot, flying instructor and float plane test pilot during the four years of General Duties following my graduation from Cranwell proved invaluable. I also owe much to the brilliant team of engineers (mostly younger than myself) that I succeeded in recruiting after I had been placed on the Special Duty List and loaned to Power Jets Ltd. as Honorary Chief Engineer.

Finally, this work owes much to the encouragement I received from Professor Andrew A. Pouring, Commander Marle D. Hewett, Chairman of the Aero-Space Department of the U.S. Naval Academy, and the help of Commander Hewett's staff, especially Mrs. Morva Hamaleinan.

Postscript

Since the foregoing was written the original of this work has been printed in limited numbers in report form for the U.S. Naval Academy as "Engineering & Weapons Report EW—7—79" dated June 1979. This book, however, differs from the original work in that Sections 3, 4, 5 and 17 have been substantially amended or rewritten with simplification as the main objective.

SECTION 1
Fundamentals

Notation and Units (for this section)

P	Absolute Pressure	lb/ft^2 (p.s.f.)
p	Pressure Ratio	
V	Specific Volume	ft^3/lb
T	Absolute Temperature	°Kelvin (°K)
t	Temperature Ratio	
ρ	Density	lb/ft^3
σ	Density Ratio	
E	Internal Energy	C.H.U/lb or ft lb/lb
H	Heat Added	C.H.U (Centigrade Heat Units)
h	Enthalpy	C.H.U/lb or kj/kg
s	Entropy	C.H.U/°K
W	Work/unit mass	C.H.U or Ft lbs/lb
C_v	Specific Heat at Constant Volume in thermal units	(C.H.U/lb/°K)
C_p	Specific Heat at Constant Pressure in thermal units	(C.H.U/lb/°K)
K_v	Specific Heat at Constant Volume in mechanical units	(ft lb/lb/°K)
K_p	Specific Heat at Constant Pressure in mechanical units	(ft lb/lb/°K)
γ	Ratio of Specific Heats $\equiv \frac{C_p}{C_v} \equiv \frac{K_p}{K_v}$	
R	Gas Constant per unit mass $\equiv K_p - K_v$	ft lb/lb/°K
H_R	Heat Added Reversibly	C.H.U.

Note:– One Centigrade Heat Unit (C.H.U.) is the amount of heat required to raise the temperature of one pound of water by 1.0°C: i.e. 1.0 C.H.U. = 1.8 B.T.U.s or 1400 ft.lbs.

Basic Definitions and Laws

All that follows (unless otherwise stated) is based on the assumption that air behaves as a perfect gas of constant specific heat, and on the use of three definitions, two thermodynamic laws and Newton's Laws of Motion. Steady flow is also assumed.

The *Definitions* are:

1) $E \equiv C_v T$ or $E \equiv K_v T$
2) $h \equiv E + PV$
3) $ds \equiv \frac{dH_R}{T}$

The *Thermodynamic Laws* are:

1) The First Law of Thermodynamics, namely $\Delta H = W + \Delta E$ i.e. Heat added equals work done plus the increase in Internal Energy. (This is the thermodynamic form of the Law of Conservation of Energy)

2) That for a *Perfect Gas*: $PV = RT$ or $P = \rho RT$ – This is known as the "Gas Equation"

(Note:–the Second Law of Thermodynamics is not used herein–except incidentally in the section on shock waves. It is variously stated; it is the thermodynamic equivalent of the axiom that energy cannot be created out of nothing. One form of stating it is:–"It is impossible for a self-acting machine, *unaided by any external agency*, to convey heat from one body to another at a higher temperature")

A Note on Entropy

Entropy is a concept which many students have difficulty in assimilating. It is a somewhat intangible quantity which, being defined as a differential, has no absolute value. One can only assign a specific value for entropy by choosing an arbitrary zero such as O°C (as in steam tables). It is a very valuable concept for thermodynamic calculations concerning vapours and non-perfect gases, and many text book writers make generous use of temp-entropy diagrams, etc. to illustrate thermal cycles with a perfect gas (or mixture of perfect gases) as the working fluid. The writer has never found this to be necessary and so there are no such diagrams herein except for Fig. 1e of Section 6 as one of eight methods of representing thermal cycles, four of which use entropy as one of the basic parameters, merely to illustrate the several alternatives for thermal diagrams.

The word "isentropic" is frequently used, however, to indicate an adiabatic change of state which is reversible i.e. without loss. At one time the word "adiabatic" was used for this but was distinctly misleading since "adiabatic" covers *any* change of state where heat is neither added nor lost. Thus a heat insulated throttling process is adiabatic but not isentropic. Indeed, any adiabatic process in which utilisable energy is converted into non-useable internal energy is non-isentropic because entropy increases. An increase of entropy is analogous to the loss of energy in a waterfall where the original potential energy is converted to unusable energy of turbulence. Again an increase of entropy may be likened to an increase of the randomness of molecular motion at the expense of the energy of orderly motion i.e. the conversion of 'order into chaos.' There can never be a decrease of entropy in an adiabatic process–which is one way of expressing the second law of Thermodynamics. The most one can do in aero-thermodynamics is to minimize the increase of entropy. This is one of the main objectives in the design of aero-thermodynamic machinery.

Isentropic Compression or Expansion of a Perfect Gas

In isentropic compression or expansion, a perfect gas obeys the law $PV^{\gamma} = \text{const.} = P_o V_o^{\gamma}$ where P_o and V_o are the pressure and specific volume of a reference state. Alternatively, writing $\rho \equiv \frac{1}{V}$ and $\rho_o \equiv \frac{1}{V_o}$, $\frac{P}{\rho^{\gamma}} = \frac{P_o}{\rho_o^{\gamma}}$. This law is of key importance in all that follows. It is derived from the first law of Thermodynamics

$$\Delta H = W + \Delta E \tag{1-1}$$

using the Gas Equation:– $PV = RT$ (1-2)

the definition of internal Energy:– $E = K_v T$ (1-3)

and the definition of Entropy:– $ds = \frac{dH_R}{T}$ (1-4)

Since no heat is added or removed, $\Delta H = 0 \therefore$ from (1)

$$W + \Delta E = 0 \tag{1-5}$$

If $\Delta H = 0$ $dH_R = 0$ $\therefore$ $ds = 0$ $\therefore$ s is constant which confirms that the process is isentropic.

Fig. 1 is a Pressure-Specific Volume (P-V) diagram drawn to illustrate the connection between W. P and V. AB shows the relationship between P and V as a gas is compressed from P_1V_1 to P_2V_2. It is not necessarily isentropic. ab represents a part of the compression through a decrease of volume $-\delta V$. The work done on the gas $-\delta W$ in compressing from a to b is seen to be given by $-\delta W = -P\delta V$ (by convention work done in compression is taken to be negative and to be positive in expansion). In the limit

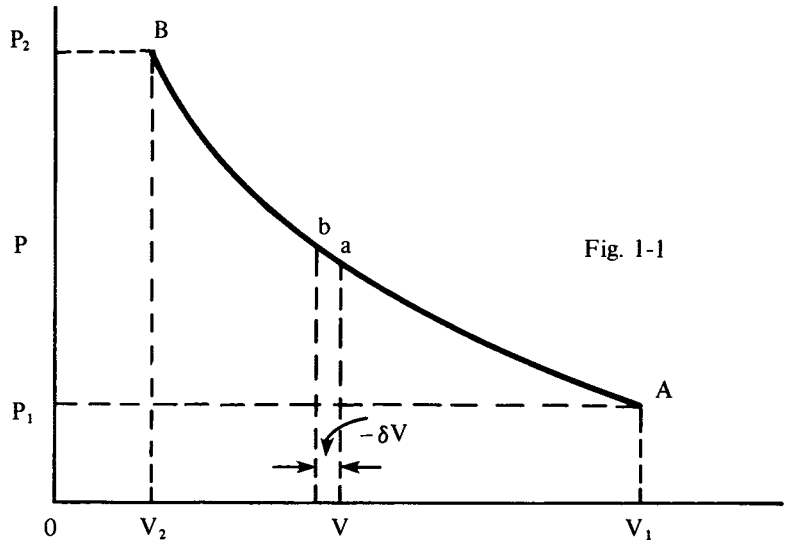

Fig. 1-1

$$dW = PdV \tag{1-6}$$

From equ.(5), for isentropic compression or expansion $dW = -dE$ and from equ. (3) $dE = K_v dT$ $\therefore$ $dW = -K_v dT$ (1-7)

therefore from (6) & (7) $PdV = -K_v dT$ (1-8)

From which $dT = -\frac{PdV}{K_v}$ (1-9)

From the Gas Equation $PV = RT$ we have $PdV + VdP = RdT$

or $PdV + VdP = K_p dT - K_v dT$ (1-10)

Substituting for PdV from (8), (10) becomes $VdP = K_p dT$ (1-11)

Substituting for dT from (9) $VdP = -\frac{K_p}{K_v} PdV$ or, since $\frac{K_p}{K_v} = \gamma$, $VdP + \gamma PdV = 0$

or $\frac{dP}{P} + \gamma \frac{dV}{V} = 0$ from which $\text{Log } P + \gamma \text{ Log } V = \text{Const.}$

or

$$PV^{\gamma} = \text{Const.} \quad (1\text{-}12)$$

An important form of (11) is $\frac{dP}{\rho} = K_p dT$ (1-11a)

Note that (11a) can be derived from the First Law when H = 0, Fig. 1, and the Gas Equation and is true whether or not the process is isentropic as long as it is adiabatic.

Important Relationships

A number of useful relationships may be derived from those stated in the foregoing using additional notation as follows:

$\theta = \Delta T$

$\theta' = \Delta T'$ where the prime indicates an isentropic process.

$\phi = \frac{\theta}{T_1}$ where T_1 is a reference temp.

$\phi' = \frac{\theta'}{T_1}$

From the Gas Equation in the form $P = \rho RT$ we may write $P_1 = \rho_1 RT_1$, where the suffix 1 means a reference condition, it follows that $\frac{P}{P_1} = \frac{\rho}{\rho_1}\frac{T}{T_1}$ or $p = \sigma t$ (1-13)

From the isentropic law $PV^{\gamma} = P_1 V_1^{\gamma}$ it follows that

$$\frac{P}{P_1} = \left(\frac{V_1}{V}\right)^{\gamma} \equiv \left(\frac{\rho}{\rho_1}\right)^{\gamma} \quad \text{or } p = \sigma^{\gamma} \text{ or } \sigma = p^{\frac{1}{\gamma}} \quad (1\text{-}14)$$

By combining (13) and (14)

$$\frac{P}{P_1} = \left(\frac{T}{T_1}\right)^{\frac{\gamma}{\gamma-1}} \quad \text{or } p = t^{\frac{\gamma}{\gamma-1}} \quad \text{or } t = p^{\frac{\gamma-1}{\gamma}} \quad (1\text{-}15)$$

$$\frac{\rho}{\rho_1} = \left(\frac{T}{T_1}\right)^{\frac{1}{\gamma-1}} \quad \text{or } \sigma = t^{\frac{1}{\gamma-1}} \quad \text{or } t = \sigma^{\gamma-1} \quad (1\text{-}16)$$

For an isentropic temp rise of θ' from temp T_1

$$t = 1 + \frac{\theta'}{T_1} \quad \text{or} \quad t = 1 + \phi' \tag{1-17}$$

$$\text{hence} \quad \sigma = (1 + \frac{\theta'}{T_1})^{\frac{1}{\gamma-1}} \quad \text{or} \quad \sigma = (1 + \phi')^{\frac{1}{\gamma-1}} \tag{1-18}$$

$$\text{and} \quad p = (1 + \frac{\theta'}{T_1})^{\frac{\gamma}{\gamma-1}} \quad \text{or} \quad p = (1 + \phi')^{\frac{\gamma}{\gamma-1}} \tag{1-19}$$

From the definition of enthalpy $h \equiv E + PV$ and the Gas Equation $PV = RT$, $dh = dE + PdV + VdP \equiv dE + RdT \equiv dE + K_p dT - K_v dT$ and since $dE \equiv K_v dT$ it follows that

$$dh = K_p dT \text{ or } dh = \frac{dP}{\rho} \text{ (from 11a)} \tag{1-20}$$

and therefore *for const. specific heat* $h = K_p T$ (1-21)

$$\text{hence} \quad \frac{h}{E} = \frac{K_p T}{K_v T} = \gamma$$

The Momentum Equation for linear Compressible Flow

Using additional notation as follows:–

u Velocity ft/sec

S Section Area sq.ft.

m Mass lbs

F Force lbs

and with the aid of Fig. 2, the very important Momentum Equation will be derived.

Fig. 2 represents a small section of a stream tube of sections S at AA′ and S+δS at

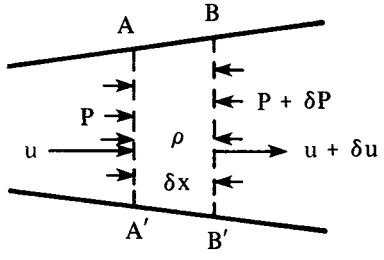

Fig. 1-2

BB′ with pressures and velocities as shown for a very small element of length δx and mean density ρ.

The net accelerating force acting on the element ABB′A′ is $PS - (P+\delta P)(S+\delta S)$ plus the mean side wall pressure $P + \frac{\delta P}{2}$ acting on the area δS i.e. $\delta F = PS - (P + \delta P)(S + \delta S) + (P + \frac{\delta P}{2})\,\delta S$ which, neglecting the products of infinitesimals, reduces to $\delta F = -S\delta P$.

Again neglecting the products of infinitesimals, the mass of the element $\delta m = pS\delta x$ and the acceleration is $u\frac{\delta u}{\delta x}$, therefore, since force equals mass times acceleration,

$$\delta F = -S\delta P = \frac{\delta m}{g}\, u \frac{\delta u}{\delta x} = \frac{\rho S \delta x}{g}\, u \frac{du}{\delta x} \text{ from which it readily follows that } \frac{dP}{\rho} + \frac{du^2}{2g} = 0 \tag{1-22}$$

It may be seen that (22) is the differential form of Bernouilli's Equation for incompressible flow, namely:– $P + \frac{\rho u^2}{2g} = \text{const.}$

The Energy Equation for Compressible Flow

This is very simply derived from (22). As we have seen, (Equation (11a)), $\frac{dP}{\rho} = K_p dT$, so, substituting for $\frac{dP}{\rho}$ in (22), we have $K_p dT + \frac{du^2}{2g} = 0$ or $dT + \frac{du^2}{2gK_p} = 0$ (1-23)

from which $\frac{u^2}{2gK_p} + T = T_T$ where T_T is total or 'stagnation' temp. (1-24)

Writing $\frac{u^2}{2gK_p} = \theta_u$ where θ_u is the 'temp equivalent of velocity' then

$$T + \theta_u = T_T \qquad (1\text{-}25)$$

i.e., in words "Total (or stagnation) Temp. equals the Static Temp. plus the Temp. equivalent of velocity"

Equation 25 is a very simple and useful form of the Energy Equation and is true whether the energy conversion is isentropic or not as long as it is adiabatic. It may be described as the 'compressible version' of Bernouilli's Equation. It will be much used in all that follows. *It is emphasised, however, that it is based on the assumption that* K_p *is constant,* otherwise Equation 23 must be used with K_p as a function of T.

Quantities etc. used for Air treated as a Perfect Gas of Constant Specific Heat

K_p = 336 ft lbs/lb/°C

K_v = 240 ft lbs/lb/°C

R = 96 ft lbs/lb/°C

C_p = 0.24 C.H.U./lb/°C

C_v = 0.171 C.H.U./lb/°C

$\gamma \equiv \frac{K_p}{K_v} \equiv \frac{C_p}{C_v} = 1.4$

$\frac{1}{\gamma - 1} = \frac{K_v}{R} = 2.5$

$\frac{\gamma}{\gamma - 1} = \frac{K_p}{R} = 3.5$

$\frac{\gamma + 1}{2} = 1.2$

u_c (the accoustic speed at stalic temp. T) $= \sqrt{gR\gamma T} = 65.786\sqrt{T}$

$\sqrt{2gK_p} = 147.1$

Note: Since 1.0°C = 1.0°K it is useful to use °K for absolute temps and °C for temp. differences.

In most of this work the numerical quantities above will be used instead of symbols to simplify formulae e.g. $\frac{P}{P_1} = \left(\frac{T}{T_1}\right)^{\frac{\gamma}{\gamma-1}}$ becomes $p = t^{3.5}$; $\frac{\rho}{\rho_1} = \left(\frac{T}{T_1}\right)^{\frac{1}{\gamma-1}}$ becomes $\sigma = t^{2.5}$; $u = 147.1\sqrt{\theta_u}$ etc.

SECTION 2
Flux Density in Isentropic Compressible Flow

Additional Notation

Q Mass Flow Rate lb/sec
ψ Flux Density lb/sec/sq ft
ψ_c Maximum Flux Density
T_c Static Temp when $\psi = \psi_c$
u_c Velocity when $\psi = \psi_c$
θ_c Temp. Equivalent of $u_c = \dfrac{u_c^2}{2g K_p} \equiv T_T - T_c$
$t_c = \dfrac{T_T}{T_c}$
ρ_c Density when $\psi = \psi_c$
$\alpha \equiv \dfrac{1}{\gamma - 1}$ (= 2.5 for air)

$k = \sqrt{2gK_p}$ (= 147.1 for air)
S_c Section Area when $\psi = \psi_c$

The suffix T implies total (or 'stagnation') temp., pressure, and density.

Flux Density Relationships

It will be obvious that $\psi = \rho u = \dfrac{Q}{S}$ (2.1)

ψ will be a maximum i.e. will equal ψ_c when $d\psi = 0$ i.e. when $d(\rho u) = 0$ or

$$\rho_c\, du + u_c\, d\rho = 0 \quad \text{or} \quad \frac{du}{u_c} + \frac{d\rho}{\rho_c} = 0 \tag{2-2}$$

Since, for isentropic flow, $\rho = \rho_T\, t^{-\alpha}$, $d\rho = -\alpha\rho_T\, t^{-\alpha-1}\, dt \therefore \frac{d\rho}{\rho} = -\frac{\alpha dt}{t}$ (2-3)

and, since $u = k\sqrt{\theta_u} = k\sqrt{T_T - T} = k\sqrt{T_T\left(1 - \frac{1}{t}\right)}$

$$du = k\sqrt{T_T}\, d\,(1 - t^{-1})^{1/2} = k\sqrt{T_T} \times \frac{1}{2}\,(1 - t^{-1})^{-1/2} \times t^{-2}\, dt$$

or

$$du = \frac{k\sqrt{T_T}}{2t^2\sqrt{1 - \frac{1}{t}}}\, dt \qquad \text{Using } u = k\sqrt{T_T\left(1 - \frac{1}{t}\right)} \text{ from above}$$

then $$\frac{du}{u} = \frac{dt}{2t^2 - 2t} \tag{2-4}$$

hence substituting for $\frac{d\rho}{\rho}$ from (3) and for $\frac{du}{u}$ from (4)

(2) becomes $$-\frac{\alpha dt}{t_c} + \frac{dt}{2t_c^{\,2} - 2t_c} = 0$$

which reduces to $$\frac{1}{t_c - 1} = 2\alpha = \frac{2}{\gamma - 1}$$

$$\therefore\ t_c - 1 = \frac{\gamma - 1}{2} \quad \text{from which} \quad \underline{t_c = \frac{\gamma + 1}{2}} \tag{2-5}$$

i.e. $\psi = \psi_c$ when $\frac{T_T}{T_c} = \frac{\gamma + 1}{2}$ (= 1.2 for air)

From $\theta_c = T_T - T_c = T_T\left(1 - \frac{1}{t_c}\right) = T_T\left(1 - \frac{2}{\gamma+1}\right) = T_T\left(\frac{\gamma-1}{\gamma+1}\right)$ it follows that, for air, $\theta_c = \frac{T_T}{6}$ or $\frac{T_c}{5}$ and, since $u_c = \sqrt{2gK_p\theta_c} = \sqrt{2gK_p\,\frac{\gamma-1}{2}\,T_c}$ then using $K_p = R\frac{\gamma}{\gamma-1}$;

$u_c = \sqrt{g\gamma RT_c}$ *which is the acoustic velocity at temp.* T_c – thus flux density is a maximum when velocity equals the local speed of sound.

For the 'critical' temp ratio t_c (total to static) the corresponding value of p_c (total to static) $= t_c^{\frac{\gamma}{\gamma-1}}$ and the critical density ratio $\sigma_c = t_c^{\frac{1}{\gamma-1}} \therefore \frac{\rho_T}{\rho_c} = \frac{\gamma+1}{2}^{\frac{1}{\gamma-1}}$

or, since $\rho_T = \frac{P_T}{RT_T}$ (from the Gas Equation); $\rho_c = \frac{P_T}{RT_T\sigma_c}$. Since $\psi = \rho u$, $\psi_c = \rho_c u_c$ and, as we have seen, $u_c = \sqrt{g\gamma RT_c}$ it follows that $\psi_c = \frac{P_T}{RT_T\sigma_c}\sqrt{g\gamma RT}$ which, using $T_c = \frac{T_T}{t_c}$ and $\sigma_c = t_c^{\frac{1}{\gamma-1}}$, reduces to $\psi_c = \frac{P_T}{\sqrt{T_T}}\, t_c^{-\frac{\gamma+1}{2\gamma-2}}\sqrt{\frac{g\gamma}{R}}$ (2-6)

For air $t_c = 1.2$ $\quad \frac{\gamma+1}{2\gamma-2} = 3$ and $\sqrt{\frac{g\gamma}{R}} = .6853$

$$\therefore \text{ for air } \psi_c = \frac{.6853}{1.2^3}\frac{P_T}{\sqrt{T_T}} = .3966\,\frac{P_T}{\sqrt{T_T}} \tag{2-7}$$

Also, for air $p_c = t_c^{3.5} = 1.2^{3.5} = 1.8929$

and $\sigma_c = t_c^{2.5} = 1.2^{2.5} = 1.5774$

$$u_c = 147.1\sqrt{\frac{T_T}{6}} = 60.053\sqrt{T_T} \tag{2-8}$$

or $u_c = 147.1\sqrt{\frac{T_c}{5}} = 65.785\sqrt{T_c}$

Thus it may be seen that ψ_c is proportional to total pressure and inversely proportional to $\sqrt{\text{total temp.}}$—a fact of much importance in many areas of aero-thermodynamics.

For flux density other than ψ_c, since $\psi = \rho u$; $u = 147.1\sqrt{T_T}\sqrt{1-\frac{1}{t}}$ and $\rho = \frac{\rho_T}{t^{2.5}} = \frac{P_T}{RT_T}\,t^{-2.5}$ it follows that $\psi = 147.1\sqrt{T_T}\sqrt{\frac{t-1}{t}} \times \frac{P_T}{RT_T}\,t^{-2.5}$ which reduces to

$$\psi = 1.532\,\frac{P_T}{\sqrt{T_T}}\,\frac{\sqrt{t-1}}{t^3} \tag{2-9}$$

$$\text{From (7) } \psi_c = .3966\,\frac{P_T}{\sqrt{T_T}} \quad \therefore \quad \frac{\psi}{\psi_c} = 3.863\,\frac{\sqrt{t-1}}{t^3} \tag{2-10}$$

The table below gives the values of ψ/ψ_c, u/u_c ρ/ρ_c and P/P_c for the temp. ratio (total to static) range 1.0 – 3.4

t	ψ/ψ_c	u/u_c	ρ/ρ_c	P/P_c
1.00	0	0	1.577	1.893
1.05	0.747	0.534	1.396	1.596
1.10	0.917	0.738	1.243	1.356
1.15	0.985	0.885	1.112	1.161
1.20	1.000	1.000	1.000	1.000
1.25	0.990	1.095	0.903	0.867
1.30	0.965	1.177	0.819	0.756
1.35	0.930	1.247	0.745	0.662
1.40	0.892	1.309	0.680	0.583
1.45	0.851	1.365	0.623	0.516
1.50	0.811	1.414	0.572	0.458
1.60	0.731	1.500	0.437	0.365
1.70	0.659	1.572	0.419	0.296
1.80	0.593	1.633	0.363	0.242
1.90	0.534	1.686	0.317	0.200
2.00	0.484	1.732	0.279	0.167
2.20	0.398	1.809	0.220	0.120
2.40	0.331	1.870	0.177	0.0884
2.60	0.278	1.922	0.145	0.0688

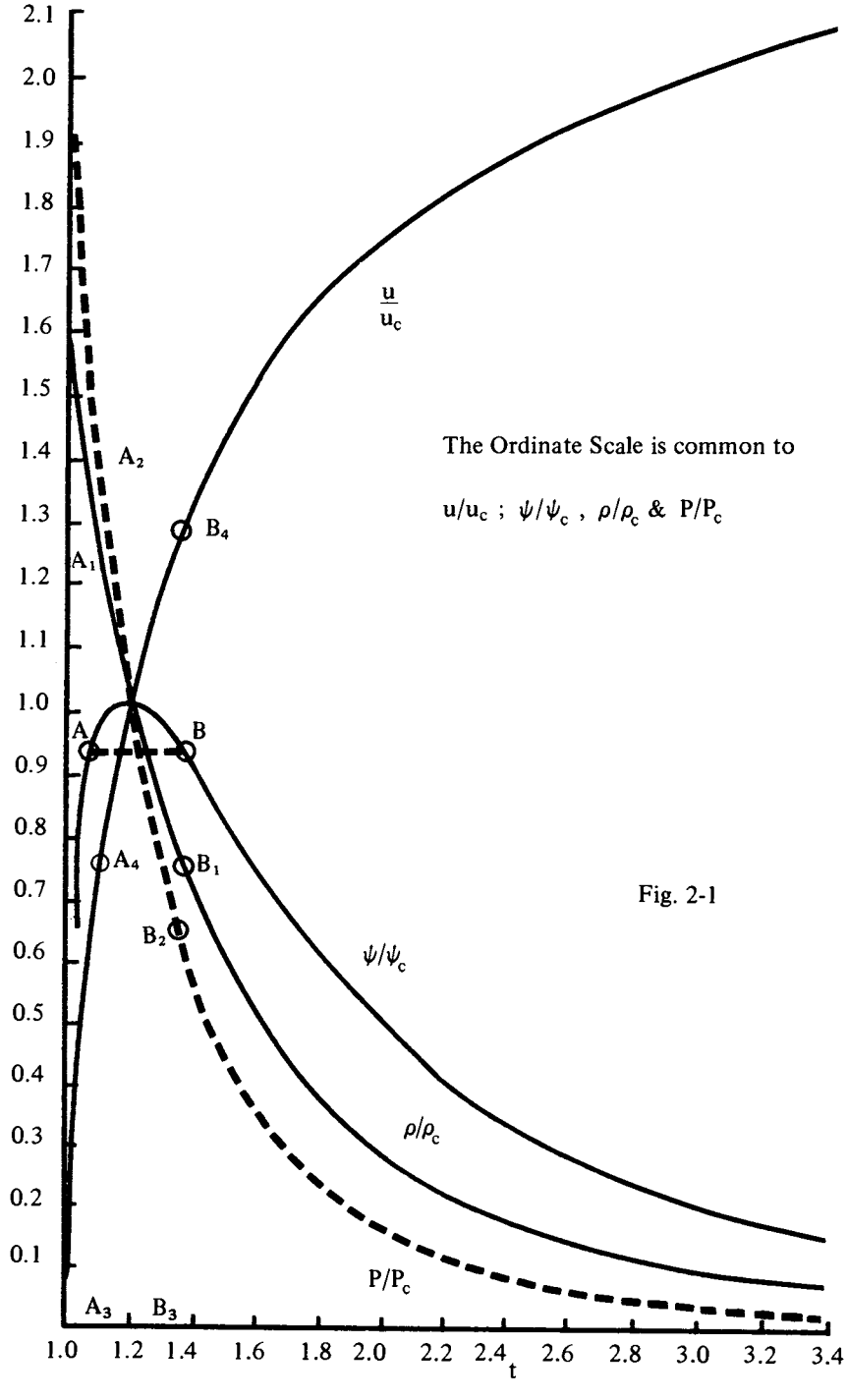
2.1
2.0
1.9
1.8
1.7
1.6
1.5
1.4
1.3
1.2
1.1
1.0
0.9
0.8
0.7
0.6
0.5
0.4
0.3
0.2
0.1
u/uc
A2
B4
A1
A
B
A4
B1
B2
ψ/ψc
ρ/ρc
P/Pc
A3
B3
1.0 1.2 1.4 1.6 1.8 2.0 2.2 2.4 2.6 2.8 3.0 3.2 3.4
t
The Ordinate Scale is common to
u/uc ; ψ/ψc , ρ/ρc & P/Pc

Fig. 2-1

2.80	0.236	1.964	0.120	0.0515
3.00	0.202	2.000	0.101	0.0405
3.20	0.175	2.031	0.086	0.0322
3.40	0.152	2.058	0.074	0.0261

These figures are plotted in Fig. 1.

The main feature to note is that below ψ_{max} ($\psi = \psi_c$) there are two possible values of ψ and, correspondingly, two each of t, p/ρ_c, P/P_c and u/u_c. Thus for $\psi/\psi_c = 0.92$ (A and B) the two possible values of ρ/ρ_c are at A_1 and B_1; for P/P_c at A_2 and B_2; for t at A_3 and B_3; and for u/u_c at A_4 and B_4. It would therefore be possible, without violating continuity, for a sudden 'jump' in pressure from B_2 to A_2 to occur with a corresponding jump in density from B_1 to A_1 and a sudden reduction of velocity from B_4 to A_4. This, of course, is the basis of shock wave phenomena. Unfortunately, as shown in Section 4, these sudden changes are not isentropic.

Another point to notice from the ψ/ψ_c curve is that, near the maximum, in the range, say, t = 1.15 to t = 1.25 the change of ψ/ψ_c is not more than 1.5% of the maximum, so that, in this range (which occurs frequently in turbo machinery) there would be little error in assuming that mass flow rate Q depends only on total temp. and pressure, i.e. that

$$Q \propto \frac{P_T}{\sqrt{T_T}}.$$

It should be noted that u/u_c is synonymous with Mach Number, i.e. $\frac{\text{actual velocity}}{\text{acoustic velocity}}$

where the acoustic velocity is that for the static temp. T in $u_c = \sqrt{g\gamma RT}$.

It is desirable to emphasize that all the relationships derived in the foregoing discussion of flux density are true only for isentropic flow, however they are a close approximation if the departure from isentropy is minor.

A point to note is that, having magnitude and direction, flux density is a vector quantity.

SECTION 3

Radial Equilibrium in Whirling Isentropic Compressible Flow

This is a subject of considerable importance in turbo machinery blade design, yet, until the mid 1930s, the effect of centrifugal force on the radial pressure gradient in modifying the velocity distribution across the annular whirling flow issuing from, say, a turbine nozzle ring was ignored. It was assumed that the flow from each pair of nozzle blades was 'straight' and that the velocity was uniform across the annulus. This was a legacy from the days of 'partial admission' when a few widely spaced individual nozzles were used too far apart for their individual jets to coalesce into a whirling flow pattern. This non recognition of radial equilibrium or vortex flow was not important when blades were very short relative to mean diameter. For longer blades it was customary to allow for increase of blade speed with radius and blades were 'twisted' accordingly, but no allowance was made for the equally important reduction of whirl velocity with increase of radius with the result that the blade twist was only about half of what it should have been. Moreover calculations of end thrust on a rotor were grossly inaccurate for long bladed turbines.

Wherever a flow has curvature there has to be a pressure gradient normal to the streamlines due to centrifugal force in addition to any tangential pressure gradient there may be due to acceleration along the streamlines. Further if there is a radial component of velocity (as in radial flow machinery, e.g. centrifugal compressors), any variation i.e. acceleration, will be superimposed on the radial pressure gradient due to centrifugal force. Forces due to radial accelerations are, however, normally small compared with centrifugal force when whirl velocities are in the range 800 - 2500 ft/sec as they usually are at entry to turbine rotor blading or exit from axial flow and centrifugal compressor rotors.

In this section the theory of radial equilibrium in whirling flow is dealt with on the assumptions that changes in temp., pressure, velocity etc. take place isentropically and that stagnation (i.e. total) temp and pressure are uniform.

If the flow has tangential velocity (i.e., whirl velocity) u_ω ; axial velocity u_a and radial velocity u_r at a given point in space, then, since these components are mutually at right angles, the resultant velocity u is given by

$$u^2 = u_\omega{}^2 + u_a{}^2 + u_r{}^2 \tag{3-1}$$

$$\text{hence } \theta_u = \theta_\omega + \theta_a + \theta_r \tag{3-2}$$

It follows that the static temp. T, at the point concerned is given by $T = T_T - \theta_u \equiv T_T - \theta_\omega - \theta_a - \theta_r$ (3-3)

from which $dT = -d\theta_u \equiv -d\theta_\omega - d\theta_a - d\theta_r$

$$\text{or } dT + d\theta_\omega + d\theta_a + d\theta_r = 0 \tag{3-3a}$$

The diagram of fig. 1 represents a section of whirling flow where the whirl velocity is u_ω at radius r and the density is ρ. If the pressure is P at r and $P + \delta P$ at $r + \delta r$, then,

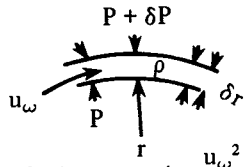

Fig. 3-1

since the acceleration towards the center is $\frac{u_\omega^2}{r}$, one may see that

$$\delta P = \frac{\rho}{g}\frac{u_\omega^2}{r}\delta r \quad \text{or} \quad \frac{dP}{\rho} = \frac{u_\omega^2}{g}\frac{dr}{r} \tag{3-4}$$

Since $\frac{dp}{\rho} = K_p dT$ (equ. 11a of Section 1) and

$$\frac{u_\omega^2}{2gK_p} = \theta_\omega \text{ it follows that } 2\theta_\omega \frac{dr}{r} = dT \tag{3-5}$$

Substituting for dT from (3a) above

$$2\theta_\omega \frac{dr}{r} = -d\theta_\omega - d\theta_a - d\theta_r$$

$$\text{or } 2\theta_\omega \frac{dr}{r} + d\theta_\omega + d\theta_a + d\theta_r = 0$$

$$\text{or } 2\frac{dr}{r} + \frac{d\theta_\omega}{\theta_\omega} + \frac{d\theta_a}{\theta_\omega} + \frac{d\theta_r}{\theta_\omega} = 0 \tag{3-6}$$

From equation (6), if the relationship between r and any two of any two of the three velocity components is known (or decided) the relationship between the third and r may be found. E.g. if $u_r = 0$ or is constant $d\theta_r = 0$ and if u_a is constant $d\theta_a = 0$, hence $\frac{2dr}{r} + \frac{d\theta_\omega}{\theta_\omega} = 0$ from which $r^2\theta_\omega = \text{const.}$ or $ru_\omega = \text{const.}$ i.e. whirl velocity is inversely proportional to radius. This is the 'law' of the 'free vortex.'

Since $ru_\omega = \text{const.}$, the angular momentum of a free vortex is the same at all radii.

It should be noted that Equation (6) above was arrived at on the assumption that the only acceleration was that due to centrifugal force. It does not take into account rates of change of u_ω u_a or u_r if present. Except within blade passages these accelerations are usually less than 2% of the centrifugal acceleration in turbo machinery.

There are several relationships between the velocity components and radius which permit easy solutions of Equation (6). Two cases are dealt with below.

Case 1 $u_r = 0$ and $\frac{u_\omega}{u_a} = \text{Const} = \tan\alpha$ where α is the angle of flow relative to the

axis. (This is representative of the flow issuing from a ring of nozzle blades of constant exit angle.)

Since $d\theta_r = 0$ and $u_a \tan\alpha = u_\omega$, $u_a^2 \tan^2\alpha = u_\omega^2$ i.e. $\theta_a \tan^2\alpha = \vartheta_\omega$ $\therefore$

$\tan^2\alpha \, d\vartheta_a = d\theta_\omega$ or $d\theta_a = \dfrac{d\theta_\omega}{\tan^2\alpha}$, hence substituting for $d\theta_a$ in equation (6) we have:–

$$\frac{2dr}{r} + \frac{d\theta_\omega}{\theta_\omega} + \frac{d\theta_\omega}{\theta_\omega \tan^2\alpha} = 0$$

or $\dfrac{2dr}{r} + \dfrac{\tan^2\alpha + 1}{\tan^2\alpha} \dfrac{d\theta_\omega}{\theta_\omega} = 0$ or, since $\dfrac{\tan^2\alpha + 1}{\tan^2\alpha} = \operatorname{cosec}^2\alpha$,

$\dfrac{2dr}{r} + \operatorname{cosec}^2\alpha \dfrac{d\theta_\omega}{\theta_\omega} = 0$ from which $2 \text{ Ln. } r + \operatorname{cosec}^2\alpha \text{ Ln. } \theta_\omega = 0$

or $r^2 \theta_\omega^{\operatorname{cosec}^2\alpha} = \text{Const.}$

Case 2 $u_r = 0$ and $u_\omega = \text{Const}$ i.e. $\theta_\omega = \text{Const.}$

Equ. (6) now becomes $\dfrac{2dr}{r} + \dfrac{d\theta_a}{\theta_\omega} = 0$ from which $\text{Ln. } r^2 + \theta_a/\theta_\omega = \text{const.}$

If, at r_m, θ_a is θ_{am} then $\text{Ln. } r^2 + \theta_a/\theta_\omega = \text{Ln. } r_m^2 + \theta_{am}/\theta_\omega$

from which $2 \text{ Ln.} \dfrac{r}{r_m} = \dfrac{1}{\theta_\omega} (\theta_{am} - \theta_a)$

or $2\theta_\omega \text{ Ln. } \dfrac{r}{r_m} = \theta_{am} - \theta_a$ or $\theta_a = \theta_{am} - 2\theta_\omega \text{ Ln. } \dfrac{r}{r_m}$

which is, perhaps, the most convenient equation to use.

Example 3-1.

If, in a free vortex flow in an annulus of inner radius 1.0 ft. and outer radius 1.6 ft., the whirl velocity at mean radius r_m is 1500′/sec and the (constant) axial velocity is 600′/sec. What are the whirl velocities at inner and outer radii and what are the flow angles at inner, mean, and outer radii?

Since, as shown above, $ru_\omega = r_m u_{\omega m}$ $u_\omega = u_{\omega m} \dfrac{r_m}{r}$. Since $r_m = 1.3$, the whirl velocity at the inner radius is $1500\left(\dfrac{1.3}{1.0}\right) = 1950$′/sec and the flow angle is $\tan^{-1} \dfrac{1950}{600} = 72.9°$. At the outer radius, $u_\omega = 1500 \left(\dfrac{1.3}{1.6}\right) = 1219$′/sec and the flow angle is $\tan^{-1} \dfrac{1219}{600} = 63.8°$. The flow angle at mean radius is $\tan^{-1} \dfrac{1500}{600} = 68.2°$.

Equation (6) has some useful variants. It may be written (since $\theta \propto u^2$):–

$$\frac{2dr}{r} + \frac{du_\omega^2}{u_\omega^2} + \frac{du_a^2}{u_\omega^2} = 0 \quad \text{(neglecting } u_r\text{)} \qquad (3\text{-}7)$$

or

$$\frac{dr}{r} + \frac{u_\omega du_\omega}{u_\omega^2} + \frac{u_a du_a}{u_\omega^2} = 0 \qquad (3\text{-}7a)$$

or

$$\frac{dr}{r} + \frac{du_\omega}{u_\omega} + \frac{u_a du_a}{u_\omega^2} = 0 \qquad (3\text{-}7b)$$

or

$$u_\omega \frac{dr}{r} + du_\omega + \frac{u_a}{u_\omega} du_a = 0 \qquad (3\text{-}7c)$$

or

$$\frac{u_\omega}{u_{\omega m}} \frac{d\frac{r}{r_m}}{\frac{r}{r_m}} + d\frac{u_\omega}{u_{\omega m}} + \frac{u_a u_{\omega m}}{u_{am} u_\omega} d\frac{u_a}{u_{am}} = 0 \qquad (3\text{-}7d)$$

where the suffix m indicates u_a and u_ω at reference radius r_m ; usually the mean radius.

Equation 7d is, of course 'doubly non-dimensional'.

From 7 b:–

$$\text{Ln. } r + \text{Ln. } u_\omega + \int \frac{u_a}{u_\omega^2} du_a = \text{const.} \qquad (3\text{-}8)$$

$$\text{or} \quad \text{Ln. } ru_\omega + \int \frac{u_a}{u_\omega^2} du_a = \text{const.} \qquad (3\text{-}8a)$$

This last may be useful for step by step integration where the relationship between u_ω and u_a is known but cannot be put into a form where $\int \frac{u_a}{u_\omega^2} u_{aD}$ can be integrated algebraically. Thus, for example, a turbine nozzle ring designed to produce a free vortex of constant axial velocity at a design mass flow rate Q, may need to be examined to find out what happens if Q is increased or decreased. For such a purpose equ. 8a is probably best used in the form $\frac{\delta r u_\omega}{r u_\omega} + \frac{u_a}{u_\omega^2} du_a = 0$ (3-8b)

Assuming the leaving flow conforms to the exit angles at all radii and that these conform to the condition that $\tan\alpha = \frac{u_\omega}{u_{aD}}$ where $u_\omega = \frac{r_m}{r} u_{\omega mD}$ and $u_a = \text{const.} = u_{aD}$ (the suffix D implying the design condition). The relationship between u_ω and u_a for the off design condition becomes $u_\omega = u_a \tan\alpha = u_a \frac{r_m}{r} \frac{u_{\omega mD}}{u_{aD}}$ whence one may substitute either for u_ω or u_a in equ. (8b).

Writing $\phi_a = \frac{\theta_a}{T_T}$ and $\phi_\omega = \frac{\theta_\omega}{T_T}$ another useful variant of Equation (6) is:–

$$2d\frac{\frac{r}{r_m}}{\frac{r}{r_m}} + \frac{d\phi_\omega}{\phi_\omega} + \frac{d\phi_a}{\phi_\omega} + \frac{d\phi_r}{\phi_\omega} = 0 \qquad (3\text{-}9)$$

which again is doubly non dimensional.

The static temp. T_s at any radius is $T_s = T_T - \theta_\omega - \theta_a - \theta_r$ (3-10)

or $\frac{T_s}{T_T} = 1 - \phi_\omega - \phi_a - \phi_r$ or $t = \frac{1}{1-\phi_\omega-\phi_a-\phi_r}$ (3-10a)

where t is the total to static temp. ratio.

If P_s is the static pressure at any radius, then $\frac{P_T}{P_s} = t^{3.5}$ or pressure ratio $p = t^{3.5}$ i.e. using Equ. 10a.

$$p = \left(\frac{1}{1-\phi_\omega-\phi_a-\phi_r}\right)^{3.5} \quad (3\text{-}11)$$

Similarly the density ratio σ (total to static) is given by $\sigma = \left(\frac{1}{1-\phi_\omega-\phi_a-\phi_r}\right)^{2.5}$ (3-12)

If p_m is the pressure ratio at reference radius r_m then from (11)

$$p_m = \left(\frac{1}{1-\phi_{\omega m}-\phi_{am}-\phi_{rm}}\right)^{3.5} \text{ so } \frac{p}{p_m} = \left(\frac{1-\phi_{\omega m}-\phi_{am}-\phi_{rm}}{1-\phi_\omega-\phi_a-\phi_r}\right)^{3.5} \quad (3\text{-}13)$$

$$\text{and } \frac{\sigma}{\sigma_m} = \left(\frac{1-\phi_{\omega m}-\phi_{am}-\phi_{rm}}{1-\phi_\omega-\phi_a-\phi_r}\right)^{2.5} \quad (3\text{-}14)$$

(It presumably being obvious that $t_m = \frac{1}{1-\phi_{\omega m}-\phi_{am}-\phi_{rm}}$ and that

$$\frac{t}{t_m} = \frac{1-\phi_{\omega m}-\phi_{am}-\phi_{rm}}{1-\phi_\omega-\phi_a-\phi_r} \text{ and } \therefore t = \frac{t_m}{(1-\phi_\omega-\phi_a-\phi_r)})$$

The above doubly non dimensional formulae enable one to draw generalised curves for the variation of temp. ratio, pressure ratio and density ratio with radius for given values of t_m, $\phi_{\omega m}$, ϕ_{am} and ϕ_{rm} at reference radius r_m.

For cases like a free vortex of constant axial velocity or where $\frac{u_a}{u_\omega}$ = const (ie constant exit angle in the case of a nozzle ring) where the differential equations (6), (7), (9) and (10) or their variants are readily solved, it is a relatively simple matter to find how temp. ratio, pressure ratio and density ratio vary with radius—as may be seen in the following example:—

Example 3-2

A free vortex nozzle ring has a mean radius r_m of 1.5 r_i where r_i is the root radius (i.e. $r_i = 1.0$) and at r_m, $u_a = 0.4u_\omega$ and $\phi_{\omega m} = 0.7$, how do the temp., pressure and density ratios vary from $r/r_i = 1.0$ to $r/r_i = 2.0$?

u_ω varies inversely as the radius, ie $u_\omega r = u_{\omega m} r_m$ from which $\frac{u_\omega}{u_{\omega m}} = \frac{r_m}{r} \therefore \frac{\phi_\omega}{\phi_{\omega m}} = \left(\frac{r_m}{r}\right)^2$ or $\phi_\omega = \phi_{\omega m} \left(\frac{1.5}{r}\right)^2 = \frac{.07 \times 2.25}{r^2} = \frac{.1575}{r^2}$; ϕ_a = const. = $0.4^2 \phi_{\omega m} = 0.16\phi_{\omega m}$

$= .16 \times .07 = .0112$

$$t = \frac{1}{1-\phi_\omega-\phi_a} = \frac{1}{1-\phi_\omega-.0112} = \frac{1}{.9888-\phi_\omega}$$

so, since (from above) $\phi_\omega = \frac{.1575}{r^2}$ $\quad t = \frac{1}{0.9888-\frac{.1575}{r^2}}$

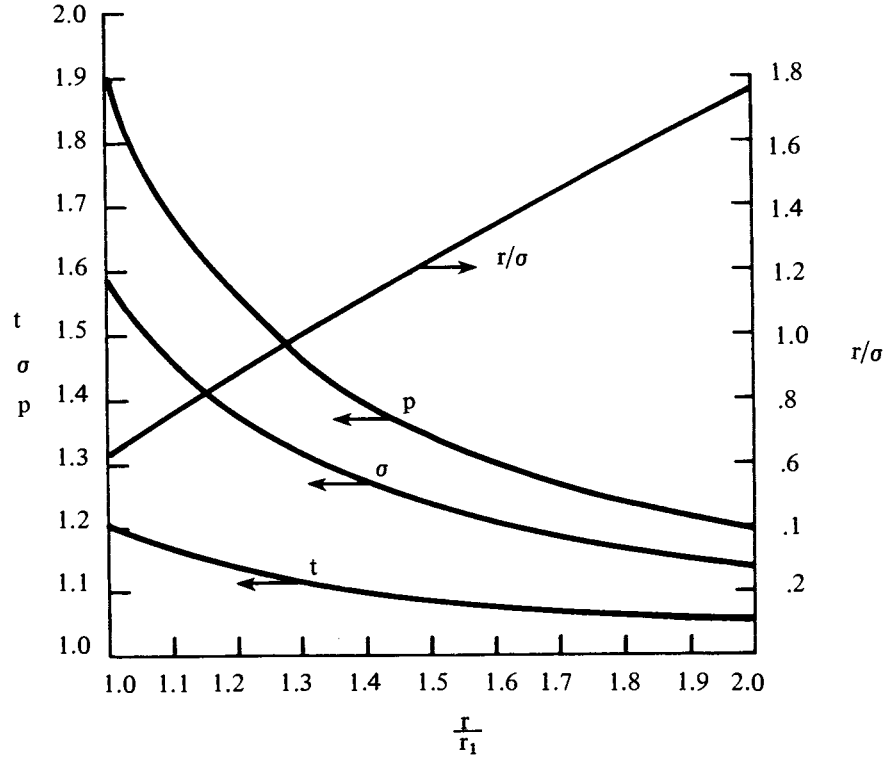

Fig. 3-2

Using $\sigma = t^{2.5}$ and $p = t^{3.5}$ the following table results:–

r	t	σ	p	$\frac{r}{\sigma}$
1.0	1.203	1.587	1.909	0.630
1.2	1.137	1.379	1.568	0.870
1.4	1.101	1.271	1.399	1.101
1.6	1.078	1.208	1.302	1.324
1.8	1.064	1.167	1.241	1.542
2.0	1.053	1.139	1.199	1.756

These figures are plotted in Fig 2. The reader will note the striking variation in p in particular. Thus, for example if the total pressure were, say, 12,000 p.s.f. the static pressure in the vortex would increase from 6286 at r_i to 10,000 p.s.f. at $r/r_1 = 2.0$

The significance of including r/σ in the above table is that the mass flow rate Q is given by:–

$$Q = 2\pi\rho_T \int_{r_1}^{r_2} \frac{r u_a}{\sigma}\, dr \qquad \text{where } \rho_T \text{ is the stagnation density.}$$

If, as in the free vortex, u_a is const then

$$Q = 2\pi\rho_T \; u_a \int_{r_1}^{r_2} \frac{r}{\sigma}\, dr$$

As may be seen from Fig. 2, $\frac{r}{\sigma}$ is virtually a straight line for a free vortex, so there would be little error in writing

$$Q = 2\pi\rho_T \; u_a \frac{r_m}{\sigma_m} (r_2 - r_1)$$

SECTION 4
A Method of Dealing with Shock Waves in Air

Part 1 – Normal Shock Waves

Introductory

With the advent of flight at supersonic speeds and the increasing trend towards supersonic relative velocities in turbo machinery blading, some knowledge of shock wave phenomena is essential.

It is not intended herein to prove that *very small* pressure disturbances in a compressible fluid travel at the acoustic speed for the fluid. It will be assumed that the reader is familiar with the fact that the acoustic speed u_c is given by $u_c = \sqrt{g\gamma RT}$ which, for air, becomes $u_c = 65.79\sqrt{T}$ where T is the static temperature in °K and u_c is in ft/sec. Thus at 288°K u_c = 1116.5 ft/sec.

With other than small pressure disturbances the speed of propagation exceeds the acoustic speed as is obvious from the fact that the portion of the shock wave immediately ahead of the nose (i.e. a 'detached shock') of a body travelling at supersonic speed must be travelling at the same speed as the body. Fig. 1 shows the kind of shock wave ahead of a blunt nosed supersonic missile, and Fig. 2 shows the kind of shock wave ahead of, say, a pitot tube of a supersonic aircraft.

When concerned with supersonic flight in the stratosphere, the temperatures involved are (except at Mach numbers well above 3.0) within the range where there is negligible error in assuming that the specific heat is constant. For shock waves in turbines operating at much higher temperatures, however, accuracy would require that γ, K_p, etc., would need to be adjusted accordingly, but for present purposes it will be assumed that K_p is constant at 336 ft lbs/lb/°K and $\gamma = 1.4$; $\frac{\gamma}{\gamma - 1} = 3.5$, etc.

The velocity u relative to the body is not affected until the shock front is crossed.

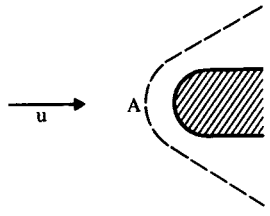

Fig. 4-1

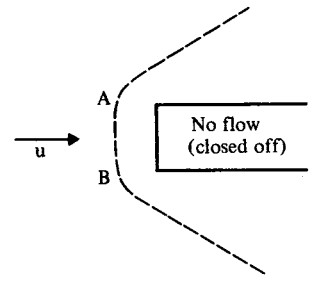

Fig. 4-2

At the point A in Fig. 1 and from A to B in Fig. 2 the shock wave is normal to the axis of the body. At points further from the axis, the wave curves as shown and (if the body of Fig. 1 is a solid of revolution and that of Fig. 2 is a closed off parallel tube—or solid cylinder) becomes an 'oblique shock' which tends to a conical shock front, eventually becoming a conical shock front, when the pressure differential across it becomes very small. The half angle of the cone will then be the 'Mach angle' α_M where $\alpha_M = \text{cosec}^{-1} M$ where M is the Mach number u/u_c. Thus for $M = 2$, i.e. $u = 2u_c$, $\alpha = \sin^{-1} 0.5 = 30°$.

It is not the writer's intention to cover the whole range of shock wave phenomena but only to indicate a method of dealing with them.

Fig. 3 represents part AB of a normal shock which is stationary relative to an observer and across which velocity drops sharply from u to zu (where z is less than unity) and there is an associated rise in static pressure, static temperature and density. The change will be adiabatic but not isentropic. However, total temperature will remain unchanged.

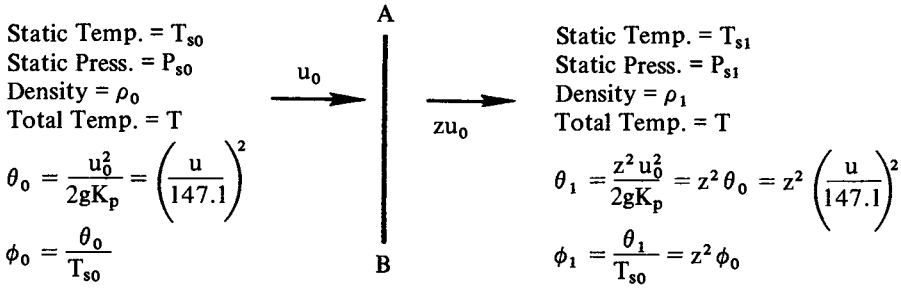

Fig 4-3

The notation used and the more simple relationships are indicated in Fig. 3. (*It should be noted that ϕ is here used as a multiple of T_{s0} and not as a multiple of total temperature T as hitherto*).

The increase of entropy which occurs is best explained by visualising AB as a very thin diaphragm across which high speed molecules can 'escape' from right to left and, by collision, raise the internal energy immediately ahead of AB, and vice versa. Also radiation from the higher temperature fluid to the right can increase the internal energy to the left and vice versa (probably negligible at temperatures of the order of 300°K).

For the solution of this problem, four equations are necessary, namely those for 1) continuity, 2) energy, 3) the gas equation and 4) the momentum equation.

From Continuity: The flux density is unchanged, i.e. $u_0\rho_0 = zu_0\rho_1 \quad \therefore \quad \frac{\rho_1}{\rho_0} = \frac{1}{z}$ (4-1)

From Energy: $T = T_{s0} + \theta_0 = T_{s1} + \theta_1 = T_{s1} + z^2\theta_0$ (4-2)

$$\text{from which } 1 + \phi_0 = \frac{T_{s1}}{T_{s0}} + z^2\phi_0 \text{ or } \frac{T_{s1}}{T_{s0}} = 1 + \phi_0(1 - z^2) \tag{4-3}$$

From the Gas Equation: $\frac{P_{s1}}{P_{s0}} = \frac{\rho_{s1}}{\rho_{s0}} \frac{T_{s1}}{T_{s0}}$ or, by substitution from (1) and (3)

$$\frac{P_{s1}}{P_{s0}} = \frac{1}{z}[1 + \phi_0(1 - z^2)] \tag{4-4}$$

From Momentum: $P_{s1} - P_{s0} = \frac{\psi}{g} u_0(1 - z)$ or, since $\psi = \rho_0 u_0 = \frac{P_{s0} u_0}{RT_{s0}}$

$$P_{s1} - P_{s0} = \frac{P_{s0} u_0^2}{RgT_{s0}}(1 - z) = P_{s0} \frac{2K_p u_0^2}{2gRK_p T_{s0}}(1 - z)$$

$$= P_{s0} \frac{2K_p}{R} \frac{\theta_0}{T_{s0}}(1 - z)$$

or, since $\frac{2K_p}{R} = 7 \left(\text{from } \frac{K_p}{R} = \frac{\gamma}{\gamma - 1} = 3.5\right)$ and $\frac{\theta_0}{T_{s0}} = \phi_0$

$$P_{s1} - P_{s0} = 7P_{s0}\phi_0(1 - z) \quad \text{or} \quad \frac{P_{s1}}{P_{s0}} - 1 = 7\phi_0(1 - z)$$

or

$$\frac{P_{s1}}{P_{s0}} = 1 + 7\phi_0\,(1 - z) \tag{4-5}$$

$\therefore$ from equations (4) and (5), $\frac{1}{z}\,[(1 + \phi_0\,(1 - z^2)] = 1 + 7\phi_0\,(1 - z)$

or

$$1 + \phi_0\,(1 - z^2) = z[1 + 7\phi_0\,(1 - z)] \tag{4-6}$$

Equation (6) reduces to $\phi_0 = \frac{1}{6z - 1}$ (4-6a)

It should be noted that when z = unity $\phi_0 = \frac{1}{5}$, i.e. $\frac{\theta_0}{T_{s0}} = \frac{1}{5}$ which is the condition for $u_0 = u_c$. (Note that if $z > 1.0$, ϕ_0 is less than 1/5, i.e. u_0 is subsonic and no shock wave will exist.)

Alternatively $z = \frac{1}{6}\left(1 + \frac{1}{\phi_0}\right)$ or $\frac{1}{z} = \frac{6\phi_0}{1 + \phi_0}$ (4-6b)

Hence by substitution in equations (1), (3), and (4) or (5) $\frac{\rho_1}{\rho_0}; \frac{T_{s1}}{T_{s0}}$ and $\frac{P_{s1}}{P_{s0}}$ may be found in terms of ϕ_0.

Thus, substituting for z from (6b), equation (1) becomes:

$$\frac{\rho_1}{\rho_0} = \frac{1}{z} = \frac{6\phi_0}{1 + \phi_0} \tag{4-7}$$

Equation (3) becomes:

$$\frac{T_{s1}}{T_{s0}} = 1 + \phi_0\,(1 - z^2) = 1 + \phi_0\left[1 - \frac{1}{36}\left(\frac{\phi_0 + 1}{\phi_0}\right)^2\right]$$

$$\therefore \quad \frac{T_{s1}}{T_{s0}} = 1 + \phi_0 - \frac{(\phi_0 + 1)^2}{36\phi_0} \tag{4-8}$$

Equation (5) becomes:

$$\frac{P_{s1}}{P_{s0}} = 1 + 7\phi_0\,(1 - z) = 1 + 7\phi_0\left[1 - \frac{1}{6}\left(1 + \frac{1}{\phi_0}\right)\right]$$

or

$$\frac{P_{s1}}{P_{s0}} = 1 + 7\phi_0\left(1 - \frac{\phi_0 + 1}{6\phi_0}\right) = 1 + 7\phi_0 - \frac{7}{6}\phi_0 - \frac{7}{6}$$

or

$$\frac{P_{s1}}{P_{s0}} = \frac{1}{6}(35\,\phi_0 - 1) \tag{4-9}$$

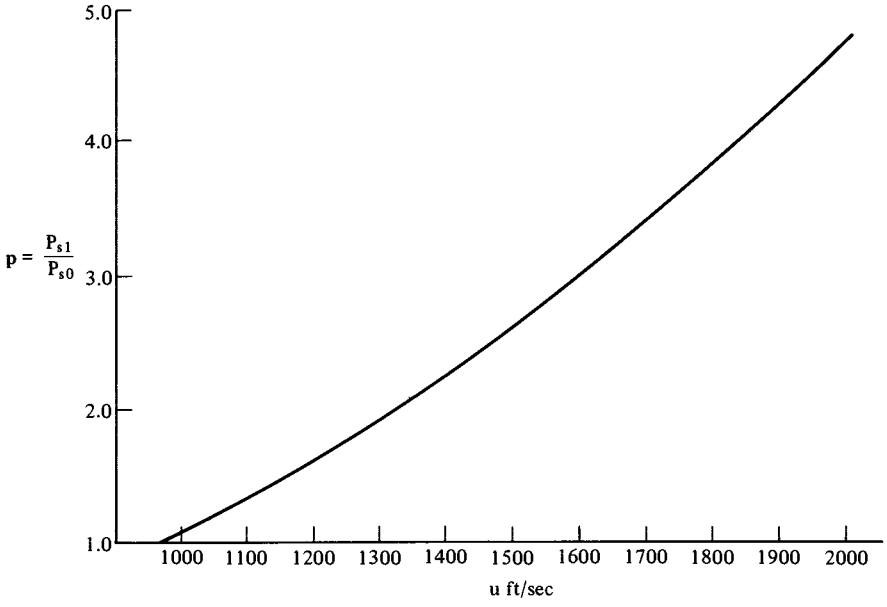

Fig. 4-4

Since $\phi_0 \equiv \frac{\theta_0}{T_{s0}} \equiv \frac{1}{T_{s0}} \left(\frac{u_0}{147.1}\right)^2$, equations (7), (8) and (9) provide a ready connection between density ratio, temperature ratio and pressure ratio and velocity u_0. In fact, since from the Gas Equation, $\frac{P_{s1}}{P_{s0}} = \frac{\rho_{s1}}{\rho_{s0}} \frac{T_{s1}}{T_{s0}}$, any two of the ratios can be used to find the third.

Fig. 4 shows the relationship between the pressure ratio across a normal shock and flight speed u for an air temperature of 220°K. This curve is, of course, readily calculated from equation (9).

Fig. 5 shows curves for pressure, density, and temperature ratios in non-dimensional form over the range $\phi = 0.2$ (Mach 1.0) to 1.0.

Example 4-1

What are the velocity, pressure, temperature and density changes across a normal shock ahead of a bluff body travelling at 2000 ft/sec through air having a static temperature of 220°K (i.e. in the stratosphere)?

$$\text{For } u = 2000, \theta_0 = \left(\frac{2000}{147.1}\right)^2 = 184.9°C \quad \therefore \quad \phi_0 = \frac{184.9}{220} = 0.84$$

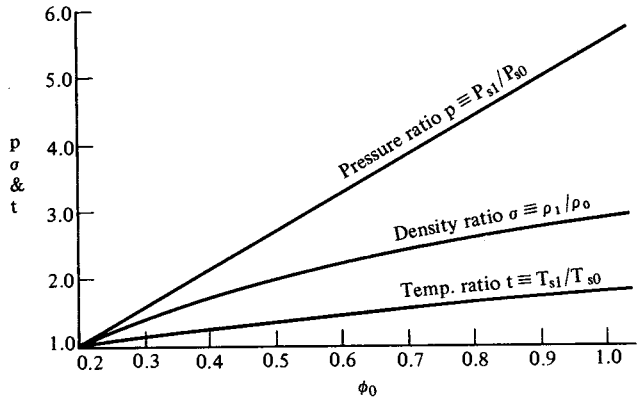

Fig. 4-5

$$\therefore \quad z = \frac{1}{6}\left(1 + \frac{1}{.84}\right) = .365$$

$\therefore$ the velocity after the shock is zu = .365 x 2000 = 730.2 ft/sec.

The total temp. T_T relative to the body is $T_T = 220 + 184.9 = 404.9°K$. T_T is the same before and after the shock. The kinetic temp. after the shock $\theta_1 = \left(\frac{730.2}{147.1}\right)^2 = 24.6°C$. $\therefore$ the static temp. $T_{s2} = T_T - \theta_1 = 404.9 - 24.6 = 380.3$ $\therefore$ the static temp. rise $\Delta T_s = 380.3 - 220 = 160.3°C$ and $\frac{T_{s1}}{T_{s0}} = \frac{380.3}{220} = 1.728.$

From equation (1) $\frac{\rho_1}{\rho_0} = \frac{1}{z} = \frac{1}{.365} = 2.74$

$$\frac{P_{s1}}{P_{s0}} = \frac{\rho_1}{\rho_0}\frac{T_{s1}}{T_{s0}} = 2.74 \times 1.728 = 4.734.$$

Referring to Fig. 5, it is obvious from equation (9) that there is a straight line relationship between p and ϕ_0. Also, as may be seen, there is a near straight line relationship between t and ϕ_0. Even when t is drawn at 10 times the scale the curve is very nearly straight at values of ϕ_0 greater than 0.6.

Example 4-2

If the pressure ratio across a normal shock is 10.0, what is the wave velocity u_0 when $T_{s0} = 220°K$?

This problem is very simply solved by re-arranging equation (9) into the form

$$\phi_0 = \frac{6p + 1}{35} \quad \text{from which} \quad \phi_0 = \frac{61}{35} \equiv 1.7429$$

$\therefore \quad \theta_0 = 1.7429 \times 220 = 383.4°C$ for which $u_0 = 147.1\sqrt{383.4} = 2880$ ft/sec, i.e. nearly three times acoustic speed at 220°K.

In Fig. 6, z is plotted against ϕ_0 over the range 0.2 to 1.0 and brings out very clearly the very large reduction of kinetic energy which can occur across a normal shock wave. Thus, at $\phi_0 = 1.0$, $z = \frac{1}{3}$, i.e. the velocity after the shock is 33.3% of u_0. This corresponds

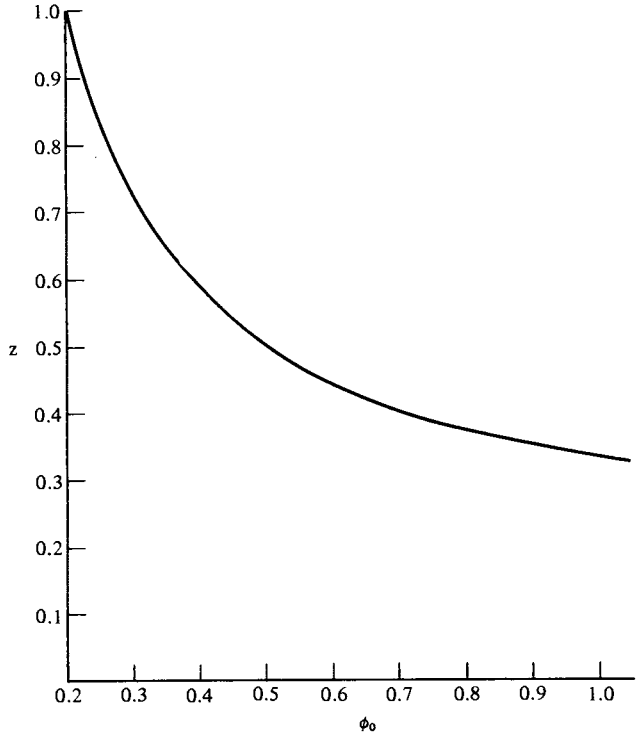

Fig. 4-6

to a reduction of kinetic energy of 89% approximately. This, however, entails a considerable conversion of k.e. into internal energy; i.e. a loss. This matter will be discussed below.

From $z = \frac{1 + \phi_0}{6\phi_0}$ it is evident that the asymptotic limit of z is $\frac{1}{6}$ with the assumption of constant K_p. In practice, at such high values of ϕ_0 one would be dealing with plasmas rather than a 'perfect gas.'

The Efficiency of Shock Compression

The efficiency of engines, gears, etc. is easily defined as $\frac{\text{energy out}}{\text{energy in}}$, but the efficiency of shock-compression is not so easily defined, and there is some inconsistency among engineers in definition. Some talk of 'pressure efficiency,' others of 'adiabatic efficiency' and so on. The difficulty is, perhaps, best illustrated by an example.

Suppose $\phi_0 = 0.8$ and T_0, the static temperature before the shock, is 220°K and P_0, the static pressure before the shock, is 400 psf, then we have the following figures:

From $\phi_0 = 0.8$, $\theta_{u0} = 0.8 \times 220 = 176°C$ which corresponds to $u_0 = 1951.5$ ft/sec.

The total temperature T before and after the shock is $220 + 176 = 396°K$. ∴ the isentropic temp. ratio (total to static) is $\frac{396}{220} = 1.8$ and the corresponding pressure ratio is $1.8^{3.5} = 7.8244$ to give a total pressure of $7.8244 \times 400 = 3129.8$ p.s.f., i.e. a pressure rise of $3129.8 - 400 = 2729.8$ p.s.f., i.e. this would be the pressure rise if there were no losses.

From equation (9), the static to static pressure ratio is $\frac{1}{6}(35 \times 0.8 - 1) = 4.5$ and from equation (7) $z = \frac{1.8}{4.8} = 0.375$ to give $u_1 = 0.375 \times 1951.5 = 731.8$ ft/sec which is equivalent to 24.75°C, i.e. the static temp. after the shock is the total temp. less 24.75°, namely $396 - 24.75 = 371.25$. Thus if the 731.8 ft/sec after the shock is brought to rest isentropically, the temp. ratio would be $\frac{396}{371.25} = 1.0667$. The corresponding pressure ratio would be $1.0667^{3.5} = 1.2534$ to give an overall total to static pressure ratio of $1.2534 \times 4.5 = 5.64$ and a total pressure of $5.64 \times 400 = 2256.2$ p.s.f., i.e. a pressure rise of $2256.2 - 400 = 1856.2$ p.s.f. compared with the isentropic rise of 2729.8 p.s.f. Thus the pressure efficiency η_p is given by

$$\eta_p = \frac{1856.2}{2729.8} = 0.68 \quad \text{or} \quad 68\%.$$

In compressors 'adiabatic efficiency' is defined as $\frac{\theta_c'}{\theta_c}$ where θ_c' is the isentropic temperature rise corresponding to the total to static pressure ratio and θ_c is the actual

temperature rise static to total. This definition is imperfect in that a proportion of the losses (converted into internal energy) are recoverable on re-expansion. Alternatively, in a thermal cycle, the heat which must be added to achieve a given maximum cycle temperature is reduced by the amount of internal energy resulting from losses. Nevertheless, 'adiabatic efficiency' is a very convenient definition for cycle calculations.

Since shock compression is of greatest interest from the point of view of supersonic aircraft intakes where it contributes substantially to the overall compression, it seems desirable to use adiabatic efficiency for shock compression. Thus, in the above example the actual pressure ratio was found to be 5.64. The corresponding isentropic temperature ratio t′ is $5.64^{0.2857} = 1.639$. $\therefore\ \theta' = 1.639 \times 220 - 220 = 140.63°C$. The actual temperature rise θ was found to be 176°C. $\therefore$ the adiabatic efficiency η_c is

$$\eta_c = \frac{140.63}{176} = 0.799 \text{ or } 79.9\%,$$ i.e. a much higher figure than pressure efficiency.

The conversion of kinetic energy into internal energy on passage through the shock is clearly $176 - 140.63 = 35.87°C$ which is 20% of the initial kinetic energy.

Example 4-3

If $T_0 = 220°K$ and $\phi_0 = 0.4$ what is η_c if there are no further losses after a normal shock wave?

$\theta_{u0} = .4 \times 220 = 88°C$. This is the actual temperature rise static to total. From equation (9), the static to static pressure ratio is $\frac{1}{6}(35 \times 0.4 - 1) = 2.1667$. The initial velocity $u_0 = 147.1\sqrt{88} = 1{,}379.9$ ft/sec.

From equation (7), $z = \frac{1.4}{2.4} = 0.5833$ $\therefore$ the velocity $zu_0 = .5833 \times 1379.9 = 804.9$ ft/sec the temperature equivalent of which is 29.94°C $\therefore$ the isentropic temperature ratio involved in reducing zu_0 to zero is $\frac{220 + 88}{220 + 88 - 29.94} = 1.1077$ for which the corresponding pressure ratio is $1.1071^{3.5} = 1.4304$ to give a total pressure ratio of $1.4304 \times 2.1667 = 3.0993$. The corresponding value of t′ is $3.0938^{0.2857} = 1.3815$ to give a θ'_c of $.3815 \times 220 = 83.93°C$.

$$\therefore\ \eta_c = \frac{83.93}{88} = 0.954 \quad \text{or} \quad 95.4\%.$$

It may thus be seen that the greater the 'strength' of a shock wave the lower the adiabatic efficiency. In fact if ϕ_0 is only a little above its lowest limit of 0.2 the adiabatic efficiency is virtually 100%.

It should be noted that, since $\phi_0 = \frac{1}{5}$ corresponds to the acoustic speed, ϕ_0 cannot be less than 0.2 for a shock wave to exist. It follows from equation (6a) that z cannot be greater than unity (corresponding to $\phi_0 = 0.2$) therefore a rarefaction shock wave cannot exist. (This point is usually made by invoking the second law of thermodynamics. It can

also be made by pointing out that if, in Fig. 3, the arrows were reversed, though the continuity, energy, gas and momentum equations would still be satisfied, there would be a decrease in entropy which is impossible in an adiabatic process–a statement which amounts to "invoking the second law . . . .")

Summary

$z \equiv \frac{u_1}{u_0}$; $\theta_{u0} \equiv \frac{u_0^2}{2gK_p}$; $\phi_0 \equiv \frac{\theta_{u0}}{T_{s0}}$; P_{s0}, ρ_0 and T_{s0} are the static pressure, density and temperature ahead of the shock wave. P_{s1}, ρ_1 and T_{s1} are the static pressure, density and temperature after the shock wave. T is the total temperature.

$$T = T_{s0} + \theta_{u0} = T_{s1} + \theta_{u1}$$

$$\sigma \equiv \rho_1/\rho_0 = 1/z \text{ or, eliminating z, } \sigma = \frac{6\phi_0}{1+\phi_0}$$

$$t \equiv T_{s1}/T_{s0} = 1 + \phi_0\,(1 - z^2) \text{ or, eliminating z, } t = 1 + \phi_0 - \frac{(\phi_0+1)^2}{36\phi_0}$$

$$p \equiv P_{s1}/P_{s0} = 1 + 7\phi_0\,(1 - z) \text{ or, eliminating z, } p = \frac{1}{6}(35\phi_0 - 1)$$

$$\phi_0 = \frac{1}{6z-1} \text{ or } z = \frac{1+\phi_0}{6\phi_0} \text{ or, eliminating z, } \phi_0 = \frac{6p+1}{35}$$

Part 2. Oblique Shock Waves

Introductory

The discussion herein is limited to two dimensional cases.

The key to the theory of oblique shock waves is that an oblique shock is a normal shock travelling in a direction perpendicular to the oblique shock.

Discussion

Fig. 7 illustrates a sharp wedge of angle β with its upper surface parallel to the direction of u_0 and generating an oblique shock AB, the angle between AB and the under surface being α.

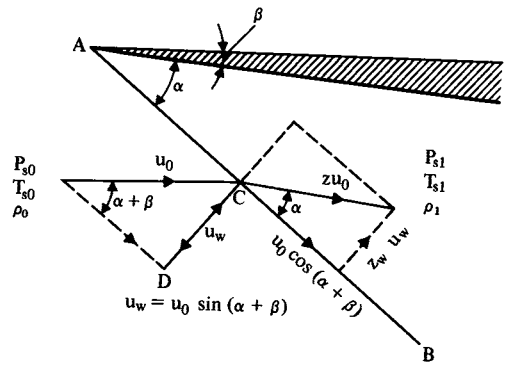

Fig 4-7

Treating AB as a normal shock travelling in the direction CD with velocity u_w one may see that $u_w = u_0 \text{ Sin } (\alpha + \beta)$ (4-10)

and that $\dfrac{z_w u_w}{u_0 \cos(\alpha + \beta)} = \tan \alpha$ (4-11)

From equation (6b) one may also see that $z_w = \dfrac{1}{6}\left(1 + \dfrac{1}{\phi_w}\right)$

or

$$z_w = \frac{\phi_w + 1}{6\phi_w} \tag{4-12}$$

By using these three equations the relationship between ϕ_0, α and β may be found as follows:

From (10), $\left(\dfrac{u_w}{u_0}\right)^2 = \dfrac{\phi_w}{\phi_0} = \text{Sin}^2(\alpha + \beta) \therefore \phi_w = \phi_0 \text{ Sin}^2(\alpha + \beta)$ (4-13)

From (10) and (11), $z_w \tan(\alpha + \beta) = \tan \alpha$,

i.e. $z_w = \dfrac{\tan \alpha}{\tan(\alpha + \beta)}$ (4-14)

From (12) and (14), $\dfrac{\phi_w + 1}{6\phi_w} = \dfrac{\tan \alpha}{\tan(\alpha + \beta)}$

or

$6\phi_w \tan \alpha = \phi_w \tan(\alpha + \beta) + \tan(\alpha + \beta)$

from which $\phi_w (6 \tan \alpha - \tan(\alpha + \beta)) = \tan(\alpha + \beta)$

or

$$\phi_w = \frac{\tan(\alpha+\beta)}{6\tan\alpha - \tan(\alpha+\beta)} \tag{4-15}$$

(Note that if $\beta = 0$ $\phi_w = 0.2$, the condition for the acoustic speed.)

Hence, using (13),

$$\phi_0 \sin^2(\alpha+\beta) = \frac{\tan(\alpha+\beta)}{6\tan\alpha - \tan(\alpha+\beta)} \tag{4-16}$$

Given α and β, ϕ_0 is readily found though some 'juggling' is still necessary to find α if ϕ_0 and β are given. (The writer finds that, for small values of β, then if an initial guess at α is a little larger than the Mach angle $\sin^{-1}\frac{u_c}{u_0}$ then two other trials are sufficient to find the value of α which satisfies (16).)

Equation (16) can, of course, be manipulated into many forms but it seems very doubtful that any of them show any advantage over (16).

For the density, temperature, and pressure ratios across an oblique shock it remains to adapt equations (7), (8), (9), etc., by substituting ϕ_w for ϕ_0.

One could substitute further for ϕ_w from (15). This will clearly lead to some distinctly clumsy equations of doubtful value and so will not be attempted herein. One would clearly prefer to determine ϕ_w from (15) and use it in equations (7), (8), (9), etc., instead of ϕ_0.

For ease of reference the oblique shock wave relationships are given below.

$$T = T_{s0} + \theta_{u0} = T_{s1} + \theta_{u1} \tag{4-17}$$

$$z_w = \frac{1+\phi_w}{6\phi_w} \tag{4-18}$$

From Fig. 7 $z = \frac{\cos(\alpha+\beta)}{\cos\alpha}$ (4-19)

$$\sigma \equiv \rho_1/\rho_0 = \frac{1}{z_w} = \frac{6\phi_w}{1+\phi_w} \tag{4-20}$$

$$t \equiv T_{s1}/T_{s0} = 1 + \phi_w(1 - z_w^2) = 1 + \phi_w - \frac{(\phi_w+1)^2}{36\phi_w} \tag{4-21}$$

$$p \equiv \frac{P_{s1}}{P_{s0}} = 1 + 7\phi_w(1 - z_w) = \frac{1}{6}(35\phi_w - 1) \tag{4-22}$$

Example 4-4

If $\beta = 5°$ what must u_0 be to give $\alpha = 30°$ assuming $T_{s0} = 220°K$?

From (16) $\phi_0 \sin^2 35 = \dfrac{\tan 35}{6 \tan 30 - \tan 35}$

$\sin 35 = .5736 \quad \tan 30 = .5774 \quad \text{and} \quad \tan 35 = .7002$

$\therefore \ \phi_0 (.5736)^2 = \dfrac{.7002}{6 \times .5774 - .7002} = .2533$

$\therefore \ \phi_0 = \dfrac{.2533}{.5736^2} = 0.77$

$\therefore \ \theta_{u0} = .77 \times 220 = 169.4°C \qquad \therefore \ u_0 = 147.1\sqrt{169.4} = 1914.5 \text{ ft/sec.}$

Example 4-5

Using the values of α, β and T_{s0} of Example 4 what are the values of σ, t and p?

From equation (15) $\phi_w = \dfrac{.7002}{6 \times .5774 - .7002} = .2533$

From equation (22) $p = \dfrac{1}{6}(35 \times .2533 - 1) = 1.3109$

From equation (20) $\sigma = \dfrac{6 \times .2533}{1.2533} = 1.2126$

$t = \dfrac{p}{\sigma} = \dfrac{1.3109}{1.2126} = 1.081$

Example 4-6

Using the data of Examples 4 and 5 what is the velocity reduction through the shock wave?

From equation (19) $z = \dfrac{\cos 35}{\cos 30} = \dfrac{.8192}{.866} = .9459 \ \therefore$, since in Example 4, u_0 was found to be 1914.5 ft/sec $u_1 = .9459 \times 1914.5 = 1810.9$ ft/sec, i.e. a reduction of 103.6 ft/sec.

Example 4-7

Using the figures of the foregoing examples what is the loss (i.e. conversion to internal energy) as a percentage of the kinetic energy reduction?

In Example 5 the pressure ratio (static to static) was found to be 1.3109 for which the corresponding isentropic temperature ratio is $1.3109^{0.2857} = 1.0804$ to give an isentropic temperature increase of $0.0804 \times 220 = 17.69°C$. The actual temperature ratio was found to be 1.081, to give an actual temperature increase of $0.081 \times 220 = 17.82°C$. $\therefore$ the conversion of part of the kinetic energy to internal energy is only $17.82 - 17.69 = 0.13°C$.

The velocity reduction was found to be from 1914.5 ft/sec ($\theta_{u0} = 169.4°C$) to 1810.9 ft/sec ($\theta_{u1} = 151.55°C$), i.e. the temperature equivalent of the kinetic energy reduction is $169.4 - 151.55 = 17.85°C$. Thus, the proportion of conversion to internal energy is $\frac{0.13}{17.85} = .0073$ or 0.73%. So, in the very unlikely event that subsequent conversion would entail negligible loss, the adiabatic efficiency of the shock compression is over 99%. This points to the obvious conclusion that a succession of weak oblique shocks can give high compression efficiency. Indeed, as will be demonstrated below, it should be possible to approximate very closely to isentropic compression at least until the velocity is reduced to the acoustic velocity corresponding to $\frac{T°}{6}$ C. (T being total temperature.)

Fig. 8 illustrates a sequence of oblique shocks from a two-dimensional surface ABCDEF for a speed u = 2000 ft/sec. with a static temperature of 220°K at station 0.

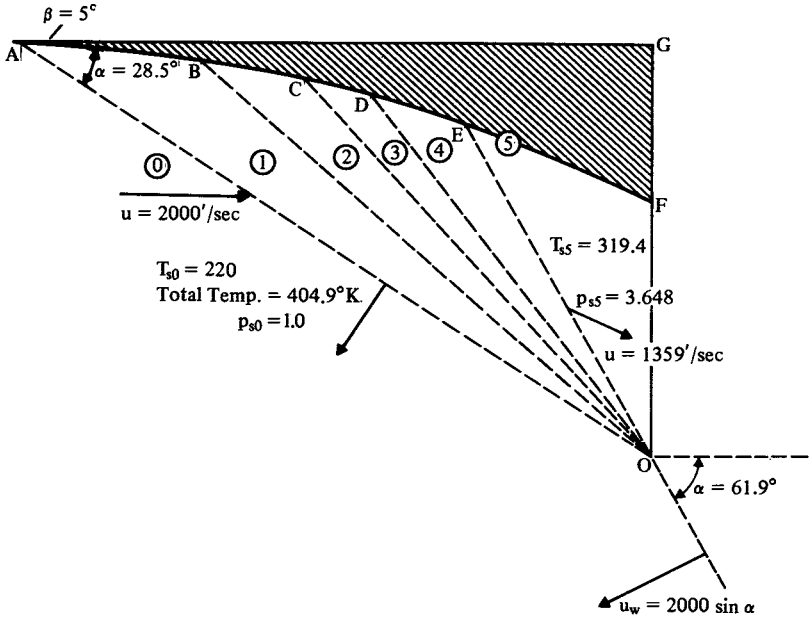

Fig. 4-8

(Total temperature = $220 + \left(\frac{2000}{147.1}\right)^2 = 404.9°K.$) The initial wedge angle at A is 5° and there are 5° increments at BCD & E. Between E and F increments of slope are not specified but would need to be very much less than 5° for the shocks to pass through 0.

It is no coincidence that all waves focus at 0. The distances AB, BC, etc., were chosen to achieve this and avoid the complexities of wave junctions at other points.

If there were no bounding surface, all waves coalescing at O would combine into a single shock as shown.

The pressure, temperature ratios across shocks OA, OB, etc., are readily calculated by the methods indicated above. The overall pressure ratio and static temp. after OE are indicated in Fig. 8. The efficiency of compression from A to E is found to be very high. The isentropic temperature ratio corresponding to $P_{s5} = 3.648$ is $3.648^{0.2857} = 1.4474$ to give an isentropic temperature increase of $0.4474 \times 220 = 98.42°C$. The actual temperature rise is $319.4 - 220 = 99.4$ $\therefore$ the loss to internal energy is 0.98°C. The kinetic energy conversion is $\left(\frac{2000}{147.1}\right)^2 - \left(\frac{1359}{147.1}\right)^2 = 184.86 - 85.35 = 99.51$ so that the loss to internal energy is less than 1.0%. The efficiency across the combined shock beyond O, however, would be distinctly lower.

Fig. 8 represents an idealised case in that it takes no account of the inevitable boundary layer which viscosity would cause along the surface AF and which would be subjected to a substantial adverse pressure jump at each 'kink'. This boundary layer would be very thin and, though it would mean a small change in the effective profile of AF, the tendency to reverse flow at the surface, i.e. 'breakaway,' would be countered by the high velocities in the outer layers of the boundary layer. Nevertheless AF should really represent the 'surface' of the boundary layer film.

It will be obvious from Fig. 8 that AF could be a smooth curve. If such were the case one may visualise an infinite number of oblique shocks each of infinitesimally small strength except at A (and even at A if the curve had zero slope at A). In reality there would be smooth rise of pressure downstream of AO and the 'rays' BO, CO, etc., would be lines of equal pressure, i.e. isobars, of equal temperature, equal density and equal velocity. It seems appropriate that they be called 'isostats' (there being no probability of confusion with its geological use in 'isostatic', 'isostasy', etc.) implying lines of equal state since every property of the fluid, including entropy and enthalpy will be uniform along them. It follows that $\frac{dP_s}{P_s} \propto \frac{dT_s}{T_s} \propto \frac{d\rho}{\rho}$ etc., from which it further follows that beyond AO, the compression is isentropic, at least until u falls to the local value of u_c ($\equiv u_{cF}$).

The geometry of the situation is represented in Fig. 9.

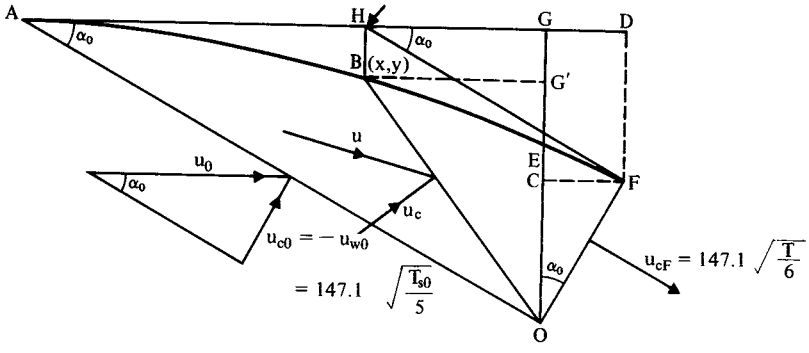

T_{s0}

$$T = T_{s0} + \left(\frac{u_c}{147.1}\right)^2$$

ρ_0

$$\sin \alpha_0 = \frac{u_{c0}}{u_0}$$

$$AG = x_0$$

$$GO = y_0$$

$$AO = r_0 = \frac{x_0}{\cos \alpha_0}$$

$$OF = r_F = \left(\frac{T_{s0}}{T_{sF}}\right)^3 r_0$$

$$GD = CF = r_F \sin \alpha_0$$

$$OB = r$$

At OF, $T_{SF} = \frac{5}{6} T$ and $\rho_F = \left(\frac{T_{sF}}{T_{s0}}\right)^{2.5}$

Fig. 4-9

Neglecting the boundary layer, AF may be described as an 'isentropic surface.'

Taking A as the origin of co-ordinates, HB ≡ y and AH ≡ x, so the isostat OB of length r ends on the isostatic surface at xy. So, to locate B, one must either find x and y, or, using polar co-ordinates, the length r and the angle BOA.

Since the compression beyond AO is assumed isentropic the relationships of isentropic compression apply, i.e. $\rho/\rho_0 = \left(\frac{T_s}{T_{s0}}\right)^{2.5}$; $\frac{P_s}{P_{s0}} = \left(\frac{T_s}{T_{s0}}\right)^{3.5}$ etc.

The scale of the diagram is one of choice. x_0, for example, may be set at ten units of length.

Assuming that $\beta_0 = 0$ then α_0 is the Mach angle for u_0, i.e. $\sin^{-1} \frac{u_{c0}}{u_0}$

where $\frac{u_{c0}}{u_0} = \sqrt{\frac{\theta_{c0}}{\theta_{u0}}} = \sqrt{\frac{T_{s0}}{5\theta_{u0}}} = \sqrt{\frac{1}{5\phi_0}}$ from which r_0, the point O and y_0 are readily determined. Evidently these are dependent on ϕ_0 which means that the isentropic surface varies with ϕ_0.

One may see that $x_0 = r_0 \cos \alpha_0$ and $y_0 = r_0 \sin \alpha_0$. These determine the general frame of the diagram.

Information can be obtained from the requirements of continuity. Thus the flow through each isostat is the same as that flowing through AO, namely $\rho_0 u_0 y_0$ or $\rho_0 u_{c0} r_0$. It follows that for any isostat of length r

$$\rho_0 u_{c0} r_0 = \rho u_c r \tag{4-23}$$

Using the fact that the total temperature T is constant and given by $T = T_{s0} + \theta_{c0}$, one may see that the static temperature T_s along an isostat such as OB may be obtained from $\theta_u = T_{s0} + \theta_{u0} - T_s$ where θ_u is the temperature of the (uniform) velocity u across OB. (Note that the direction of u is parallel to the tangent at B.)

Equation (23) may be manipulated as follows:

$$\frac{r}{r_0} = \frac{\rho_0}{\rho} \frac{u_{c0}}{u_c} = \left(\frac{T_{s0}}{T_s}\right)^{2.5} \sqrt{\frac{\theta_{c0}}{\theta_c}} = \left(\frac{T_{s0}}{T_s}\right)^{2.5} \sqrt{\frac{T_{s0}}{5} \times \frac{5}{T_s}} = \left(\frac{T_{s0}}{T_s}\right)^{3} \tag{4-24}$$

(Remembering that the temperature equivalent of the critical velocity is $0.2 \times T_s$.)

Hence, for given values of r_0 and T_{s0} there is a very simple relationship between r and T_s. For any selected value of T_s the length r is readily determined but, unfortunately, not its direction except for OE and OF.

For some time the writer supposed that Fig. 9 contained enough information to find the shape of the isostatic surface but, after many fruitless hours, was forced to the conclusion that it is indeterminate. It must, however, satisfy the following conditions:

1) If $\beta = 0$ then AG is the tangent at A.
2) The slope must continually increase from A to F.
3) The tangent at F must be parallel to AO.
4) The length r_F of OF must be consistent with (24).

For the last, T_{SF}, the static temperature at OF, is determined by the fact that the critical velocity u_{cF} across OF coincides with the actual velocity

$$\therefore \theta_{ucF} = \frac{T}{6}, \text{ hence } T_{sF} = T_0 + \theta_{uc} - \frac{T}{6} \text{ or } T_{sF} = \frac{5}{6} T$$

Example 4-8

What is the length of OF given that x_0 is 100 units of length, $T_{s0} = 220°K$ and $u_0 = 1600$ ft/sec?

The temperature equivalent of 1600 ft/sec is $\left(\frac{1600}{147.1}\right)^2 = 118.3°C$

$\therefore$ the total temperature $T = 220 + 118.3 = 338.3°K$

$$\text{Sin } \alpha_0 = \frac{u_{c0}}{u_0} \text{ and } \theta_{uc0} = \frac{T_{s0}}{5} = 44°C \therefore u_{c0} = 147.1\sqrt{44} = 975.8 \text{ ft/sec}$$

$$\therefore \text{Sin } \alpha_0 = \frac{975.8}{1600} = 0.6098 \text{ and Cos } \alpha_0 = 0.7925$$

$$\text{Since } \frac{\alpha_0}{r_0} = \text{Cos } \alpha_0, r_0 = \frac{x_0}{\text{Cos } \alpha_0} = \frac{100}{0.7925} = 126.18 \text{ units}$$

$$\text{At OF, } T_{sF} = \frac{5}{6}T = \frac{5}{6} \times 338.8 = 281.7°K$$

$$\therefore \text{ from (24) (using } r_F \equiv \text{OF}) \frac{r_F}{T_0} = \left(\frac{T_{s0}}{T_{sF}}\right)^3 = \left(\frac{220}{281.7}\right)^3 = 0.4765$$

$$\therefore r_F = 0.4765\, r_0 = 0.4765 \times 126.18 = 60.12 \text{ units of length.}$$

To make the isentropic surface determinate it is necessary to specify a relationship between two of the several variables. For example one might decide that T_s should rise in proportion to x. More simply it might be specified that $\frac{dy}{dx} = kx$. This, of course, defines the parabola $y = \frac{k}{2}x^2$. AF thus becomes a segment of a parabola where $\frac{dy}{dx}$ at F is Tan α_0. At F, $x = x_0 + r_F \text{ Sin } \alpha_0$

$$\therefore \text{ at F, } \frac{dy}{dx} \equiv \text{Tan } \alpha_0 = k(x_0 + r_F \text{ Sin } \alpha_0), \text{ which gives the value of k, namely}$$

$$k = \frac{\text{Tan } \alpha_0}{x_0 + r_F \text{ Sin } \alpha_0}$$

Example 4-9

Using figures from the preceding example and assuming that AF is a segment of the parabola $y = \frac{1}{2}\left(\frac{\text{Tan } \alpha_0}{x_0 + r_F \text{ Sin } \alpha_0}\right)x^2$, what are the values at B of r; T_s; u; u_c; ρ/ρ_0 and P/P_0 if, in Fig. 9, the value of x at B is 60 units of length?

$$\text{Tan } \alpha_0 = \frac{\text{Sin } \alpha_0}{\text{Cos } \alpha_0} = \frac{0.6098}{0.7925} = 0.7695 \quad \therefore \text{ at B,}$$

$y = \frac{3600}{2}\left(\frac{.7695}{100 + 60.12 \times 0.6098}\right)$ from which $y = 10.13$. Now $y_0 = \sqrt{r_0^2 - x_0^2} = 76.95$
$\therefore$ the length of $OG' = 76.95 - 10.13 = 66.82$ units and $BG' = 40$ units $\therefore$ the length of OB is given by $r = \sqrt{66.82^2 + 1600} = 77.88$ units.

Having found r, then, from (24) T_s is obtained from $\frac{r}{r_0} = \left(\frac{220}{T_s}\right)^3$

$$\therefore \quad \sqrt[3]{\frac{77.88}{126.18}} = \frac{220}{T_s} = .8514, \text{ from which } T_s = 258.4^\circ K$$

All the other required quantities readily follow.

From $\theta_u = T - T_s = 338.3 - 258.4 = 79.91^\circ C$, $u = 147.1\sqrt{79.91} = 1315$ ft/sec.

From $\theta_{uc} = \frac{T_s}{5}$, $u_c = 147.1\sqrt{\frac{258.4}{5}} = 1057.5$ ft%sec

From $\frac{\rho}{\rho_0} = \left(\frac{T_s}{T_{s0}}\right)^{2.5}$, $\frac{\rho}{\rho_0}\left(\frac{258.4}{220}\right)^{2.5} = 1.4951$

From $\frac{P}{P_0} = \frac{\rho T_s}{\rho_0 T_{s0}}$, $\frac{P}{P_0} = 1.4951 \times \frac{258.4}{220} = 1.7561$

Check

If the above figures are correct then, from continuity

$$u_{c0}\, r_0 = \frac{\rho}{\rho_0}\, u_c\, r$$

For the left hand side, $975.8 \times 126.18 = 123.126$.
For the right hand side, $1.4951 \times 1057.5 \times 77.88 = 123.134$. This is an exceptionally close agreement in view of the numbers of significant figures used in the calculations.

We have thus verified that between A and F the equation for the isentropic surface is $y = \frac{x^2}{2}\left(\frac{\tan \alpha_0}{x_0 + r_F \sin \alpha_0}\right)$. This of course is only one of several possible surfaces, but r_F, T_{sF} and α_0 would be the same for all for the same values of x_0, T_{s0}, and u_0.

In practice a value of $\beta = 0$ at A would be impracticable so for $\beta > 0$ AO would in

fact be a weak oblique shock entailing a very modest loss. Nevertheless, even allowing for boundary layer loss, the adiabatic efficiency as far as the throat OF should be over 98%.

In the case on which Fig. 9 was based ($u_0 = 2000$ ft/sec and $T_{s0} = 220°K$), $u_{cF} = 1208.3$ ft/sec which represents 36.5% of the initial kinetic energy. Further reduction of velocity beyond OF would require an increase of section, i.e. a subsonic diffuser in which, without special devices, one might expect a further loss of the order of 10% of the residual kinetic energy at OF.

It should be noted that if β_0 is greater than 0°, then the relevant values of u_0, T_{s0}, etc., for calculating the isentropic surface are those immediately *after* the oblique shock, and that the initial isostat is some distance from the nose of the wedge at the under surface. If A′ denotes the leading edge and A denotes the initial point of the first isostat then A′A is straight conforming to the wedge angle β. Also if the oblique shock and the initial isostat are to meet at O then the length of A′A is given by

$\text{Cos A'OA} = \dfrac{r_s^2 + r_0^2 - (A'A)^2}{2r_s r_0}$ where r_s is the length of the oblique shock. The isentropic surface begins at A where $\dfrac{dy}{dx} = \tan \beta_0$.

The question arises, does the isentropic surface have any practical use? From the point of view of an intake for a supersonic aircraft engine, the direction of u_{cF} is undesirable. However, this might be dealt with by accepting a 'reflected' oblique shock from O, of such strength as to change the direction of flow as desired and accept the comparatively small loss which would result (because the velocity through it would not be all that much above u_{cF}). Again, a 'cascade' of curves similar to AF might have some useful function as, for example, in a supersonic compressor.

A more interesting case is that of successive reflections as shown in Fig. 10 where from A to E the slope is constant at 5° and BH is parallel to AO.

The effect of the initial shock AB is to deflect the flow (as shown in broken lines) parallel to AC. The reflected shock BC must be such that the flow between BC and CD is parallel to BD. The second reflection CD must be such that the flow becomes parallel to CE. The reflection DE must once more cause the flow to be parallel to BDF.

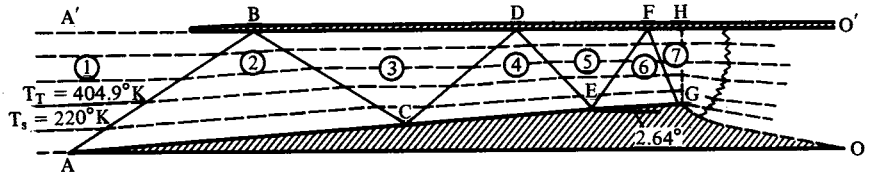

Fig. 4-10

At E and F the calculation becomes 'delicate'. Referring to (16) it is found that a curve for $\phi \sin^2(\alpha + \beta)$ does not intercept a curve for $\frac{\tan(\alpha + \beta)}{6 \tan \alpha - \tan(\alpha + \beta)}$ if the slope EG is maintained at 5°. It was found necessary to reduce it to 2.64° to obtain the reflection EF to give the final reflection FG. The figures for station 7 in Fig. 10 are therefore somewhat uncertain.

Station	1	2	3	4	5	6	7
ϕ	0.840	0.699	0.575	0.465	0.365	0.268	0.201
$\alpha°$	33.4	36.9	41.15	46.9	55.9	69.4	$90_{\text{approx.}}$
$\alpha - \beta°$	28.4	31.9	36.15	41.9	50.9	66.76	$0_{\text{approx.}}$
T_s°K	220.0	238.2	257.1	276.4	296.6	319.3	$337_{\text{approx.}}$
θ_u°C	184.9	166.5	147.7	128.5	108.3	85.6	67.9
u′/sec.	2000	1898	1788	1667	1531	1360.7	1212
p/stage	←1.3273→	←1.3012→	←1.2858→	←1.2781→	←1.2922→	←1.2058→	
σ/stage	←1.2241→	←1.2062→	←1.9662→	←1.1910→	←1.2003→	←1.1425→	
t/stage	←1.0843→	←1.0788→	←1.0749→	←1.0731→	←1.0756→	←1.0554→	
p	1.000	1.3273	1.7272	2.2209	2.8385	3.6680	4.4228

p ≡ cumulative static pressure ratio

At HG the velocity is the local acoustic velocity and so if a further velocity reduction is desired the channel must diverge to become a subsonic diffuser. But, as pointed out in Section 5, when a divergence follows a choking throat, over-expansion with acceleration occurs followed by sudden recompression through a normal shock. The lower the value of ϕ ahead of this shock the lower the loss through it, so it seems desirable to 'induce' it as near to the beginning of the divergence as possible by making the initial divergence much larger than that after the recompression shock—as indicated in Fig. 10 between G and O. The efficiency of compression from AA′ to HG is remarkably high—over 99%—for an energy conversion of about 63%. So, with a small wedge angle, there would be no great error in assuming isentropic compression from AA′ to HG.

Obviously the pattern of shocks shown in Fig. 10 is particular to the initial value of ϕ, i.e. to u and T_s at station 1. Moreover, if Fig. 10 represents the engine intake of a supersonic aircraft, it would be very sensitive to any change of direction of u at station 1, i.e. to yaw.

Further, some very careful design would be necessary if reflection DE is to coincide exactly with the sudden reduction of slope at E. This difficulty might be alleviated by avoiding such a sudden change of slope.

If diffusion between G′ and OO′ were reasonably efficient the velocity at OO′ would be about 500 ft/sec. which is a 'comfortable' figure for the velocity ahead of an engine compressor intake. It is emphasised, however, that Fig. 10 is a two dimensional diagram while a compressor entry is annular.

If the line A′O′ in Fig. 10 were regarded as a mirror, the solid boundary removed, and the system below it inverted above A′O as a mirror image then one would have a diagram of what happens at oblique shock wave interceptions.

Though, as we have seen, a rarefaction shock wave is impossible, the information that the pressure along a surface is dropping must be transmitted at sonic speed. Here again, the concept of a system of rays or isostats is useful. These, however, must diverge because as the pressure drops the velocity increases and the static temperature drops. The latter means a reduction of the acoustic velocity u_c, therefore as u increases and u_c decreases the Mach angle $\sin^{-1} \frac{u_c}{u}$ decreases.

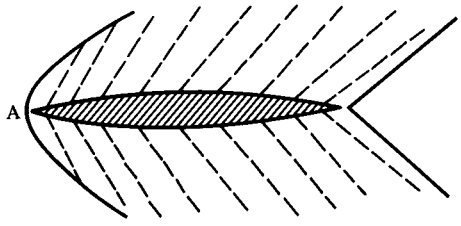

Fig. 4-11

A guess at what happens in the case of a two dimensional body is shown in Fig. 11. Being wholly convex there can be no shock waves along its length. A single nose shock would exist which would be normal at A and the point of highest pressure would be at the nose. Thereafter the pressure drops from nose to tail. There would be a tail shock of recompression to the initial ambient pressure before A.

At this point it should be emphasised that though a convex surface cannot generate a rarefaction shock, it *can* reflect a compression shock (as at the point E in Fig. 10) weakening it in the process.

The rarefaction isostats will intercept the front and rear shocks and progressively reduce their strength and therefore their angle relative to the axis of the body. Also, owing to losses across the front shock, at a sufficient distance from the body the velocity ahead of the rear shock will be less than that ahead of the front shock. It would seem, therefore, that the nose and tail shocks must eventually merge into a single oblique shock. This is contrary to the general belief that the 'double boom' often heard from supersonic aircraft is due to separate nose and tail shocks. In the opinion of the writer the second boom is more likely to be a ground reflection of the first. If this belief is correct then the time interval between the booms would depend on the observer's height from the ground, the slope of the latter, etc.

SECTION 5
Isentropic Flow Through Nozzles

The discussion of flux density in Section 2 clears the way for a brief discussion of flow through convergent and convergent-divergent nozzles neglecting losses due to wall friction (for the time being).

For simplicity, only the formulae applicable to air acting as a perfect fluid will be used.

It will be obvious that the flow dQ through a small section δS is given by $dQ = \psi \delta S$, and that if the flow is uniform across a section S, then $Q = \psi S$. Further, that the maximum value of Q cannot exceed $\psi_c S_c$ where S_c is the minimum section, and will, in fact, be less than this if the flow at S_c is non-uniform due to curvature.

Fig. 1a represents a convergent nozzle of exit area S discharging isentropically into a region, e.g. the atmosphere, where the ambient pressure is P_0, from a reservoir where total temp. and total pressure are T_T and P_T (assumed maintained constant by continuous replacement).

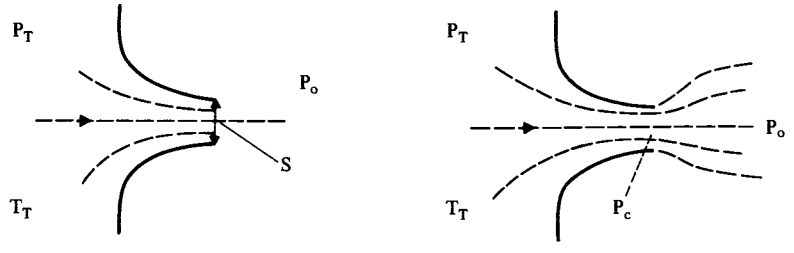

Fig. 5-1

If it be assumed that the effect of flow curvature at nozzle exit is negligible, i.e. that pressure and velocity is uniform across S, then, if the pressure ratio is less than the critical, i.e. that $\frac{P_T}{P_0} < 1.893$, one may assume that the pressure at S is P_0 and that $t = p^{\frac{\gamma-1}{\gamma}} = \left(\frac{P_T}{P_0}\right)^{\frac{1}{3.5}}$, i.e. $t < 1.2$. The flux density at exit from equation (2-9) is given by $\psi = 1.532 \frac{P_T}{\sqrt{T_T}} \frac{\sqrt{t-1}}{t^3}$, so the discharge flow is $Q = 1.532\ S \frac{P_T}{\sqrt{T_T}} \frac{\sqrt{t-1}}{t^3}$ lb/sec.

Example 5-1

Air is discharged through a convergent nozzle of exit area of 0.5 ft^2 from a reservoir, where $P_T = 3000$ p.s.f. and $T_T = 800°K$, to atmosphere where ambient pressure $P_0 = 2116$ p.s.f. What are the values at exit of a) ψ_e; b) $\frac{\psi_e}{\psi_c}$; c) u_c; d) $\frac{u_e}{u_c}$; e) T_e; f) ρ_e; and g) Q?
h) What should be the value of P_T for max. possible Q assuming the same T_T and that pressure at S_e is still 2116 p.s.f.?

The pressure ratio $\frac{P_T}{P_o} = \frac{3000}{2116} = 1.418 \therefore t = \frac{T_T}{T_e} = 1.418^{.286} = 1.105$ and $\frac{\rho_T}{\rho_e} = 1.105^{2.5} = 1.284$. $\rho_T = \frac{P_T}{RT_T} = \frac{3000}{96 \times 800} = .0391$ lb/ft.^{3} $\therefore \rho_e = \frac{.0391}{1.284} = .0304$ lb/ft.^{3}

$T_e = \frac{800}{1.105} = 724°K \therefore \theta_{ue} = 800 - 724 = 76°C \therefore u_e = 147.1\sqrt{76} = 1282'$/sec. $\therefore \psi_e = u_e \rho_e = 1282 \times ,0304 = 38.98$ lb/sec./ft.^{2} $\therefore Q = \psi_e S_e = 19.49$ lb/sec.

$u_c = 147.1\sqrt{\frac{800}{6}} = 1698.6 \therefore u_e/u_c = \frac{1282}{1698.6} = .755$. $\rho_c = \frac{\rho_T}{1.2^{2.5}} = .0248$

$\therefore \psi_c = \rho_c u_c = 42.1$ lb/sec/ft.^{2} $\therefore \psi/\psi_c = \frac{38.98}{42.1} = .926.$

Hence the answers for a) to g) are:– a) $\psi_e = 38.98$ lb/sec./ft.^{2}; b) $\frac{\psi_e}{\psi_c} = 0.926$; c) $u_e = 1282'$/sec.; d) $\frac{u_e}{u_c} = 0.755$; e) $T_e = 724°K$; f) $\rho_e = 0.0304$ lb/ft.^{3}; g) $Q = 19.49$ lb/sec. For h) the max. flow will occur when $\frac{P_T}{2116} = 1.2^{3.5} = 1.893 \therefore P_T$ would be $1.893 \times 2116 = 4005$ p.s.f.; ρ_T would be $\frac{4005}{96 \times 800} = .0521$ lb/ft.^{3} and ρ_e would be $\frac{.0521}{1.2^{2.5}} = .0331$ lb/ft.^{3} $\therefore \psi_e = \psi_c = .0331 \times u_c = .0331 \times 1698.6 = 56.15$ (which could have been obtained from equation (2-7) to give a Q_{max} of 28.075 lb/sec.)

It is of interest to note that in the sub critical case of the above example (i.e. $P_T = 3000$ p.s.f., etc.) the reactive thrust on the reservoir would be $\frac{Q}{g} \times u_e$, i.e. $\frac{19.49}{32.2} \times 1282 = 776$ lbs. while ΔP acting on $S_e = .5(3000 - 2116) = 442$ lbs. The difference, of course, is due to the reduction of internal pressure as the air accelerates into the nozzle. The proportion of thrust accounted for by this is $\frac{776 - 442}{776} = .43$ or 43%. In the critical case where $P_T =$ 4005 p.s.f., $u_c = 1698.6$ and $Q_{max} = 28.075$, the reactive thrust is $\frac{28.075}{32.2} \times 1698.6 = 1481$ lbs. while $0.5(4005 - 2116) = 944.5$ lbs., so the reduction of internal pressure accounts for a proportion equal to $\frac{1481 - 944.5}{1481} = .362$, i.e. 36.2% of the thrust. When the pressure ratio to a convergent nozzle exit is the value corresponding to max. flow, i.e. 1.893, the nozzle is said to be 'choking'. Then, as we have already seen, $Q_{max} = .397\ S. \frac{P_T}{\sqrt{T_T}}$ where S is the minimum section.

Fig. 1b illustrates what happens in a convergent nozzle when the pressure ratio $\frac{P_T}{P_o}$ exceeds 1.893 (i.e. the temp ratio exceeds 1.2). The pressure at nozzle exit plane is $\frac{P_T}{1.893}$ and further expansion to P_o occurs external to the nozzle exit as shown. For complete expansion within a nozzle when $\frac{P_T}{P_o}$ exceeds 1.893 there must be a divergent section beyond the throat, though without a divergent section and for pressure ratios not greatly above the critical, the velocity a short distance downwind from the exit would not differ greatly from that corresponding to complete expansion.

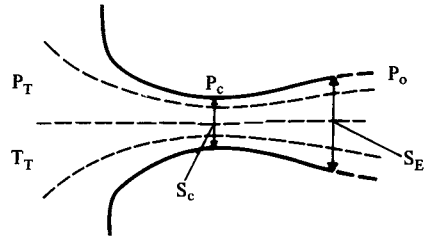

Fig. 5-2

Fig. 2 illustrates a 'con-di' nozzle for complete expansion from P_T to P_o where $\frac{P_T}{P_o}$ is well in excess of 1.893.

The size of S_E can readily be calculated from the fact that continuity requires that $\psi_c S_c = \psi_E S_E$, i.e. that $\frac{S_c}{S_E} = \frac{\psi_E}{\psi_c}$ and, as we have seen (equation 2-10), $\frac{\psi_E}{\psi_c} = \frac{3.864\sqrt{t-1}}{t^3}$

$\therefore \frac{S_c}{S_E} = \frac{3.864\sqrt{t-1}}{t^3}$. Thus *exit area/throat area is determined by the value of t only (and vice versa).*

Example 5-2

If P_T is $4P_o$ and $T_T = 1000°K$ what is the exit area of a con-di nozzle of throat section $S_c = 0.5$ ft.^{2} for complete expansion. And if $P_o = 2116$ p.s.f. what are the values of a) u_c; b) u_e; c) ρ_c; d) ρ_e; and e) Q.?

For $p = 4$ $t = 4^{.286} = 1.486$ $\therefore \frac{S_E}{S_c} = \frac{1.486^3}{3.864\sqrt{.486}} = 1.218$

$\therefore S_E = .609$ ft.^{2}

for a) $u_c = 147.1\sqrt{\frac{1000}{6}} = 1899'/\text{sec.}$

for b) $u_e = 147.1\sqrt{1000\left(\frac{t-1}{t}\right)} = 147.1\sqrt{1000\left(\frac{.486}{1.486}\right)} = 2660'/\text{sec.}$

for c) $\rho_c = \frac{\rho_T}{1.577}$ and $\rho_T = \frac{P_T}{RT_T} = \frac{4 \times 2116}{96 \times 1000} = .08817$

$\therefore \rho_c = \frac{.08817}{1.577} = .0559$ lb/ft.^{3}

for d) $\rho_e = \frac{\rho_T}{t^{2.5}} = \frac{.08817}{1.486^{2.5}} = .0328$ lb/ft.^{3}

for e) One may use either $Q = \rho_c u_c S_c$ or $Q = \rho_e u_e S_e$ or $Q = \psi_e S_e$ using equation (2-9) for ψ, or $Q = \psi_c S_c$ using equation (2-7) for ψ_c.

From $Q = \rho_c u_c S_c$ $Q = .0559 \times 1899 \times .5 = 53.08$ lb/sec.

From $Q = \rho_e u_e S_e$ $Q = .0328 \times 2660 \times .609 = 53.13$ lb/sec.

From $Q = \psi_e S_e$ $Q = .609 \times 1.532 \frac{P_T}{\sqrt{T_T}} \frac{\sqrt{t-1}}{t^3} = .933\left(\frac{8464}{\sqrt{1000}}\right)\frac{\sqrt{.486}}{1.486^3}$

$= 53.05$ lb/sec.

From $Q = \psi_c S_c$ $Q = .5 \times .397 \times \frac{8464}{\sqrt{1000}} = 53.13$ lb/sec.

(The minor differences are, of course, due to using a limited number of significant figures.)

The first two alternatives are to be preferred since they involve the memorisation of fewer constants.

It is of interest to note what would happen to the reactive thrust if the divergent portion were omitted. The pressure at S_c is $\frac{8464}{1.893} = 4471$ p.s.f. and the velocity $u_c = 1899'$/sec. Thus there would be a pressure thrust of $0.5\,(4471 - 2116) = 1177.5$ lb. and a reaction thrust of $53.1 \times \frac{1899}{32.2} = 3131.6$ lb. to give a total thrust of 4309.1 lb., whereas, with complete expansion the reactive thrust $= 53.1 \times \frac{2660}{32.2} = 4386.5$ lb.; i.e. an increase of 1.8%.

In practice, flow through nozzles is not quite isentropic, though nearly so if correctly designed. The inevitable boundary layer due to surface friction reduces the effective pressure drop and, though very thin in a sharply descending pressure gradient, reduces the effective flow area. Also, if wall curvature is appreciable at the throat, one cannot assume uniform flux density because of the pressure gradient across the section due to centrifugal force. In a symmetrical nozzle with a straight axis ψ_c can occur only on the axis so that ψ between the axis and the wall is less than ψ_c. If the axis were curved this effect would be even more pronounced and the streamline for ψ_c would not be on the axis (except for one special case).

If, in the case of a con-di nozzle designed for a pressure ratio well above the critical ratio 1.893, the pressure ratio (total to static) is reduced, either by increasing exit static pressure or reducing entry total pressure, so is the temp. ratio, and the nozzle no longer conforms to the requirement that $\frac{S_c}{S_E} = \frac{3.864\sqrt{t-1}}{t^3}$. There will be a section between S_c and S_E which does conform and beyond which the divergent portion no longer runs full. Referring to this intermediate section as S_i one would expect that there would be recompression from S_c to S_i until $\frac{S_c}{S_i} = \frac{3.864\sqrt{t-1}}{t^3}$ and that at S_i the flow would break away with the static pressure equal to the ambient pressure at discharge. But in practice this does not happen. For a short distance beyond S_c there is over expansion to a pressure well below exit static P_o and then sudden recompression to P_o across a normal shock wave much as shown in Fig. 3.

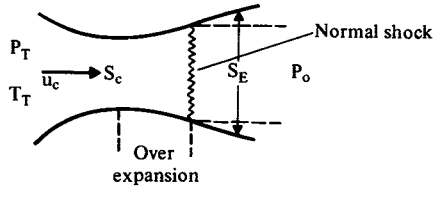

Fig. 5-3

Recompression through a shock wave entails loss not only in the compression across it but also in the turbulence in the space between the discharge flow and the nozzle wall downstream of the shock. Moreover, the effect of the sudden pressure rise on the boundary layer tends to cause a fluctuating flow breakdown where the shock contacts the wall and this in turn acts as an effective reduction in section, the net result being a complex interaction which causes a rapid fluctuation in the position of the shock.

Even if $\frac{P_T}{P_o}$ were reduced to the critical ratio 1.893 this over expansion and shock recompression would still occur, but if reduced below 1.893 the throat would cease to choke, the shock would disappear and the divergent portion would become a diffuser. Recompression in a diffuser, however, is inefficient even if the divergence is very gradual because of the adverse pressure gradient effect on the boundary layer, so the flow would be far from isentropic beyond S_c. The pressure ratio would need to be appreciably below the critical for the divergent portion to become fully established as a subsonic diffuser. When the flow through S_c becomes 'stably' subsonic then S_E becomes the flow controlling section.

Nozzles in Series

If two or more nozzles are in series and the flow is isentropic (i.e. no friction losses) and there is no power extraction between them then clearly the flow will be determined by the smaller (or smallest) throat. But if there is some loss of total pressure between them this may not be so if the difference in throat sections is small.

Fig. 4 represents such a situation in which S_2 is slightly larger than S_1. The 'grid' AB symbolises a cause of total pressure loss from P_{T1} to P_{T2} where P_{T2} is only a little less than P_{T1}. There will be no change of total temperature T_T if the flow is adiabatic.

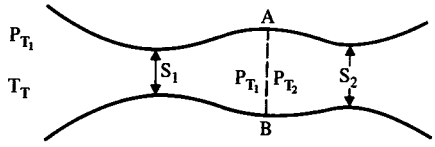

Fig. 5-4

For the throat S_1, if choking, $\psi_{c1} = k\frac{P_{T1}}{\sqrt{T_T}}$. For the throat S_2, if choking, $\psi_{c2} = k\frac{P_{T2}}{\sqrt{T_T}}$, so, for simultaneous choking $\psi_{c1}S_1 = \psi_{c2}S_2$, i.e. $\frac{P_{T1}}{\sqrt{T_T}}S_1 = \frac{P_{T2}}{\sqrt{T_T}}S_2$ (for continuity) from which $\frac{P_{T1}S_1}{P_{T2}S_2} = 1$. This could be a highly unstable state of affairs if $P_{T1} - P_{T2}$ varied according to which nozzle was choking. Choking might oscillate rapidly

between the nozzles and cause a rapid fluctuation in mass flow Q. To avoid this $\frac{P_{T1}S_1}{P_{T2}S_2}$ would need to be significantly larger or smaller than unity to ensure steady flow.

We will now proceed to examine nozzle combinations which are very relevant to later portions of this work.

In the diagrams a vertical axis is chosen for the various arrangements. This makes it easier to include many of the relevant relationships on the diagrams rather than in the text.

Case 1. Two Choking Nozzles in Series with Energy Extraction between them

This is analagous to the situation in a simple jet engine. The turbine driving the compressor may be, in effect, a choking nozzle beyond which total temperature and total pressure are reduced. The final exhaust includes the second choking nozzle.

The situation is represented diagrammatically in Fig. 5.

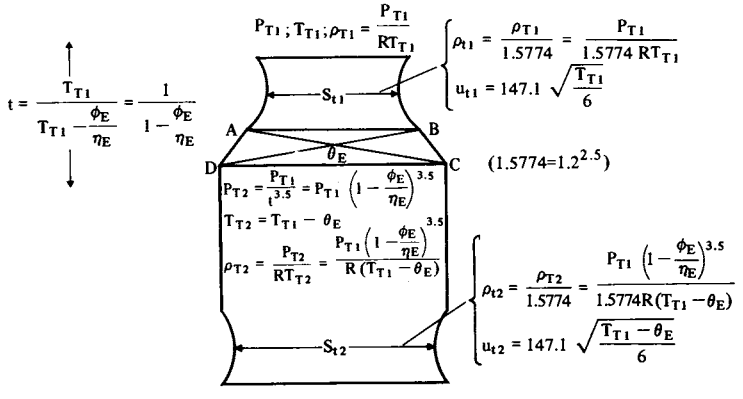

Fig. 5-5

ABCD represents a turbine or other means of energy extraction θ_E with efficiency η_E which reduces the total temperature from T_{T1} to T_{T2}, and the total pressure from P_{T1} to P_{T2}. The corresponding 'total' densities are ρ_{T1} and ρ_{T2}.

The suffixes t1 and t2 pertain to conditions at the throats S_1 and S_2.

With efficiency η_E, the isentropic energy drop $\theta'_E = \frac{\theta_E}{\eta_E}$; hence, as shown, the total to total temperature ratio t across S_1 and ABCD is given by

$$t = \frac{1}{1 - \frac{\phi_E}{\eta_E}} \qquad \left(\text{where } \phi_E = \frac{\theta_E}{T_{T1}}\right)$$

Many of the relevant relationships are indicated in Fig. 5.

For continuity, $\frac{S_{t2}}{S_{t1}} = \frac{\rho_{t1}\, u_{t1}}{\rho_{t2}\, u_{t2}}$. (5-1)

From Fig. 5 we see that $\rho_{t1} = \frac{P_{T1}}{1.5774\, RT_{T1}}$ and $\rho_{t2} = \frac{P_{T1}\left(1 - \frac{\phi_E}{\eta_E}\right)^{3.5}}{1.5774\, R\,(T_{T1} - \theta_E)}$

$$\therefore \frac{\rho_{t1}}{\rho_{t2}} = \frac{P_{T1}}{1.5774 RT_{T1}} \times \frac{1.5774 RT_1\,(1 - \phi_E)}{P_{T1}\left(1 - \frac{\phi_E}{\eta_E}\right)^{3.5}} = t^{3.5}\,(1 - \phi_E) \tag{5-2}$$

Also $u_{t1} = 147.1\sqrt{\frac{T_{T1}}{6}}$ and $u_{t2} = 147.1\sqrt{\frac{T_1 - \theta_E}{6}} = 147.1\sqrt{\frac{T_1}{6}\,(1 - \phi_E)}$

$$\therefore \frac{u_{t1}}{u_{t2}} = 147.1\sqrt{\frac{T_{T1}}{6}} \times \frac{1}{147.1\sqrt{\frac{T_1}{6}\,(1 - \phi_E)}} = \sqrt{\frac{1}{1 - \phi_E}} \tag{5-3}$$

Substituting in (1) from (2) and (3)

$$\frac{S_{t2}}{S_{t1}} = t^{3.5}\,(1 - \phi_E)\sqrt{\frac{1}{1 - \phi_E}} = t^{3.5}\sqrt{1 - \phi_E} \tag{5-4}$$

Note that if $\eta_E = 1.0$

$$t = \frac{1}{1 - \phi_E} \quad \text{so (4) becomes} \quad \frac{S_{t2}}{S_{t1}} = t^3. \tag{5-5}$$

This result is relevant to relatively moving nozzles in Case 6 on page 60.

Numerical Check

Using assumptions as follows: $T_{T1} = 1000°K$, $P_{T1} = 12{,}000$ p.s.i.;

$\theta_E = 300$ (so that $\phi_E = 0.3$) and $\eta_E = 0.87$, we have:

$$\rho_{T1} = \frac{12000}{96 \times 1000} = 0.125 \quad \text{and} \quad \rho_{t1} = \frac{0.125}{1.5774} = .07924$$

$$u_{t1} = 147.1\sqrt{\frac{1000}{6}} = 1899.1 \text{ ft/sec.}$$

$$T_{T2} = 1000 - 300 = 700; \quad t = \frac{1}{1 - \frac{0.3}{.87}} = 1.5263,$$

$$\therefore P_{T2} = \frac{12.000}{(1.5263)^{3.5}} = 2731.7 \quad \therefore \rho_{T2} = \frac{2731.7}{96 \times 700} = .04065,$$

$$\therefore \rho_{t2} = \frac{.04065}{1.5774} = .02577$$

$$u_{t2} = 147.1\sqrt{\frac{700}{6}} = 1588.9 \text{ ft/sec.}$$

$$\therefore \frac{\rho_{t1}}{\rho_{t2}} \frac{u_{t1}}{u_{t2}} = \frac{S_{t2}}{S_{t1}} = \frac{.07924}{.02577} \times \frac{1899.1}{1588.9} = 3.675.$$

From equation (4) $\frac{S_{t2}}{S_{t1}} = 1.5263^{3.5}\sqrt{1 - 0.3} = 3.675$ Q.E.D.

Note that if there had been no less, i.e. $\eta_T = 1.0$, then t would be $\frac{1}{0.7} = 1.4286$ which, from (5), would make $\frac{S_{t2}}{S_{t1}} = t^3 = 1.4286^3 = 2.9155$. Thus it may be seen that losses in energy extraction have an appreciable effect on the throat area ratio.

Equation (4) brings out three very important facts, namely, that if $\frac{S_{t2}}{S_{t1}}$ is fixed and η_E may be regarded as constant then *i) ϕ_E is fixed, i.e. θ_E is proportional to T_{T1} ii) t is also fixed, iii) T_{T2} is proportional to T_{T1}*. Thus if one wishes to vary ϕ_E and t it is necessary to vary $\frac{S_{t2}}{S_{t1}}$. If S_{t1} represents turbine nozzle throats in parallel and S_{t2} represents the final nozzle of a jet engine, it is no problem to vary S_{t2} but, up to now, S_{t1} cannot be varied (though attempts to achieve this are probably in progress).

Case 2. Three Choking Nozzles in Series with Energy Extraction after the First and Second

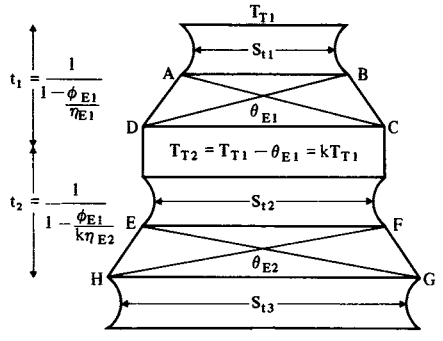

Fig. 5-6

This, shown diagrammatically in Fig. 6, is relevant to a two-spool jet engine with a choking final nozzle preceded by two choking turbines in series.

For the expansion across S_{t1} and ABCD, the situation is the same as Case 1,

$$\therefore \quad \frac{S_{t2}}{S_{t1}} = t_1^{3.5}\sqrt{1-\phi_{E1}} \tag{5-6}$$

and the total temperature after CD is proportional to T_{T1}, so we can write $T_{T2} = kT_{T1}$.

For an observer at EF the situation is also the same as Case 1 except that kT_{T1} replaces T_{T1} and the temperature ratio t_2 across S_{t2} and EFGH becomes

$$t_2 = \frac{kT_{T1}}{kT_{T1} - \frac{\theta_{E2}}{\eta_{E2}}} = \frac{1}{1-\frac{\phi_{E2}}{k\eta_{E2}}}$$

as shown on Fig. 6.

$$\text{Hence} \quad \frac{S_{t3}}{S_{t2}} = t_2^{3.5}\sqrt{1-\frac{\phi_{E2}}{k}} \tag{5-7}$$

Multiplying (6) and (7) we obtain

$$\frac{S_{t3}}{S_{t1}} = (t_1 t_2)^{3.5}\sqrt{(1-\phi_{E1})\left(1-\frac{\phi_{E2}}{k}\right)} \tag{5-8}$$

As with Case 1, θ_{E2} is proportional to T_{T2} which in turn is proportional to T_{T1}, and,

since θ_{E1} is also proportional to T_{T1} it follows that if $\frac{S_{t3}}{S_{t1}}$ is fixed, so is $\frac{\theta_{E2}}{\theta_{E1}}$ (so long as η_{E1} and η_{E2} may be regarded as constants). Thus *there is a 'thermodynamic lock' between ABCD and EFGH* which may be 'broken' by variation of the throat S_{t3}.

These 'fixed links' in expansion imposed by choking nozzles are very useful for calculating the part load performance of jet engines over the range where η_{E1} and η_{E2} may be assumed constant.

If there is an energy loss between BC and EF it may be allowed for by adjusting η_{E1} to include it. Similarly if there is an energy loss between GH and S_{t3} it may be allowed for by adjusting η_{E2} to include it.

In summary, if S_{t1}, S_{t2}, and S_{t3} are fixed so are $\frac{T_{T1}}{T_{T2}}, \frac{\theta_{E1}}{\theta_{E2}}, \frac{\theta_{E1}}{T_{T1}}, \frac{\theta_{E2}}{T_{T1}}$, etc. Also t_1 and t_2 are fixed as long as η_{E1} and η_{E2} may be assumed constant.

Finally, if $\eta_{E1} = \eta_{E2} = 1.0$ $\quad t_1 = \dfrac{1}{1 - \phi_{E1}}$ $\quad$ and $\quad t_2 = \dfrac{1}{1 - \dfrac{\phi_{E2}}{k}}$

So, substituting in (8) we get

$$\frac{S_{t3}}{S_{t1}} = (t_1 t_2)^3. \tag{5-9}$$

This result is relevant to relatively moving nozzles (see below).

Case 3. A Non-Choking Nozzle in Series with a Choking Nozzle with Energy Extraction between them

This is relevant to a gas turbine with open exhaust or a jet engine with a variable final nozzle opened up to a non-choking condition for operational reasons.

In the cases considered in the foregoing, the temperature ratio across the final nozzle did not enter into the picture but it must be taken into account if the temperature ratio (total to static) is less than the critical value (= 1.2) at all points from entry to exit of the final nozzle. The static pressure of final discharge must also be taken into account.

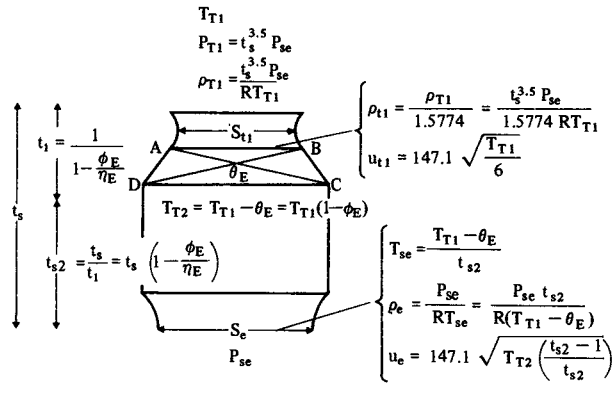

Fig. 5-7

Figure 7 is a diagrammatic representation of the system. In it the suffix s implies static quantities or total to static ratios; thus t_s is the overall total to static temperature ratio and P_{se} is the static pressure at S_e.

This case is somewhat more complex than the two already considered above.

Again, for continuity $\dfrac{S_e}{S_1} = \dfrac{\rho_{t1}\, u_{t1}}{\rho_e\, u_e}$.

Using the relationships shown on Fig. 7 and the fact that $T_{T2} = T_{T1}(1-\phi_E)$

$$\frac{\rho_{t1}}{\rho_e} = \frac{t_s^{3.5}\, P_{se}}{1.5774\, RT_{T1}} \times \frac{RT_{T1}(1-\phi_E)}{P_{se}\, t_{s2}} = \frac{t_s^{3.5}}{t_s^2}\left(\frac{1-\phi_E}{1.5774}\right) \tag{5-10}$$

$$\frac{u_{t1}}{u_e} = 147.1\sqrt{\frac{T_{T1}}{6}} \times \frac{1}{147.1\sqrt{T_{T1}(1-\phi_E)\left(\frac{t_{s2}-1}{t_{s2}}\right)}} = \sqrt{\frac{t_{s2}}{6(1-\phi_E)(t_{s2}-1)}} \tag{5-11}$$

Multiplying (10) by (11) gives

$$\frac{S_e}{S_1} = \frac{1}{1.5774}\frac{t_s^{3.5}}{t_{s2}}\sqrt{\frac{t_{s2}(1-\phi_E)}{6(t_{s2}-1)}} \quad \text{or, since } t_s = t_1 t_{s2}$$

$$\frac{S_e}{S_1} = \frac{1}{1.5774}\, t_1^{3.5}\, t_{s2}^3\sqrt{\frac{1-\phi_E}{6(t_{s2}-1)}} \quad \text{or, since } t_1 = \frac{1}{1-\frac{\phi_E}{\eta_E}}$$

$$\frac{S_e}{S_1} = \frac{1}{1.5774}\left(\frac{1}{1-\frac{\phi_E}{\eta_E}}\right)^{3.5} t_{s2}^3 \sqrt{\frac{1-\phi_E}{6(t_{s2}-1)}} \qquad (5\text{-}12)$$

Numerical Check

Using assumptions as follows: $T_{T1} = 1000°K$, $\theta_E = 300°C$, $\eta_E = 0.87$, $P_{se} = 2000$ p.s.f. and $t_{s2} = 1.15$, we have: $t_1 = \dfrac{1}{1-\frac{0.3}{0.87}} = 1.5263$

$\therefore\ t_s = t_1 \times t_{s2} = 1.5263 \times 1.15 = 1.7553\ \therefore\ P_{T1} = 1.7553^{3.5} \times 2000 = 14{,}329$ p.s.f.

$\therefore\ \rho_{T1} = \dfrac{14\,329}{96 \times 1000} = 0.1493$ and $\rho_{t1} = \dfrac{0.1493}{1.5774} = .09463$

Since $T_{T2} = 1000 - 300$, $T_{se} = \dfrac{700}{1.15} = 608.7\ \therefore\ \rho_e = \dfrac{2000}{96 \times 608.7} = .03423$

$\therefore\ \dfrac{\rho_{t1}}{P_a} = \dfrac{.09463}{.03423} = 2.7649$

$u_{t1} = 147.1\sqrt{\dfrac{1000}{6}} = 1899.1$ ft/sec and $u_e = 147.1\sqrt{700 \times \dfrac{0.15}{1.15}} = 1405.6$ ft/sec.

$\therefore\ \dfrac{u_{t1}}{u_e} = \dfrac{1899.1}{1405.6} = 1.3511\ \therefore\ \dfrac{S_e}{S_1} = 2.7649 \times 1.3511 = 3.736$

Using equation (12) we have $\dfrac{S_e}{S_1} = \dfrac{1}{1.5774}\left(\dfrac{1}{1-\frac{0.3}{0.87}}\right)^{3.5} \times 1.15^3 \times \sqrt{\dfrac{1-0.3}{6 \times 0.15}} = 3.736$ Q.E.D.

If $\eta_E = 1.0$ (12) becomes $\dfrac{S_e}{S_1} = \dfrac{1}{1.5774}\left(\dfrac{1}{1-\phi_E}\right)^{3.5} t_{s2}^3 \sqrt{\dfrac{1-\phi_E}{6(t_{s2}-1)}} =$

$$\frac{1}{1.5774}\left(\frac{t_{s2}}{1-\phi_E}\right)^3 \sqrt{\frac{1}{6(t_{s2}-1)}} \qquad (5\text{-}13)$$

This is relevant to relatively moving nozzles (see over).

Case 4. Choking Nozzle in Series with a Non-Choking Nozzle with Energy Extraction between them

This is representative of a turbine with non-choking blading followed by another turbine or final nozzle across which the total to static temperature ratio is above the critical ratio 1.2.

In this case the situation reverts to that in which the system is unaffected by the static pressure at exit from the choking nozzle.

The system is represented in Fig. 8.

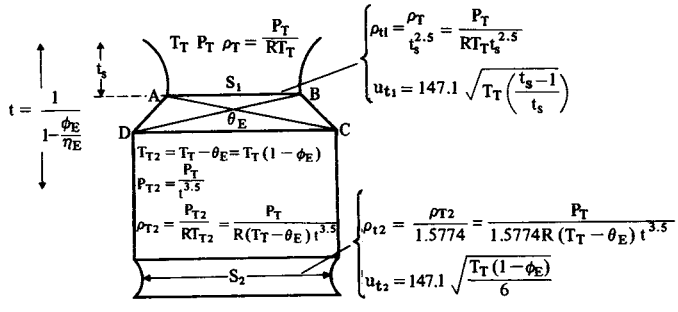

Fig. 5-8

Using the relationships shown on Fig. 8, we have:

$$\frac{\rho_{t1}}{\rho_{t2}} = \frac{P_T}{RT_T t_s^{2.5}} \times \frac{1.5774\,RT_T\,(1-\phi_E)t^{3.5}}{P_T} = 1.5774\,(1-\phi_E)\frac{t^{3.5}}{t_s^{2.5}} \tag{5-14}$$

$$\frac{u_{t1}}{u_{t2}} = 147.1\sqrt{T_T\left(\frac{t_s-1}{t_s}\right)} \times \frac{1}{147.1\sqrt{\frac{6}{T_T(1-\phi_E)}}} = \sqrt{\frac{6(t_s-1)}{t_s(1-\phi_E)}} \tag{5-15}$$

Hence, multiplying (14) by (15)

$$\frac{S_2}{S_1} = 1.5774\,(1-\phi_E)\frac{t^{3.5}}{t_s^{2.5}} \times \sqrt{\frac{6(t_s-1)}{t_s\,(1-\phi_E)}} = 1.5774\,\frac{t^{3.5}}{t_s^{2.5}}\sqrt{\frac{6(t_s-1)(1-\phi_E)}{t_s}} \tag{5-16}$$

or, using $t = \dfrac{1}{1-\dfrac{\phi_E}{\eta_E}}$, $\dfrac{S_2}{S_1} = 1.5774\left(\dfrac{1}{1-\dfrac{\phi_E}{\eta_E}}\right)^{3.5} t_s^{-2.5}\sqrt{\dfrac{6(t_s-1)(1-\phi_E)}{t_s}}$

$$\text{or,} \quad \frac{S_2}{S_1} = \frac{1.5774}{t_s^3}\left(\frac{1}{1-\frac{\phi_E}{\eta_E}}\right)^{3.5}\sqrt{6(t_s-1)(1-\phi_E)} \qquad (5\text{-}17)$$

from which it is more readily seen that, for a given value of η_E, if any two of $\frac{S_2}{S_1}$, t_s or ϕ_E are fixed, so is the third.

Numerical Check

Assuming that $T_T = 1000°K$; $P_T = 12000$ p.s.f.; $\theta_E = 300$; $\eta_E = 0.87$ and $t_s = 1.15$;

we have: $\rho_T = \frac{12000}{96 \times 1000} = 0.125$; $\rho_{t1} = \frac{0.125}{1.15^{2.5}} = .08814$;

$$t = \frac{1}{1-\frac{0.3}{0.87}} = 1.5263 \therefore P_{T2} = \frac{12000}{1.5263^{3.5}} = 2731.7 \text{ p.s.f.},$$

$$\therefore \rho_{T2} = \frac{2731.7}{96 \times 700} = .04065$$

$$\therefore \rho_{t2} = \frac{.04065}{1.5774} = .02577 \therefore \frac{\rho_{t1}}{\rho_{t2}} = \frac{.08814}{.02577} = 3.4203$$

$$u_{t1} = 147.1\sqrt{1000\left(\frac{0.15}{1.15}\right)} = 1680 \text{ ft/sec}, \quad u_{t2} = 147.1\sqrt{\frac{700}{6}} = 1588.9 \text{ ft/sec}$$

$$\therefore \frac{u_{t1}}{u_{t2}} = \frac{1680}{1588.9} = 1.0574 \therefore \frac{S_2}{S_1} = 1.0574 \times 3.4203 = 3.616.$$

$$\text{From (17)} \ \frac{S_2}{S_1} = \frac{1.5774}{1.15^3}\left(\frac{1}{1-\frac{0.3}{0.87}}\right)^{3.5}\sqrt{6 \times 0.15 \times 0.7} = 3.616 \text{ Q.E.D.}$$

If, in (17), $\eta_E = 1.0$ the equation becomes:

$$\frac{S_2}{S_1} = \frac{1.5774\sqrt{6(t_s-1)}}{[t_s(1-\phi_E)]^3} \qquad (5\text{-}18)$$

which is again relevant to relatively moving nozzles (see over).

Case 5. Two Non-Choking Nozzles in Series with Energy Extraction Between them

This is relevant to a two stage turbine in which neither stage is choking and there is no choking restriction in the exhaust.

In this case the exhaust static pressure has to be taken into account once more.

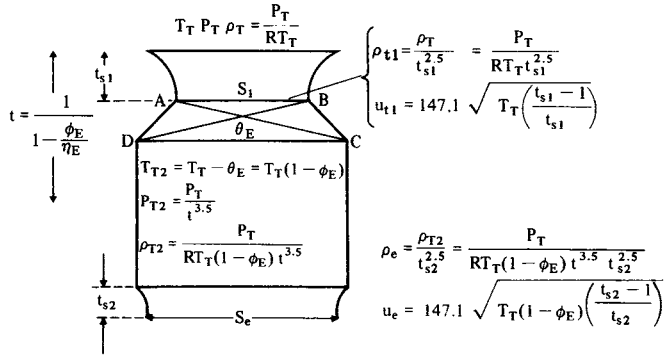

Fig. 5-9

The situation is represented in Fig. 9 on which as before several of the major relationships are indicated.

For continuity, $\dfrac{S_E}{S_1} = \dfrac{\rho_{t1}\ u_{t1}}{\rho_e\ u_e}$.

Using the relationships shown on Fig. 9:

$$\frac{\rho_{t1}}{\rho_e} = \frac{P_T}{RT_T t_{s1}^{2.5}} \times \frac{RT_T(1-\phi_E)t_{s2}^{2.5}}{P_T} = (1-\phi_E)t^{3.5}\left(\frac{t_{s2}}{t_{s1}}\right)^{2.5} \tag{5-19}$$

$$\frac{u_{t1}}{u_e} = 147.1\sqrt{T_T\left(\frac{t_{s1}-1}{t_{s1}}\right)} \times \frac{1}{147.1\sqrt{T_T\,(1-\phi_E)\left(\frac{t_{s2}-1}{t_{s2}}\right)}} =$$

$$\sqrt{\frac{t_{s2}}{t_{s1}}\,\frac{(t_{s1}-1)}{(t_{s2}-1)}\,(1-\phi_E)} \tag{5-20}$$

Multiplying (19) by (20):

$$\frac{S_e}{S_1} = (1-\phi_E)\,t^{3.5}\left(\frac{t_{s2}}{t_{s1}}\right)^{2.5}\sqrt{\frac{t_{s2}}{t_{s1}}\left(\frac{t_{s1}-1}{t_{s2}-1}\right)(1-\phi_E)} = \left(\frac{t_{s2}}{t_{s1}}\right)^3 t^{3.5}\sqrt{(1-\phi_E)\left(\frac{t_{s1}-1}{t_{s2}-1}\right)} \tag{5-21}$$

Numerical Check

Assuming that $T_T = 1000°K$; $P_T = 12{,}000$ psi; $\theta_E = 300$; $\eta_E = 0.87$

$t_{s1} = 1.17$ and $t_{s2} = 1.15$ then:

$$\rho_T = \frac{12000}{96 \times 1000} = 0.125; \quad \rho_{t1} = \frac{0.125}{1.17^{2.5}} = .08442$$

$$t = \frac{1}{1 - \frac{0.3}{0.87}} = 1.5263 \quad \therefore P_{T2} = \frac{12000}{1.5263^{3.5}} = 2731.7 \text{ p.s.f.}$$

$$\therefore \quad \rho_{T2} = \frac{2731.7}{96 \times 700} = .04065$$

$$\therefore \quad \rho_e = \frac{.04065}{1.15^{2.5}} = .02866 \quad \therefore \frac{\rho_{t1}}{\rho_e} = \frac{.08442}{..02866} = 2.9456$$

$$u_{t1} = 147.1\sqrt{1000 \times \frac{0.17}{1.17}} = 1773.1 \text{ ft/sec, and } u_e = 147.1\sqrt{700 \times \frac{0.15}{1.15}} = 1405.6 \text{ ft/sec.}$$

$$\therefore \quad \frac{u_{t1}}{u_e} = 1.2615 \qquad \therefore \frac{S_e}{S_1} = 1.2615 \times 2.9456 = 3.715.$$

Using equation (21) we have:

$$\left(\frac{1.15}{1.17}\right)^3 \left(\frac{1}{1 - \frac{0.3}{0.87}}\right)^{3.5} \sqrt{0.7 \times \frac{0.17}{0.15}} = 3.715 \text{ Q.E.D.}$$

At this point, a word of caution is necessary. In the numerical check, with $\theta_E = 300°$, $t = 1.5263$ which is well above the critical ratio 1.2, so that if the energy extractor were a turbine it would need to have at least two stages to avoid choking in either the stationary or moving blading

Referring to equation (21), if $\eta_E = 1.0$, $t^{3.5} = \left(\frac{1}{1 - \phi_E}\right)^{3.5}$ and (21) then becomes

$$\frac{S_e}{S_1} = \left(\frac{t_{s2}\, t}{t_{s1}}\right)^3 \sqrt{\frac{t_{s1} - 1}{t_{s2} - 1}} \tag{5-22}$$

which is again relevant to relatively moving nozzles (see over).

Case 6. Relative Movement between Nozzles

Figure 10 represents a nozzle B receding from fixed nozzle A with velocity v. The broken lines indicate a confining channel between them.

Improbable as it may seem from the diagram, this is relevant to the stationary and moving blades of a turbine.

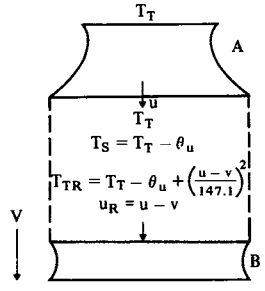

Fig. 5-10

As will now be shown, the relative movement of B away from A is equivalent to energy extraction between them, this energy being without loss if the flow is wholly isentropic as will be assumed.

The key fact is that the static temperature T_s is the same relative to both nozzles in the internozzle space, but the total temperature T_{TR} relative to B is reduced by the relative movement.

Using the relationships shown on the diagram, the reduction of total temperature is

$$T_T - \left\{T_T - \theta_u + \left(\frac{u-v}{147.1}\right)^2\right\} = \theta_u - \left(\frac{u-v}{147.1}\right)^2 .$$

This reduction is equivalent to energy extraction θ_E, so one may write

$$\theta_E = \theta_u - \left(\frac{u-v}{147.1}\right)^2 = \theta_u - \left(\frac{u^2}{147.1^2} - \frac{2uv}{147.1^2} + \frac{v^2}{147.1^2}\right)$$

or

$$\theta_E = \theta_u - \left(\theta_u - \frac{2u^2\,\frac{v}{u}}{147.1^2} + \theta_v\right) = 2\theta_u \frac{v}{u} - \theta_v$$

or, since $\frac{v}{u} = \sqrt{\frac{\theta_v}{\theta_u}}$,

$$\theta_E = 2\theta_u\sqrt{\frac{\theta_v}{\theta_u}} - \theta_v = 2\sqrt{\theta_u\theta_v} - \theta_v.$$

Dividing throughout by T_T we have

$$\phi_E = 2\sqrt{\phi_u\phi_v} - \phi_v \,. \tag{5-22}$$

Hence in Cases 1 to 5 above, if relatively moving nozzles are substituted for energy extraction between non-relatively moving nozzles with $\eta_E = 1.0$, then the 'presumptive' value of $t\left(= \frac{1}{1-\phi_E}\right) = \frac{1}{1-2\sqrt{\phi_u\phi_v} + \phi_v}$. Thus in Case 1, for $\eta = 1.0$ it was found that $\frac{S_2}{S_1} = t^3$ (equation (5)) so, for a second choking nozzle receding from a first choking nozzle with velocity v, (5) becomes $\frac{S_2}{S_1} = \left(\frac{1}{1-2\sqrt{\phi_u\phi_v} + \phi_v}\right)^3$ or $1 - 2\sqrt{\phi_u\phi_v} + \phi_v = \sqrt[3]{\frac{S_1}{S_2}}$ from which it may be seen that if $\frac{S_1}{S_2}$ is fixed ϕ_v is a function of ϕ_u.

Similar substitutions for t and/or ϕ_E may be made in equations (9), (13), (18) and (22).

It is not recommended that the reader attempts to memorise the numerous formulae of this Section. The writer's main purpose has been to demonstrate the methods to be used for finding them and to bring out the 'links' and 'locks' which nozzles in series can impose, especially in the cases involving choking nozzles.

One final point: it is emphasised that only non-choking convergent nozzles can run full in off design conditions. For choking con-di nozzles to run full, as has been shown, the temperature ratio across them must conform to the exit/throat area ratio and vice versa. If this conformity does not exist the flow tends to fluctuate because in the instant following 'detachment' from the wall of the divergent portion the rapidly moving detached flow tends to pump away the relatively stagnant fluid between it and the wall and to re-attach at one point while becoming detached from another. Thus there would be a rapid fluctuation in direction superimposed on a fluctuation in flow rate. One may surmise that this phenomenon would be a serious source of noise.

SECTION 6
Representation of Thermal Cycles for Perfect Gases

The state of a perfect gas is determined by any two of the six quantities Pressure P, Specific Volume V (or $1/\rho$), Temp. T, Internal Energy E, Enthalpy h, and Entropy s. Hence changes of state can be represented on diagrams using any pair for coordinates or even pairs of combinations.

Figs. 1a–1h show eight of many possible ways of representing an *ideal* constant pressure cycle for a heat engine (or heat pump) using air as working fluid, it being assumed that the specific heats C_v and C_p (or K_v and K_p) are constant. Each diagram is for the same cycle–the well known 'Brayton Cycle'–in which, in a heat engine, air is compressed isentropically from A to B, heated at constant pressure from B to C, expanded isentropically from C to D, and cooled at constant pressure from D to A. This is the basic cycle of most modern gas turbines, though, in practice, except for 'closed cycle' engines, the 'spent' fluid is exhausted to atmosphere at D.

None of the diagrams involve enthalpy or internal energy because, with constant specific heats they would be similar to those with T as one of the ordinates but to a different scale. The same applies to the product PV. Even allowing for increase of specific heat with temperature, P–h, P–E, h–s diagrams etc., would be quite similar to their constant specific heat counterparts.

Any of the diagrams can be represented in non-dimensional form, thus the $p-v$ diagram of Fig. 1d is the non-dimensional version of the P–V diagram of Fig. 1a.

Entropy, by reason of its definition as a differential, has no absolute value. So, where it is used, it is necessary to stipulate an arbitrary datum. For the purpose of the diagrams involving s (Figs. 1c, 1e, 1f and 1g) the datum chosen was $s = 0$ when $T = 200°K$.

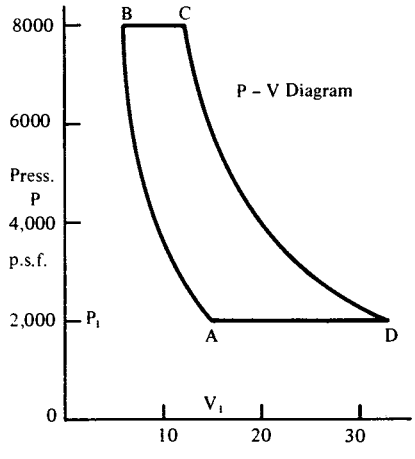

Fig. 6-1a

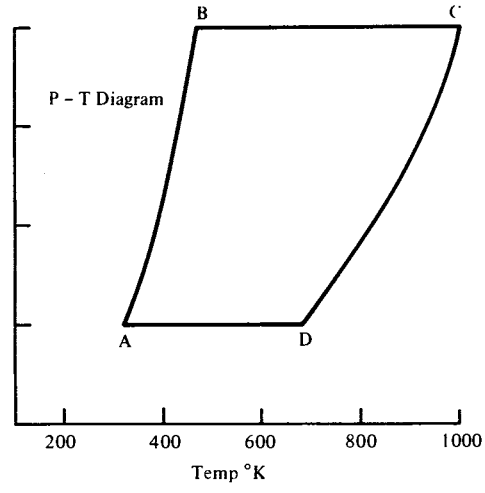

Fig. 6-1b

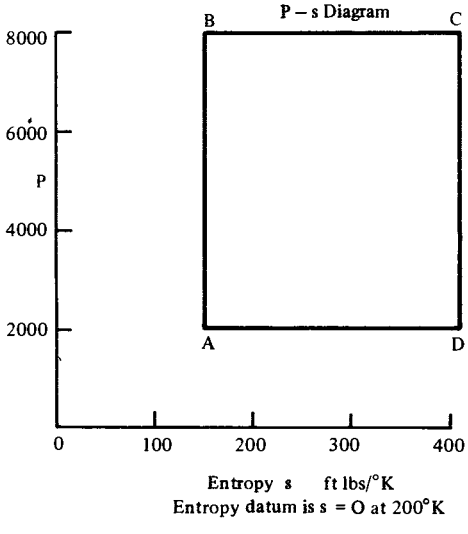

Fig. 6-1c

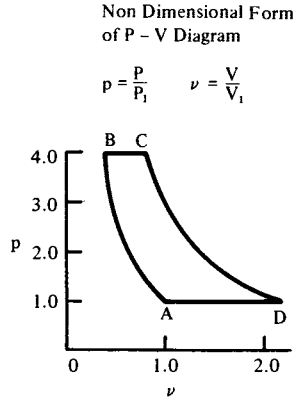

Fig. 6-1d

Of the diagrams shown, the P–V diagram (Fig. 1a) and the T–s diagram (Fig. 1e) are the most frequently used in text books. The P–V diagram because areas on it are a measure of mechanical energy, e.g. the area below AB, i.e. $\int_A^B PdV$; is the work done in (ideal) compression from A to B and $\int_C^D PdV$ is the ideal work of expansion from C to D. The area ABCD is the net work of the cycle. On the T–s diagram, areas on it are a measure of heat.

Thus $\int_B^C Tds$ equals the heat added between B and C and $\int_D^A Tds$ is the heat rejected from D to A. The area ABCD represents the net heat converted to mechanical energy.

Many writers of text books on gas turbines make generous use of T-s diagrams but the writer, in many years of gas turbine design, has never had occasion to use them with a perfect gas as working fluid (or mixtures of perfect gases). The use of entropy is, however, invaluable when dealing with steam and other vapours or mixtures of vapours and gases.

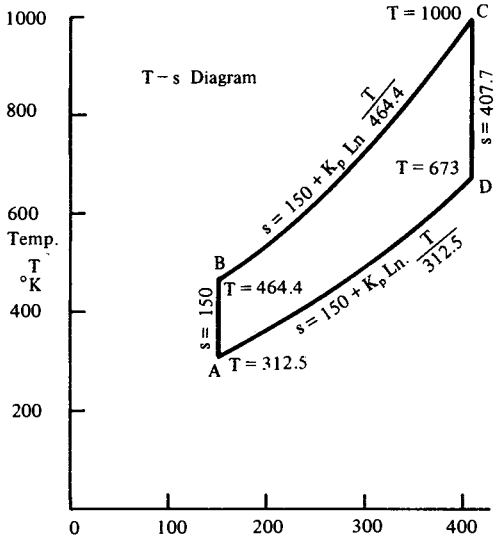

Fig. 6-1 e

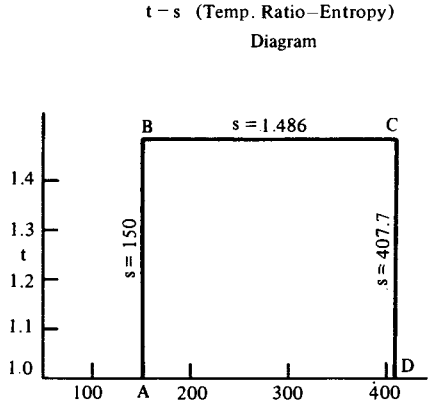

Fig. 6-1 f

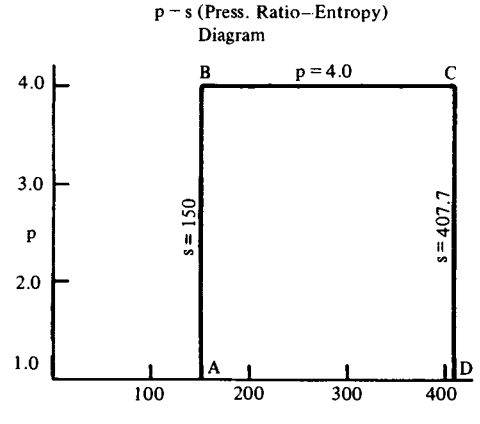

Fig. 6-1 g

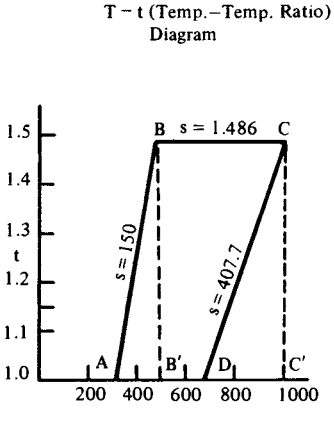

Fig. 6-1 h

The main value of thermal diagrams is to illustrate theoretical propositions.

The P–T diagram of Fig. 1b is rarely used, if at all. But, as may be seen, if set alongside the corresponding P–V diagram (as in Fig. 1) or superimposed on it, one may find temperatures by reading across from one to the other.

Figs. 1c, 1f and 1g are of interest because of their simplicity.

The T–t diagram is of academic interest in that all isentropics radiate from the hypothetical point $T = 0 \quad t = 0$.

Another interesting feature of Fig. 1h is that projections on the Temp. scale allow one to read off energy changes. Thus AB' indicates the temp. rise of compression, $B'C'$ ($\equiv BC$) the temp. rise due to heat addition, AD is the temp. equivalent of the heat rejected, $C'D$ is the temp. drop in expansion and $C'D - AB'$ gives the temp. equivalent of net work. A defect of this diagram, as shown, is that an isothermal is a mere point on the temp. scale so the Carnot cycle cannot be depicted.

As will be seen hereafter, the writer evolved methods of cycle calculations based on Fig. 1f using, for constant specific heats, temps. T, temp. ratios t and temp. differences θ. And, for variable specific heat, enthalpy h, pressure ratios p, and enthalpy differences Δh.

SECTION 7

Gas Turbine Cycle Calculations Using Approximate Methods

The approximate methods referred to in the heading are those referred to in the last paragraph of Section 6, i.e., cycles are dealt with almost entirely in terms of absolute temperatures, temperature differences and temperature ratios, it being assumed a) that specific heats are constant at C_V = 0.171 C.H.U./lb/°C; C_P = 0.24 C.H.U./lb/°C; K_V = 240 ft lbs/lb/°C and K_P = 336 ft lbs/lb/°C and therefore that $\gamma = 1.4$ and R = 96 ft lbs/lb/°C; b) that increase of mass due to fuel addition in combustion may be neglected.

All energy and other quantities are for unit mass flow rate (designated by the word 'specific' where necessary).

The adiabatic efficiency of compression η_C is defined as $\eta_C = \frac{\theta'_C}{\theta_C}$ shere θ'_C is the isentropic total temperature rise and θ_C is the actual total temperature rise for the pressure ratio. (total to total).

The adiabatic efficiency of expansion η_E is defined as $\eta_E = \frac{\theta_E}{\theta'_E}$ where θ_E is the actual total temperature drop and θ'_E is the isentropic total temperature drop for the pressure ratio concerned (the suffixes T or J may be used where it is necessary to distinguish between expansion through a turbine and expansion through a jet).

The Brayton Cycle With No Losses

Fig. 1a is a representation of the P-V diagram of Fig. 6-1a of Section 6 in diagrammatic form (i.e., not to scale as are all the diagrams of Section 6) with certain additional features. $T_O T_C$ is isentropic compression from P_1 to P_2 and $T_M T_E$ is isentropic expansion from P_2 to P_1. T_M-T_C is heat addition at constant pressure P_2 and $T_E - T_O$ is heat rejection at constant pressure P_1. The shaded area $T_O\ T_C\ P_2\ P_1$ represents the 'negative work' of compression W_C, and is given by $W_C = \int_{P_1}^{P_2} VdP$ or $\int_{P_1}^{P_2} \frac{dP}{\rho}$.

As we have seen from Section 1, $\frac{dP}{\rho} = K_P dT \therefore W_C = \int_{T_O}^{T_C} K_P dT$, i.e., $W_C = K_P(T_C - T_O)$.

Similarly the positive work of expansion W_E, i.e., the shaded area $P_2 T_M T_E P_1$ is given by $W_E = K_P(T_M - T_E)$.

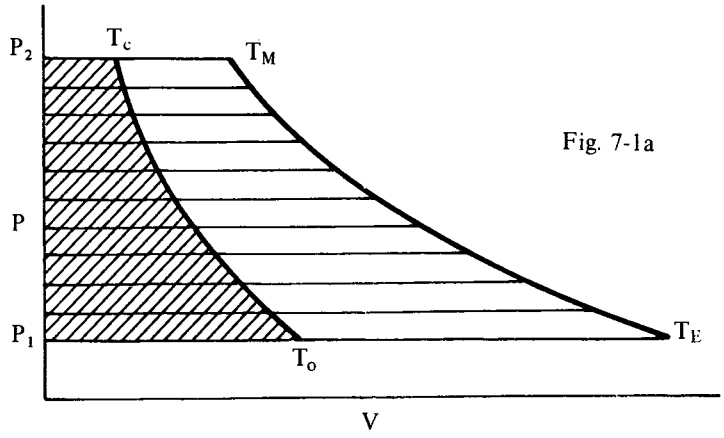

Fig. 7-1a

Since the pressure ratio p is the same for compression and expansion so is the temperature ratio t, i.e., $t = \frac{T_C}{T_O} = \frac{T_M}{T_E} \left(= \left(\frac{P_2}{P_1} \right)^{0.286} \right)$. It follows that $\frac{T_M}{T_C} = \frac{T_E}{T_O} = K$ where K is the positive/negative work ratio.

Fig. 1b is a modification of Fig. 1a using $T_C = tT_O$ and $T_M = kT_O$ from which it follows that Figs. 1a and 1b can be represented non-dimensionally as in Fig. 1c.

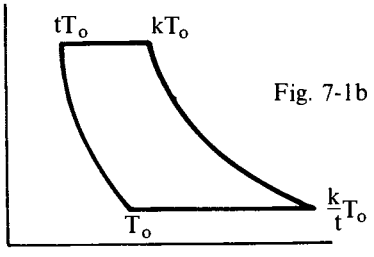

Fig. 7-1b

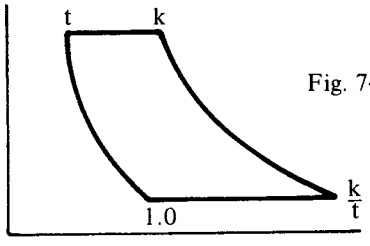

Fig. 7-1c

In Fig. 1c, the positive work W_e is proportional to $k - \frac{k}{t}$ while the negative work W_C is proportional to $t - 1$ $\therefore$ the net work $W_E - W_C$ is proportional to $k\left(\frac{t-1}{t}\right) - (t-1)$ or $(k-t)\left(\frac{t-1}{t}\right)$. The heat added H is proportional to $k - t$ (the constants of proportionality being the same for W_E, W_C, and H, namely $K_P T_O$ in mechanical units).

The overall efficiency η_O is $\frac{\text{net work}}{\text{heat added}}$ (or since net work equals heat added less heat rejected, $\eta_O = \frac{\text{heat added-heat rejected}}{\text{heat added}}$). $\therefore \eta_O = \frac{k\left(\frac{t-1}{t}\right) - (t-1)}{k-t}$ which reduces to $\eta_O = \frac{t-1}{t}$ or $\eta_O = 1 - \frac{1}{t}$.

Note that, in the ideal case, i.e., 100% efficiency in compression and expansion, η_O is independent of k and depends only on t.

$1 - \frac{1}{t}$ is the 'Air Standard Efficiency'

The specific work W_S, however, depends on k since it is proportional to $\eta_O(k - t)$, i.e., $W_S \equiv W_E - W_C = \eta_O K_P T_O (k - t)$ or, since $\eta_O = 1 - \frac{1}{t}$, $W_S = K_P T_O \left(1 - \frac{1}{t}\right)(k - t)$.

Brayton Cycle With Losses

This is depicted in the P-V diagram of Fig. 2.

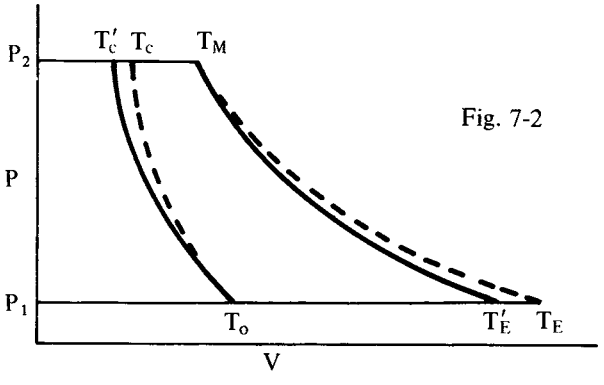

Fig. 7-2

$T_O T'_C$ is isentropic compression and $T_O T_C$ represents the actual compression (assumed adiabatic) in which losses are converted to internal energy thus causing an increase of temperature (and therefore of V) at any given value of P.

$T_M T'_E$ is isentropic expansion and $T_M T_E$ is the actual expansion (also assumed adiabatic) in which again losses take the form of an increase of internal energy (and entropy).

Unfortunately, areas bounded by the broken lines are no longer measures of work done. $T'_C T_C$ and $T'_E T_E$ represent the conversion of losses into heat. And, as may be seen, losses are not totally lost. The heating effect of compression losses reduces the amount of heat needed to raise the temperature to T_M at constant pressure P_2 and the expansion losses are partially recovered in the portion of the expansion following their heating effect. The lower down the expansion curve they occur the less the recovery.

F.W. Representation of the Ideal Brayton Cycle

As indicated in Section 6 the writer has always preferred to think in terms of diagrams similar to Fig. 6-1f of that section, i.e., using vertical lines for isentropics and horizontal lines for constant temperature ratio (and therefore constant pressure or pressure ratio) but further simplifying by omitting ordinands and scales. Thus the ideal Brayton cycle would be represented (or merely imagined) as in Fig. 3a.

Fig. 7-3a

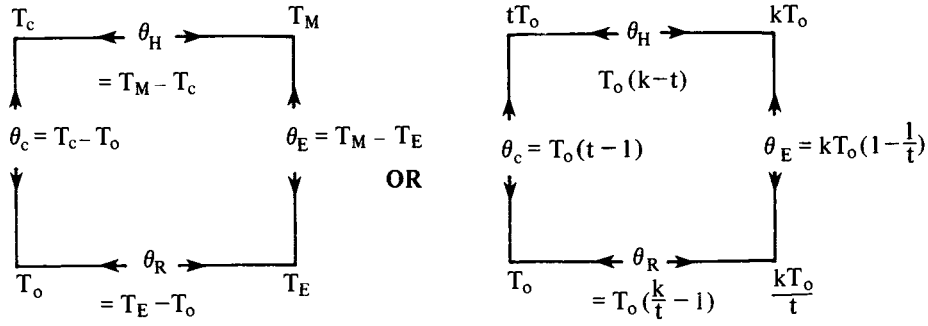

The non-dimensional form will be obvious from the right hand diagram of Fig. 3a – division by T_o at all points.

Fig. 3b gives a numberical example for $T_O = 288°K$, $T_M = 1200°K$, and $\theta_C = 300°C$, $t = \frac{588}{288} = 2.042$.

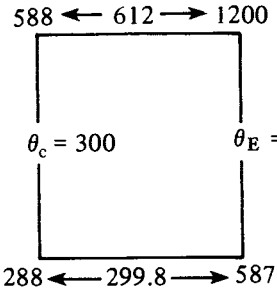

Fig. 7-3b

The specific compression work $W_C = K_P \times 300$
The specific expansion work $W_E = K_P \times 612.2$
The specific net work $W_E - W_C = K_P \times 312.2$

$\therefore \eta_O = \frac{312.2}{612} = 0.51 \left(\text{note that this equals } 1 - \frac{1}{t}\right)$

Representation of the Actual Cycle with Losses

This is shown in Fig. 4a. The temperature ratio t of the cycle is now $t = \frac{T'_C}{T_O} = \frac{T_O + \eta_C \theta_C}{T_O} = 1 + \frac{\eta_C \theta_C}{T_O}$

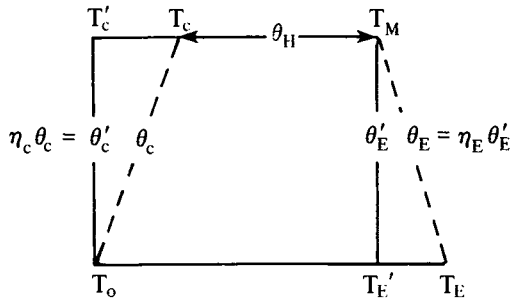

Fig. 7-4a

(Note: The 'slope' of the broken lines is exaggerated to accommodate the symbols, and their length is not representative of their magnitudes thus $T_M T_E = T_M - T_E = \eta_E \theta'_E$ which should be shorter than $T_M T'_E$. (This would be rectified if a diagram similar to Fig. 6-1h of Section 6 were used.)

Figure 4b shows a numerical example for $T_O = 288°K$; $T_M = 1200°K$; $\theta_C = 300°C$; $\eta_C = 0.85$ and $\eta_e = 0.87$.

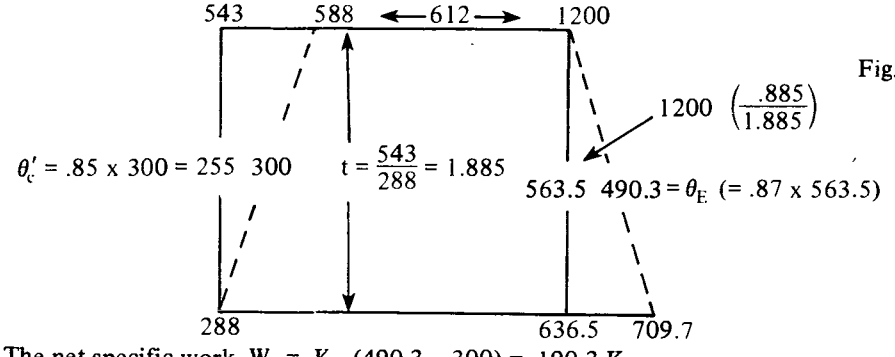

Fig. 7-4b

The net specific work $W_s = K_p\,(490.3 - 300) = 190.3\,K_p$.

Heat added $H = K_p\,(1200 - 588) = 612\,K_p$ $\therefore$ $\eta_o = \dfrac{190.3}{612} = .311$

Once one is familiar with the layout, it is unnecessary to draw a diagram. The spatial relationship of figures only will serve the purpose, thus the example shown in Fig. 7-4b may be set out thus:

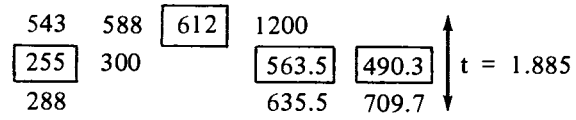

The temperature differences are distinguised from absolute temperatures by 'boxing'.

For most practical purposes one may omit T'_C, θ'_C, θ'_E and T'_E and reduce the layout to:

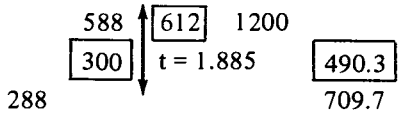

since t may be obtained from $t = 1 + \frac{\eta_C \theta_C}{T_O}$ and $\theta_E = \eta_E T_M \left(1 - \frac{1}{t}\right)$

Fig. 5 is a repeat of Fig. 4a in non-dimensional form where all temperatures and temperature differences are multiples of T_O.

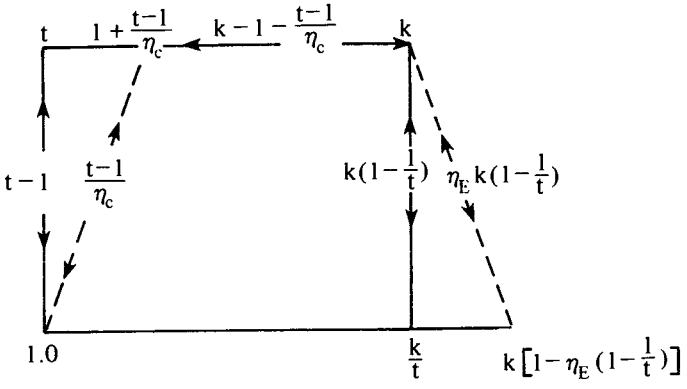

Fig. 7-5

In non-dimensional terms, the positive work of expansion is seen to be $W_E = \eta_E k \left(1 - \frac{1}{t}\right)$ and the negative work of compression is seen to be $\frac{t-1}{\eta_C}$, hence the net work is given by

$$W_E - W_C = \eta_E k \left(1 - \frac{1}{t}\right) - \frac{t-1}{\eta_C}$$

The heat added is H (non-dimensional) $= k - 1 - \frac{t-1}{\eta_C}$ $\therefore \eta_O = \frac{\text{net work}}{\text{head added}} = \frac{\eta_E k \left(\frac{t-1}{t}\right) - \frac{t-1}{\eta_C}}{k - 1 - \frac{t-1}{\eta_C}}$ which reduces to

$$\eta_O = \left(\frac{t-1}{t}\right)\left(\frac{\eta_C \eta_E k - t}{\eta_C (k-1) - t + 1}\right) \qquad (7\text{-}1)$$

Since $\frac{t-1}{t}$ is the air standard efficiency, the quantity in the second pair of brackets may be described as the 'thermodynamic efficiency,' which, if $\eta_C = \eta_E = 1.0$ reduces to 1.0.

The above formula for η_O shows that η_O is zero if $\eta_C \eta_E \frac{k}{t} - 1 = 0$, i.e., if $\eta_C \eta_E \frac{k}{t} = 1$. This explains the many failures to evolve practical gas turbines in the

early part of this century when component efficiencies were about 70% or below and the maximum temperature of the cycle was severely limited by the materials available.

As may be seen from Figure 5 $\frac{k}{t}$ is the 'positive/negative work ratio' of the ideal cycle.

It should also be fairly obvious that expansion efficiency is relatively more important than compression efficiency and that this relative importance increases with increase of $\frac{k}{t}$.

For any particular values of k, η_C and η_E the optimum value of t can be found from $\frac{d\eta_O}{dt} = 0$. The result is a somewhat clumsy quadratic for t. It is preferable to plot η_O as a function of t to get the optimum and also a picture of the sensitivity of η_O to t, especially if one allows for the normal decrease of η_C and increase of η_E with increase of t (i.e., with pressure ratio). (The increase of η_E will normally more than offset the decrease of η_C.)

SECTION 8
Turbo Gas Generators

Gas turbines operating with the constant pressure (or Brayton) cycle can take many forms. Such engines as the piston engine operating with the constant volume (or 'Otto') cycle or with the Diesel cycle (in which heat is added at substantially constant pressure and rejected at constant volume) are limited in variety by the fact that all the cycle stages - inspiration (or 'suction'), compression, combustion and exhaust, all take place in a single organ, the cylinder, so variations are basically limited to number, size, and arrangement of cylinders. In the gas turbine, on the other hand, each phase of the cycle takes place in separate 'organs' - the compressor or compressors, the combustion chamber or chambers and the turbine or turbines, and this fact makes possible a large number of arrangements. Moreover such devices as heat exchangers, compressor intercoolers (rarely used) add further to the possible range of types of gas turbine power plant. However, one of the commonest features is to use a combination of compressor, combustion chamber/s and compressor turbine to generate a supply of heated and pressurized gas for use in one or more power turbines (or propelling jet, etc.) more or less mechanically independent of the compressor-combustion-compressor turbine combination which is usually known as a 'gas generator.' A gas generator for use with a power turbine is depicted schematically in Figure 1.

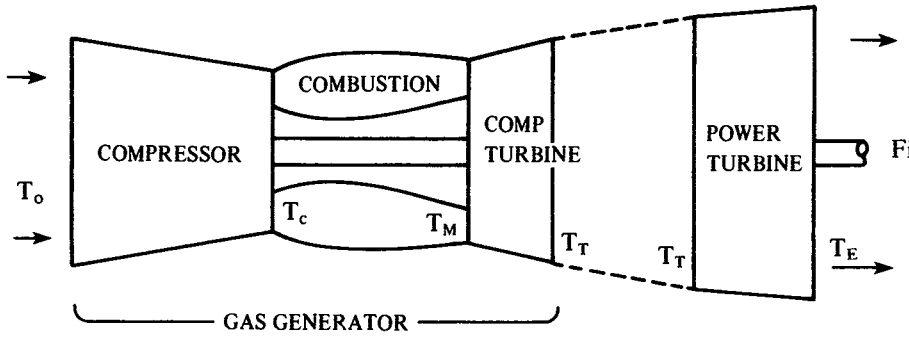

Fig. 8-1

The corresponding P–V diagram is shown in Fig. 2 and the F. W. diagram in Fig. 3a where, for convenience, the relationships between temperature differences, efficiencies and temperature are also shown.

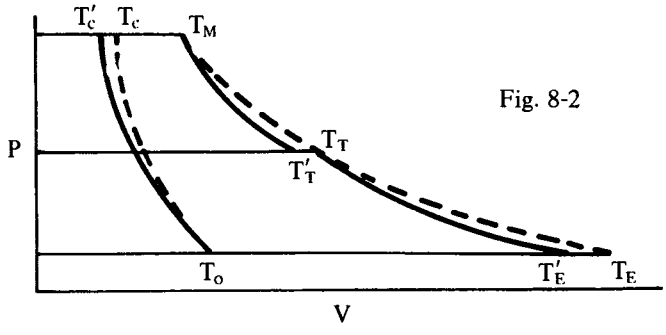

Fig. 8-2

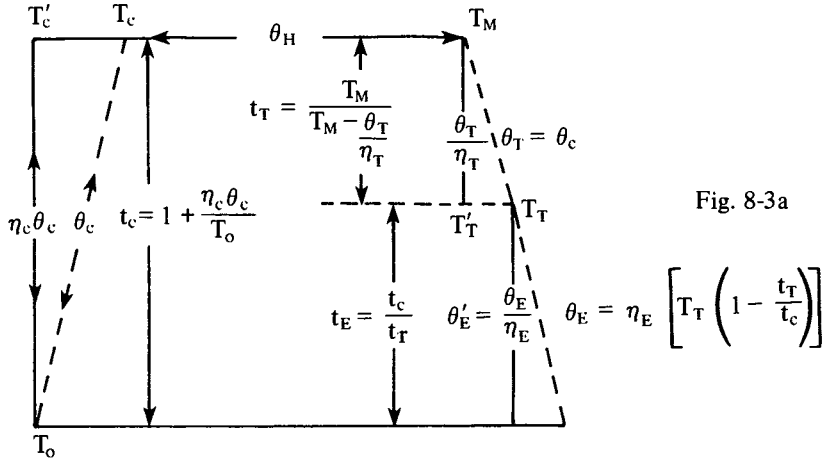

Fig. 8-3a

The compressor turbine usually also drives auxiliaries such as a fuel pump, etc., but the power for such purposes is very small compared with that required by the compressor, so that there is negligible error in assuming that $\theta_T = \theta_C$, i.e., the actual temperature drop in the compressor turbine is equal to the actual temperature increase in the compressor.

Two other important things should be noted, namely: (1) the product of the temperature ratios in expansion must equal the overall temperature ratio, i.e., $t_T \times t_E = t_C$, and (2) that since $T_C = T_O + \theta_C$ and $T_M = T_C + \theta_H = T_O + \theta_C + \theta_H$ and $T_T = T_M - \theta_C = T_O + \theta_C + \theta_H - \theta_C = T_O + \theta_H$ then $\theta_H = T_T - T_O$. (This must be so since, at T_T, the negative work of the cycle has been dealt with, so the total temperature at compressor turbine exhaust (T_T) must exceed the initial temperature T_O by the temperature rise in combustion (θ_H).)

A further point: the exhaust kinetic energy of the compressor turbine is a loss in relation to that turbine but contributes to the energy available for the power turbine. The kinetic energy of exhaust from the power turbine is, however, a total loss (unless made use of in some way). Nevertheless the efficiency of the power turbine η_E is normally higher than that of the compressor turbine η_T, especially if T_M is so high that blade cooling means are necessary in the gas generator turbine (i.e., compressor turbine).

θ_E represents the net specific work of the cycle, i.e., specific power = $K_P\theta_E$,

$\therefore \eta_O = \dfrac{\theta_E}{\theta_H}$.

From Fig. 3a it may be seen that $\theta_E = \eta_E T_T \left(1 - \dfrac{t_T}{t_C}\right) = \eta_E (T_M - \theta_C) \left(1 - \dfrac{t_T}{t_C}\right)$

hence, since T_O, T_M, θ_C, η_C, η_T and η_E are normally known (or assumed) θ_E may be readily calculated.

Example 8-1

Fig. 3b shows a numberical example for $T_O = 288°K$; $T_M = 1200°K$; $\theta_C = \theta_T = 300°C$; $\eta_C = 0.85$; $\eta_t = 0.87$ and $\eta_E = 0.90$, the isentropics being omitted.

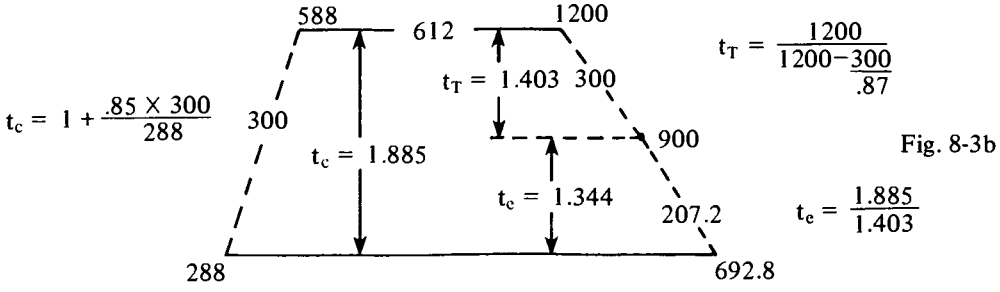

Fig. 8-3b

$$\theta_E = .9 \times 900 \left(1 - \frac{1}{1.344}\right) = 207.2 \qquad \therefore \eta_O = \frac{207.2}{612} = .339$$

The specific fuel consumption f_S for fuel of calorific value of 10,500 CHU/lb is $\therefore f_S = \dfrac{C_P\theta_H}{10{,}500} = \dfrac{0.24 \times 612}{10{,}500} = 0.014$ lb/sec. The specific power $W_S = 207.2 \times 336 = 69{,}612$ ft/lbs/sec or 126.6 HP. (It is useful to remember that the multiplier to convert θ_E to HP is 0.611.)

Note that, in the above example, the fuel represents a mass addition of 1.4%.

Figs. 2, 3a and 3b could equally well represent a simple jet engine at *static sea level* operation, in which case the expansion from T_T to T_E would represent the kinetic energy of the jet. The efficiency of this expansion, however, would be much higher than the 90% assumed for the example of Fig. 3b.

With the layouts of Figures 3a and 3b in mind, it is a simple matter to find how η_O, etc., vary with t_C by tabulation. For example the table below shows the effect of varying θ_C and therefore t_C assuming $T_O = 288°K$, $T_M = 1200°K$, $\eta_C = 0.85$, $\eta_T = 0.87$, $\eta_E = 0.90$ (i.e., the same assumptions as for Fig. 8-3b except for the variation of θ_C).

θ_C	t_C	T_C	θ_H	T_T	t_T	t_E	θ_E	η_O	f_S	W_S(HP)
200	1.590	488	712	1000	1.237	1.286	200.0	0.281	0.0163	122.2
250	1.738	538	662	950	1.315	1.322	208.1	0.314	0.0151	127.1
300	1.885	588	612	900	1.403	1.344	207.2	0.339	0.0140	126.6
350	2.033	638	562	850	1.504	1.351	198.9	0.354	0.0128	121.6
400	2.181	688	512	800	1.621	1.345	184.7	0.361	0.0117	112.9
450	2.328	738	462	750	1.758	1.325	165.4	0.358	0.0106	101.1

$$\left(t_C \text{ from } t_C = 1 + \frac{\eta_C \theta_C}{288} \quad T_C = 288 + \theta_C \quad \theta_H = 1200 - T_C \quad T_T = 1200 - \theta_C \right.$$

$$t_T = \frac{1200}{1200 - \frac{\theta_C}{\eta_T}} \quad t_E = \frac{t_C}{t_T} \quad \theta_E = \eta_E T_T \left(1 - \frac{1}{t_E}\right) \quad \eta_O = \frac{\theta_E}{\theta_H} \quad f_S = \frac{0.24 \times \theta_H}{10{,}500}$$

$$\left. W_S = 0.611 \theta_E \cdot \right)$$

The variation of η_O with θ_C is plotted in Fig. 4a which also shows the effect of changing T_M to 1100°K and 1300°K, using the same turbine efficiencies. This assumption means that the curve for T_M = 1300°K may be over optimistic and that for 1100°K a little pessimistic in that turbine efficiencies tend to fall with increase of T_M owing to losses resulting from blade cooling, etc. Also, as already indicated above it is unreasonable to assume that η_C, η_T and η_E are unaffected by θ_C, i.e., by the cycle temperature ratio t_C. This effect will be examined briefly below.

The values of W_S are shown in Fig. 4b. Fig. 4c shows pressure ratio p v. θ_C.

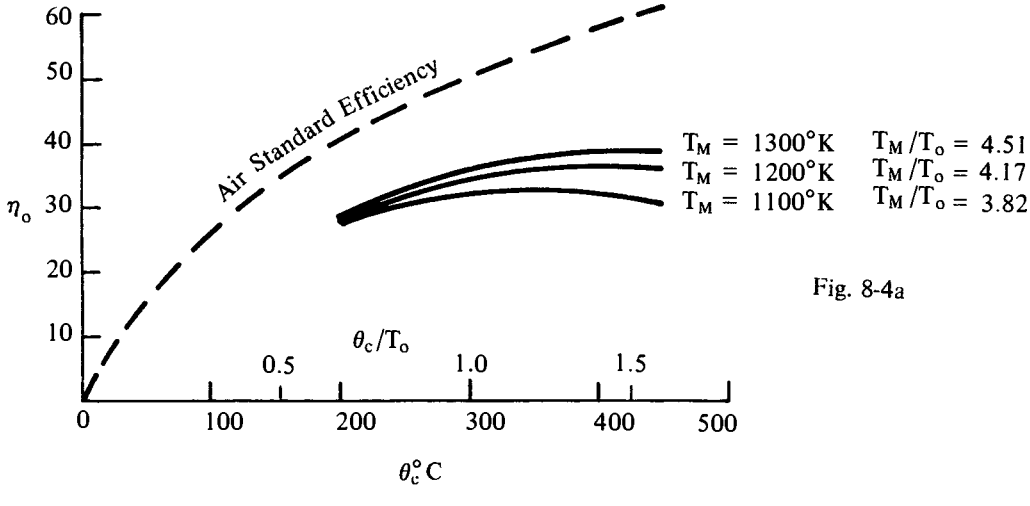

Fig. 8-4a

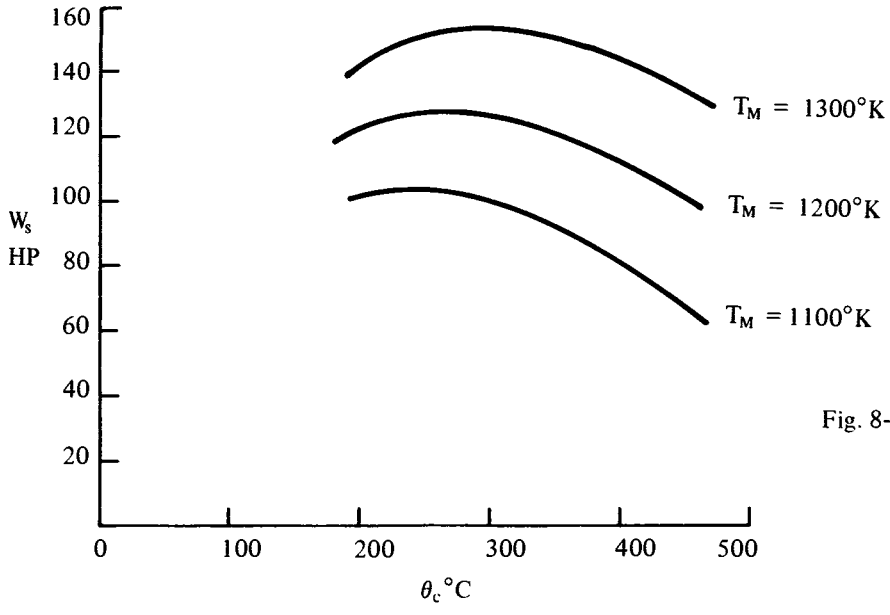

Fig. 8-4 b

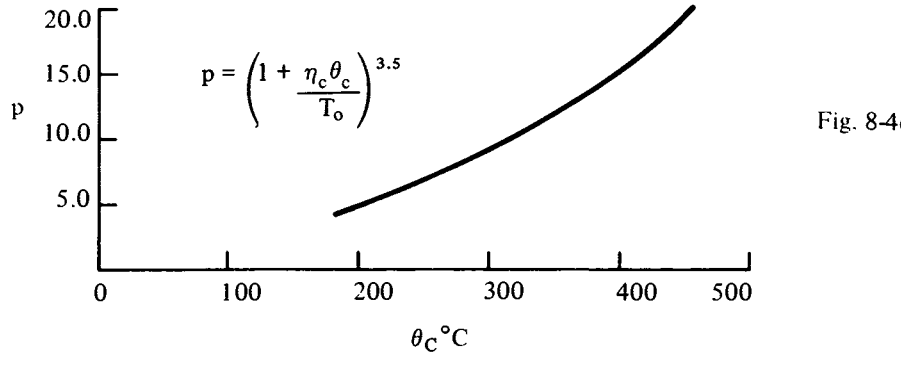

Fig. 8-4c

Polytropic Efficiency

It can be shown that if a compressor has n stages and it is assumed that each stage has the same temperature ratio t_s and the same stage efficiency η_{CS} then $\eta_C = \dfrac{t_s^n - 1}{\left(1 + \dfrac{t_s - 1}{\eta_{CS}}\right)^n - 1}$ from which η_C is found to be increasingly less than η_{CS} as n is increased. The proof is not difficult but it is not proposed to include it here because it is unrealistic to assume equal efficiency per stage because of the differences of geometry of successive stages (blade length, etc.) and the fact that, except for the first stage, each stage is receiving the disturbed flow from all the preceding stages.

The corresponding formula for a turbine of n stages each having stage temperature ratio t_{TS} and stage efficiency η_{TS} is

$$\eta_T = \frac{1 - \left[1 - \eta_{TS}\left(\frac{t_{TS} - 1}{t_{TS}}\right)\right]^n}{1 - \frac{1}{t_{TS}^n}}$$

from which η_T is found to be appreciably larger than η_{TS}, but again the assumptions are unrealistic. Nevertheless, it is a fact that compressor efficiency falls and turbine efficiency increases as temperature ratio increases.

Example 8-2

Assume that a compressor of 350° for θ_C can be regarded as three groups of stages of temperature rises and efficiencies as follows: 1st group 125° at 89%; 2nd group 100° at 89%; 3rd group 150° at 88%. What is the overall compressor efficiency if T_O = 288°K?

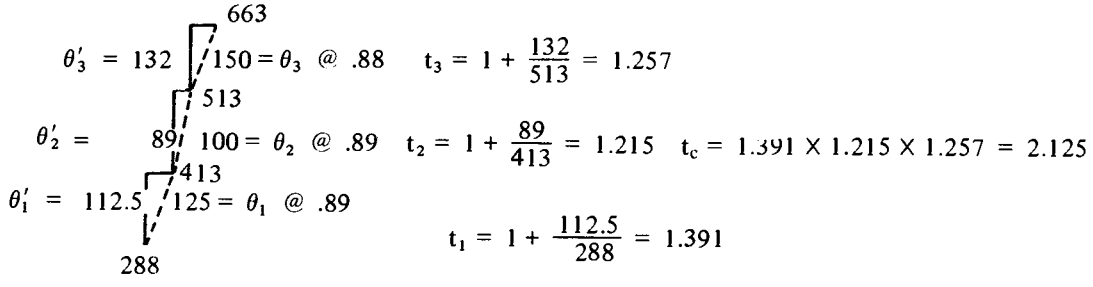

Fig. 8-5

From the layout of Fig 5, one may see that $\theta_C = 663 - 288 = 375°C$ and that $t_C = t_1 \times t_2 \times t_3 = 2.125 \therefore \theta_C' = 1.125 \times 288 = 324 \therefore \eta_C = \frac{324}{375} = 0.864$.

Example 8-3

It would be possible to drive the compressor of Example 2 with a single stage turbine in certain circumstances, but let it be supposed that with a T_M of 1300°K it is considered desirable to use a three stage turbine (to limit the need for blade cooling to the first stage and for other reasons) and that the temperature drops and stage efficiencies are as follows:

1st stage θ_{T1} = 200°C at η_{T1} = 0.86
2nd stage θ_{T2} = 90°C at η_{T2} = 0.91
3rd stage θ_{T3} = 85°C at η_{T3} = 0.91

What is the value of η_T for the compressor turbine?

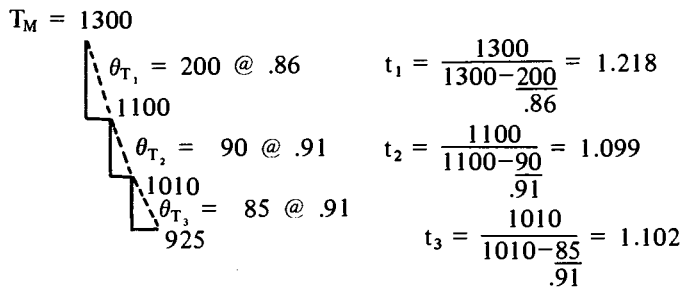

Fig. 8-6

From the layout of Fig. 6, $t_T = 1.218 \times 1.099 \times 1.102 = 1.475$ $\therefore \theta'_T = 1300 \left(\frac{0.475}{1.475}\right) =$ 418.6 and since $\theta_T = 200 + 90 + 85 = 375$ $\eta_T = \frac{375}{418.6} = 0.896$.

Example 8-4

Using the figures of Examples 2 and 3, and assuming that final expansion efficiency $\eta_E = 0.9$, what is η_O?

Since, (from Example 2), $t_C = 2.125$ and, (from Example 3), $t_T = 1.475$ $t_E = \frac{2.125}{1.475} =$ 1.4407 $\therefore \theta_E = 0.9 \times 925 \left(\frac{0.4407}{1.4407}\right) = 254.7°C$. From Example 2, $T_C = 663°K$

$\therefore \theta_H = 1300 - 663 = 637°C$ $\therefore \eta_O = \frac{\theta_E}{\theta_H} = \frac{254.7}{637} = 0.40$

This improvement as compared with the curve for 1300°K in Fig. 4a is, of course, due to the higher values of η_C and η_T.

It may be seen from the tabulation associated with Example 1 that specific power peaks at a much lower value of θ_C than that for maximum efficiency but this is greatly offset by the effect of pressure ratio on the mass flow rate. This is the subject of the following section.

SECTION 9
Mass Flow Rate in Gas Turbines

The thermal cycles discussed in Sections 7 and 8 provide means for calculating directly such quantities as specific fuel consumption, specific power, etc., but for complete performance calculations it is, of course, essential to know the mass flow rate Q.

A simple 'axiom' may be stated here: "What flows in is determined by what can get out." In the limit, if the exhaust (and any other means of escape) is completely blocked off there can be no through flow (as in the case of a pitot tube). One would think that the above stated axiom is self evident, yet one of the longest and most costly patent infringement actions in British history (Rateau vs. Rolls Royce and others) turned on it, in that Rateau claimed that, in jet engines and the like, a divergent intake ahead of a compressor 'controlled' the axial velocity at the compressor inlet, which was tantamount to arguing that the shape of the intake duct was a controlling factor in determining the throughput. In fact, unless it has a choking throat, the only way in which the intake duct can influence the mass flow is by the small effect its efficiency has on overall pressure ratio.

The design value of Q is determined by the designer to meet the power W_D needed for the design purpose. If the design specific power is W_{SD} then $Q_D = \frac{W_D}{W_{SD}}$. The value of Q_D thus decided determines the size of the power plant and 'fixes' a number of critical apertures, e.g., turbine nozzle throats, exhaust duct dimensions, etc. These critical areas then determine the value of Q at all running conditions.

In short, Q depends primarily on the geometry of the expansion part of the system. (As will be seen later, there are circumstances where 'variable geometry' may be used to obtain more desirable values of Q in certain modes of operation.)

There is, however, a limiting factor of considerable importance, namely the maximum permissible value of the axial velocity at entry to the first stage compressor rotor blades. In the limit this cannot exceed the local speed of sound, but, in the present state of the

art, it normally has to be well below this to keep down the Mach number relative to the moving blades at full speed. The axial velocity at entry to the first compressor rotor is usually designed to be in the range 500–550′/sec. This, coupled with the largest possible tip/hub ratio, i.e., $\frac{\text{blade tip diameter}}{\text{blade root diameter}}$ at the entry plane, for the first rotor often determines the diameter of an engine (almost always in the case of aero–engines other than helicopter engines).

It will be obvious that, for geometrically similar engines with the same thermal cycles, the power will be proportional to the square of the diameter while the weight would be proportional to the cube of the diameter, i.e., the 'square–cube law' would apply, so it would seem to pay to use, say, 4 small engines instead of one engine of twice the size, but unfortunately, though the 'aerodynamic' scale down is feasible (at the expense of some loss due to scale effects, i.e., the effect of reduced Reynolds Number) the apparent potential 50% weight saving would not be achieved at reasonable cost because mechanical and manufacturing problems are greatly increased by size reduction. It is in fact, far easier to design efficient high power gas turbines than low power units of acceptable efficiency– hence the failure, to date, of the gas turbine to 'invade' the automotive and light aircraft fields.

Multiple small engines would also greatly complicate control problems, instrumentation, etc. In any case, designers have been very skilful in 'defeating' the square-cube law.

It has been shown in Section 2 that flux density ψ for isentropic flow is given by $\psi = 1.532\frac{P_T}{\sqrt{T_T}}\frac{\sqrt{t-1}}{t^3}$ for air (see Eq. 2-9) hence the flow Q through a duct of section S is given by $Q = \psi S = 1.532\frac{S \cdot P_T}{\sqrt{T_T}}\frac{\sqrt{t-1}}{t^3}$. It has also been shown that the maximum value of ψ is $\psi_C = 0.397\frac{P_T}{\sqrt{T_T}}$, (see Eq. 2-7) and occurs in choking throats when the temperature ratio from total to static in the throat is $t_C = 1.2$. It has further been shown that $\psi = 0.397\frac{P_T}{\sqrt{T}}$ is a good approximation for total to static temperature ratios in the range 1.15-1.25 which largely covers the values of t which occur in turbine nozzle and rotor blade rings.

Though the flow through a gas turbine is not isentropic due to losses it is nevertheless reasonable to assume that though the constant of proportionality will be affected by this fact, the magnitude of Q will still be proportional to the total pressure at entry to the first turbine stage and inversely proportional to $\sqrt{T_M}$, i.e., to assume that $\frac{Q}{Q_D} = \frac{P_D}{P}\sqrt{\frac{T}{T_D}}$ where the suffix D signifies a reference condition (e.g., the design values of P_{max} and T_{max}).

The value of Q can be affected by the compressor and combustion chamber characteristics in that if the power output is reduced by reduction of T_M, (i.e., cutting back on fuel injection) while maintaining speed of rotation, the resulting increase of mass flow will usually reduce compressor delivery pressure which tends to counteract the effect of reduced

T_M, the net effect being small. It is unusual, however, for a gas generator to maintain speed with reduction of fuel, but it can be done by manipulating the effective 'back pressure' at compressor turbine exhaust, e.g., by opening up the final nozzle in the case of a jet engine (a means used by the writer in the early days of jet engine development to obtain a limited range of compressor characteristics).

Referring to the curves of Figs. 8-4a and 8-4b of Section 8, one may see that for optimum efficiency for the values of T_M the following figures apply:

For T_m = 1100 max η_O occurs at θ_C = 350 and W_S = 92.6 HP/lb/sec (η_O = 0.33)
For T_m = 1200 max η_O occurs at θ_C = 400 and W_S = 112.9 HP/lb/sec (η_O = 0.36)
For T_m = 1300 max η_O occurs at θ_C = 450 and W_S = 134.0 HP/lb/sec (η_O = 0.39)

Thus, over the range considered, there is virtually a linear relationship between T_M and θ_C for optimum efficiency and between either T_M or θ_C and optimum efficiency.

As mentioned above, it is undesirable to exceed 500-550'/sec for the axial velocity at compressor entry and this fact will therefore decide the first stage compressor diameter for a given horse power.

Example 9-1

What is the diameter D of the first stage compressor for a 10,000 HP gas turbine, given T_O = 288°K, P_O = 2116 p.s.f. T_{max} = 1300°K; axial velocity at compressor entry = 550'/sec; θ_C = 450°C, and compressor tip/hub ratio = 2.0?

From above, W_S = 134 HP/lb/sec $\therefore Q = \frac{10{,}000}{134}$ = 74.63 lb/sec $\therefore 74.63 = \rho u S$ where S is the entry annulus = $\frac{0.75\pi D^2}{4}$. For u = 550'/sec. $\theta_u = \left(\frac{550}{147.1}\right)^2 = 13.98$ $\therefore$ t (total to static) for acceleration from u = 0 to u = 550 is given by $t = \frac{288}{288 - 13.98} = 1.051$ for which $\sigma = 1.051^{2.5} = 1.132$. The stagnation density $\rho_O = \frac{2116}{288 \times 96} = 0.0765$ $\therefore \rho$ at compressor entry = $\frac{0.0765}{1.132} = 0.0676$. $\therefore$ $74.63 = 0.0676 \times 550 \times \frac{0.75\pi D^2}{4}$ from which $D^2 = 3.408$ and D = 1.85 ft or 22.2".

For T_M = 1100°K and θ_C = 350, D would need to be increased in the ratio $\sqrt{\frac{134}{92.6}} = 1.203$. Why, therefore, one might ask, might a design be chosen which has a 20% larger diameter and substantially lower efficiency. The answer is that there are certain circumstances in which capital cost is more important than running costs, e.g., 'peak load lopping' in electric power generation where 'boost power' is required for only a fraction of total generating time. The machine with a lower T_{max} though larger in diameter, might be much cheaper by reason of fewer compressor and turbine stages and freedom from the complications of blade cooling, etc.

The above example illustrates the difficulty of scaling down. For a geometrically similar unit of 100 HP, the diameter would be 2-1/4" approximately which would be quite impractical from the manufacturing point of view, and the efficiency would be seriously

affected by scale effect. (This is a very hypothetical case and somewhat contradictory in that to obtain the 100 HP with efficiency reduced by scale effect, Q would have to be somewhat larger than is implied.)

The geometry having been 'frozen' for the design condition, Q for conditions other than design is, as stated above, given by $\frac{Q}{Q_D} = \frac{P}{P_D}\sqrt{\frac{T_D}{T}}$ where the suffix D again means the design condition.

Example 9-2

Taking the figures of Example 9-1 above and referring to Figs. 8-4a, 8-4b and 8-4c of Section 8, what would be the effect on power if 'throttling back' reduced θ_C to 400 with T_M = 1200°K and θ_C to 350 with T_M = 1100°K? (This example ignores the 'lock' which may exist between T_M and θ_C to be discussed later.)

For 400/1200 (this is an abbreviation for θ_c = 400°C and T_M = 1200°K) the overall pressure is ratio 15.31 as compared with 19.25 for the design case (450/1300)

$$\therefore \frac{Q}{Q_D} = \frac{15.31}{19.25}\sqrt{\frac{1300}{1200}} = 0.828, \text{ while } W_S \text{ is reduced from 134 HP/lb/sec}$$

to 107.3 HP/lb/sec $\therefore \frac{W_S}{W_D}\frac{Q}{Q_D} = \frac{107.3}{134} \times 0.828 = 0.6629$ $\therefore$ Total HP is reduced from 10,000 to 6,629 HP.

For 350/1100 the pressure ratio is 11.98 $\therefore \frac{Q}{Q_D} = \frac{11.98}{19.25}\sqrt{\frac{1300}{1100}} = 0.677$. W_S is reduced to 92.6 HP/lb/sec $\therefore$ Power = $0.677 \times \frac{92.6}{134} \times 10{,}000 = 4{,}675$ HP.

This example assumes that, over the range considered, component efficiencies are unchanged. While this may be reasonable for the gas generator for the range covered it is not so acceptable for the power turbine unless its function allows it to 'keep in step' with the gas generator unit. The variation of efficiency with load for the power turbine therefore depends upon its purpose. Thus, if driving an AC generator it must run at constant speed whatever the load. If driving a variable pitch airscrew or propellor the load would depend on pitch setting, aircraft speed, etc.

As will be shown later (and as might be guessed from the fact that temperature changes are measures of kinetic energy changes) θ_C tends to be proportional to the square of rotational speed N, hence in the last example $\frac{N}{N_D}$ for T_M = 1200°K and θ_C = 400°C would be $\sqrt{\frac{400}{450}} = 0.943$ and, for T_M = 1100°K and θ_C = 350°, would be $\sqrt{\frac{350}{450}} =$ 0.882, thus power varies very rapidly with N. Thus, in the last Example, at 88% of full speed the power is 46.7% of full power and at 94.3% of full speed the power is 66.3% of full power; again assuming that the nature of the load allows the efficiency of the power turbine to be maintained.

It will be noted, however, that for the speed range 88% to 100% the variation of $\frac{Q}{Q_D}$ is from 67.7% to 100%. Unfortunately the variation of axial velocity at compressor

entry is greater than this because the reduced axial velocity due to reduced Q means an increased density at compressor entry. The effect, however, is small for the range under discussion, and would be much smaller if the design speed axial velocity were more conservative—at the expense of increased diameter.

The foregoing suggests that in cases where gas turbine power plant is used at full power for only a small proportion of total running time it would be preferable to design the components to suit the part load condition which is most used and accept a small loss of component efficiency at full load.

The foregoing discussion does not take into account the sensitivity of compressor delivery pressure and efficiency to mass flow rate, especially in the case of multi stage axial flow compressors. This matter will also be discussed later.

SECTION 10

More on Part Load Performance of Gas Generators

The subject of part load performance has been dealt with in general terms in the preceding section. It is the purpose of this section to take a closer look at the relevant theory.

Since the output of pressurized and heated air (and combustion products) may be used for many different purposes – not necessarily involving power turbines – it is useful to think in terms of the gas power generated, and to use the concept of gas generator efficiency η_{GG}, defined as gas power generated/heat energy of combustion. The overall efficiency of the total power plant is then given by $\eta_O = \eta_{GG}\eta_E$. Thus, referring to Example 9-1 the 'gas horsepower' available would be $\frac{10{,}000}{0.9} = 11{,}110$ and η_{GG} would be $\frac{\eta_O}{0.9}$, i.e., $\frac{0.39}{0.9} = 0.433$ or 43.3%.

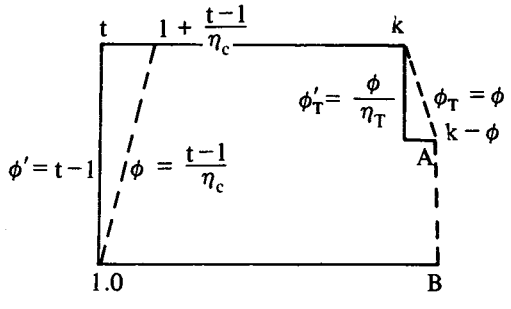

$$t_T = \frac{k}{k - \frac{\phi}{\eta_T}}$$

Fig. 10-1

The non-dimensional cycle for a gas generator is shown in the diagram of Fig. 1. All temperatures are shown as multiples of T_O and $\phi \equiv \frac{\theta_C}{T_O}$ etc. Expansion AB after the compressor turbine is unspecified.

If the pressure at k is P then the pressure at A is $\frac{P}{t_T^{3.5}} = P_A$ Q for expansion AB is the same as for the compressor turbine, ∴ if one may assume that, between A and B, there are nozzle rings or equivalent fixed areas such that $Q_{AB} \propto \frac{P_A}{\sqrt{k-\phi}}$ then we have $Q \propto \frac{P}{\sqrt{k}}$ for the compressor turbine. Since $Q = Q_{AB}$ it follows that $K_1 \frac{P}{\sqrt{k}} = K_2 \frac{P_A}{\sqrt{k-\phi}}$ where K_1 and K_2 are constants which include equivalent fixed areas.

Since $P_A = \frac{P}{t_T^{3.5}}$, $K_1 \frac{P}{\sqrt{k}} = K_2 \frac{P}{t_T^{3.5}} \sqrt{k-\phi}$ from which

$$t_T^{3.5} \sqrt{1 - \frac{\phi}{k}} = \frac{K_2}{K_1} = \text{const.} \qquad (10\text{-}1)$$

From the diagram of Fig. 1, $t_T = \frac{k}{k - \frac{\phi}{\eta_r}}$ or $\frac{1}{1 - \frac{\phi}{\eta_r k}}$

Substituting in (1) for t_T gives

$$\left(\frac{1}{1 - \frac{\phi}{\eta_r k}}\right)^{3.5} = \frac{K_2}{K_1} \frac{1}{\sqrt{1 - \frac{\phi}{k}}} \quad \text{or} \quad \left(1 - \frac{\phi}{\eta_r k}\right)^{3.5} = \frac{K_1}{K_2} \left(1 - \frac{\phi}{k}\right)^{0.5} \qquad (10\text{-}2)$$

From (2) one may see that, for the range over which η_T is substantially constant, $\frac{\phi}{k}$ = const. Thus it may be seen that the linear relationship between θ_C and T_M, found in Section 9, was no fluke. Since $\phi = \frac{t-1}{\eta_C}$ it follows that, over the range for which η_C may be considered virtually constant, $k \propto t - 1$. So $\frac{k}{k_D} = \frac{t-1}{t_D - 1}$.

Since $t_T = \frac{k}{k - \frac{\phi}{\eta_T}}$ and $k \propto \phi$, it further follows that the compressor turbine temperature ratio remains constant and equal to the design value. This being so, η_T will be substantially constant, hence there will cease to be any gas power available when t is reduced to t_T, i.e., when $\frac{k}{k - \frac{\phi}{\eta_r}} = t$. Then, of course $\eta_{GG} = 0$.

Summarizing the foregoing, we have the following useful conclusions: For the part load range over which η_C and η_T may be regarded as substantially constant; (a) $\frac{T_M}{\theta_C} = \text{const.} = \frac{T_{MD}}{\theta_{CD}}$ (b) $\frac{t-1}{t_D - 1} = \text{const.} = \frac{T_M}{T_{MD}}$ (c) $t_T = \text{const.} = t_{TD}$.

Example 10-1

If the design conditions of a gas generator unit are $T_O = 288°K$, $\theta_{CD} = 450°C$, $T_{MD} = 1300°K$, $\eta_C = 0.85$, and $\eta_T = 0.87$, at what values of θ_C and T_M would the gas power be nil?

$$k_D = \frac{1300}{288} = 4.514 \quad \phi_D = \frac{450}{288} = 1.5625 \quad \therefore t_T \text{ (at all conditions)} = \frac{4.514}{4.514 - \frac{1.5625}{0.87}} =$$

$1.661 = t = 1 + \eta_C\phi$ at zero gas power $\therefore \phi = \frac{0.661}{0.85} = 0.777 \quad \therefore \theta_C = 0.777 \times 288 = 223.9°C$

$\frac{k}{\phi} = \frac{k_D}{\phi_D} = \frac{4.514}{1.5625} = 2.889 \quad \therefore T_M = 2.889 \times 223.9 = 646.8$. The zero power values of θ_C and T_M are thus seen to be approximately half the design values which means that the speed of rotation would be about 71% of design.

Example 10-2

Using the data of Example 1, how would the zero power mass flow and fuel consumption compare with design?

The design temperature ratio of compression $t_D = 1 + \frac{0.85 \times 450}{288} = 2.328 \quad \therefore$ the pressure ratio is $2.328^{3.5} = 19.254$.

At zero power $t = 1.661 \quad \therefore$ the corresponding pressure ratio is $1.661^{3.5} = 5.91$. Also at zero power $T_m = 646.8 \quad \therefore \frac{Q}{Q_D}$ for $W = 0$ is given by $\frac{Q}{Q_D} = \frac{5.91}{19.254}\sqrt{\frac{1300}{646.8}} = 0.435$.

Since θ_C at $W = 0$ is 223.9; $\theta_H = T_M - T_C = 646.8 - (288 + 223.9) = 134.9$ while $\theta_{HD} = 1300 - (288 + 450) = 562 \quad \therefore$ the relative fuel consumption is $\frac{134.9}{562} \times \frac{Q}{Q_D} = 0.24 \times 0.435 = 0.104$, i.e., the fuel consumption at $W = 0$ is about 10% of that at design speed. In practice, whatever follows the gas generator is bound to cause some back pressure unless completely by-passed, which means that fuel consumption, idling speed, etc., would be somewhat greater than those calculated in the above two examples.

In Section 9 and referring to Fig. 4a of Section 8 the apparent linear relationship between η_O and θ_C at the higher values of θ_C was purely fortuitous since, as seen above, $\eta_O = 0$ when $\theta_C = 223.9$. In fact η_O falls off very rapidly below $\theta_C = 350$.

As previously indicated, the efficiency and power of any device which uses the energized gas generated by the gas generator are not necessarily simple multiples of η_{GG} and W_{gg} (i.e., gas power) but the part load behavior of the gas generator will give a useful indication of the characteristics of the complete system.

From the foregoing reasoning, and using $a = \frac{k_D}{\phi_D}$ it is now possible to draw a 'doubly non-dimensional' diagram for the gas generator portion of the cycle as shown in Fig. 2.

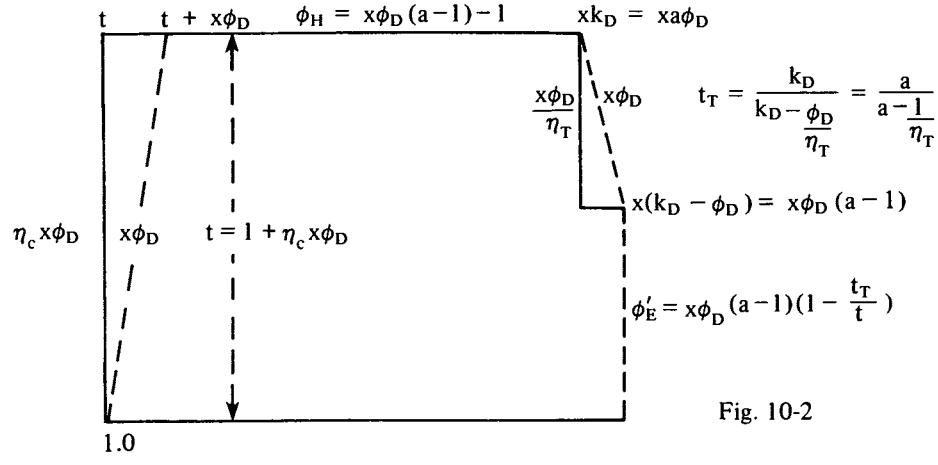

Fig. 10-2

ϕ'_E, of course, is the specific gas power available as a multiple of T_O. Writing $\phi'_E = W_S$ then

$$\frac{W_S}{W_{SD}} = \frac{x\left(1 - \frac{t_T}{t}\right)}{1 - \frac{t_T}{t_D}} \tag{10-3}$$

where the suffix D again implies the design condition.

For mass flow,

$$\frac{Q}{Q_D} = \frac{P}{P_D}\sqrt{\frac{T_{MD}}{T_M}} = \left(\frac{t}{t_D}\right)^{3.5}\sqrt{\frac{1}{x}} \tag{10-4}$$

Hence, multiply (1) and (2) $\frac{W}{W_D} = \sqrt{x}\left(\frac{t}{t_D}\right)^{3.5}\left(\frac{1 - \frac{t_T}{t}}{1 - \frac{t_T}{t_D}}\right)$ which may be written

$$\frac{W}{W_D} = \sqrt{x}\left(\frac{t}{t_D}\right)^{2.5}\left(\frac{t - t_T}{t_D - t_T}\right) \tag{10-5}$$

For given values of ϕ_D and a, t_D and t_T are constants $\therefore$ one may write

$$\frac{W}{W_D} = A\sqrt{x}(1 + Cx)^{2.5}(1 + Cx - B) \tag{10-6}$$

where $A = \frac{1}{t_D^{2.5}(t_D - t_T)}$; $C = \eta_C\phi_D$ and $B = t_T = \frac{a}{a - \frac{1}{\eta_T}}$. Again, it may be seen that if $1 + Cx = B = t_T$ then $\frac{W}{W_D} = 0$.

Points to note are that (i) $\sqrt{x}$ is a measure of rotational speed N and (ii) since torque x N is proportional to W the torque-speed variation is very rapid for gas turbine engines so that though reduction gears may be (and often are) necessary there should rarely be need for change speed gears.

Example 10-3

Given the following data (a) $\phi_D = \frac{\theta_C}{T_C} = 1.5$; (b) $a = \frac{T_N}{T_O}\frac{1}{\phi_D} = 4.0$; (c) $\eta_C = 0.86$; (d) $\eta_T = 0.88$ and assuming that $\frac{N}{N_D} = \sqrt{x}$, what is the value of $\frac{N}{N_D}$ for $\frac{W}{W_D} = 0.75$?

$t_D = 1 + 0.86 \times 1.5 = 2.290$: $t_T = \frac{4}{4 - \frac{1}{0.88}} = 1.397$ $\therefore$ the constants for Equation (4) are: $A = \frac{1}{2.29^{2.5}}(2.290 - 1.397) = 0.141$ $C = 0.86 \times 1.5 = 1.29$

$B = t_T = 1.397$ $\therefore$ from (6) $0.75 = \sqrt{x} \times 0.141\ (1 + 1.29x)^{2.5}(1 + 1.29x - 1.397)$

or $\frac{0.75}{0.141} = \sqrt{x}\,(1 + 1.29x)^{2.5}(1.29x - 0.397) = 5.319$: from this x is found to be 0.917

hence $\frac{N}{N_D} = \sqrt{0.917}$, i.e., N is just under 96% of N_D.

SECTION 11

Gas Turbines With Recuperators

If the exhaust temperature of a gas turbine unit is higher than the temperature at compressor delivery, it should be possible in theory to transfer some of the waste heat of exhaust to the compressed air by means of a heat exchanger or recuperator (sometimes 'regenerator' is used) and thereby to reduce the amount of heat addition in combustion. The effect on overall efficiency can be very large when the pressure ratio is modest and T_M is high as may be seen from the diagrams of Figures 1a and 1b which have the same values of θ_C, T_m, η_c (= 0.87), η_T (= 0.87) and η_E (= 0.90). In Figure 1b it is assumed that a recuperator of 80% transfer efficiency (of counter flow type) is used to transfer exhaust heat to the compressor delivery air thereby raising its pre-combustion temperature to 793.2°K, thereby cutting θ_H from 862°C to 606.8°C. The effect on efficiency is striking. For the cycle of Figure 1a $\eta_o = \frac{293}{862} = 0.34$ or 34%. With the recuperator $\eta_o = \frac{293}{606.8} = 0.483$ or 48.3%.

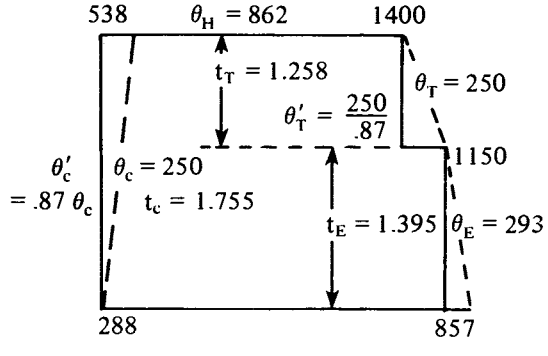

Fig. 11-1a

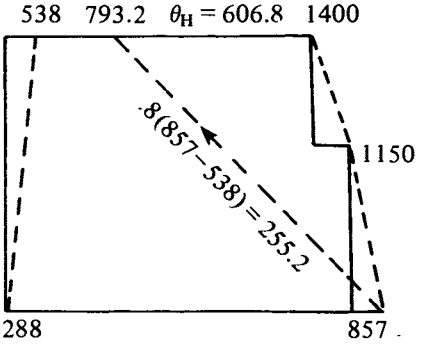

Fig. 11-1b

This example was a more or less random selection and is not an illustration of the whole possibilities of the use of a recuperator. Further, it is not a true comparison in that recuperator pressure loss would reduce both the effective power turbine efficiency and the effective delivery pressure, i.e., the effective value of η_c, but even if one reduces η_C to 0.85, and η_E to 0.88 to allow for recuperator losses, η_O is still 47%.

Unfortunately, recuperators of a capacity sufficient to achieve heat transfers of the order of 80% present severe technical problems in addition to pressure loss. Those problems include great bulk and weight, manufacturing costs, installation, thermal expansion, cleaning difficulties, and so on.

Heat exchangers are familiar features of everyday life, e.g., steam boilers, car radiators and cylinder jackets in liquid cooled piston engines, air conditioning units, refrigerators, etc., but, except for massive steam boilers, the rate of heat transfer is minute compared with that necessary in gas turbines. Thus, for example, if the cycles of Figure 1 were for 1000 HP the mass flow would be $\frac{1000}{293 \times 0.611} = 5.586$ lb/sec, hence the rate of heat transfer would need to be 5.586 x 255.2 x 0.24 = 342 CHU/sec, equal to 871 HP or 87.1% of the power output. (A reader might say "yes!, but what of it?" auto engines have to get rid of about 25% of the heat value of the fuel consumed via the radiator and this is roughly the same as the power produced." The reply to this is that the transfer is from liquid (water plus anti freeze) to air and not from air to air as in the case of gas turbines.)

There are several types of heat exchanger, but it is not proposed to deal with the various alternatives - parallel flow, cross flow, rotating matrices (in which a cylindrical 'honeycomb' rotates with one portion in the low pressure hot stream, becoming heated up, and with the other portion in the high pressure 'cool' stream where it parts with the heat picked up in the hot stream. So far as is known to the writer, none of the many attempts to solve the sealing problem has succeeded.), etc., because only in the case of the counter flow type can there by any hope of transfers of the order of 80%. Any other type, even if the transfer were 100%, could not raise the pre-combustion temperature by more than 50% of the difference between exhaust temperature and compressor delivery temperature.

The theory of heat transfer in recuperators is very complex and is beyond the scope of this present work. A few major factors will, however, be pointed out, as follows:

(1) The main 'mechanism' of heat transfer from a gas to a metal dividing surface is by convection through the boundary layer. Radiation and conduction are negligible by comparison with convection (gases have a very low thermal conductivity as compared with metals) thus, as was pointed out by Osborne Reynolds about a century ago, there is a close relationship between surface drag and convection. Indeed, as a rough approximation, the rate of heat transfer per unit area from air to surface and vice versa is, like drag, proportional to ρu^2. This apparently simple rule, however, is complicated by the fact that as the fluid is heated or cooled the density varies inversely with the temperature, so that, in a duct of uniform section, since the product $u\rho$ remains constant u must be proportional to temperature, from which it follows that ρu^2 is proportional to temperature (changes in pressure being considered negligible).

(2) It will be fairly obvious that the rate of heat transfer from fluid to metal and vice versa will be proportional to the surface area and the temperature difference.

(3) The conductivity of metals is so high compared with gases that for thin tubes or plates separating gas streams, the temperature drop in the metal may be regarded as negligible.

(4) From (1) and (2) above it follows that the rate of heat transfer per unit area is proportional to velocity, since, if area is increased (by, say, increasing tube diameter) u is decreased.

Since pressure loss is proportional to surface drag it follows that a recuperator for large heat exchange and low pressure loss must be very bulky if of tubular construction. Even so, the potential fuel saving is so great that it is worth taking a more detailed look at gas turbine cycles with recuperators assuming that a transfer coefficient of 0.8 can be achieved. This may be conservative since the writer has heard that 0.85 has been obtained in at least one case though at what expense in pressure loss he was not told.

Figure 2 is a repeat of Figure 1b in non-dimensional form (T_E, T_C, H, etc., are multiples of T_O) in which it is assumed that 80% of the difference between T_E and T_C is added to T_C by a recuperator, to give a pre-combustion temperature of T_R.

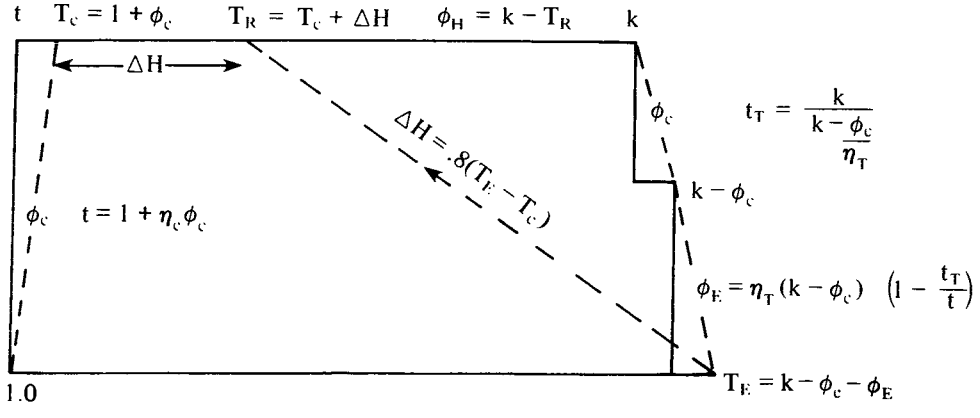

Fig. 11-2

Specific power for given values of ϕ_C and k is the same as for a power unit without a recuperator but, as long as T_E exceeds T_C, ϕ_H is reduced by $\Delta H = 0.8(T_E - T_C)$ and the overall efficiency correspondingly increased.

With a recuperator ϕ_H is found to be $\phi_H = 0.2k + 0.6\phi_C + 0.8\phi_E - 0.2$. Without a recuperator $\phi_H = k - \phi_C - 1$, hence the recuperator increases η_o in the ratio

$$\frac{0.2k + 0.6\phi + 0.8\phi_E - 0.2}{k - \phi_C - 1}$$

if one neglects recuperator pressure losses (an admittedly dubious assumption).

The curves of Figures 3a and 3b show the effect of an 80% recuperator as compared with non regenerated units for values of k = 4.0, 4.5 and 5.0 and over a range of ϕ_C = 0.3 to 1.1. The curve for air standard efficiency is also shown.

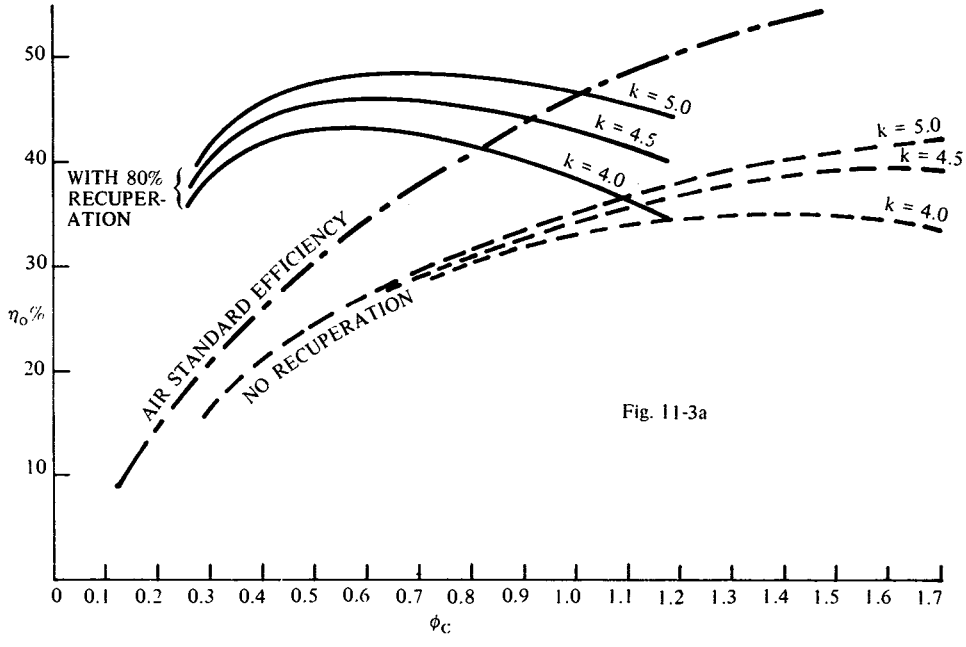

Fig. 11-3a

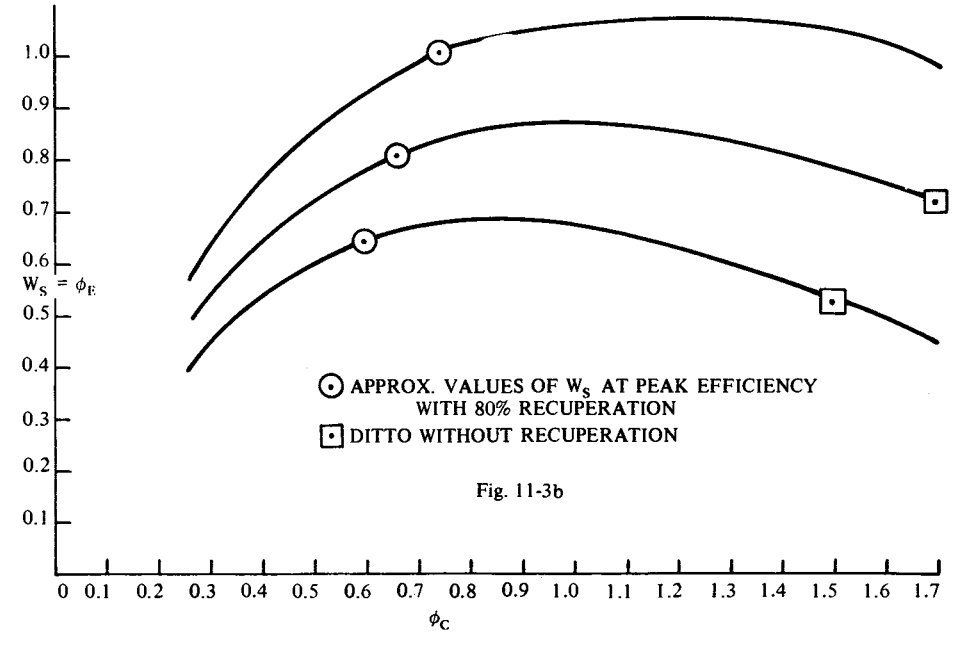

Fig. 11-3b

In calculating these curves it was assumed that η_C decreased linearly from 0.88 at ϕ_C = 0.3 to 0.85 at ϕ_C = 1.1 and that η_T decreased from 0.9 at k = 4.0 to 0.87 at k = 5.0 (to allow for blade cooling) but η_E was left unaltered at 0.88 which is probably rather 'unfair' for the unregenerated edition.

If the curves were prolonged beyond $\phi_C = 1.1$, then, for a given value of k they would intercept when $T_E = T_C$.

The most striking thing to note is, that with a recuperator, peak efficiencies occur at much lower pressure ratios. Indeed they exceed air standard efficiency very substantially. This means, however, that though specific power is the same at given values of ϕ_C and k and, for a given value of k, would not differ greatly at corresponding peak efficiencies (see Figure 3b), the much lower pressure ratio of the 'recuperated' plant means that for a given total power, the diameter of compressors and turbines would have to be substantially larger—which can be a very helpful fact for power units of low design power. Even so, a 100 HP unit with axial velocity at compressor entry of, say, 300′/sec and a tip hub ratio of 1.3 would still be under 4.5″ diameter with first stage blades about 0.5″ long. Nevertneless, this seems to be in the range of practicable possibility and well worth development effort to achieve it, even if efficiencies of less than 30% have to be accepted. Indeed, if a single stage centrifugal compressor could achieve 80% efficiency at the modest pressure ratio of 3.25, overall efficiencies of well over 30% should be possible, and with a centrifugal compressor there might be a reasonable hope that production cost could be competitive with the reciprocating engine.

Using some crude and rather hasty methods, the writer estimates that a counter flow heat exchanger of 80% transfer capacity in which the compressed air flows through a number of unfinned tubes in parallel would require a volume of about 21 cubic feet for a 100 HP unit at the expense of about 5 HP in pressure loss. The effective HP loss would, however, be less than this because some of the friction heating in the high pressure ducting (i.e., between compressor delivery and combustion) would be partially recovered in expansion (as in the case of compressor losses) and the dynamic pressure of the inevitable exhaust velocity from the power turbine might well be sufficient to discount the pressure loss in the hot low pressure ducting.

By using longitudinal fins on the tubing and other devices, the above quoted volume could probably be reduced by 50% or more, at the expense of a considerable increase in manufacturing cost.

Figure 4 is a diagrammatic representation of a counter flow heat exchanger in which the low pressure hot exhaust flows from right to left through the annulus of section $S_h - S_C$, and the cooler compressed air from the compressor delivery flows left to right through a tube of diameter d and section S_C. It is assumed that there is no heat loss through the outer wall of the insulated annulus.

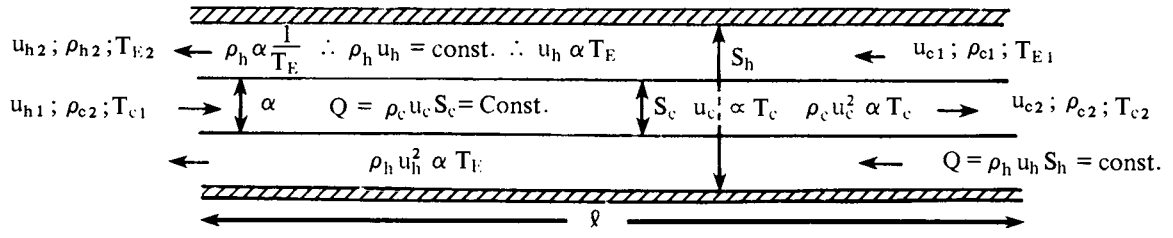

Fig. 11-4

It may be seen that the area available for heat transfer from annulus to tube per unit length is proportional to d. It will be obvious that if the single tube shown is subdivided into n tubes in parallel, each of section $\frac{S_c}{n}$ then the surface per unit length will be increased n times, so that for a given total transfer surface, ℓ may be reduced to $\frac{\ell}{n}$, hence the volume $\ell \times S_h$ tends to vary inversely as n (the word 'tends' is used because there will be scale effects on the heat transfer coefficients). For a given pressure difference, the thickness of the tube walls may also be decreased by $\frac{1}{n}$ but there is a practical limit to this.

If ΔT_1 is the temperature difference between the annulus and the surface of the tube (or tubes) and ΔT_2 is the temperature difference between the tube wall and the flow in the tube, though $\Delta T_1 + \Delta T_2$ will tend to remain constant, the ratio $\frac{\Delta T_1}{\Delta T_2}$ will be affected by the fact that ρu^2 increases in the direction of flow within the tube (or tubes) and therefore the rate of heat transfer per °C, while the opposite happens external to the tubes, therefore $\frac{\Delta T_1}{\Delta T_2}$ will increase from right to left. Again, how this will happen will depend on scale effect, the effect of temperature on viscosity, etc.

In short, in order to keep down the volume and weight of a tubular type counter flow heat exchanger, it is desirable to have the largest practicable number of tubes in parallel for the desired rate of flow and to mount them in such a manner as to avoid thermal expansion and other problems.

It is not intended to imply in the foregoing that only tubular types are feasible, but the writer does not wish to become involved in a long dissertation on ways of preventing distortion by pressure differences across non-tubular surfaces.

SECTION 12
Turbo-Compressors and Turbines

The wording of the heading is chosen to exclude discussion of many types of compressors which are not used as major components of gas turbines, e.g., piston type compressors, rotary compressors such as the 'Rootes Blower,' sliding vane types, etc.

The words 'continuous flow' are also implied in the heading, since it is not intended to cover intermittent flow 'explosion' turbines such as proposed by Holzwarth and others.

The compression process in a gas turbine is performed in a centrifugal compressor or an axial flow compressor or a combination of both. If both types are used, the axial flow compressor invariably precedes the centrifugal type.

In the case of air breathing aircraft engines, the deceleration of the intake air can contribute substantially to the total compression ('ram compression'). Indeed in ramjets, ram compression is the only compression.

The expansion process in gas turbines takes place in turbines having 'full peripheral admission.' They may be either of axial flow type or radial flow type, the former being by far the most common.

In the case of aircraft gas turbines, the latter part of the expansion is used to produce a 'propelling jet,' the expansion in the turbine stage or stages being just sufficient to drive the compressor or compressors (and low power auxiliaries such as fuel pumps, generators, etc.)

Torque and Angular Momentum

Newton's second law of motion states that the rate of change of momentum is proportional to the applied force and takes place in the line of action of the force. ('Momentum' is the product of velocity and mass.)

For many purposes, this law may be re-stated as 'the rate of change of angular momentum is proportional to the applied torque.' This may be regarded as the 'key law'

for turbo machinery, the torque and angular momentum being measured relative to the axis of rotation. It should be pointed out, however, that the law is not particular to rotating components; it is absolutely general as may be seen by reference to Figure 1.

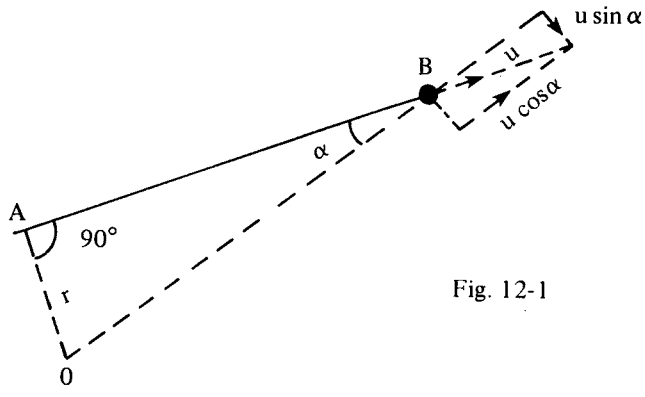

Fig. 12-1

If a particle of mass m is at B and is travelling at uniform velocity u in the direction AB then, if O is *any* point in space, the component of u normal to OB is $u\sin\alpha$, and the component in the direction OB is $u\cos\alpha$. This latter, passing through O, has no component of angular momentum about O $\therefore$ the angular momentum about O is $u\sin\alpha$ x OB, i.e., since $OB\sin\alpha = AO \equiv r \therefore u \times OB \sin\alpha = ur$. Thus, if the linear momentum mu is constant so is the angular momentum about *any* point in space. (The 'rotational version' of Newton's first law.)

If the particle is being acted upon by a force F, also in the direction AB, then $Fr = mr\frac{du}{dt}$ or $Fr = \frac{d}{dt}(mru)$, i.e., torque about O equals the rate of change of angular momentum about O.

This elementary piece has been included because, in dealing with rotary machinery one may be apt to forget that the relevant reference point is not necessarily the axis. For example, suppose Figure 2 represents a small disc A mounted near the rim of a large disc B on a frictionless bearing at O′, then however great the angular acceleration of B there is no torque acting on A about O′ so A will have reverse rotation relative to B, i.e., one revolution clockwise for every revolution of B, hence relative to a stationary observer the tangental velocity about O at a point on A at a radius greater than OO′ will be less than if A were fixed to B and conversely for any point on A less than OO′ from O. (This example is relevant to the concept of the 'relative eddy' which, inter alia, explains why the whirl velocity of the fluid leaving the tips of centrifugal compressor blading, is somewhat less than the tip velocity of the blades, i.e., there is a 'slip factor'.)

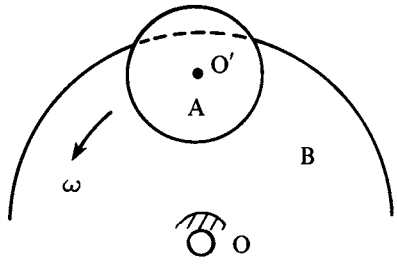

Fig. 12-2

Nevertheless, in the case of turbo machinery, the axis of rotation is the reference for torque and angular momentum. Thus *the torque generated by a turbine is equal to the rate of reduction of angular momentum in the driving fluid.* Similarly *the torque required to drive a compressor or pump is equal to the increase induced in the rate of angular momentum.* (These statements require minor modifications in that bearing friction and windage losses detract slightly from the effective torque generated by a turbine and add to the torque necessary to drive a compressor.) It follows that when a turbine is directly driving a compressor at uniform speed, except for the minor qualifications mentioned above, the rate of change of angular momentum in turbine and compressor must be equal and opposite. An interesting example of this principle is furnished by Nernst's proposal illustrated diagrammatically in Figure 3. Nernst proposed a 'U tube' arrangement rotating at high speed around axis AB, with combustion at C. Air in the ascending leg was compressed by centrifugal force, heated at C and then expanded down the descending leg to exhaust with a greater pressure and temperature than at entry thus having had its energy augmented. There being no net change of angular momentum between entry and exit no driving torque was necessary except for bearing friction and air resistance (which would be high unless there were an enclosing drum). Unfortunately this simple gas generator was impracticable because of the low compression obtainable at C with available materials. Moreover, the potential for increased compression by utilizing the kinetic energy at C could not be used. Nevertheless the device contains the germ of the concept of combining a radial flow compressor with a radial flow turbine as has been done, notably by Von Ohain in the first German turbo-jet engine.

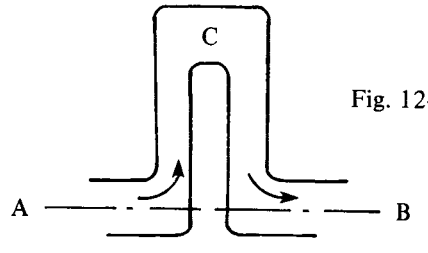

Fig. 12-3

Definition of Efficiencies

An outstanding characteristic of turbo machinery is the enormous volumetric capacity in proportion to size as compared with all other types of power generating machinery, e.g., reciprocating piston engines. So much so that heat loss through casings may be taken as negligible in comparison with the energy changes involved. In other words, the processes

of compression and expansion may be regarded as 'adiabatic.' Hence, if there were no losses, i.e., no conversion of kinetic energy into internal energy by friction and turbulance, etc., the processes of compression and expansion would be isentropic. These losses, however, are unavoidable, hence the measure of the efficiency of a compressor – the 'adiabatic efficiency' – is the ratio of the energy input required to achieve a given pressure ratio isentropically to the energy input actually required, i.e., the isentropic increase of enthalpy divided by the actual increase of enthalpy for the pressure ratio. For constant specific heat, enthalpy is proportional to temperature, hence one may define adiabatic efficiency of compression as $\eta_c = \frac{\theta'_c}{\theta_c}$ where θ'_c is the isentropic total temperature increase and θ_c is the actual total temperature increase for the pressure ratio (total to total).

It could be argued that this definition of compression efficiency leaves something to be desired in that a part of the losses are recoverable on expansion and to that extent they are not a 'dead loss,' but this fact can be readily allowed for in cycle calculations.

In expansion through a turbine the adiabatic efficiency η_T is given by $\eta_T = \frac{\theta_T}{\theta'_T}$ if one assumes constant specific heat, where θ_T is the actual temperature drop (total to total) and θ'_T is the isentropic temperature drop (total to total) corresponding to the pressure ratio (total to total).

Occasionally, when the axial velocity at exhaust is high, it may be necessary to think in terms of shaft efficiency η_{TS} defined as $\eta_{TS} = \frac{\theta_T - \theta_a}{\theta'_T}$ where θ_a is the temperature equivalent of the kinetic energy of the exhaust axial velocity, i.e., treating θ_a as a loss so far as shaft power is concerned, though normally it is not a real loss because it forms part of the energy available for further expansion through another turbine or propelling jet.

Example 12-1

A compressor takes in air from the atmosphere of temperature = 288°K and pressure = 2116 lb/sq ft and compresses it to a total pressure of 14000 lb/sq ft; the total temperature at delivery is found to be 531°K. What is the adiabatic efficiency?

The pressure ratio is $\frac{14000}{2116} = 6.616$ $\therefore$ the isentropic temperature ratio is $6.616^{0.286} = 1.717$ $\therefore$ the isentropic temperature rise = 0.717 x 288 = 206.5, i.e., $\theta' = 206.5$. The actual temperature rise $\theta = 531 - 288 = 243$ $\therefore \eta_c = \frac{206.5}{243} = 0.85$ or 85%.

Example 12-2

Expansion in a turbine takes place from a total pressure of 1650 p.s.f. and total temperature of 1150°K to a total pressure at exhaust of 778 p.s.f. The total temperature at exhaust is found to be 950°K. Assuming the driving fluid is air and that specific heat is constant at $C_P = 0.24$, what is the adiabatic efficiency?

The pressure ratio $p_T = \frac{1650}{778} = 2.121$ $\therefore$ the temperature ratio (isentropic) t_T is given by $p_T^{0.286} = t_T$ $\therefore t_T = 2.121^{0.286} = 1.24$ $\therefore$ the isentropic temperature drop θ'_T =

$1150\left(1-\frac{1}{1.24}\right) = 222.6°C$; θ_T, the actual temperature drop, $= 1150 - 950 = 200°C$

$\therefore \eta_T = \frac{200}{222.6} = 0.899$ or 89.9%.

Example 12-3

If the turbine of Example 2 above has an exhaust axial velocity of 800′/sec, what is the shaft efficiency and the static pressure at exhaust?

The temperature equivalent of 800′/sec $= \left(\frac{800}{147.1}\right)^2 = 29.6°C$ hence $\eta_{TS} = \frac{200 - 29.6}{222.6} =$ 0.766 or 76.6%.

The total temperature at exhaust being 950°K, the static temperature at a velocity of 800′/sec $= 950 - 29.6 = 920.4°K$ $\therefore$ the total to static temperature ratio $= \frac{950}{920.4} = 1.032$. The corresponding total to static pressure ratio is $1.032^{3.5} = 1.117$ $\therefore$ the static pressure is $\frac{778}{1.117} = 696.4$ p.s.f.

This example illustrates the large difference there may be between adiabatic efficiency and shaft efficiency if exhaust axial velocity is high.

CENTRIFUGAL COMPRESSORS

Centrifugal (or 'radial flow') compressors and pumps have a longer history in engineering because of their fundamental simplicity but have been largely overtaken in gas turbine technology by axial flow types because intensive development of the latter has led to the achievement of substantially higher adiabatic efficiencies at the high pressure ratios of modern gas turbines. Centrifugal types are still extensively used, however, for many engineering purposes. Also there are a few gas turbine engines in which a centrifugal compressor is used for the final stage of compression where efficiency is rather less important than in the initial stages of compression. Moreover, there are still many Rolls Royce 'Dart' turbo-prop engines in service having two stage centrifugal compressors. Further, in small gas turbines for auxiliary purposes where efficiency is not all important, centrifugal compressors still have their uses, largely again because of their simplicity and the fact that they 'scale down' more easily.

(The terms 'radial flow' and 'axial flow' are somewhat unsatisfactory descriptions because the flow in compressors is never purely radial or axial except at entry or discharge. 'Radial flow' means that the component of velocity which carries the fluid through the compressor is radial. 'Axial flow' means that the component of velocity which carries the fluid through is parallel to the compressor axis. 'Radial flux' and 'axial flux' might be better descriptions.)

The large diameter of the centrifugal compressor is another big disadvantage as compared with the axial flow type. This is of special importance in aircraft gas turbines and more than compensates for the much greater length of the axial flow type. However, the use of a centrifugal stage at the high pressure end of a compound compressor is much less of an embarrassment from the size point of view because the volumetric capacity necessary is much reduced by the preceding compression.

There are several types of centrifugal compressors, but by far the most common is the unshrouded radial vane type as used in aero engine superchargers for many years before the advent of the jet engine, and as used by the writer in his early jet engine designs.

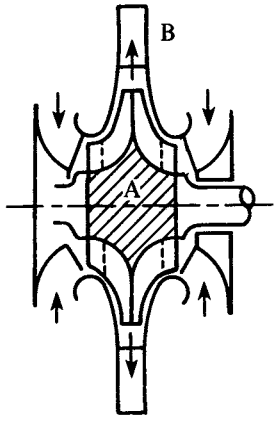

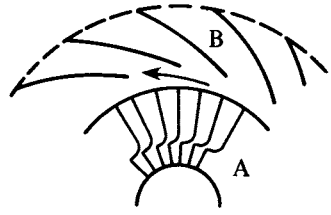

Fig 12-4

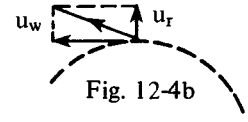

Fig. 12-4b

Figure 4 is a rough representation of the double sided radial vaned centrifugal compressor used in the first jet engine, the left hand sketch being a section through the axis and the right hand sketch being a partial view of the impellor A and diffuser blade ring B. The volute into which the diffuser channels discharged is not shown.

The velocity vector diagram for the air leaving the impellor periphery is shown in Figure 4b.

The choice of a double sided compressor was based on the necessity to get the maximum possible flow in proportion to size and thereby reduce the surface friction and other losses as compared with a single sided compressor of the same volumetric capacity. Moreover, this arrangement resulted in a much better match with its directly coupled driving turbine.

The design tip speed was 1470′/sec hence, with the materials available, stress considerations precluded the use of other than radial vanes and the fitting of shrouds. (Shrouds are 'cover plates' attached to the edges of the radial vanes to prevent leakage from the high pressure to the low pressure sides of the blading through the clearance between the high speed impellor and the stationary casing. Shrouded impellors are generally considered to be more efficient where rotational speeds are low enough to permit their use, despite the inevitable inward leakage from tip to intake through the clearance between shroud and casing.)

At the annular entrance to the impellor, axial extensions of the radial blades were curved to conform with the relative velocity of the air entering the impellor. Later, it became more usual to use rings of blades separately mounted to perform the same function, namely to 'steer' the inflowing air into the impellor with minimum turbulance. They came to be known as 'inducers.'

As may be seen from the left hand sketch of Figure 4, the initial direction of flow of the intake air was radially inwards. This was a necessity imposed by the general arrangement of the whole engine. But, at the entry, the air had no angular momentum, and therefore the change of angular momentum in the impellor was from nil to $u_w r_o$ where u_w was the tangential (or 'whirl') component of velocity at the tip radius r_o. (The radial velocity component u_r contributes nothing to angular momentum.) Thus the specific torque Ω_s is given by $\Omega_s = \frac{u_w r_o}{g}$ from which, since energy input per unit mass flow W_s equals $\frac{\omega\Omega}{g}$, where ω is the angular velocity of the impellor, $W_s = \frac{u_w r_o \omega}{g}$, or since $r_o\omega = u_b$, where u_b is the tip speed of the blading, $W_s = \frac{u_w u_b}{g}$. If the number of blades were infinite, u_w would equal u_b and so W_s would equal $\frac{u_b^2}{g}$. The corresponding temperature rise would thus be $\theta_c = \frac{u_b^2}{gK_p}$, i.e., $2\left(\frac{u_b^2}{2gK_p}\right)$ or $2\theta_b$. Thus, if $u_w = u_b$, the temperature rise θ_c is twice the temperature equivalent θ_b of the tip speed u_b. For 1470'/sec the temperature equivalent is 99.9°C and twice this is 199.8°. The actual temperature rise at design speed in the first jet engine was 190° approximately, which was in accordance with expectations; the pressure ratio, however, was well below design initially because the adiabatic efficiency hoped for, namely 80%, could not be obtained by a considerable margin. This efficiency was ultimately achieved after numerous modifications to the intake assembly and the diffuser system.

The fact that θ_c is always somewhat less than $2\theta_b$ in a radial bladed compressor is due to the 'slip factor' which in turn is a consequence of the 'relative eddy.' The relative eddy is explained by reference to Figure 5 which represents a 'cell' between two adjacent blades.

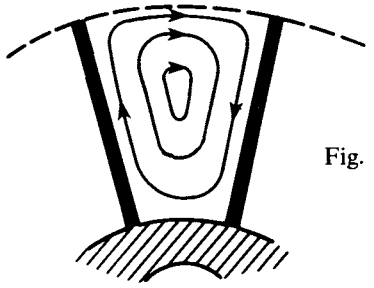

Fig. 12-5

If there were no through flow, then, if the impellor were started from rest and rotated anticlockwise, the body of fluid in the cell would also be accelerated anticlockwise as a whole, but, *relative to the cell itself*, except for skin friction there is no torque and therefore no change in angular momentum, i.e., there is a clockwise circulation within and relative to the cell as shown in Figure 5. This is the relative eddy which, when there is through flow, is superimposed on it, thus reducing u_w at the tip below u_b. Clearly, the 'slip' due to the relative eddy depends on the number of blades and would be

zero for an infinite number. Hence, the slip factor is usually taken to be $1 - \frac{1}{n}$ where n is the number of blades, i.e., $u_w = \left(1 - \frac{1}{n}\right) u_b$ at the tip $\therefore \theta_c = \left(1 - \frac{1}{n}\right) \frac{u_b^2}{gK_p} = 2\left(1 - \frac{1}{n}\right) \theta_b$.

Though the total temperature rise is the result of the specific energy input to the impellor, the rise in static pressure is partly due to centrifugal force within the impellor and partly due to the conversion of kinetic energy into pressure by the effect of the divergent channels in the diffuser blade ring; i.e., the total compression is shared between the impellor and the diffusers, though the latter, being stationary, do no work on the fluid.

If the radial velocity were small compared with the tangential velocity within the impellor then the pressure increase (assuming a very large number of blades) in the impellor would correspond to that due to the 'solid' rotation of a 'forced vortex' in which tangential velocity $u_w = r\omega$. Hence we would have $\frac{\delta P}{\delta r} = \frac{\rho}{g} \frac{u_w^2}{r}$ or $\frac{dP}{\rho} = \frac{r\omega^2 dr}{g}$ $\therefore$ from the relationship $\frac{dP}{\rho} = K_p dT$

$$dT = \frac{\omega^2}{gK_p} rdr \quad \therefore \Delta T = \frac{\omega 2}{2gK_p} (r_0^2 - r_1^2) \equiv \frac{u_{wo}^2 - u_{wi}^2}{2gK_p} \equiv \theta_b - \theta_1$$

So, for $r_i = 0$, $\Delta T = \theta_b$. (But, in this, T is static temperature, so that total temperature at the tip radius would be increased by the temperature equivalent of the tip tangential velocity, i.e., tip blade speed, to give a total temperature increase of $2\theta_b$ as before.) Assuming an isentropic relationship between P and T, $1 + \frac{\Delta P}{P_1} = \left(1 + \frac{\Delta T}{T_i}\right)^{3.5}$ or $\frac{\Delta P}{P_1} = \left(1 + \frac{\theta_b}{T_1}\right)^{3.5} - 1$ where ΔP is the increase of static pressure within the impellor due to centrifugal force. (Note that the assumption that $r_1 = 0$ is equivalent to assuming that the inducers 'impose' a tangential velocity and pressure on the fluid 'as if' the fluid had in fact entered at $r_1 = 0$ which of course, is impossible.) The foregoing ignores the affect of the relative eddy, i.e., an infinite number of blades is assumed.

In practice what happens within the impellor is far more complex than the foregoing suggests. The mechanical simplicity is not matched by the aerodynamic simplicity. At a given radius the pressure on the 'driving face' of a blade must be higher than on the rear face otherwise there would be no torque. This pressure difference must increase with mass flow rate so, in every channel there has to be a substantial tangential pressure gradient superimposed on the radial pressure gradient with a corresponding variation of radial velocity, so that the vector diagram of Figure 4b represents an 'average' state of affairs. Moreover, the implication in Figure 5, that the channels run 'full' is almost certainly never true. Fig. 6 is more likely to represent what actually happens, i.e., a detachment of the flow from the rear face of each blade so that it issues from the impellor periphery in a series of 'jets' having a much higher radial velocity than one would calculate from the axial width at the tip.

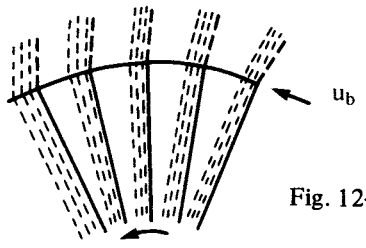

Fig. 12-6

In pre-jet engine days, superchargers and the like usually had about 16 blades, ostensibly to keep down skin friction over the blade surfaces; but, from the first, the writer contended that there ought to be as many blades as was practically possible. With the manufacturing techniques then available, 30 was the largest number which could be milled out of a solid forging. This was later reduced to 29 because tip failures were thought to be a consequence of some kind of resonant interaction between the 30 impellor blades and the 10 diffusers.

It is hard to say what happened in the divergent diffuser passages; a series of waves in all probability, i.e., a far from steady flow. At the design speed of 17,750 r.p.m. and with 29 blades, the flow at entry to each diffuser must have been fluctuating at the rate of 8,580 times/second.

As previously indicated, the torque necessary to drive the impellor is equal to the rate of change of angular momentum induced plus some torque resistance due to casing friction. At a given speed this latter would remain more or less constant irrespective of the mass flow rate and therefore becomes of decreasing importance with increase of flow rate. (The skin friction due to the radial component of flow cannot affect the torque.)

Once the fluid leaves the impellor its angular momentum remains constant (except for the small retarding effect of casing drag) until it engages and enters the diffusor blade ring, hence the tangential velocity decreases with radius, i.e., $u_w r$ = const., and there is a corresponding rise in pressure. It follows that it is possible to obtain a conversion of kinetic energy into pressure energy in a bladeless diffuser space, but unfortunately this greatly increases diameter. Thus, to reduce the tangential velocity to half that at the impellor tip would require that the diameter be twice that of the impellor, and even then 25% of the tip tangential kinetic energy would still remain. Nevertheless, in some commercial compressors where size is not of great importance, bladeless diffuser spaces are used. (On one occasion, the writer persuaded the designer of one such compressor – a diesel engine supercharger – to add a ring of diffuser blades at about twice the impellor diameter. There was an appreciable improvement in delivery pressure and efficiency.) Another big disadvantage of a bladeless diffuser space is the structural problem of bracing the casings against the pressure acting to force them apart.

The performance of a compressor is represented as in Figure 7 in the form of 'characteristic curves' in which pressure ratio is plotted against a mass flow rate parameter for a series of speeds, usually represented non dimensionally.

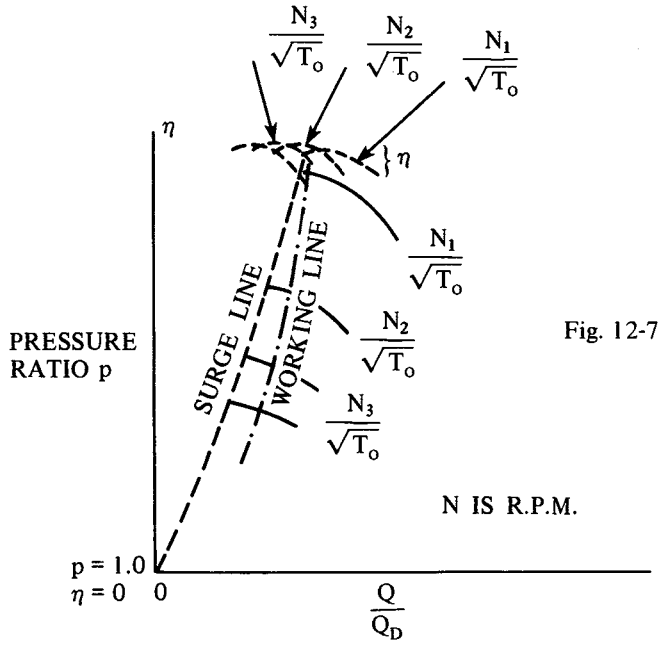

Fig. 12-7

In Figure 7, the speed parameter $\frac{N}{\sqrt{T_o}}$ is not truly non dimensional, but is frequently regarded as such for a given compressor because the quantities needed to make it so, namely diameter D, g and K_P, are constants. It would be more correct to use $\frac{ND}{\sqrt{2gK_PT_o}}$ or $\frac{u_b}{u_c}$ where u_b is tip speed and u_c the acoustic speed for temperature T_o (since $u_c \propto \sqrt{T_o}$), in which case the same curves would apply to a family of geometrically similar compressors.

The 'surge line' defines a region of instability. To the left of it, stable running cannot be obtained. There is a rapid series of flow reversals often quite violent depending to a large extent on what follows compressor delivery. Surging often makes its presence known by explosive bangs.

There is another kind of flow instability in addition to total flow reversal, namely a rotating stall where there is a 'domino effect' caused by a breakdown of flow in one channel 'triggering off' a breakdown in the next, and that in the next, and so on. This was first noted by the writer and his co-workers when a perspex casing was fitted to a centrifugal type jet engine compressor in an effort to detect the flow pattern with a stroboscope and showers of sparks. The main object of the experiment was not achieved but the rotating stall which developed, when the flow was reduced to a certain point, was very obvious. It was quite slow compared to the speed of rotation and in the opposite direction.

Stationary intake guide vanes are often used in both centrifugal and axial flow compressors, so shaped and disposed as to generate 'pre-whirl' in the fluid entering the compressor. Though this reduces the work capacity for a given tip speed, in that it reduces

the rate of change of angular momentum induced by the impellor, it enables mass flow to be increased relative to intake size up to a point without exceeding the maximum permissible Mach number at the outer diameter of the inducers. It also reduces the amount of deflection necessary in the inducers. When intake guide vanes were introduced in early jet engines the improvement in overall performance was quite striking. (They had been in use for some time before the Rolls Royce Nene was designed, nevertheless, they were not used in the Nene as first designed. They were fitted into the engine later and, as a result, the static thrust jumped from 4000 to 5000 lbs.)

The 'working line' shown in Figure 7 represents the locus of the points at which the compressor operates and is determined by what happens after compressor discharge. It represents the points at which the compressor is 'in balance' with, say a combination of combustion chambers and driving turbine. It might also appropriately be called the 'matching line.' As may be seen it tends to approach the surge line as $\frac{N}{\sqrt{T_o}}$ is increased. It has often happened that a jet engine, completely surge free at ground level, has run into surging trouble at heights where the reduction of atmospheric temperature T_o has caused $\frac{N}{\sqrt{T_o}}$ to increase to the point where the working line intercepted the surge line.

Another point which has to be taken into account is that, during acceleration, extra driving power is needed to overcome rotor inertia. This means extra fuel and increased temperature at entry to a driving turbine, this in turn causes a temporary reduction in mass flow, i.e., the working line for acceleration is to the left (Figure 7) of that for normal operation thus increasing the tendency to surge. This must be allowed for in design, i.e., the steady speed working line must be sufficiently far to the right of the surge line to prevent the risk of surging during acceleration, or devices such as 'blow off valves' must be provided to allow for a temporary increase of mass flow through the compressor during acceleration. (This is particularly important in aircraft gas turbines where a rapid increase of power is frequently essential.)

Other forms of centrifugal compressors are depicted in Figures 8 and 9, having blades swept forward and backward respectively.

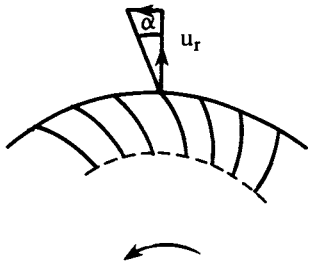

Fig. 12-8

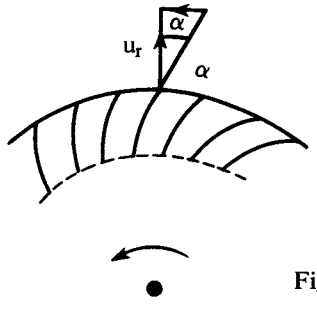

Fig. 12-9

In the Figure 8 arrangement the tip whirl induced is increased by $u_r \tan\alpha$ where α is the angle with which the flow relative to the impellor leaves relative to the radius, so, as compared with the radial vaned type, the rate of change of angular momentum is greater,

i.e., the specific work capacity is greater for a given tip speed. Moreover, since the radial velocity u_r increases with mass flow rate the specific work capacity also increases with mass flow rate. The opposite happens in the case of the back swept blades of Figure 9. The latter arrangement, however, is the only arrangement used in practice so far as is known to the writer.

Referring to Figure 7, the characteristic curves would, if efficiency did not vary with mass flow, tend to be horizontal with a radial vaned impellor (in the absence of stationary intake guide vanes), but would tend to have a positive slope with forward swept blades and a negative slope with back swept blades. The former is a very 'surge prone' state of affairs. The back swept blading has the further advantage that the curvature of the impellor blade channels helps to prevent the type of breakaway of flow depicted in Figure 6, so that improvement in efficiency may well offset the reduction in specific work capacity, especially if the blades are shrouded (as they usually are with this type of impellor).

There seems little doubt that compressors with impellors having back swept radial blading are intrinsically more efficient than any other kind of centrifugal compressor; indeed, when the writer visited the Swiss firm of Oerlicken in 1948, he saw a gas turbine with a compressor consisting of three stages of centrifugal compression; each stage having shrouded and back swept impellor blades, and was astonished to learn that the compressor efficiency was as high as 86% despite the fact that, in his opinion, the size of the compressor was far larger than it need have been for the design mass flow rate. Another unusual feature of this machine was that two intercoolers were used between stages. Seemingly the reduction of the negative work of the cycle by this means more than compensated for the increase in combustion heat addition for a given T_M due to the reduced compressor delivery temperature. And, of course, the pressure ratio of the second and third stages was increased by reduced inlet temperature. Further, since the machine also had a heat exchanger (or recuperator), the effectiveness of heat recovery was increased by the increased difference between turbine exhaust and compressor delivery temperatures.

Material developments and improvements in manufacturing techniques, especially the big advances in titanium technology, may well cause a notable increase in the use of centrifugal compressors using shrouded back swept bladed impellors in gas turbine compressors assemblies, if only as a replacement for several axial flow stages at the high pressure end of a compound compressor, especially where the optimum pressure ratio is reduced by the use of a recuperator (see Section 11).

AXIAL FLOW COMPRESSORS

Figure 10 is a rough representation of a seven stage axial flow compressor. The upper diagram represents a section through the axis and below is a partial view of the first stage rotor blades viewed from the front.

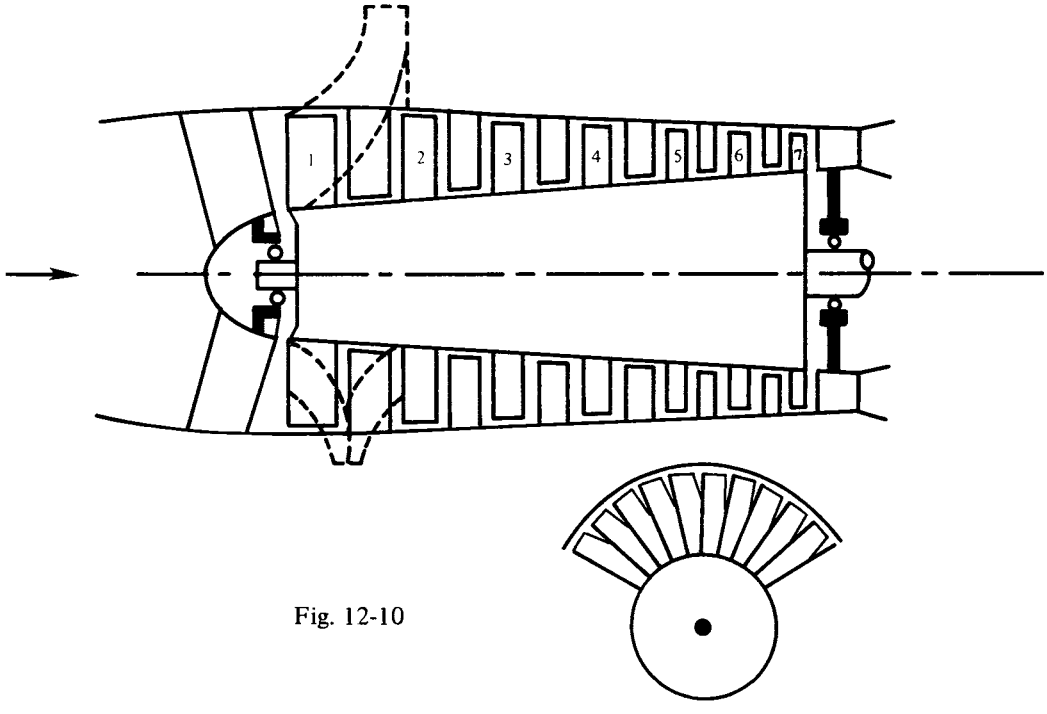

Fig. 12-10

Superimposed on the upper half of the longitudinal section is the 'ghost' of a single sided centrifugal compressor impellor of about the same volumetric and work capacity. The 'ghost' of the equivalent double sided impellor is superimposed on the lower half, (the speed of which would be about 41% greater than that of the single sided one for the same tip speed, i.e., same work capacity). This comparison gives some indication of the extent to which, in the axial flow compressor, efficiency and small diameter is 'traded' for mechanical complexity, length, etc. The design time alone required for the axial flow type is measured in months as compared with a matter of a day or two for the centrifugal type. The development time and cost is also vastly greater. Nevertheless, after many years of intensive development and accumulated experience, the axial flow type has virtually completely displaced the centrifugal type in modern gas turbines (research and development of the centrifugal type in the past thirty years or so has been sadly neglected).

In the sectional view of Figure 10, the rotor blade rings are numbered and the construction of the discs or drum on which they are mounted is not shown. The stationary stator blades (unnumbered) are 'rooted' in the casing which is normally made in two halves having longitudinal flanges by means of which they are bolted together. This is necessary for assembly purposes.

The vanes shown ahead of the first stage support the hub which carries the front bearing. They are usually three or four in number often offset from the radial direction,

partly to avoid thermal expansion problems and partly to distribute their wakes between several first stage rotor blades. These supporting vanes have no deflecting function. When a ring of intake guide vanes is fitted to generate pre-whirl in the fluid entering the first stage rotor, they may also be used to support the hub.

The divergent intake duct shown in Figure 10 is characteristic of aircraft gas turbines. A convergent inlet is more appropriate in all other gas turbines where there is no requirement for the efficient conversion of kinetic energy of the entering fluid into 'ram pressure' as is necessary in aircraft engines.

The basic functions of the rotors and stators are the same as those of the impellor and diffusers of a centrifugal compressor. The rings of rotor blades impose an increase in angular momentum on the fluid and the torque required to drive them is proportional to the rate of increase. Also, due to the divergent shape of the channels the rotors act as rotating diffusers and so contribute part of the pressure rise per stage. The kinetic energy of the whirling flow at exit from a rotor is converted into pressure energy in the divergent channels of the stator blade ring which thus acts as a stationary ring of diffuser blades. Thus, as in the centrifugal type, the pressure, temperature and density increase per stage is shared between rotors and stators. The latter, however, being stationary, do no work on the fluid. But here, the similarity with the centrifugal type really ends. The flow pattern is very different, and, to some extent, more predictable.

Figure 11 shows a section at, say, mean radius, of a few rotor blades and their following stator blades with the relevant vector diagrams for the upper pair of blades shown.

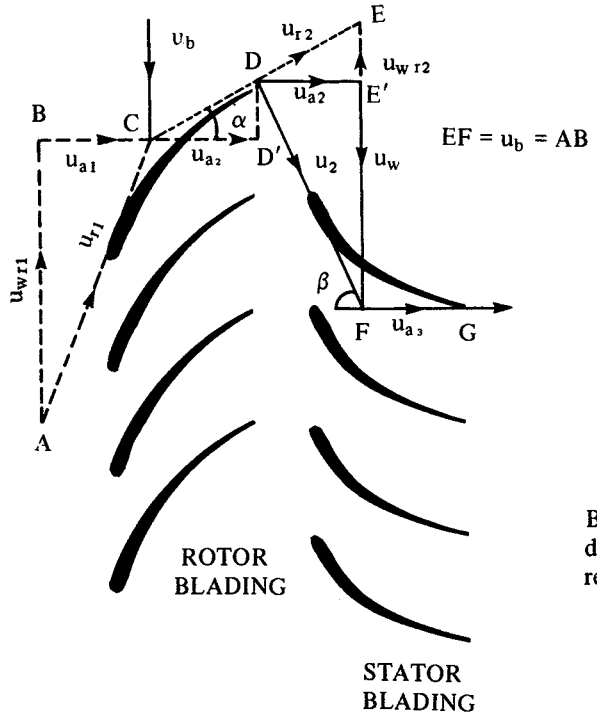

Fig. 12-11

Broken lines in the vector diagram indicate velocities relative to rotor

There are other ways of drawing the vector diagrams. The one shown in Figure 11 is the preferred one because it makes it easy to define the 'skeleton line' of the blade profiles.

In the diagram, the degree of deflection with its accompanying large increase in channel width, is exaggerated. It must, however, be remembered that the diagram is two dimensional and for one particular radius. The actual area change depends also upon what happens at other radii and on whether or not blade height (i.e., the length of the blade normal to the plane of the paper) varies from front to back of a blade row; thus if the trailing edges of the rotor blades were shorter than the leading edges as in Figure 12, the effective increase in channel section would be greatly reduced. Such a change in blade height would mean a substantial increase in the axial component of velocity at blade exit and this, in turn, would decrease the degree of deflection in the stator blading and increase it in the rotor blading, i.e., an increase of u_{a2} in Figure 11 would reduce the exit angle α of the rotor blading and the entry angle β of the stator blades.

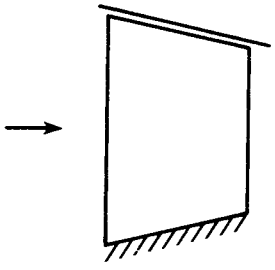

Fig. 12-12

The vector diagram of Figure 11 is drawn for a case where the flow into the rotor is purely axial ahead of the rotor (i.e., no intake guide vanes) and also purely axial flow at discharge from the stator blading.

If the blade speed is u_b at radius r then the vector AB is the whirl at entry relative to the rotor, i.e., $u_{wr1} = -u_b$. The vector BC is the entry axial velocity u_{a1}, so the resultant relative velocity u_{r1} is the vector AC. It is obvious that $u_{r1}^2 = u_{a1}^2 + u_b^2$ and that the temperature equivalents of these relative velocities are related by the equation $\theta_u = \theta_a + \theta_b$. If the total temperature of the entering air is T_o then the static temperature is $T_o - \theta_a$ so that the total temperature relative to the moving blade T_{TR} is $\therefore$

$$T_{TR} = T_o - \theta_a + \theta_u = T_o + \theta_b \qquad (12\text{-}1)$$

Since there can be no change of total temperature in the blade channel, $T_o + \theta_b$ is also the total temperature relative to the rotor at exit. Total pressure (relative to the blade) would be reduced by blade friction and possible detachment of the flow on the convex face with resulting turbulence, especially if the adverse pressure gradient due to divergence is excessive.

Vector DE represents the relative velocity at exit from the rotor u_{r2} which is the resultant of the relative whirl u_{wr2} (= E'E) and the axial velocity u_{a_2} (= DE'). Since $u_{r_2}^2 = u_{wr2}^2 + u_{a2}^2$ then $\theta_{ur2} = \theta_{ua2} + \theta_{wr2}$, the static temperature in the interblade space; (which will be the same for both rotor and stator blades) T_S is thus $T_{Tr} - \theta_{ur2}$

or

$$T_s = T_o + \theta_b - \theta_{ua} - \theta_{wr2} \qquad (12\text{-}2)$$

The whirl relative to the stator blade u_w (i.e., the 'absolute whirl' induced by the rotor) is seen (from Figure 11) to be given by E'F

$$\text{i.e., } u_w = u_b - u_{wr2} \tag{12-3}$$

It follows that the temperature equivalent of u_2 (= DF) is given by $\theta_{u2} = \theta_{ua2} + \theta_{uw}$.

From (3), $$\theta_{uw} = \frac{(u_b - u_{wr2})^2}{2gK_P} = \theta_b + \theta_{wr2} - \frac{u_b u_{wr2}}{gK_P} \tag{12-4}$$

hence $$\theta_{u2} = \theta_{ua2} + \theta_b + \theta_{wr2} - \frac{u_b u_{wr2}}{gK_P} \tag{12-5}$$

$\therefore$ the total temperature at stator entry (and exit). T_T is given by

$$T_T = T_S + \theta_{u2} \tag{12-6}$$

Substituting for T_S from (2) and for θ_{u2} from (5)

$$T_T = T_o + \theta_b - \theta_{ua2} - \theta_{wr2} + \theta_{ua2} + \theta_b + \theta_{wr2} - \frac{u_b u_{wr2}}{gK_P}$$

which reduces to $$T_T = T_o + 2\theta_b - \frac{u_b u_{wr2}}{gK_P} \tag{12-7}$$

Writing $\Delta T = T_T - T_o$ (the total temperature increase across the stage)

$$\Delta T = 2\theta_b - \frac{u_b u_{wr2}}{gK_P} \tag{12-8}$$

ΔT is, of course, a measure of the specific work done by the stage.

(Note that if $u_{wr2} = 0$ the total temperature rise for the stage would be twice the temperature equivalent of the blade speed as in the case of a radial vaned centrifugal impellor with a very large number of blades having a negligible slip factor).

As may be seen from Figure 11, the whirl leaving (and relative to) the rotor u_{wr2} depends on the axial velocity u_{a2} and the angle α, i.e., $u_{wr2} = u_{a2} \tan\alpha$. It follows that, since u_{a2} depends upon the mass flow rate Q and the area of the annulus, from (8) ΔT decreases with increase of Q (as in the case of the centrifugal impellor with back swept blades).

At this point it is appropriate to point out that exit angles of both rotor and stator blades govern the performance of the compressor to a far greater extent than the entry angles. These latter, however, are important in that if they are not reasonably consistent with the flow direction then flow breakdown is likely due to stalling. Axial flow compressors are much more sensitive in this respect than axial flow turbines because of the

adverse pressure gradient within the blade channels. Clearly a reduction of Q below the 'correct' value would be much more harmful than an increase. (See Figure 11. If a reduction of u_{a1} occurs as a result of a reduction of Q the 'angle of attack' is increased.)

Example 12-4

Given the following data: (1) $T_Q = 300°K$; (2) $u_{a2} = 600'/sec$; (3) angle $\alpha = 45°$; (4) u_b at radius r (unspecified) is $900'/sec$; and (5) $u_{a1} = 550'/sec$ ∴ what is (a) the specific work capacity measured as ΔT, (b) the total temperature relative to the rotor, and (c) the static temperature between rotor and stator?

Figure 13 is the vector diagram differing slightly in arrangement from that of Fig. 11 (yet another variant would be to have joined C and F as the resultant velocity at entry to the stator) with the component and resultant velocities being shown with their temperature equivalents.

The total temperature relative to the rotor is seen to be 300 + 37.4 = 337.4°K (i.e., 300 + 37.4 + 14 − 14) ∴ the static temperature after the rotor is 337.4 − 33.27 = 304.13°K which is also the static temperature ahead of the stator ∴ the total temperature before, through, and after the stator is 304.13 + 20.8 = 324.93°K, thus ΔT for the stage is just below 25°. The same result is obtained by using Equation (8).

The static temperature before the rotor is 286° for which $u_c = 1112.5'/sec$ ∴ the Mach No. at rotor entry $= \frac{1055}{1112.5} = 0.948$. This is sufficiently high to indicate that great care would be necessary to avoid a choking throat in the rotor blade channels.

This last point emphasizes the importance of designing the channels rather than the blade profiles. (In the early days of axial flow compressor design the tendency to regard the blades as a 'cascade' of aerofoils was so strong that designers tended to design the blade profiles on aerofoil principles and to overlook the greater importance of the channels.)

The fact that u_{a2} is greater than u_{a1} in the above example implies that the rotor blade annulus decreases from entry to exit as in Figure 12.

Other points to notice from the example are: (1) though the specific work done by the rotor blading is about that which was usual in the early days of axial flow compressor development, the rotor blade curvature is quite small at the radius at which $u_b = 900'/sec$; (2) the deceleration in the rotor blading is from $1055'/sec$ to $848.5'/sec$; (3) the axial velocity at exit from the stator blading (unspecified) would be determined by the annulus, density etc.; It *could* be made to equal the entry velocity of $671'/sec$ by reducing the annulus (as in Figure 12) in which case there would be no deceleration in the stator blading at the radius concerned, and therefore no pressure rise. This point is mentioned to show that the way the stage pressure rise is distributed between rotors and stators is very much under the control of the designer; and (4) at the radius concerned the whirl velocity on leaving the rotor is $300'/sec$ hence the centrifugal field is $\frac{300^2}{rg}$, thus if r equalled, say, $1.0'$, the centrifugal acceleration would be nearly 3000g. Thus, from entry to exit of the rotor, the centrifugal force field increases from zero to 3000g approximately, while the reverse happens in the stator blading. Such powerful force fields would have a big effect on the retarded flow in the boundary layers and cause it to have a radial component of flow, i.e., the boundary layer is 'scavenged' away from the inner portions of the blading

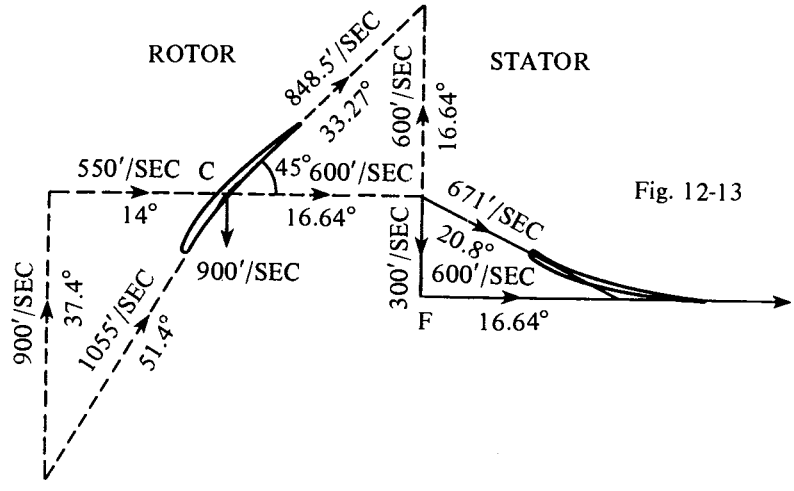

Fig. 12-13

where the blade deflection is greater. The writer believes this to be a major factor contributing to the high efficiency obtainable with axial flow compressors despite the normal poor efficiency of diffuser channels in general.

Figure 14 illustrates the effect of reducing u_{a2} as compared with the example shown in Figure 13. By increasing the exit annulus of the rotor blading u_{a2} is shown reduced from 600 to 500'/sec without change of rotor blade profile.

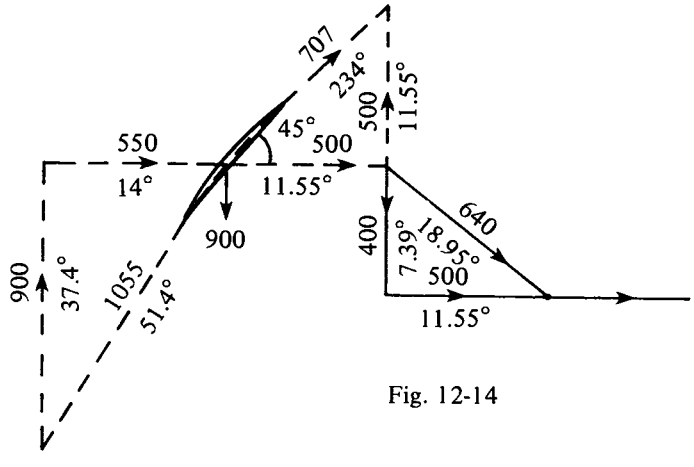

Fig. 12-14

From Equation (8) $\Delta T = 2 \times 37.4 - \frac{900 \times 500}{32.2 \times 336} = 33.2°$, i.e., a very substantial increase of work capacity. As may be seen, the velocity reduction in the rotor is much greater while that in the stator is reduced unless the leaving axial velocity is substantially below that of Figure 13 (not given). The increase in ΔT is, of course, due to the 33%

increase of whirl imparted by the rotor, which latter also increases the centrifugal acceleration in the ratio $\left(\frac{400}{300}\right)^2$ by approximately 78%.

The stator blades of Figure 13 would no longer be appropriate since the relative flow angle at entry of the Figure 13 example is $\tan^{-1} 0.5 = 26.6°$ while for Figure 14 it is $\tan^{-1} 0.8 = 38.7°$ approximately, so that if the stators of Figure 13 were used in the circumstances of Figure 14, the angle of attack would be 12.1° which would almost certainly cause them to stall.

There are some interesting variants of Equation (8), i.e., $\Delta T = 2\theta_b - \frac{u_b u_{wr2}}{gK_P}$. Multiplying the second term on the right by $\frac{2u_b}{2u_b}$ we obtain $\Delta T = 2\theta_b - \frac{2u_b^2}{2gK_P} \frac{u_{wr2}}{u_b}$ and, since $\frac{u_b^2}{2gK_P} = \theta_b$, this becomes

$$\Delta T = 2\theta_b \left(1 - \frac{u_{wr2}}{u_b}\right) \tag{12-8a}$$

or, since u_{wr2}, the relative whirl from the rotor, $= u_{a_2} \tan\alpha$

$$\Delta T = 2\theta_b \left(1 - \frac{u_{a_2}}{u_b} \tan\alpha\right) \tag{12-8b}$$

or, since $u_{wr2} = u_b - u_w$, from (8a)

$$\Delta T = 2\theta_b \left(1 - \frac{u_b - u_w}{u_b}\right) = 2\theta_b \left(\frac{u_w}{u_b}\right) \tag{12-8c}$$

The foregoing may be described as the 'temperature equivalent method' of dealing with the subject, and illustrates the point that moving objects such as rotor blading may be regarded as having a temperature equivalent of their velocity. One simply has to multiply temperatures and temperature equivalents by K_P to obtain the energy values in mechanical units. It must be remembered, however, that, in the foregoing, ΔT is a measure of the *specific work*, and must be multiplied by Q to obtain the power input. Thus, if an axial flow compressor has a temperature rise of ΔT_1 in the first stage, ΔT_2 in the second and so on, then the power required W in mechanical units is given by $W = QK_P(\Delta T_1 + \Delta T_2 + \ldots . \Delta T_n)$ for n stages.

An alternative method might be described as the 'linear momentum method.' If the change of whirl is Δu_w in passing through a rotor, then the component of tangential force F_S per unit mass in the plane of the rotor at the radius where Δu_w occurs then $F_S = \frac{\Delta u_w}{g}$ and the specific rate of doing work $W_S = F_S \times u_b = \frac{u_b \Delta u_w}{g}$.

Since $u_b = r\omega$ where ω is the angular velocity of the rotor $F_S \times r\omega = \frac{r\omega\Delta u_w}{g}$ or $F_S = \frac{r\Delta u_w}{g}$ and since $F_S r$ is the specific torque and $\frac{r\Delta u_w}{g}$ is the specific change of angular

momentum at radius r, we are back to torque = rate of change of angular momentum. However, in each of these methods Δu_w and flux density may vary with radius so that the relationship between Δu_w and r and between ψ and r must be known for torque, etc., to be obtainable by integration. Thus the two dimensional analysis so far discussed is by no means the whole story, though, as will be seen hereafter, there are certain circumstances in which the two dimensional analysis may substitute for a three dimensional one for some of the performance characteristics, but a three dimensional study is essential for blade design.

Referring to Equation (8c), i.e., $\Delta T = 2\theta_b \left(\frac{u_w}{u_b}\right)$, this was arrived at on the assumption that there was no whirl in the fluid entering the rotor. More generally,

$$\Delta T = 2\theta_b \left(\frac{\Delta u_w}{u_b}\right) \qquad (12\text{-}8d)$$

and since $\theta_b = \frac{u_b^2}{2gK_p}$ then $\Delta T = \frac{u_b^2}{gK_p}\left(\frac{\Delta u_w}{u_b}\right)$ or

$$gK_p\Delta T = u_b(\Delta u_w) \qquad (12\text{-}8e)$$

Hence, since u_b is proportional to radius, for ΔT to be the same at all radii Δu_w must be inversely proportional to radius.

As shown in Section 3 on radial equilibrium, this condition is best satisfied if the whirl velocity conforms to that of a free vortex of uniform axial velocity, i.e., $u_w r$ = const. and u_a = const. both before and after blade rings.

In the following three dimensional analysis of the effect of radial equilibrium on blade design, a specific example is used on the basis of the following assumptions

(1) ΔT (i.e., the total temperature rise for the stage) is 35°C at all radii

(2) The air has axial velocity only at entry to the rotor and at exit from the stator which, with (1), means that the rotor induces a free vortex flow in the interblade space, i.e., $u_w r$ = const. = $u_{wm} r_m$ where the suffix m implies conditions at mean radius r_m

(3) The tip/hub ratio at rotor entry is 2:1, i.e., $\frac{r_o}{r_1} = 2$ where r_o and r_i are outer and inner radii respectively

(4) r_m is constant from entry to exit of the stage

(5) The blade annulus section varies to conform with the condition that axial velocity is 550′/sec at entry to and exit from the rotor

(6) The rotor blade speed at r_m is 1050′/sec

(7) Total temperature before the rotor is 288°K

(8) Total pressure before the rotor is 2116 p.s.f.

From Equation (8e), at r_m, $u_{wm} = \frac{gK_p\Delta T}{u_{bm}} = \frac{32.2 \times 366 \times 35}{1050} = 360.6'/\text{sec}.$

u_b and u_w (at rotor exit) at r, r_m and r_o are then as follows

	u_b	u_w
r_o	1400	270.5
r_m	1050	360.6
r_i	700	540.9

The resulting vector diagrams for root mean and tip are shown in Figure 15 with resultant and component velocities and their temperature equivalents shown for each vector.

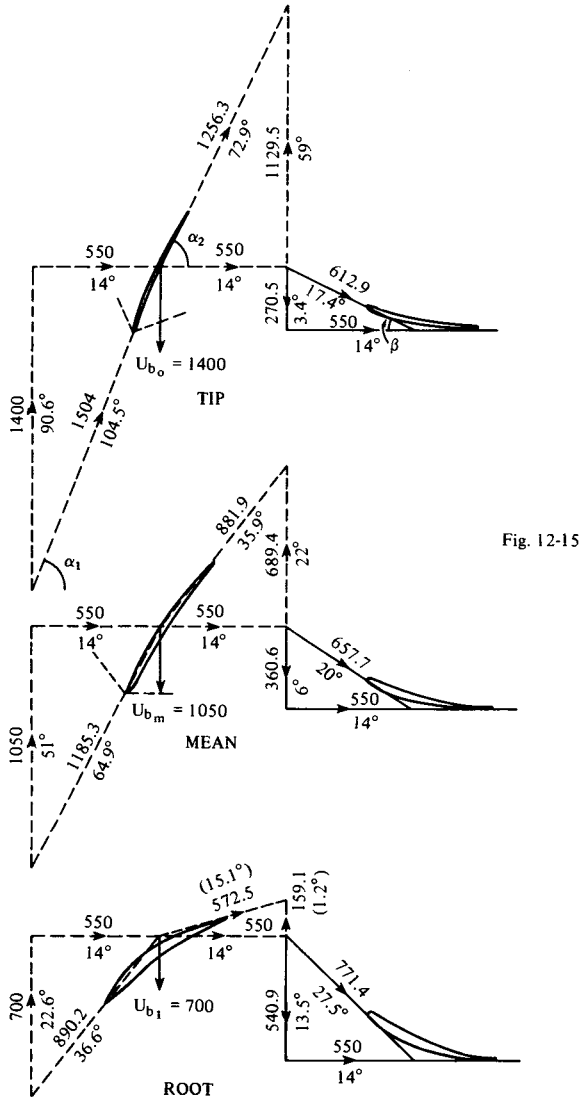

Fig. 12-15

The table below lists some of the salient features obtained from these diagrams.

	T_o	T_{S1}	θ_{r1}	T_R	θ_{r2}	T_{S2}	σ	$r\sigma$	α_1	α_2	$\beta_{\beta 2}$	T_{S2}	θ_{rs}	T_2	ΔT	M_1	M_1'
r_o	288	274	104.5	378.5	72.9	305.6	1.314	2.628	68.6°	64.0°	26.2°	305.6	17.4	323.0	35	1.38	1.29
r_m	288	274	64.9	338.9	35.9	303.0	1.286	1.930	62.4°	51.4°	33.2°	303.0	20.0	323.0	35	1.09	1.01
r_i	288	274	36.6	310.6	15.1	295.5	1.208	1.208	51.8°	16.4°	44.5°	295.5	27.5	323.0	35	0.82	0.76

In the above T_{S1} and T_{S2} are the static temperatures before and after the rotor. $\sigma \equiv \frac{\rho_{S2}}{\rho_{S1}}$ where ρ_{S1} and ρ_{S2} are the densities before and after the rotor, and σ is calculated from $\sigma = \left(\frac{T_{S2}}{T_{S1}}\right)^{2.5}$, i.e., on the assumption that the flow through the blading is isentropic i.e., making no allowance for blade losses.

The mass flow rate Q through the annulus is given by

$$Q = 2\pi u_a \int_{r_1}^{r_o} \rho r dr \quad \text{or} \quad Q = \frac{2\pi u_a}{\rho_{S1}} \int_{r_1}^{r_o} \sigma r dr \text{ at rotor blade exit.}$$

Hence the significance of $r\sigma$ in the table. The mean of the values of $r\sigma$ at r_i and r_o is 1.923 as compared with the value of 1.930, namely a difference of less than 0.4%, thus the error is very small if one assumes that $Q = \rho_m u_a S$ where S is the area of the annulus, and ρ_m is the density at mean radius. As, in the above example, u_a is the same before and after the rotor, the annulus decreases from entry to exit in the ratio $\frac{1}{1.286}$, and, since r_m remains the same, the width of the annulus decreases from 1.0 to 0.778, i.e., r_o decreases from 2.0 to 1.889 and r_i increases from 1.0 to 1.111 to maintain the same axial velocity before and after the rotor blading.

Columns M and M′ require some explanation. M is the Mach No. at rotor entry based on the acoustic speed for the static temperature of 274°K. M′ is the value of $\frac{u_r}{u_c'}$ where u_c' is the choking velocity for the total temperature relative to the rotor blade (T_R), i.e., $u_c' = 147.1 \sqrt{\frac{T_R}{6}}$.

As may be seen, both M and M′ are above unity for more than half the blade length. At one time this would have been considered unthinkable but is now quite usual. As may also be seen, blade profiles become very thin near r_m and beyond, so the shock waves to which they give rise are very weak. Their pattern, however, is complicated by the fact that the leading edge of each rotor blade lies behind the shock waves emanating from one or more preceding blades, and, for other than the first stage, their reflections from the preceding stator ring. To this extent the vector diagrams are a little misleading at high Mach Nos. since they do not take into account the small changes in flow direction which occur on passage through a shock wave.

The diagrams of Figure 15 and the tabulated figures illustrate a number of interesting points as follows:

(1) Though the deceleration is from 1504 to 1256′/sec at the rotor tip the deflection is less than 5° but increasing to nearly 36° at the root. Fortunately, at the root the pitch is half that at the tip, and, if necessary, channel divergence can be reduced by increasing the axial width of the blades.

(2) In the stators also, deflection and channel width increase from tip to root, but Mach numbers are well below unity.

(3) The centrifugal field in the interblade space is far more intense at the root than at the tip. In fact, in a free vortex, it varies inversely as the cube of the radius (since $u_w \propto \frac{1}{r}$, $u_w^2 \propto \frac{1}{r^2}$ $\therefore \frac{u_w^2}{r} \propto \frac{1}{r^3}$). This suggests that, to prevent breakaway due to the effect of divergence on the boundary layer, it would be desirable to design the rotor channels to have increasing rate of divergence from entry to exit, and vice versa for the stator channels.

(4) It is obvious that increased axial velocity would increase the deflection in the rotor channels and reduce it in the stators.

(5) The increase of blade section from tip to root is very satisfactory from the point of view of blade stress due to centrifugal force.

The relative eddy, briefly explained in the discussion of the centrifugal compressor, must also occur between each pair of rotor blades of an axial flow compressor but owing to the much greater number of blades its influence would be much reduced. It's effect would differ in that while still tending to cause slip at the blade tips it would tend to cause 'negative slip' at the root radius. It's effect could be countered by slight adjustments to the blade exit angles.

A Note on Cascade Tests

It has long been established that what happens in the boundary layer is crucial to the whole aerodynamic behavior of a body moving through a fluid, yet many researchers have spent much time on experiments with stationary finite 'cascades' of blades in the belief that the information obtained is applicable to the blading of axial flow compressors and turbines. In the opinion of the writer there can be little resemblance between the flow through such cascades and what happens in the blading of high speed rotors or even rings of stator blades. Any results from tests with cascades which may seem to correlate must be presumed to be purely coincidental for the following reasons:

(1) The intense centrifugal fields which are present in both rotors and stators cannot be reproduced in a cascade, yet these forces must have a profound effect on boundary layers.

(2) A ring of rotor or stator blades is, in effect, an infinite cascade varying from blade root to blade tip in relative velocity, blade angles and profiles, blade pitch and chord, etc.

(3) Rings of blades discharge into an annulus of fixed section area which largely determines the axial velocity which, in turn, in conjunction with exit blade angles, boundary layer effects and the (relatively minor) effect of the relative eddy, determines the angle and velocity of flow at blade exit.

(4) The effects of compressibility can rarely be reproduced in a stationary cascade.

There have been efforts to deal with (3) above by using extensions of the end blades of a cascade to simulate the controlling effect of the exit area on the axial velocity component in the hope that this will cause a finite cascade to be representative of an infinite cascade.

Of the above objections, (1) is almost certainly the most cogent. Even if means of meeting the others could be devised, the differences in boundary layer phenomena would alone be so great as to destroy any resemblance in the flow behavior. One might think that a cascade could be least be made to be reasonably representative of a ring of stator blades, but, as seen above, the whirling flow entering a compressor stator has a centrifugal field of force of great magnitude at entry diminishing to zero at exit if the exit flow is purely axial (or having negligible residual whirl). And vice versa for a turbine nozzle ring.

In the case of the rotor blading the state of affairs in the boundary layer is further complicated by the fact that it is subject to much larger centrifugal forces than the main flow, especially those portions of it in contact or near contact with the blade surface. This is best visualized by imagining that a very small diameter tube is 'buried' radially in the blade and open to the flow at its inner end. Since it would be rotating with the angular velocity of the blade the centrifugal pressure gradient within it would be defined by $\frac{dp}{dr} = \frac{pr\omega^2}{g}$ from which $\frac{dp}{\rho} = \frac{\omega^2 r dr}{g}$ or, since $\frac{dp}{\rho} = K_p dT$, $K_p dT = \frac{\omega^2 r dr}{g}$ whence ΔT between r_1 and r_o is given by $\Delta T = \frac{\omega^2 (r_o^2 - r_1^2)}{2gK_p}$ or $\Delta T = \frac{u_{bo}^2}{2gK_p} - \frac{u_{bi}^2}{2gK_p}$ where u_{bo} is the blade tip speed and u_{bi} is the root speed; or, using temperature equivalents, $\Delta T = \theta_{bo} - \theta_{bi}$.

Thus, assuming an isentropic relationship between temperature and pressure, i.e., $1 + \frac{\Delta P}{P_i} = \left(1 + \frac{\Delta T}{T_1}\right)^{3.5}$ (i.e., for air), $\frac{\Delta P}{P_i} = \left(1 + \frac{\Delta T}{T_i}\right)^{3.5} - 1$.

Taking the example used for Figure 15 as an illustration, $T_i = 288°$ and $P_1 = 2116$ p.s.f. (total temperature and pressure): $u_{bi} = 700'/\text{sec}$ $\therefore \theta_{bi} = 22.64°C$; $u_{bo} = 1400'/\text{sec}$ $\therefore \theta_{bo} = 90.58°C$ $\therefore \Delta T = 90.58 - 22.64 = 67.94°C$, hence $\frac{\Delta P}{2116} = \left(1 + \frac{67.94}{288}\right)^{3.5} - 1 = 1.1$ $\therefore \Delta P = 2325$ p.s.f.

If one now imagines that our radial tube has a series of holes along its length, fluid would flow through them into the 'outer' parts of the boundary layer and the main flow, especially at entry to the rotor blading where the main flow has not yet 'acquired' a centrifugal pressure gradient.

Our imaginary tube would be replenished by inflow at its inner end.

The outflow from a similar tube near the exit of a rotor blade would be diminished by the fact that the main flow has a centrifugal pressure gradient 'imposed' upon it in its passage through the rotor blade channels corresponding to that of a free vortex, but which would still be less than that of the forced vortex within the 'tube.'

There is, thus, a strong tendency for boundary layer fluid to be 'pumped' into the main stream. But it must be replaced. To guess how this happens it is necessary to take into account the pressure gradient across the blade channels at a given radius due to the

curvature of the flow through them and which causes the pressure on the concave side of a blade to be substantially higher than on the convex side.

Matters are further complicated by the pressure rise along the flow path which varies from root to tip to conform with the free vortex generated by the blading. The three dimensional pressure distribution which exists in the channels is so complex that one can do no more than guess at the kind of secondary flows which are induced by the effect of the pressure field on the boundary layers along the blade surfaces.

Two of the many possibilities for the innermost part of the boundary layer are suggested in Figure 16. The type of secondary flow indicated in the left hand sketch is possibly representative of what happens at rotor entrance while at and near the exit the 'cross channel' pressure increase added to whirl pressure increase might be sufficient to cause an inward flow on the concave side of a blade, i.e., to overcome the centrifugal pumping effect. In any event the scavenging effect will be strongest at the exit on the convex side of a blade at the root where it is most needed to prevent breakaway.

In the stators, the secondary flows are likely to be quite different and less favorable to the prevention of breakaway owing to the absence of the centrifugal pumping effect.

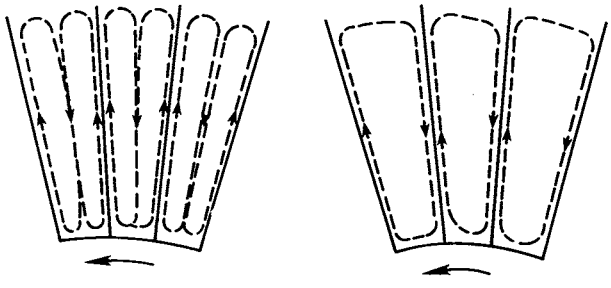

Fig. 12-16

In the case of the rotor blades, matters are yet further complicated by the 'spill' which must occur from the high pressure to the low pressure sides (i.e., from concave to convex) through the clearance between the blade tips and the casing. This could be prevented by mounting a shroud ring round the blade tips, but experience seems to indicate that this reduces compressor efficiency; presumably because it has some kind of adverse effect on the secondary flows within the channels. The use of shrouding would also provide a 'leakage path' from the exit to entry at the rotor tips through the clearance between shroud and casing which, without shrouding, would be obstructed to some extent by the 'tangential' tip leakage mentioned above.

Multi-Stage Axial Flow Compressors

Up to this point, the discussion of axial flow compressors has been limited to a single stage combination of rotor and stator of a kind which might well be representative of the first stage of a multi stage compressor as illustrated in Figure 10.

Multi stage units are essential to obtain the degree of compression required in gas turbines, because, in the present state of the art, about 40° rise per stage is the most that can be obtained with good efficiency. This, at 90% adiabatic efficiency and from an initial total temperature of 288°K, would yield a temperature ratio of 1.125 and a pressure ratio of

1.51. For a 400° compressor, i.e., one capable of producing a temperature rise of 400°, 10 stages would be necessary. It is, however, somewhat doubtful if this degree of compression can be achieved in a single compressor without special measures to prevent blade stalling and surging at low speeds. The need for these special measures is based on the fact that a design suitable for full design speed is mismatched from entry to exit at speeds less than design, primarily due to the difference in the increase of density as between low speed and full speed. The density increase calls for a progressive reduction of blade annulus from entry to exit as shown in Figure 10. If it were physically possible to have variable blade length so as to increase annulus area at the high pressure end for low speed operation in such a manner as to keep the axial velocity proportional to blade speed, the problem would not exist. But this, of course, is not practical and so other methods have to be employed to prevent the excessive changes in flow direction at entry to blading which would otherwise occur at 'off design' speeds, when the axial velocity at entry tends to be too low and that at exit too high. The former is more harmful than the latter because a reduction of axial velocity relative to blade speed increases the 'angle of attack' and therefore the tendency to blade stalling.

The usual preventive measures comprise one or more of the following:

(1) The provision of blow off valves part way along the compressor to increase the mass flow through the first few stages at low speeds.

(2) The use of variable stators for the first few stages. (This is characteristic of many General Electric Co. designs.)

(3) The division of the total compression between two or more compressors in series independently driven by turbines in series. Thus, if 14 stages were necessary then, say, two seven stage compressors might be used running at different speeds. In such cases (which are now common) the shaft of the L.P. turbine–L.P. compressor combination is 'threaded' through the HP assembly, the speed of the latter being the higher. Such arrangements are known as 'two spool' engines.

(4) Making possible a reduction of the effective back pressure of the expansion system so as to increase mass flow in proportion to speed. As, for example, by the opening up of a variable jet nozzle in a jet engine. (This, however, is not very effective with an axial flow compressor owing to its pressure ratio, mass flow characteristics – see below.)

As already mentioned, the temporary increase of turbine inlet temperature during acceleration aggravates the surging problem.

Some of these measures are partly self defeating; for example, the provision of blow off valves increases the power required to drive the compressor. Thus, if driven by a turbine, the turbine inlet temperature is increased which, since Q for the turbine is proportional to $\frac{P}{\sqrt{T}}$, in turn reduces the mass flow.

The nature of the problem of finding what happens at off design speeds is best explained (up to a point) by taking a specific case.

Figure 17 is a diagram for a design cycle based on the following assumptions: (1) $T_o = 288°K$ and $P_o = 2116$ p.s.f.; (2) $T_{max} = 1150°K$; (3) $\eta_T = 0.87$; (4) $\eta_T = 0.9$; (5) $\theta_c = 245$; (6) the mean radius for all stages is the same; (7) u_a at entry and exit is

550′/sec; (8) we are not concerned with what happens after the compressor turbine; and (9) the compressor has 7 stages, each having $\Delta T = 35°C$

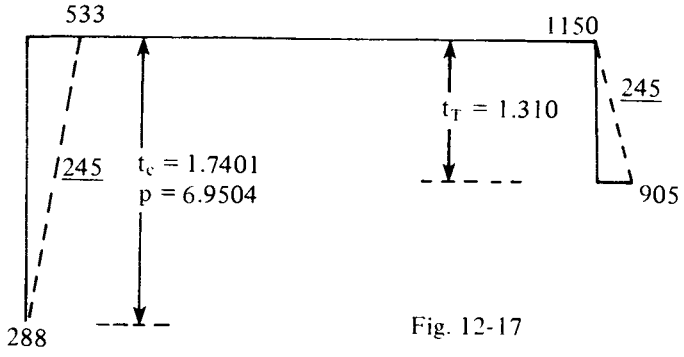

Fig. 12-17

The temperature and pressure ratios corresponding to the above assumptions are shown on the diagram. The stagnation density before entry ρ_o is $\frac{P_o}{RT_o}$ and is found to be 0.766. The temperature equivalent of 550′/sec is 14° ∴ the density ρ_i at rotor entry is $\rho_1 = \rho_o \left(\frac{288-14}{288}\right)^{2.5}$ from which $p_i = 0.0675$.

At compressor rotor exit, with compression total pressure of $1.7401\,P_o$ and total temperature of 533°K, the stagnation density ρ_E is $\frac{1.7401\,P_o}{533\,R}$ which is found to be 0.2874 hence at 550′/sec exit axial velocity, the static density ρ_{ES} is given by $\rho_{ES} = \rho_E \left(\frac{533-14}{533}\right)^2$ and is found to be 0.269.

If S_i is the annulus area at entry and S_E is the annulus area at exit then $Q = \rho_1 \times 550 \times S_E$ from which $\frac{S_E}{S_i} = \frac{\rho_1}{\rho_{ES}}$. Since mean radius r_m is assumed the same, $S_i = 2\pi r_m \ell_i$ where ℓ_i is the annulus width (i.e., blade length) at entry, and $S_E = 2\pi r_m \ell_E$ where ℓ_E is the annulus width at exit. Therefore $\frac{S_E}{S_i} = \frac{\ell_E}{\ell_i} = \frac{\rho_1}{\rho_{ES}}$ i.e., $\frac{\ell_E}{\ell_i} = \frac{0.0675}{0.269} = 0.251$. Thus the blade length at exit is approximately 1/4 of that at entry.

Fig. 12-18 represents the cycle of the same assembly with θ_c reduced to 61.2°C and assumes that the off design conditions drop the compressor efficiency to 0.8 and the compressor turbine efficiency also to 0.8. It is further assumed that the assembly is just self-driving, i.e., that whatever follows the compressor turbine is 'absent,' i.e., the temperature and pressure ratios for the compressor and its driving turbine are the same and as shown in the diagram.

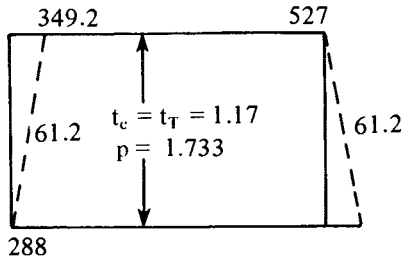

Fig. 12-18

It is readily found that to give an actual temperature drop of 61.2°C at 80% efficiency with a temperature ratio of 1.17 then $T_{max} = 527°K$ as shown. The temperature ratio of 1.17 is sufficiently near the critical ratio 1.2 to assume that $Q \propto \frac{P}{\sqrt{T_M}}$. If now Q_D is the design mass flow of the cycle shown in Figure 17, then Q for the cycle of Figure 18 is given by $\frac{Q}{Q_D} = \frac{1.733P_o}{6.95P_o}\sqrt{\frac{1150}{527}} = 0.368$

A θ_c of 61.2°C being 0.25 x design θ_c(= 245) would correspond to 50% design speed in a radial bladed centrifugal compressor but this would not be so in a multi stage axial flow machine, nevertheless, it is evident that Q decreases more rapidly than blade speed.

It now remains to find out what happens (so far as is possible) to axial velocities. This is not difficult if one makes the rather sweeping assumption that, in the off design condition, one may take the axial velocity at mean radius as representing an average for the annular section concerned. (Which would be true at entry to the first rotor.)

We have the following data from above:

(1) $Q = 0.368Q_D$

(2) $Q_D = S_i$ x 550 x 0.0675 at entry

(3) $Q_D = 0.25S_i$ x 550 x 0.269 at exit

For the off design condition of Figure 18, at entry we have: $Q = S_i u_{ai} \rho_i$, but ρ_i depends upon u_{ai} since $\rho_i = \rho_o \left(\frac{288 - \theta_{ai}}{288}\right)^{2.5}$. However, the approximations involved do not justify the successive approximation necessary to obtain 'exact' values of u_{ai} and ρ_i so it will be assumed that $\theta_{ai} \cong 2°C$, from which $\rho_1 = 0.0766 \left(\frac{286}{288}\right)^{2.5} = 0.0753$. S_i being unchanged, it follows from (1) and (2) that u_{ai} is reduced in the ratio $\frac{0.0675}{0.0753}$ x 0.368 = 0.33, i.e., u_{ai} = 0.33 x 550 = 181′/sec (for which $\theta_{ai} \cong 1.5°$, hence the error in assuming 2° is negligible).

Thus it may be seen that a reduction of blade speed by something of the order of 50% means a reduction of axial velocity of the order of 67% at entry, which, of course, means quite a large increase in angle of attack and therefore in the tendency to stall.

At compressor exit, the opposite happens owing to the lower exit density and small annulus.

Using $Q = 0.368Q_D$ and (3) we have

$$0.368 \times 0.251S_1 \times 550 \times 0.269 = 0.251S_1 \times u_{aE} \times \rho_{ES}$$

and given that the total pressure and temperature are $1.733P_0$ and 349.2°K (see Figure 18) ρ_{ES} is found to be 0.108 and u_{aE} = 505'/sec, i.e., 92% of design value though again the blade speed will probably be in the 50-60% range.

But this is by no means the whole picture. For the design cycle of Figure 17 it was assumed that the total temperature rise of 245°C was equally divided between the stages, but, as seen from the vector diagram of Figure 19 where AB is the relative whirl at rotor entry (= $-u_b$), DE is the relative whirl u_{wr2} at rotor exit and EF is the absolute whirl u_w, (i.e., relative to the stator). The length of DF is equal to AB, i.e., to u_b. BC, CE and FG are the axial velocity vectors as indicated.

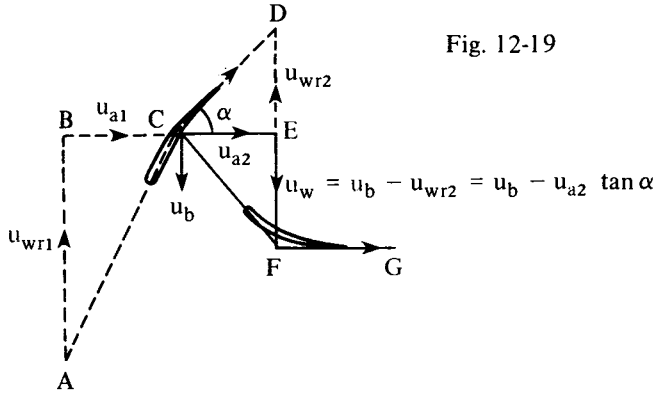

Fig. 12-19

As we have seen (Equation (8e)), with no whirl prior to rotor entry, $gK_p\Delta T = u_b u_w$. As seen in Figure 19, $u_w = u_b - u_{a2}\tan\alpha$

$$\therefore gK_p\Delta T = u_b(u_b - u_{a2}\tan\alpha) \qquad (12\text{-}8f)$$

Tanα, of course, varies with radius and the relationship between tanα and r is determined by the design condition where, for free vortex whirl at rotor exit, $u_w r = u_{wm} r_m$ or $u_w = u_{wm}\frac{r_m}{r}$ and $u_{bD} = r\omega_D$ (suffix D implying the design value). It follows that $\tan\alpha = \frac{u_{bD} - u_{wD}}{u_{a2D}}$ or $\tan\alpha = \frac{r\omega_D - u_{wmD}\frac{r_m}{r}}{u_{a2D}}$ (12-9)

Writing $a = \frac{\omega_D}{u_{a2D}}$ and $b = \frac{u_{wmD}}{u_{a2D}}$, Equation (9) may be written

$$\tan\alpha = ar - \frac{b}{r} \qquad (12\text{-}9a)$$

whence Equation (8f) becomes

$$gK_p\Delta T = u_b^2\left[1 - u_{a2}\left(ar - \frac{b}{r}\right)\right] \qquad (12\text{-}8g)$$

ΔT, being the increase of total temperature across a stage, is thus seen to be a function of radius when u_b is different from the design value. It also depends on the axial velocity after each rotor, decreasing as u_{a2} increases from entry to exit of the assembly. Indeed ΔT for the first stage may well be two or three times greater than for the last at, say, 70% design speed assuming that the flow angle at rotor exit differs little from the blade angle.

Using variable stators to create pre-whirl in the direction of rotation at rotor entry both reduces ΔT and the angle of attack of the entering flow and therefore the risk of stalling and flow breakdown.

No attempt will be made herein to deal with the complex calculations necessary to determine how ΔT varies across the radius and from stage to stage in off design conditions. Enough has been said in the foregoing to indicate the nature of the complexities involved and to indicate that multi stage axial flow compressors call for great skill in design and development – plus a large measure of intuition.

Figure 20 is based on Figure 15 in which only single blade sections were drawn for root, mean, and tip radii, and is drawn to illustrate the blade channels at root, mean, and

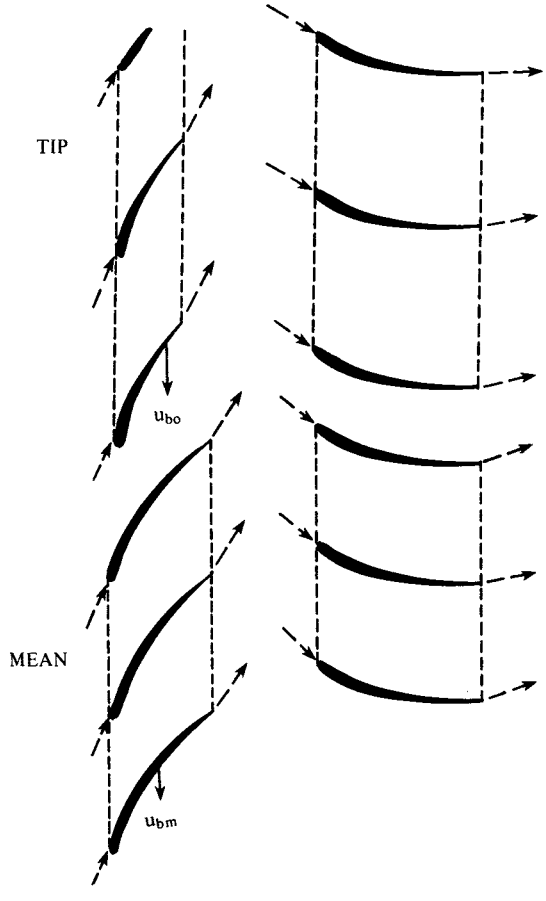

Fig. 12-20

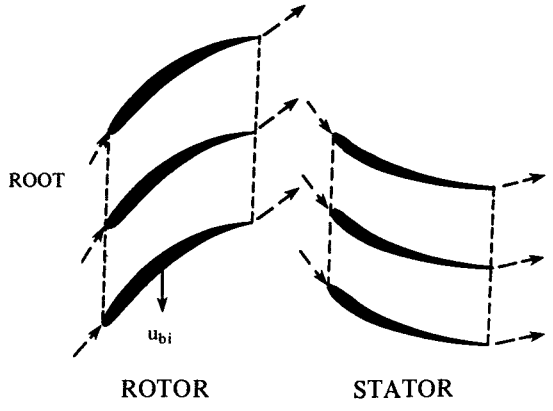

tip. For the rotor blades the pitch/chord ratio has been chosen to be approximately 0.5 at the root, and somewhat less for the stator blades. The pitch is, of course, proportional to radius, so the pitch/chord ratio increases from root to tip, especially in the case of the rotor where, as shown, the chord decreases from root to tip.

It will be recalled that Figure 15 was based on an example for the first stage of a multi stage compressor. Subsequent stages have progressively shorter blades so that if, say, all stages have the same mean radius, the root blade speed increases and the tip speed decreases. This latter fact coupled with the progressive rise in temperature means a decrease in Mach No. at the blade tips.

It will be noted from Figure 20 that there is considerable 'overlap' at the rotor blade roots but virtually no overlap at mean radius, while at the tips the trailing edges are pitched well ahead of the leading edges of the following blades. This is probably not a 'good thing' for supersonic relative velocity at entry in that the leading edge shock waves on the forward face side will 'miss' the trailing edge of the blade ahead, and no deflection can occur before passage through the shock wave. It seems desirable that the leading edge shock wave should at least 'strike' the trailing edge of the blade ahead.

The way the pitch/chord ratio will vary in successive stages will depend on the variation in the number of blades. As the blades get shorter it is usual to reduce the axial width and progressively increase the number of blades especially in aero engines where weight is all important.

The stator blades of Figure 20 are seen to have no overlap throughout their length.

The axial clearances shown in Figure 20 are purely arbitrary. From the aerodynamic and noise points of view, the larger the axial clearance the better to minimize the effect of the pressure field ahead of leading edges on the flow leaving trailing edges and to minimize the 'siren effect.' Large axial clearances, however, increase the overall length and therefore the weight, and increase sundry structural problems, which are themselves matters of considerable complexity in axial flow compressor design.

A Note on Axial Velocity

The choice of axial velocities for the design condition is a matter of judgement for the

designer, but on balance, it seems desirable to design for high axial velocity for the following reasons:

(1) reduction of overall size for a given mass flow rate

(2) reduction of the change of flow angles in off design conditions

(3) increase of resultant velocities relative to blading which has the effect of reducing the load coefficient (analogous to lift coefficient of an airplane wing).

There is, however, an upper limit. The axial velocity cannot exceed the local speed of sound otherwise choking would occur. Indeed it is desirable to keep the Mach No. of the axial velocity well below unity to allow for aerodynamic disturbances which well might provoke choking. Moreover, though in (3) above the increase of resultant velocity is suggested as an advantage there could be an undesirable increase of Mach No. relative to rotor blading at entry at outer radii.

In any event the effect on size reduction tends to become small when at high axial velocity Mach Nos., the density reduction increasingly offsets the velocity increase (and offsets it completely at Mach 1.0).

Another disadvantage which partially offsets the above advantages is that reduction of blade length is not accompanied by a proportionate reduction of tip clearance, the necessity for which contributes to losses.

Characteristic Curves

The form of the characteristic curves for a centrifugal compressor are shown in Fig. 7 of this section. The characteristics of an axial flow compressor may be similarly plotted. There are substantial differences however. The negative slope of the $\frac{N}{\sqrt{T_o}}$ curves is far greater, tending almost to the vertical especially at high values of $\frac{N}{\sqrt{T_o}}$. This is because, as has been shown, ΔT decreases sharply with increase of Q and so does the efficiency, hence, at a given value of $\frac{N}{\sqrt{T_o}}$, very small changes in Q result in large changes of pressure ratio. To some extent this is a stabilizing factor in a gas turbine since anything which tends to cause a reduction of Q is offset by the increase of delivery pressure which results.

The surge line may well start from a point on the ordinate for a pressure ratio well above p = 1.0 and may often show a pronounced 'kink' at an intermediate value of $\frac{N}{\sqrt{T_o}}$

Losses

At the design condition, if the design is good, the main source of loss is blade skin friction and turbulence associated with the boundary layer. There is also possible flow breakaway if the rate of channel divergence is excessive, due to the adverse pressure gradient. But as already mentioned, the centrifugal scavenging effect on the boundary layer must be a big saving factor in spite of the secondary flows caused. These latter, however, inevitably have a disturbing effect on the flow leaving a blade row and probably induce increased losses as the flow progresses from entry to exit of a multi stage compressor.

Tip leakage and its effect on secondary flows has already been discussed above. It is obviously desirable to keep the tip clearance as small as possible. The limitations to this will be discussed briefly below.

The axial velocity at exit would be a loss if it were not utilized, but in gas turbines it invariably is used. It may well more than compensate for combustion chamber pressure loss.

A Note on Tip Clearance

The problem of tip clearance increases from entry to exit of an axial flow compressor because of decrease in blade length and increase of temperature. The designer must allow for possible mechanical distortion, thermal distortion, the effect of coefficients of thermal expansion, the thermal capacity of the components, changes in dimensions due to stresses, etc. Thermal capacities of components in particular are of special importance in gas turbines and is possibly one of the main reasons why aircraft gas turbines adapted for industrial purposes have, surprisingly, proved more successful than machines designed specifically for such purposes by steam turbine manufacturers who tend to cling to the heavy scantling usual in steam turbines but which are quite inappropriate with gas turbines.

As we have seen, rotor blade tips are very thin so a tip rub can be disastrous. Hence the quest for casing linings which will render a tip rub relatively harmless.

The temperature changes which can occur as operating conditions are varied can be quite large, thus, for example, a rapid shut down or speed reduction may, and probably will, reduce tip clearances because the casing cools, and therefore contracts, more rapidly than rotor blades and discs. On the other hand, the light scantlings of aircraft gas turbines allow them to adjust to rapid changes in operating conditions almost as rapidly as the changes themselves. (The writer knows of one rather extreme case, where a marine gas turbine, built by a steam turbine manufacturer, had to be 'barred over' for 24 hours after shut down to counter damaging thermal distortions.)

TURBINES

General

The function of a turbine is exactly the opposite of that of a compressor. Whereas the function of the latter is to convert mechanical work into enthalpy as near isentropically as possible, the objective in a turbine is to convert enthalpy into mechanical work, also as near isentropically as possible. To that extent the basics of turbine theory have been covered 'in reverse' in the preceding discussion of compressor theory; thus, in the depiction of the centrifugal compressor of Figure 4, if one reversed the flow directions the result would represent a radial flow turbine (though these are always single sided so far as is known to the writer). The diffuser then becomes a nozzle ring, etc.

The same basic law applies, namely 'Torque equals the Rate of Change of Angular Momentum.' Also the flow must conform to the requirements of radial equilibrium wherever it is whirling.

Turbines are, however, altogether easier design propositions than compressors except for the limitations imposed by the ability of the blading, etc. materials to withstand the combination of high stress and high temperatures.

One great advantage of a turbine as compared with a compressor is that the heat (i.e., enthalpy) change per stage can be far higher than in an axial flow compressor. A single stage turbine for example can be adequate to drive a seven stage axial flow compressor.

Another big advantage is that the flow is in the direction of the pressure gradient (except in occasional designs, e.g., the first jet engine - which called for a small degree of recompression in the rotor channels at and near the root radius) and so the tendency of an adverse pressure gradient to cause flow breakdown is absent.

Yet another advantage is that the conversion of losses into heat at the early part of the expansion is partially recovered in the later part of the expansion, thus the heating effect of blade friction in a nozzle (or stator) ring partly compensates for the loss of total pressure. Similarly, in a multi stage turbine, the heating effect of losses in one stage adds to the energy available in subsequent stages.

A further advantage is that the high temperatures, because of their effect on raising the local acoustic velocity, permit the use of high axial velocities. (Though the energy value of high axial velocity at exhaust is lost as far as shaft power is concerned, it usually contributes to the energy available for further expansion – especially in the case of a jet engine, to be discussed later.) As will be seen below, high axial velocities are desirable for several reasons.

Turbine Types

It is beyond the scope of this treatise to attempt to cover the vast range of turbine types – from windmills, water wheels, Hero of Alexandria's 'aelopile' (perhaps the first known heat engine) through Pelton wheels, DeLaval's partial admission 'impulse' turbine to Parson's full peripheral admission 'reaction' turbine and Ljungström's contra rotating, multi stage radial flow type, and many others. Even radial flow turbines, though used in the first German jet engine designed by Von Ohain, and still a component of small gas turbine units, will not be further discussed. The reader must be satisfied with the statement in the foregoing, that they are centrifugal compressors acting in reverse, plus the additional statement that flow conditions in a radial flow turbine are much more favorable than those in a centrifugal compressor because of the absence of adverse pressure gradients. The following discussion is, therefore, limited to the common forms of full peripheral admission axial flow turbines used in nearly all modern gas turbines. (There are one or two small gas turbine designs having radial flow turbines.)

The terms 'impulse' and 'reaction' call for some explanation. They are really obsolete and are 'left overs' from days before the importance of radial equilibrium was recognized, i.e., when turbine blading was designed on the assumption that the tangential and axial components of the velocity of the steam or other fluid issuing from the nozzle ring was constant across the annulus. In the case of blades which were short in proportion to the mean radius they usually had the same profile section from root to tip. In the case of longer blades there would be a certain amount of 'twist' to compensate for the variation of blade speed, but no attempt to compensate for the variation in whirl speed since the presence of this variation was not recognized. (When the writer's first jet engine was built he left the design of the turbine blades to the blade design specialists of the manufacturing firm – The British Thompson-Houston Co., otherwise known as the B.T-H Company, assuming that they were fully aware of the variation in whirl velocity which must occur to satisfy radial equilibrium or 'vortex flow' as the writer then called it.

He was then quite unaware that there was any novelty in the concept, and did not find out that there was a major difference in thinking between himself and the B.T-H designers until the latter proposed a design change which, they said, would cause a large increase in end thrust to a figure well beyond the capacity of the then existing thrust bearings. This completely mystified the writer and he started to inquire into the matter. He casually asked one of the designers most concerned, "What pressure difference do you calculate between root and tip in the annular gap between nozzle discharge and rotor entry?" and was astonished to receive the reply, "What pressure difference?" This started a somewhat acrimonious controversy, not helped by the fact that the writer, realizing that his views on turbine design were novel to the turbine industry, filed and obtained a patent for 'vortex design.' The B.T-H designers were, however, under the terms of the contract, obliged to conform to the writer's insistence that the blades be made to be compatible with a free vortex flow from the nozzle ring. So, so far as is known to the writer, the first jet engine had also the first turbine to incorporate design for radial equilibrium. This meant that the blades had about double the twist compared with those in which only variation in blade speed with radius was allowed for. It also meant that the calculated end thrust was negligible - a fact subsequently verified experimentally.

In fairness it should be mentioned that other designers were beginning to be suspicious of the then conventional design assumptions. In one of their bulletins, Escher Wyss reported their finding of a substantial pressure difference between root and tip ahead of a turbine rotor but did not explain it. Also the small gas turbine group at the Royal Aircraft Establishment, at that time in the early stages of the design of a turbo-prop engine for aircraft, recognized the need for designing for radial equilibrium and supported the writer in his controversy with the B.T-H.)

In order to explain the terms 'impulse' and 'reaction' the reader is asked to visualize blades so short in proportion to mean radius that the blade profiles are not affected by variation of whirl velocity and blade speed with radius.

An impulse turbine is then one in which the entire pressure drop (neglecting blade losses) takes place in the nozzles and the rotor blades merely reverse the direction of relative whirl. This means that, if the direction of the flow at rotor exit is purely axial, the absolute whirl before the rotor is exactly twice the blade speed so that the whirl relative to the rotor is equal to blade speed both at entry and exit. The appropriate vectors and blade profiles are shown in Figure 21.

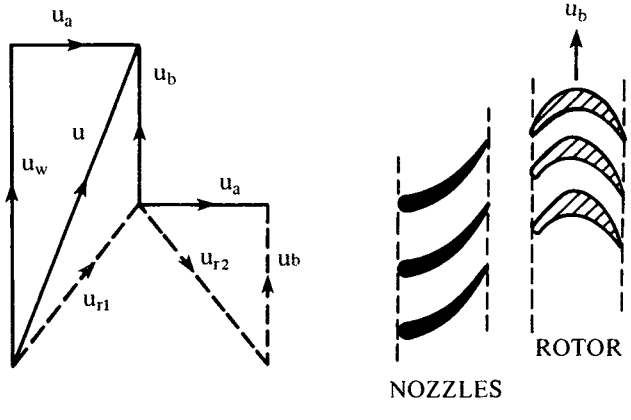

Fig. 12-21
Impulse Blading

In the left hand (vector) diagram the full lines represent absolute velocities and the broken lines represent velocities relative to the rotor. The axial component u_a is, of course, common to both nozzles and rotor blades, and has been chosen to be the same before and after the rotor blades.

The few blades sketched in the right hand diagram are drawn to conform with the vectors shown. As may be seen, the channel width of the rotor blading is substantially constant from entry to exit. In practice the rotor blades have leading edges 'rounded off' to a greater extent than shown to render them less sensitive to changes in flow direction at off design speeds.

Since, at design speed, $u_w = 2u_b$ the whirl velocity relative to the rotor equals u_b both at entry and exit $\therefore \Delta u_w = 2u_b$ and the change in angular momentum $\Delta r u_w = 2u_b r$ $\therefore$ the specific torque is proportional to $2u_b r$ and the specific power $W_S \propto 2u_b r\omega$, so, since $r\omega = u_b$, $W_S \propto 2u_b^2$, or $W_S \propto 2\theta_b$. More exactly, $W_S = \frac{2u_b^2}{g} = \frac{2u_b^2}{g}\left(\frac{2gK_p}{2gK_p}\right) =$

$4K_p\left(\frac{u_b^2}{2gK_p}\right)$, so writing $\frac{u_b^2}{2gK_p} = \theta_b$, $\quad W_S = 4K_p\theta_b$

In a 'pure reaction' turbine, the whirl component of the flow issuing from the nozzles is equal to the blade speed and, for axial exit flow so is the whirl relative to the rotor at exit. The fact that the absolute whirl before the rotor equals blade speed means that there is no relative whirl at rotor entry, i.e., the resultant velocity relative to the rotor is purely axial and so expansion takes place in the rotor blade to generate the relative whirl at exit. The appropriate vectors and blade profiles are shown in Figure 22, for the same blade speed and axial velocities as in Figure 21. This arrangement is usually referred to as '50% reaction' in that half the conversion of heat drop into kinetic energy occurs in the nozzles and the other half in the rotor blades, which are, in effect, rotating nozzles.

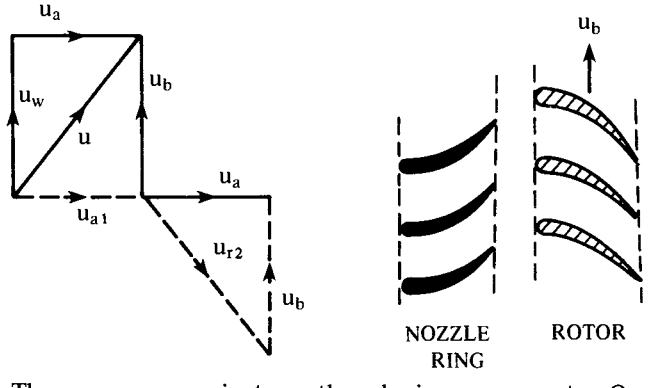

Fig. 12-22
Reaction Blading

There are many variants on these basic arrangements. One may design for 'residual whirl' and thereby increase the specific torque of rotor blading. This residual whirl would, of course, be a loss unless either (a) the kinetic energy it has is efficiently reconverted into heat energy by a ring of stator blades in the same manner as in an axial flow compressor, or (b) its energy contributes to the power generated in subsequent expansion as, for example, by driving a contra-rotating turbine. (It should be noted that residual whirl is unavoidable and unusable in a turbine which consists of a single rotor only, e.g., most windmills and so called 'wind turbines.')

As may be seen from Figure 22, $\Delta u_w = u_b$, i.e., half that of Figure 21 $\therefore$ the specific torque is proportional to $u_b r$ and the specific work W_S is proportional to u_b^2, i.e., half that of impulse type blading for a given blade speed, i.e., $W_S = 2K_p\theta_b$.

Figure 23 shows the vector diagram and blade arrangement of a 'two row Curtis Wheel' as often used at the high pressure end of a steam turbine and as proposed to be used to drive a compressor in the writer's first jet engine patent. As shown, the initial whirl u_{w1} is four times u_b and the 'residual whirl' is twice u_b on leaving the first rotor (of impulse sections). The intermediate stator acts like a stationary set of impulse blading and merely reverses the direction but not the magnitude of the absolute velocity from the first rotor, i.e., $u_3 = u_2$. Thus the whirl at entry to the second rotor is $2u_b$ (as in Figure 21).

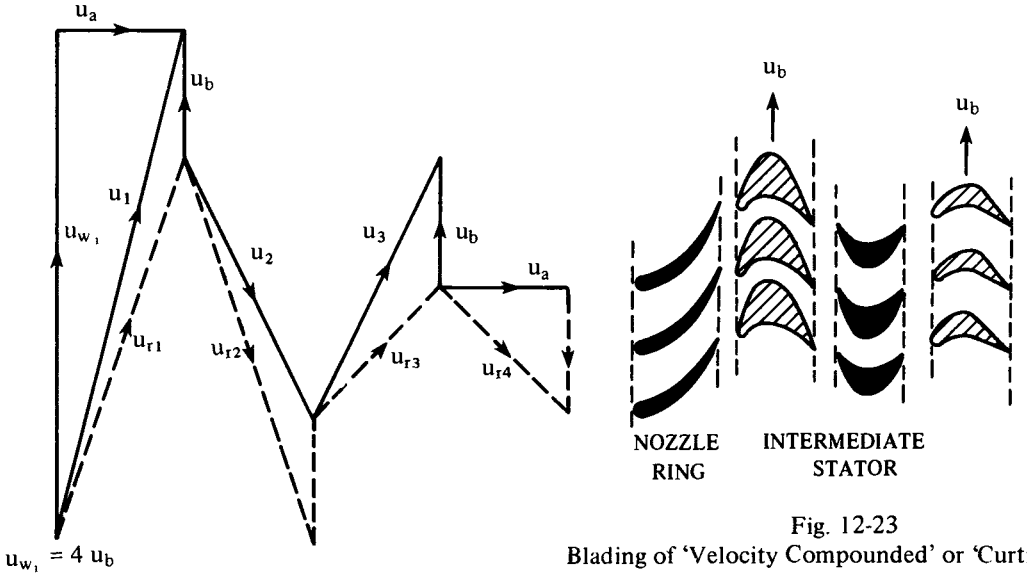

Fig. 12-23
Blading of 'Velocity Compounded' or 'Curtis' Type

The change of whirl in the first rotor is seen to be $6u_b$ and to be $2u_b$ in the second rotor to give a total of $\Delta u_w = 8u_b$. Thus the specific torque and power for a given blade speed is four times that of impulse blading (as in Figure 21). Conversely, the blade speed could be reduced by half for a given specific power.

There are many variants on the arrangements shown in Figures 21, 22, and 23. For example the one of Figure 23 might be converted to a contra rotating two stage turbine by removing the intermediate stator and reversing the direction of rotation of the second rotor. The total specific power would remain unchanged.

The foregoing discussion is, however, somewhat unrealistic in the light of the need to design for radial equilibrium which requires that the 'degree of reaction' must increase from root to tip.

In the writer's opinion, the terms 'impulse' and 'reaction' should be abandoned. One might define a turbine type by the ratio of blade speed to change of whirl at the mean radius, i.e., by $\frac{u_{bm}}{\Delta u_{wm}}$. Alternatively one might use $\frac{\theta_{bm}}{\Delta T}$ where θ_{bm} is the temperature equivalent of blade speed at mean radius. Thus, for blading which, at mean radius, had

profiles corresponding to 50% reaction (as in Figure 22), $\frac{u_{bm}}{\Delta u_w} = 1.0$, or since $\Delta T = \frac{u_b \Delta u_w}{gK_p}$ (see Equation (8e) of this section) and for '50% reaction' $\Delta u_w = u_b$ and $\theta_{bm} = \frac{u_{bm}^2}{2gK_P}$ then $\frac{\theta_{bm}}{\Delta T} = 0.5$.

It is now necessary to take a look at the effects of radial equilibrium on blade design, and for this purpose a specific example will be chosen, it being assumed that the whirl distribution before the rotor is that of a free vortex (which is the condition for constant ΔT at all radii, as has been shown earlier), i.e., $u_w r = u_{wm} r_m$, and that the exhaust flow is purely axial.

The assumptions are based on a single stage turbine to drive directly a 245° compressor with a mass flow of 350lb/sec and which, at entry to the first stage, has a blade speed of 700'/sec at a root radius of 1.0ft (note that these figures are basically those of a seven stage compressor for which the blade sections, etc. of the first stage are shown in Figure 15).

Though, in practice, at the high temperatures concerned, the value of C_p would be well above 0.24 and the value of $\frac{\gamma}{\gamma - 1}$ slightly above 4.0, these mild complicatons are not taken into account. Neither is the increase of mass flow by fuel addition. So it is assumed that the mass flow through the turbine is the same as that through the compressor, namely 350 lb/sec, and that $K_p = 336$ ft. lb/lb°C and $\frac{\gamma}{\gamma - 1} = 3.5$.

In order to keep the blades as short as possible and thus avoid excessive tip speed, it will be assumed that at the root radius, $u_w = 2u_b$ (i.e., an impulse section) and that the axial velocity at rotor exit has the high value of 1450'/sec (equivalent to 97.2°C).

Other assumptions are: (1) Total temperature T_{max} before the nozzles = 1200° K; (2) Total pressure P_{max} before the nozzles is 14,700 p.s.f.; and (3) Adiabatic efficiency $\eta_T = 0.9$.

The actual temperature drop θ_T is thus 245 + 97.2 = 342.2°C (since the energy remaining in the axial velocity contributes nothing to the shaft power) ∴ the static temperature of exhaust is 1200 − 342.2 = 857.8°K (for which the acoustic velocity is 1927'/sec. hence the Mach No. of exhaust is $\frac{1450}{1927} = 0.75$); θ'_T, the isentropic temperature drop (total to static) is $\frac{342.2}{0.9} = 380.2$ to give a temperature ratio $t_T = \frac{1200}{1200 - 380.2} = 1.464$ for which the pressure ratio p_T is $p_T = 1.464^{3.5} = 3.795$ to give a static pressure at exhaust $P_E = \frac{14,700}{3.795} = 3,874$ p.s.f. which, with a static temperature of 857.8, gives the density ρ_E at exhaust, i.e., $\rho_E = \frac{3874}{96 \times 857.8} = 0.047$. It now remains to find the annulus area S from $S = \frac{Q}{\rho u_a} = \frac{350}{0.047 \times 1450} = 5.13$ ft.^{2}

From $gK_P\Delta T = 2u_{b_1}^2$ for the root radius r_i, $u_{bi} = \sqrt{\frac{gK_P\Delta T}{2}} = \sqrt{\frac{32.2 \times 336 \times 245}{2}} =$ 1151′/sec. It follows that, since the blade speed of the compressor was taken to be 700′/sec at a radius of 1 ft., r_i for the turbine must be $\frac{1151}{700} = 1.645'$. The tip radius may now be found from $S = \pi(r_o^2 - r_i^2)$ and with S = 5.13 (from above) r_o = 2.083 ft. to give a tip speed $u_o = \frac{2.083}{1.645} \times 1151 = 1457'$/sec. The mean radius $r_m = \frac{2.083 + 1.645}{2} = 1.864$ ft.

It now remains to find the axial velocity before the rotor on the assumption that the annulus area does not change in the rotor, i.e., S is also 5.13 sq. ft. at rotor entry.

As we have seen in the case of the axial flow compressor with free vortex whirl distribution the density at mean radius may be used to calculate axial velocity from mass flow and vice versa. Having assumed that root whirl is twice blade speed at the root, i.e., $2 \times 1151 = 2302'$/sec, the whirl velocity u_{wm} at mean radius is given by $\frac{r_1}{r_m} \times 2302 = \frac{1.645}{1.864} \times 2302 = 2031'$/sec the temperature equivalent of which is 190.7°C $\therefore$ the static temperature at mean radius $T_m = 1200 - 190.7 - \theta_a = 1009.3 - \theta_a$ where θ_a is the temperature equivalent of the (uniform) axial velocity before the rotor.

The total density before the nozzles $\rho_{max} = \frac{P_{max}}{RT_{max}} = \frac{14{,}700}{96 \times 1200} = 0.128$ $\therefore$ assuming substantially isentropic expansion through the nozzles, the density at mean radius ρ_m after the nozzles is given by $\rho_m = \rho_{max}\left(\frac{T_m}{T_{max}}\right)^{2.5} = 0.128\left(\frac{1009.3 - \theta_a}{1200}\right)^{2.5}$. Also, $\rho_m = \frac{Q}{Su_a} = \frac{350}{5.13\,u_a} = \frac{68.2}{u_a}$. Using $u_a = 147.1\sqrt{\theta_a}$, $\rho_m = \frac{68.2}{147.1\sqrt{\theta_a}} = \frac{0.464}{\sqrt{\theta_a}}$.

It follows that $\frac{0.464}{\sqrt{\theta_a}} = 0.128\left(\frac{1009.3 - \theta_a}{1200}\right)^{2.5}$ or $\sqrt{\theta_a}\left(\frac{1009.3 - \theta_a}{1200}\right)^{2.5} = 3.623$ from which (by trial) θ_a = 38°C and u_a = 907′/sec. Thus there is a very considerable increase of axial velocity in passage through the rotor blades if the annulus area remains constant. This means acceleration in the moving blades even at the root which is, therefore, not a true impulse section.

All the information is now available to draw the vector diagrams and blade sections and this is done in Figure 24 with the aid of the following table:

	r	u_w	u_{a1}	u_b	u_{a_2}
r_i =	1.645	2302	907	1151	1450
r_m =	1.864	2032	907	1304	1450
r_o =	2.083	1818	907	1457	1450

AT NOZZLE ENTRY Total Temp = 1200°K; Total Press. = 14,700 psf.
Stagnation Density = 0.128 lb/ft.^{3}

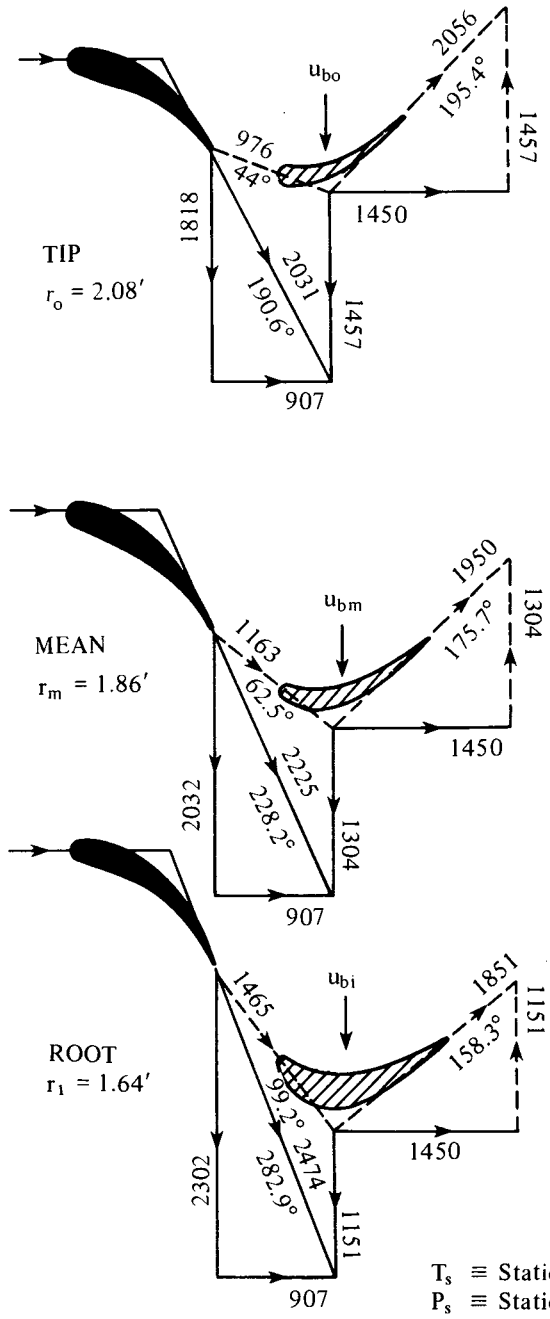

T_s = 1009.4
T_R = 1053.4
t_n = 1.189
t_R = 1.228
P_s = 8024
ρ = .083
ρr = .173

T_s = 971.2
T_R = 1034
t_n = 1.236
t_R = 1.205
P_s = 7011
ρ_s = .075
$\rho_s r$ = .141

T_s = 917.1
T_R = 1016
t_n = 1.308
t_R = 1.184
P_s = 5736
ρ_s = .0655
$\rho_s r$ = .1075

At rotor exit, static pressure = 3874 psf, static temp = 858°K
and density = .047

Fig. 12-24

$T_s \equiv$ Static Temp after nozzles °K
$P_s \equiv$ Static Press after nozzles psf
$\rho_s \equiv$ Density after nozzles lb/ft^3
$T_R \equiv$ Total Temp relative to rotor blades °K
t_n = Temp ratio (total/static) for nozzles
t_R = Temp ratio (total/static) for rotor blades

In Figure 24, full lines indicate absolute component and resultant velocities and broken lines whirl (at exit) and resultant velocities relative to the rotor blades. The velocities are shown on all vectors and their temperature equivalents on resultant velocity vectors. To the right of each diagram the values of several important variables are listed. From these a number of important points should be noted, namely:

(1) The total temperature relative to the rotor blades decreases from tip to root which is a good thing from the temperature–stress point of view.

(2) The temperature ratio (total to static) across the nozzles is above the critical ratio 1.2 from root to mean radius and below at greater radii, i.e., the nozzles are choking, but 'only just.'

(3) The reverse is the case for the rotor blading, i.e., the greatest temperature ratio is at the tips.

(4) The static pressure upstream of the rotor blades increases from 5736 p.s.f. at the roots to 8024 p.s.f. at the tips.

(5) The increase of flux density is also considerable from root to tip in the inter-blade space, which means that there has to be an outward radial component of flow in the nozzles and vice versa in the rotor blading. The effect of these radial velocity components on radial equilibrium would, however, be insignificant, i.e., $\frac{d\theta r}{\theta_w}$ would be negligible.

(6) The value of $\rho_s r$ at mean radius is within 1% of the mean of its values at root and tip which, since $Q \propto \int_{r_i}^{r_o} \rho r dr$, justifies the use of density at mean radius for calculating the axial velocity ahead of the rotor blades.

The tip/root radius ratio is $\frac{2.08}{1.64} = 1.27$ approximately, i.e., the blades are relatively short, yet, as may be seen, the 'degree of reaction' increases considerably from root to tip. The effect of this on blade profile section is very useful from the stress point of view.

It is, of course, possible to deal with vector diagrams, etc., entirely non dimensionally by making all velocities multiples of a reference velocity (which might conveniently be the blade speed at mean radius); all dimensions multiples of, say, mean radius; all temperatures and temperature equivalents multiples of, say, T_{max}, and using pressure ratios, etc., rather than absolute pressures as was done for the calculations relating to Figure 24. The writer, however, deemed it preferable to present a picture of actual magnitudes, especially in relation to the temperatures to which the rotor blades are subjected.

If non-dimensional methods had been used then the diagrams in Figure 24 would be appropriate for a range of geometrically similar turbines.

The high axial velocity at rotor exhaust would be a serious loss if not utilized, since its energy represents a considerable proportion of the heat drop. In fact though the adiabatic efficiency in the case on which Figure 24 is based was taken to be 0.9 the shaft efficiency η_s would be given by $\eta_s = \frac{245 \times 0.9}{245 + 97.2} = 0.644$ (since θ_a at exhaust = 97.2°C). But normally the energy of the exhaust contributes to the energy available for further expansion in,

say, a succeeding turbine or propelling jet. If exhaust axial velocity energy cannot be so utilized, then it would be desirable to design for a far lower value or reduce it in a diffusing exhaust annulus. In the latter case, the static pressure at rotor exit would be substantially lower than that of final exhaust, i.e., there would be recompression in the exhaust ducting.

It will be noted that the tip radius of the turbine of Figure 24 is only 4% greater than that of the first stage rotor of the compressor. It was designed to drive directly so that compressor and turbine are well matched from the point of view of size. They could in fact have been made equal by reducing the turbine root diameter if there was good reason to do so.

With the temperatures used, blade speed, and the relatively short rotor blades, blade cooling should not be necessary with present day materials, but for aircraft gas turbines at least, the trend is for much higher turbine inlet temperatures, greater tip speeds, etc., for which blade cooling becomes essential.

Calculation of End Thrust

At root radius of 1.64′ the static pressure before the rotor is 5736 p.s.f. and after is 3874 p.s.f. ∴, neglecting the shaft section, the end thrust due to differential pressure across the rotor disc is $(5736 - 3874)\,\pi \times 1.64^2 = 15.730$ lbs. To this must be added the pressure differential across the blading which increases from root to tip and is given by $2\pi \int_{r_i}^{r_o} (P_S - 3874) r\,dr$, and is found by plotting, to be 15,800 lbs. approximately, to give a total 'downstream' end thrust of 31,500 lbs. approximately. If coupled directly to the compressor rotor by shafting able to transmit the tension this goes some way to countering the opposite end thrust of the compressor rotor (not calculated).

Losses

These are generally of the same type as those already covered in the discussion of losses in compressors earlier in this section. As with compressors, the boundary layers in the blading will be profoundly affected by the intense centrifugal field, but with turbine blading, losses due to fluid friction are much reduced by the fact that the flow is in the direction of 'descending' pressure gradient so that the likelihood of flow breakaway is much reduced. For the same reason turbine blades are far more tolerant of changes of flow direction at rotor entry at off design conditions. With sufficiently rounded leading edges a variation of angle of attack of the order of $\pm 15^\circ$ would not cause serious flow breakdown unless the pitch/chord ratio were too large. (In the writer's experience the number of rotor blades should be as large as structural and stress considerations will permit.)

Tip leakage is probably the largest source of loss with uncooled blading and is a bigger problem than in a compressor. For stress and temperature reasons the turbine rotor is the most massive component in a gas turbine and, therefore, the one with the largest thermal capacity, hence there is a considerable time lag before contraction or expansion is complete after temperature changes, and this must be allowed for by relatively large tip clearance. This coupled with the large difference in static pressure from entry to exit means a very undesirable 'short circuit' of fluid. If stresses will permit, shrouding the tips (each blade carrying a shroud segment) is very beneficial.

Blade cooling adds to blade losses and reduces turbine efficiency but reduced turbine efficiency is more than offset by the gain in overall cycle efficiency resulting from the increase in allowable turbine entry (i.e., maximum cycle) temperatures.

SECTION 13
Aircraft Propulsion General

Introductory

Up to this point this work has been concerned with air breathing gas turbines in general. From here on we shall be studying their application to aircraft propulsion in the forms of turbo jets, turbo fans, etc., plus a brief discussion of the ram jet.

In its use for aircraft propulsion the gas turbine has several advantages as compared with its use for power generation at sea level which are the reasons for the fact, in general, that its application in such fields as marine propulsion, power generation, oil pipe line pumping, etc., has lagged badly behind its aircraft applications.

Except for light aircraft the gas turbine in various forms has completely displaced the piston engine-propeller combination which, until World War II, was the sole form of aircraft power plant.

The main advantages referred to above are:

(1) Part of the total compression is provided at high efficiency by ram compression due to forward speed (though at the expense of momentum drag).

(2) The low atmospheric temperatures at height substantially increase the cycle efficiency for a given maximum thermal cycle temperature.

(3) Power plant weight and bulk are greatly reduced in proportion to power.

(4) Because of (1) and (2), overall efficiency increases with height and speed.

(5) Only part of the expansion is subject to turbine losses. The part which provides the energy of a propelling jet takes place at very high efficiency.

There are certain disadvantages, however, e.g., though the aircraft gas turbine can operate with a much wider range of fuels than the piston engine it is less amenable in this respect than sea level gas turbines which can operate with almost all the range of distillate fuels whereas the aircraft gas turbine is restricted to fuels with a waxing point not above

-40°C approximately. (It is possible that this restriction may be eased for supersonic aircraft or if fuel tank heating should prove to be practicable for subsonic aircraft.) This means that the fuel must be in the kerosene-gasolene range.

Another disadvantage is the greater complexity of the combustion and fuel system due to the far greater range of fuel consumption requirements as between that for take off and initial climb on the one hand and idling on descent from great heights on the other.

As compared with the piston engine-propeller combination, the advantages are immense—far higher power/weight ratio, lack of vibration, an astonishing increase in reliability, etc.

International Standard Atmosphere (ISA)

The physical properties of the atmosphere vary so much from day to day, from season to season, with latitude, height, etc., that comparisons of performance of aircraft and engines would be very poorly based unless corrected to some generally accepted 'standard atmosphere.' This difficulty was recognized some fifty years ago and led to the international acceptance of such a standard atmosphere on which design could be based and to which observations of performance could be corrected. The result was the now generally accepted "International Standard Atmosphere."

The properties of I.S.A. are summarized as follows:

Temperature: taken as 288.3°K at sea level and the rate of fall with height (the 'lapse rate') as 6.5°C per km. which is almost exactly 2°C per thousand feet. The drop off of temperature at this lapse rate is assumed to extend to the 'tropopause' at 36,090′ (11 km) above which (the 'stratosphere') temperature is assumed constant at 216.8°K, i.e., the stratosphere is isothermal and is deemed to extend to heights far above the foreseeable operational limits of aircraft. (At very great heights – the mesosphere – the absorption of short wave solar radiation causes temperature to increase with height.)

Pressure: taken as 2116.2 p.s.f. (= 760mm of mercury at 0°C) at sea level and to decrease with height in the troposphere (below the tropopause) according to the law $\frac{P_h}{P_o} = \left(\frac{T_h}{T_o}\right)^{5.256}$ (which may be deduced from $P = \rho RT$ and $dP = -\rho dh$). In the stratosphere, the pressure at 36,090′ is 472.7 p.s.f. and above that is given by $20{,}813 \text{ Ln.}\frac{472.7}{P_h} = h - 36{,}090$ (which may be deduced from the isothermal relationship $P = \rho R \times 216.8$ and $dP = -\rho dh$).

Density: taken as 0.07646 lb/ft^3 at sea level and to decrease with height in the troposphere according to the law $\frac{\rho_h}{\rho_o} = \left(\frac{T_h}{T_o}\right)^{4.256}$ to the value 0.02272 lb/ft^3 at the tropopause. In the stratosphere, density is proportional to pressure.

Viscosity: the coefficient of viscosity μ decreases with temperature up to the tropopause and remains constant in the stratosphere. According to Sutherland's formula $\mu = A\left(\frac{T^{3/2}}{T+B}\right)$ in slugs/ft sec where $A = 3.059 \times 10^{-8}$ slug/ft sec and $B = 114°$.

The kinematic viscosity $\nu = \frac{\mu}{\rho}$ increases with height the rate of increase being greater in the stratosphere than in the troposphere.

In practice the 'real' atmosphere varies very widely from I.S.A. For example, according to season, the tropopause may be as high as about 70,000′ in tropical latitudes and as low as 25,000′ over polar regions. Moreover, in unstable atmospheric conditions such as those associated with thunderstorms or when winds are forced up or down by ground contours the lapse rate will tend to conform to the 'isentropic value' of 3°C per thousand ft. These facts coupled with the very large variations of sea level temperature with season, latitude and weather must mean that the occasions when the real atmosphere coincides with I.S.A. above any given point on the earth's surface must be very rare. Nevertheless the I.S.A. is essential for design purposes and for performance corrections. But the designer must make allowance for departures from I.S.A., e.g., the loss of power for take off which occurs with high sea level temperature as in the tropics.

In all that follows, the atmosphere is assumed to conform to I.S.A.

Aircraft Drag

For subsonic aircraft in steady horizontal flight there are two major components of drag, namely 'parasite' drag (or aerodynamic resistance drag) and 'induced' drag or 'lift drag' which is the penalty paid for lift.

Parasite drag may be broken down into 'skin friction' due to viscosity, form drag due to 'shape' and 'interference drag' arising from junctions of components, e.g., wings and fuselage. These components have one thing in common – that they are proportional to the dynamic pressure relative to the aircraft, namely $\frac{\rho u^2}{2g}$ (where u is the air speed) and to the surface area. They (especially skin friction) are also a function of Reynold's number R_e where R_e is defined as $R_e = \frac{u\ell\rho}{\mu}$ or $R_e = \frac{u\ell}{\nu}$ where ℓ is a characteristic dimension of length in the direction of u, e.g., wing chord or fuselage length and ν is kinematic viscosity. But, for a given airplane, the effect of $f(R_e)$ is normally small so one may assume that parasite drag $D_P = C_D \frac{\rho}{2g} Su^2$ where S is the 'wetted area' and C_D is the coefficient of parasite drag. The effect of R_e cannot, however, be ignored when relating the results of wind tunnel model tests to full scale aircraft.

Induced or lift drag is a consequence of obtaining lift by the downward displacement of air by the aircraft's wings. It is beyond the scope of this work to explain how this gives rise to induced drag. In brief, with a wing of finite span, the wing tip vortices resulting from wing tip 'spill' from the under (high pressure) side to the upper (low pressure) side are a continuation of the 'bound vortex' surrounding the wing which, superimposed on the general flow, constitutes 'circulation' which, ahead of the wing, causes an upward component of flow or 'upwash' which compliments the 'downwash' astern. The aircraft is, as it were, flying uphill. This effect is inversely proportional to wing span and ρu^2. With infinite wing span there would be no induced drag. So, for a finite span, induced drag $D_i \propto \frac{1}{\rho u^2}$.

Total drag D is therefore given by $D = A\rho u^2 + \frac{B}{\rho u^2}$ and the constants A and B are such that D is a minimum when parasite drag and induced drag are equal, i.e., Lift/Drag ratio is a maximum when $D_P = D_i$.

At transonic and supersonic speeds the aerodynamic situation changes dramatically due to the formation of shock waves, and the fact that the air ahead of the aircraft cannot sense its approach (since small pressure disturbances cannot propagate faster than the speed of sound). There is therefore an additional shock drag, and the lift drag arises from the downward deflection of the air passing through the shock wave. The net result is a large increase of drag and therefore reduction of lift drag ratio as the penalty for supersonic speeds. Fortunately, improvement in propulsion efficiency with speed goes quite a long way to offsetting the reduction of lift drag ratio.

In fact, aircraft drag begins to rise sharply at speeds a little below Mach 1.0 because air velocity over aircraft surfaces (outside the boundary layer) is greater than flight speed especially over the forward parts of wings, etc. The drag rise 'peaks' at values of Mach No somewhat greater than unity and then begins to drop quite rapidly at higher Mach Nos though always being well above low and moderate subsonic drag.

Aircraft Weight

Aircraft weight is, of course, greatest at take off and diminishes as fuel is consumed. Hence since total fuel weight may be as much as 50% of take off weight, there is a very considerable weight change with time and distance flown.

At modern and future heights and speeds, certain small factors affecting weight are beginning to become significant, e.g., at a height of 12 miles g is reduced by nearly 2/3 of 1%, but this is about half offset by the negative buoyancy of a pressurized cabin, which for a civil aircraft flying at 50,000′ and pressurized to 5,000′ is nearly 1/3 of 1%. This is equal to about 8 passengers in a 'wide bodied' airliner. Again as speeds rise to, say, 2,000 mph relative to the earth's surface, there is a significant reduction of effective weight due to centrifugal force relative to the earth's axis. At orbital speed, i.e., 26,000′/sec approximately, W = 0.

The reduction of the effective weight is proportional to the square of the speed about the earth's axis and this is affected by latitude and direction of flight, thus a supersonic aircraft travelling at 2,000 mph from west to east (i.e., in the direction of the earth's rotation) over the equator would have a speed of 3,000 mph or 4,400′/sec approximately relative to the axis so its effective weight would be reduced by $\left(\frac{4400}{26000}\right)^2 = 0.029$ approximately, i.e., a reduction of nearly 3% which could be worth about 116 miles of extra range for a 'normal' still air range of 4,000 miles. But if flying from east to west the speed relative to the axis would be only 1,000 mph and the effective reduction of weight only 0.003 approximately, i.e., less than 1/3rd%.

Functions of Aircraft Power Plant

Apart from important but minor functions such as cabin pressurization, powering electric and hydraulic systems, the primary function of aero engines is to provide thrust to overcome drag and for climb and acceleration.

The 'ceiling' is reached when the thrust is sufficient only for drag at or near the maximum value of lift drag ratio. This ceiling, of course, increases slowly as fuel consumption reduces weight.

If an aircraft is climbing at angle α to the horizontal then the component of weight W along the flight path is W sin α and the component normal to the flight path is W Cos α, i.e., Lift L = W Cos α.

The thrust required for acceleration $F_{acc} = \frac{W}{g}\frac{du}{dt}$ or $\frac{W}{g}\,u\,\frac{du}{ds}$ where du and ds are along the flight path.

Hence to deal with drag D, climb $\frac{dh}{dt}$, and acceleration, total thrust F is given by

$$F = D + W \sin\alpha + \frac{W}{g}\,u\,\frac{du}{ds} \qquad (13\text{-}1)$$

Since $D = \frac{W \cos\alpha}{\ell}$ where ℓ is the lift/drag ratio, Equation (1) may be written

$$\frac{F}{W} = \frac{\cos\alpha}{\ell} + \sqrt{1 - \cos^2\alpha} + \frac{1}{g}\frac{du}{dr} \qquad (13\text{-}1b)$$

$$\text{or} \quad \frac{F}{W} - \frac{1}{g}\frac{du}{dt} = \frac{1}{\ell}\cos\alpha + \sqrt{1 - \cos^2\alpha} \qquad (13\text{-}1c)$$

It should be noted that if the angle of climb α is large and the lift component normal to the flight path correspondingly reduced then induced drag is reduced and the weight/drag ratio correspondingly increased. In the extreme case of a straight vertical climb the lift is zero and so induced drag disappears.

For most aircraft α is significantly large only in the initial stages of climb. As the angle flattens out to the point where $\alpha \simeq \tan\alpha \simeq \sin\alpha$ equation (1) may be simplified

$$\text{to} \quad \frac{F}{W} - \frac{1}{\ell} = \frac{1}{u}\frac{dh}{dt} + \frac{1}{g}\frac{du}{dt} \qquad (13\text{-}2)$$

F, W, and ℓ, however, vary with height and speed so Equation (2) can only be used for time intervals sufficiently short for reasonably accurate mean values of F, W, and ℓ to be used.

Equations (1) and (2) are mainly of use in rate of climb calculations. In such calculations where take off thrust is high in proportion to weight (e.g., S.S.T.s) the writer finds it is sufficient to take height intervals of 5,000′ up to heights where acceleration has ceased and the rate of climb is approaching zero. Such calculations are necessary for calculating the weight at the end of climb and the horizontal distance covered during climb – usually of the order of 150–250 miles in still air.

The Breguet Range Formula

According to this well known formula the still air cruising range R from the end of climb to the beginning of descent is given by $R = \eta \ell C \text{ Ln. } \frac{W_1}{W_2}$ where η is the overall efficiency of the power plant, ℓ is the lift/drag ratio, C is the calorific value of the fuel, in ft lb/lb W_1 is the weight at end of climb and W_2 is the weight at beginning of descent, i.e., $W_1 - W_2$ is the weight of fuel consumed during cruise. W_2, of course, includes fuel for descent and reserves for diversion and 'stand off.'

The formula assumes that as weight is decreased by fuel consumption the aircraft climbs slowly to maintain constant indicated air speed which is the condition for constant lift/drag ratio ℓ.

The Breguet range formula is easily obtained as follows: If the fuel consumed is $-\delta W$ in distance δs, the work done against drag is $\frac{W}{\ell}\delta s$. The power for this must come

from the power plant, hence $-\eta C\delta W = \frac{W}{\ell}\delta s$ or $\delta s = -\eta\ell C\frac{\delta W}{W}$ from which $s_2 - s_1 \equiv R = \eta\ell C \text{Ln}\frac{W_1}{W_2}$.

Example 13-1:

If the take of weight is W_o; climb fuel is $0.1W_o$; reserve fuel is $0.1W_o$; and fuel for descent is $0.01W_o$, what is the still air range if 1) take off fuel = $0.5W_o$, 2) $\eta = 41\%$, 3) $\ell = 7.5$, and 4) the calorific value of the fuel is 10,500 C.H.U./lb? (1 C.H.U. = 1400 ft lbs.)

The fuel available for cruise is $W_o(0.5 - 0.1 - 0.1 - 0.01) = 0.29W_o$ $\therefore W_1 = 0.9W_o$ and $W_2 = W_o(0.9 - 0.29) = 0.61W_o$ $\therefore R = 0.41 \times 7.5 \times 10{,}500 \times 1{,}400 \text{ Ln. } \frac{0.9}{0.61} =$ 17,581,000 ft = 3,330 statute miles.

The distance covered on climb would be 200 miles and on descent about 150 miles to give a total still air range of 3,680 miles. (This example is roughly based on the Concorde.)

It should be mentioned that the slow climb required by the Breguet equation is not allowed by Air Traffic Control regulations except in the case of aircraft such as Concorde which cruises far above the usual traffic lanes.

Both η and ℓ vary with height and speed especially η in the case of jet engines where it increases almost linearly with speed up to very high speeds, so, until the ceiling is reached, the maximum value of the product $\eta\ell$ occurs at a higher speed than that for the maximum value of ℓ. Even at the ceiling, if the indicated air speed remains constant, the true speed is inversely proportional to $\sqrt{\sigma}$, where σ is the relative density, and therefore increases as the aircraft's ceiling increases (if permissible) with decrease of weight.

The importance of the product $\eta\ell$ is more relevant to climb and diversion than to continuous cruise at ceiling height were its greatest value is used anyway. On the climb one may not be able to operate at maximum $\eta\ell$ because of gust load limitations on indicated air speed (Concorde is limited to 400 knots I.A.S. for climb to about 40,000'). If conditions at the intended destination (weather, traffic congestion, etc.) require that diversion to an alternate airfield is necessary, this normally occurs at heights far below that for optimum cruise and again gust load limitations may prevent flying at optimum $\eta\ell$ especially as the power required for level flight at low height is much below maximum cruise power which means that η for low level cruise is considerably less than for full cruise power. (This situation could be alleviated by shutting down, say, two out of four engines, but this procedure is apparently not so far considered acceptable.) For stand off the fuel consumption per mile is irrelevant. The requirement here is that the time rate of fuel consumption should be as low as possible.

Propulsion in Fluids

In all forms of propulsion in fluids, i.e., in water or air, other than rocket devices, the 'drive' is obtained by generating sternwards momentum in the fluid. This is true of birds, insects, fish, etc., as well as ships, aircraft, etc.

The propulsive force is proportional to the rate of change of momentum induced and, if steady, is given by $dF = \frac{dQ(u - u_o)}{g}$ or, since $dQ = u\rho\delta S$

$$\delta F = \frac{\rho}{g} u(u - u_o)\,\delta S \tag{13-3}$$

where u_o is the speed of motion of the main mass of fluid relative to the body and u is the increased velocity passing through an element of area δS in a plane behind and normal to the direction of motion. If the momentum increase is not steady as with a squid, the waving tail of a fish, the flapping wings of a bird, the oars of a rowing boat, etc., then u would be a function of time and the matter would be much more complicated and equation (3) would be quite inadequate. Herein, however, it will be assumed that we may limit ourselves to a continuous and steady rate of change of momentum.

$$\text{From (3)} \quad F = \frac{\rho}{g} \int_o^S u(u - u_o)\,\delta S \tag{13-4}$$

where S is the total area outside which $u - u_o$ is negligibly small.

The expenditure of energy, i.e., the increase of kinetic energy corresponding to the increase of momentum, is given by $\delta E = \frac{\rho}{2g} u(u^2 - u_o^2)\,\delta S$ (13-5)

$$\text{from which} \quad E = \frac{\rho}{2g} \int_o^S u(u^2 - u_o^2)\,dS \tag{13-6}$$

The 'useful' work done (or effective power) W_p by increasing momentum is Fu_o

$$\text{which, from (4) is} \quad W_p = \frac{\rho u_o}{g} \int_o^S u(u - u_o)\,dS \tag{13-7}$$

Propulsive efficiency η_p may thus be defined as $\eta_p = \frac{W_P}{E}$ This, from (6) and (7) is given by

$$\eta_p = \frac{\frac{\rho u_o}{g}\int_o^S u(u - u_o)dS}{\frac{\rho}{2g}\int_o^S u(u^2 - u_o^2)dS} \quad \text{or} \quad \frac{2u_o \int_o^S u(u - u_o)\,dS}{\int_o^S u(u^2 - u_o^2)\,dS} \tag{13-8}$$

which by writing $u = u_o \frac{u}{u_o}$ converts to

$$\eta_p = \frac{2\int_o^S \left[\left(\frac{u}{u_o}\right)^2 - \frac{u}{u_o}\right] dS}{\int_o^S \left[\left(\frac{u}{u_o}\right)^3 - \frac{u}{u_o}\right] dS} \tag{13-8a}$$

Beyond this we cannot go unless the values of $\frac{u}{u_o}$ are known at all points within the area S. We shall, however, be concerned with cases in which $\frac{u}{u_o}$ may be presumed uniform

over S. With this assumption (8a) reduces to

$$\eta_p = \frac{2}{\frac{u}{u_o} + 1} \tag{13-9}$$

Equation (9) is the well known 'Froude efficiency' originally derived by Froude for aircraft and ship propellors using the rather dubious assumption that $\frac{u}{u_o}$ was uniform immediately behind these devices. It is a safe assumption to make with jet engines if $\frac{u}{u_o}$ is calculated or measured for a plane sufficiently close to the jet nozzle for the interchange of momentum between the jet and the external air to be taken as negligible. This interchange would not affect the total momentum increase but would have a very marked influence on the variation of $\frac{u}{u_o}$ at some distance downstream from the jet nozzle.

For the purpose of calculating propulsive efficiency with jet propulsion, Equation 9 is sufficient and (3) to (8a) may be disregarded unless for some special purpose (e.g., noise reduction) devices are used to produce a non-uniform jet discharge. Neither can it be used directly for turbo fans with separate cold and hot jets.

As may be seen from (9), η_p approaches 100% as $\frac{u}{u_o}$ nears unity, but if $\frac{u}{u_o} = 1$, $u - u_o = 0$, i.e., no thrust. However, it is obvious from (9) that for high propulsive efficiency it is better to obtain a given thrust by a combination of high mass flow rate and low values of $\frac{u}{u_o}$ than vice versa. (In the early jet engines $\frac{u}{u_o}$ at full speed was approximately 3.0 to give a propulsive efficiency of 50%. With high bypass ratio turbo fans η_p can be in the neighborhood of 80%.)

Note: The foregoing neglects the modification to thrust if expansion in the propelling nozzle is incomplete, (see the early part of Section 5) but the effect is normally negligible.

SECTION 14
'Ram' Compression and Intake Design

With stationary (or slow-moving) gas turbines the appropriate kind of intake is a convergent or 'bell shaped' duct in which the air accelerates from zero to the axial velocity at the compressor face. Since the inspired air has no kinetic energy relative to the intake before entering, there is no contribution to the total compression ratio of the thermal cycle. Indeed there may be a slight loss, but this is negligible unless the intake is very badly designed. With aircraft gas turbines, however, at high speeds, the relative kinetic energy is utilized to contribute to the total pressure ratio in the form of 'ram compression,' and it is essential that the process of conversion should be as efficient as possible.

A useful 'rule of thumb' is that the temperature equivalent or 'kinetic temperature' of the entering air is proportional to the square of the speed in hundreds of miles per hour. (This arises from the fact that to convert from mph to ft/sec the multiplying factor is 1.467 and the value of $\sqrt{2gK_p} = 147.1$ so $\frac{147.1}{1.467} = 100.27$.) Thus if θ_u is the temperature equivalent of the flight speed u then for u = 100 mph θ_u = 1°C, for u = 500 mph θ_u = 25°, for u = 1000 mph θ_u = 100° and so on. Thus the kinetic heating problems of high supersonic speeds can be readily seen, e.g., at 4000 mph the 'rule' gives a kinetic temperature of 1600°C. At these and higher speeds, however, the effects of increased specific heat, dissociation, ionization, etc. would make the 'rule' very unreliable. But it is reasonably valid up to 2000 mph.

For other systems of units, one may use $\frac{\theta_u}{\theta_{u_1}} = \left(\frac{u}{u_1}\right)^2$ where θ_{u_1} is a known kinetic temperature rise for a flight speed u_1

Except at take off and low subsonic speeds, for reasons which will be given below, the efficiency of ram compression is very high at moderate and high subsonic speeds if the axis

of the intake differs little from the line of flight, i.e., in the absence of yaw or other aerodynamic deflection of the air at intake entry, and there is no error of significance in assuming that the efficiency of ram compression is 100%. It may therefore be assumed that the temperature ratio of ram compression t_u is given by $t_u = \frac{T_o + \theta_u}{T_o}$ or $t_u = 1 + \frac{\theta_u}{T_o}$ (14-1)

and that the corresponding pressure ratio $p_u = \left(1 + \frac{\theta_u}{T_o}\right)^{3.5}$ (14-2)

and the density ratio $\sigma = \left(1 + \frac{\theta_u}{T_o}\right)^{2.5}$ (14-3)

(these ratios being total/static) where T_o is the atmospheric temperature.

Example 14-1

If the atmospheric temperature is 220°K and the flight speed 600mph (= 880′/sec) what are the temperature and pressure ratios t_u and p_u of ram compression assuming 100% for adiabatic efficiency, i.e. η_u = 100%?

$$\theta_u = 36° \therefore t_u = 1 + \frac{36}{220} = 1.164 \text{ and } p_u = 1.164^{3.5} = 1.70$$

Example 14-2

Using the same T_o and u as in Example 1 and assuming that the relative density σ of the atmosphere is 0.2463 (=I.S.A. at 40,000′) what is the static temperature T_s, pressure P_s, and density ρ_s at compressor entry if the entry axial velocity u_a is 550 ft/sec.

Sea level density being 0.0766 the density (atmospheric) for σ = 0.2463 is ρ_o = 0.2463 x 0.0766 = 0.01887. The temperature equivalent θ_a for 550′/sec is $\left(\frac{550}{147.1}\right)^2$ = 14° ∴ the static temperature increase ΔT = 36 – 14 = 22°C to give T_s = 242°K.

The temperature ratio (static to static) = $1 + \frac{22}{220} = 1.10$ ∴ the density ratio (static to static) = $1.1^{2.5} = 1.269$ ∴ $\rho_s = 1.269 \times 0.01887 = 0.02395$.

$$P_s = \rho_s R T_s = 0.02395 \times 96 \times 242 = 556.3 \text{ p.s.f.}$$

Subsonic Intakes

In these it is usual to allow, at design speed, a substantial proportion of the intake deceleration to take place ahead of the intake orifice as shown in Figure 1. Thus much of the ram compression is entirely loss free.

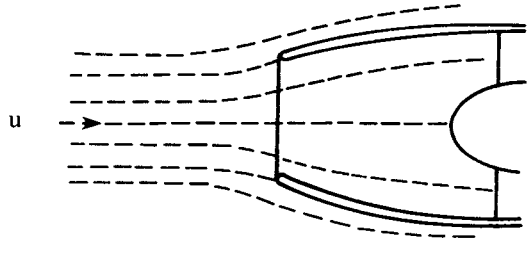

Fig. 14-1

It would be desirable to have the intake orifice as large as possible for take off and low speed, but the limit to this is set by the degree of divergence of the streamlines permissible at the rim of the orifice at design speed which, if too great, would cause flow breakaway external to the casing. This could be avoided by increasing the external diameter of the casing and 'rounding off' the lip of the entry orifice but at the price of increased nacelle drag.

(In the case of the first British jet plane (the Gloster-Whittle E28/39) the centrifugal type engine was mounted in a 'plenum chamber' in the fuselage behind the cockpit and fuel tank, i.e., the fuselage was also the engine nacelle. The air intake was at the nose of the fuselage, so, because of the size of the latter, the outer casing was well rounded at the intake orifice so it was possible to have most of the ram compression take place ahead of the orifice. In fact, there was deceleration from flight speed to 200'/sec at orifice entry. Behind the intake orifice two ducts led to the plenum chamber and were designed to reduce the velocity down to 100'/sec at plenum chamber entry.)

It is possible to increase the effective entry orifice for take off and low speeds by various means, e.g. by providing intake 'doors' to allow additional air to be drawn in through the wall of the intake duct between the entry orifice and compressor entry.

If intake ducts are alongside and close to a large adjacent surface such as a fuselage or wing it would be very undesirable for the boundary layer air of the said surface to enter the intake, so slots are used between the intake and the surface to allow the surface boundary layer to bypass the intake. (The first U.S. jet – the Bell XP59A – was the first jet plane to use this device on the writer's advice.)

Supersonic Intakes

The type of intake illustrated in Figure 1 would be quite unsuitable for supersonic speeds. There would be a shock wave ahead of the intake orifice somewhat as shown in Figure 2 much of which would comprise a 'normal shock' as indicated, across which there would be a very sharp pressure rise without change of direction with a corresponding big velocity reduction. The adiabatic efficiency of compression through a normal shock wave is very low as compared with that for oblique shocks (see Section 4). At Mach 2.0 in the stratosphere it would be about 80% or less, whereas one may expect about 95% or even more for an intake designed for oblique shocks as in Figures 3 and 4 (based on guesswork). Figure 3 illustrates the kind of intake used on Concorde and Figure 4 shows an alternative arrangement for breaking down shock compression into stages of oblique conical shocks ending in a weak normal shock.

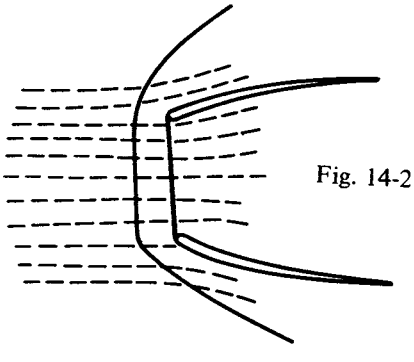

Fig. 14-2

Such intakes, unfortunately, unless of variable geometry, are suited to one particular speed and so variable geometry is virtually essential. Thus it is usually necessary for the forebody of Figure 4 to be capable of being moved fore and aft, and for the arrangement of Figure 3 to have adjustable 'ramps.'

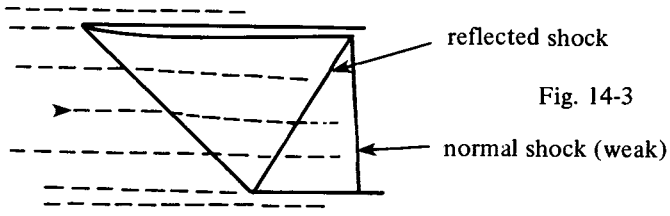

Fig. 14-3

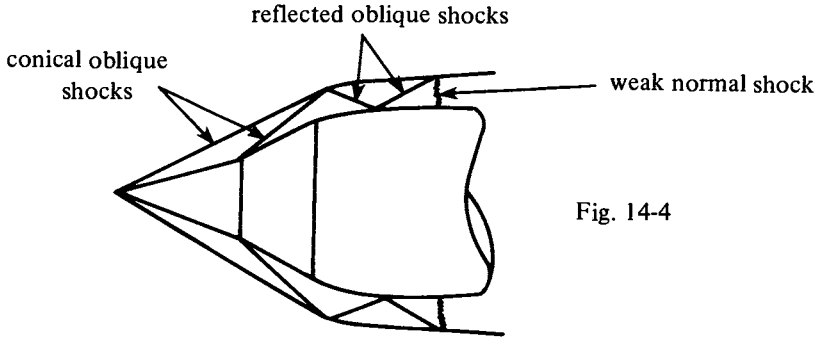

Fig. 14-4

Much development is still in progress on the forebody type of intake to reduce adverse boundary layer effects, sensitivity to yaw, etc. These disturbances apparently cause rapid fore and aft fluctuations in the position of the shocks.

Ramjets

At high supersonic speeds ram compression can be so high that additional compression becomes unnecessary, hence no compressor–compressor turbine combination is needed. It follows that the maximum temperature of the thermal cycle is no longer restricted by the stress–temperature properties of turbine blade materials and so, if desired, it is possible to use air/fuel ratios up to the stoichiometric limit of approximately 15.1. The ramjet thermal cycle therefore comprises only ram compression, combustion at substantially constant pressure, and expansion through a propelling jet. There are no major moving parts but there must be a certain amount of auxiliary apparatus for such purposes as fuel injection, for varying intake and exhaust geometry, etc.

The ramjet can never be the sole means of propulsion because of its dependence on high speed for adequate compression, but if 'boosted' to speeds of the order of Mach 3 by rockets it can 'take over' the propulsion for missiles. Similarly, if boosted to high speeds by turbo jets it could take over the propulsion for aircraft.

Figure 5 is the cycle diagram for the simple ramjet cycle.

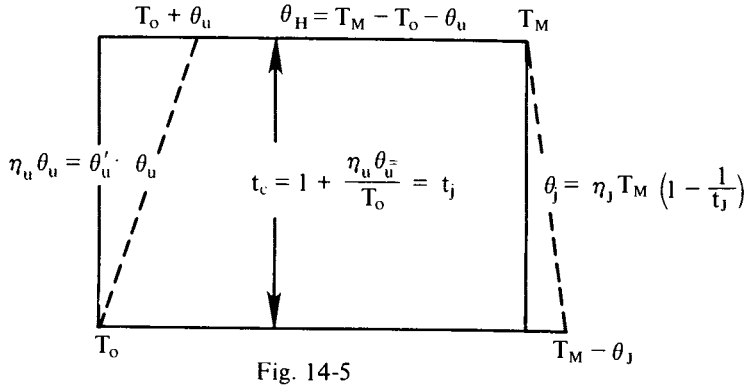

Fig. 14-5

It would be desirable to have a ram-jet body with a purely cylindrical casing and have complete expansion in the final nozzle, but this, however, is not possible at the speeds at which ramjets have good efficiency. This will be demonstrated by example. Figure 6 shows the cycle diagram for a ramjet based on the following assumptions: (1) T_o = 220°K, (2) u = 3000mph = 4400′/sec (θ_u = 900°C), (3) the efficiency of ram compression η_u = 85% (allowing for combustion pressure loss), (4) the efficiency of expansion is 100% to the nozzle throat and 98% thereafter, and (5) T_{max} = 2000°K.

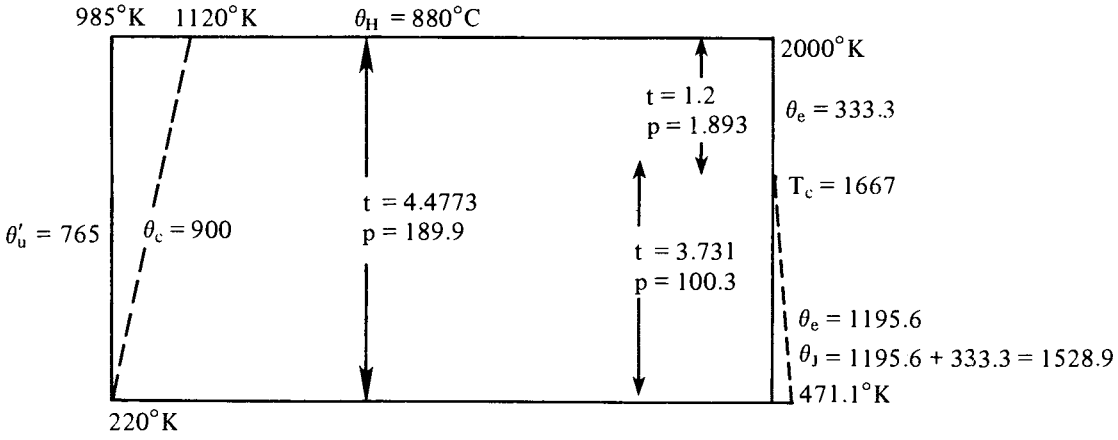

Fig. 14-6

Several of the relevant figures are shown on the diagram. Others are as follows:

Jet velocity (for complete expansion) $u_j = 147.1\sqrt{1528.9} = 5751.8'/sec$

Specific thrust $F_s = \frac{5751.8 - 4400}{32.2} = 41.98$ lbs/lb/sec

Overall efficiency $\eta_o = \frac{F_s u}{K_p \theta_H} = \frac{41.98 \times 4400}{336 \times 880} = 0.625$

If S_o is the cross section of the entering air ahead of the intake and S_e the nozzle

exit section then $S_e\rho_e u_j = S_o u\rho_o \therefore \frac{S_e}{S_o} = \frac{u\rho_o}{u_j\rho_e}$.

Since the exit temperature is 471.1°K, $\frac{\rho_o}{\rho_e} = \frac{471.1}{220} = 2.141$ and $\frac{u}{u_j} = \frac{4400}{5751.8} = 0.765$

$\frac{S_e}{S_o} = 2.141 \times 0.765 = 1.638$ the square root of which is 1.28.

So for complete expansion to P_o the nozzle exit diameter would need to be 28% greater than that of the entering stream tube and the casing would be conical which would, of course, cause considerable shock drag. Thus to have a casing of uniform diameter one would have to accept incomplete expansion in the final nozzle.

The small losses due to this would be more acceptable than the shock drag of a conical casing. For a 'parallel pipe' casing the writer finds (by trial) that at the exit plane the pressure $P_o = 2.049\,P_o$, $u_j = 5561'$/sec and $T_e = 1096°K$ thus the further acceleration after discharge would only be 5751 - 5561 = 190′/sec.

This external expansion would itself be 'bounded' by a shock wave as the issuing and expanding jet encounters the external air somewhat as shown in Figure 7.

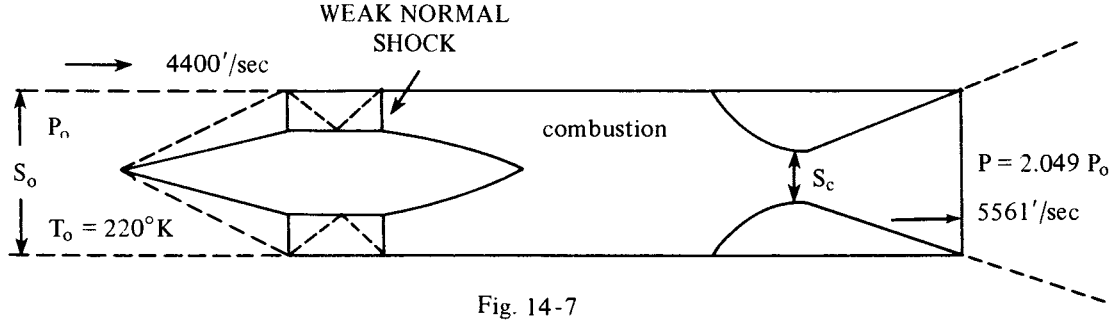

Fig. 14-7

For a flow of 1.0 lb/sec. $S_o\rho_o u = 1 \therefore S_o = \frac{1}{\rho_o u} = \frac{RT_o}{P_o u}$. So for incomplete expansion

$F_s = \frac{5561 - 4400}{32.2} + 1.049 P_o S_o = 36.06 + 1.049 \frac{RT_o}{4400}$

$1.049 \frac{RT_o}{4400} = 1.049 \times \frac{96 \times 220}{4400} = 4.8$lb hence total thrust (specific) $F_s = 36.06 + 4.8 = 40.86$ c.f. 41.98 for complete expansion. This reduces the overall efficiency η_o from 62.5% to $\frac{40.86}{41.98} \times 62.5 = 60.8\%$ which is still a very high figure.

In the foregoing example, the figure of 2000°K used for maximum temperature is far below that which would result from near stoichiometric combustion, but much higher values of T_{max} would increase the degree of under expansion and reduce propulsive efficiency. Specific thrust would, of course, be increased.

It should be mentioned that the choice of 85% for ram compression efficiency was purely arbitrary and has no basis on information available to the writer. To achieve it

would probably require a much more elaborate intake design than that shown very diagrammatically in Figure 7. Obviously, however, ramjets would be acceptable propulsive devices with far lower efficiencies (overall) than 60%. If, in the above example, the ram efficiency had been taken as low as 70%, the overall efficiency would still be 40% approximately, but F_s would be greatly reduced (to 26.5 lb/lb/sec. c.f. 40.86).

SECTION 15
Combustion

Introductory

In the early development of the jet engine the greatest of the several technical problems was that of obtaining the very high intensity of combustion with reliability of combustion chamber components coupled with low pressure loss and high combustion efficiency. The need was to reduce the volume of combustion chambers to about 5% of the best then obtained for industrial applications in proportion to the rate of fuel consumption, e.g. as in steam boilers, etc. There seemed no chemical or physical reason why the target should not be achieved and it was in fact quite quickly achieved in combustion chamber test experiments but it took some three years before the promising results of these experiments could be obtained in seemingly identical combustion chambers installed in a complete engine. The main reason for this very frustrating situation was that the pattern of air flow at combustion chamber entry (i.e. from compressor delivery), in the engine was very different from that in the component testing. Eventual realisation of this underlined the fact that there were major aerodynamic factors to be taken into account in combustion chamber design. Unfortunately these are too complex for analysis so, for this and other reasons, combustion chamber design is still more an art than a science. There are, however, certain basic principles which must be observed and these will be discussed below.

The limitations imposed by size and weight in aircraft gas turbines are not, of course, so stringent in gas turbine power units for other than aircraft propulsion, but it is generally desirable for installation and other reasons that the bulk and weight of the combustion apparatus should not be disproportionate to the other major components of the power plant.

The Composition of the Atmosphere

The atmosphere for all practical purposes is almost entirely a mixture of nitrogen and oxygen in the proportions 78.1% N_2 to 20.95% O_2 by volume or 75.52% N_2 to 23.15% O_2

by weight. The balance is made up of the inert gases Argon, Neon, Helium, Krypton and Xenon; carbon dioxide, methane, oxides of nitrogen, hydrogen and ozone, and variable quantities of water vapour. With the exceptions of Argon (1.3% by weight), CO_2 (0.5%) and water vapour, the other constituents range from 0.4 to 12 p.p.m. For combustion purposes one may therefore safely assume that air is a mixture of nitrogen and oxygen.

Hydrocarbon Fuels

Virtually all fuels derived from the 'fossil fuel' petroleum are hydrocarbons, i.e. compounds of carbon and hydrogen and fall into two main groups namely the paraffinic series with the general formula C_nH_{2n+2} and the aromatic series of the genral formula C_nH_n. Both series have hundreds of members, especially the paraffinic series ranging from CH_4 (methane) with boiling point of $-160°C$ approx. to bituminous compounds which are solids at room temperature.

Crude liquid petroleum is rarely used directly as a fuel (though some crudes are so 'light' that this is possible). It is refined in a number of processes of which the principle one is distillation whereby the crude is 'divided' into distillates ranging from heavy fuel oil to light and volatile gasolenes. The residue after distillation and many other refining processes comprises residual fuel oil, bituminous asphalts, etc. (And even coke after certain cracking processes) which contain most of the mineral impurities of the original crude.

Many attempts have been made to use 'residual' (and even powdered coal and peat) in industrial gas turbine power plant but without success to date because of the erosive effect of the ash on turbine blades. Also, since much of the ash is molten at combustion temperatures, it tends to solidify on the blading. In short, gas turbines are limited to distillate fuels whereas steam powered ships, power stations, etc. may, and usually do, operate on the much cheaper heavy residuals.

Even distillates are unusable if the content of sulphur, vanadium, etc. exceeds certain small limits.

For aircraft gas turbines the range of distillates which may be used is further limited by certain strict specification requirements the chief of which is that the waxing point must not exceed $-40°C$ owing to the low temperatures to which the tanks and fuel lines are subjected. Further the water content must be extremely low, and the proportion of aromatics is restricted: this last because aromatics are more prone to soot formation than the paraffin series hydrocarbons. All this adds up to the fact that distillate fuels for aircraft must be in the kerosene-gasolene range. (The degree to which low grade gasolene may be used has been the subject of much controversy because of the fire risk in a crash—kerosene is undoubtedly much safer in this respect). Vapour pressure with temperature, flash point, etc. are other factors to be considered (it has been claimed that as much as 18% of a low grade gasolene can be lost through boiling on a rapid climb). It is in any case desirable to replace air in fuel tanks with an inert gas as fuel is consumed to prevent the formation of explosive mixtures of fuel vapour and air which may form at certain temperatures and which may be ignited by static electricity.

The calorific value of hydrocarbon fuels varies little from 10,500 C.H.U./lb (1 C.H.U. = 1.8 B.Th.U = 1400 ft lbs) so the slightly denser kerosene occupies a somewhat lower volume than gasolene for a given fuel weight.

The Basic Chemistry of Combustion

Though kerosenes and gasolenes are mixtures of many hydrocarbons one may select any member of the family as representative of the mixture for the chemistry of the combustion process. So the writer elects to choose octane C_8H_{18} for the purpose. The chemical equation of combustion is then:–

$$C_8H_{18} + 12\tfrac{1}{2}\,O_2 = 8\,CO_2 + 9\,H_2O + \text{Heat}$$

The molecular weights are as follows:–

$$C_8H_{18} = 8 \times 12 + 18 \times 1 = 114$$
$$O_2 = 32$$
$$CO_2 = 12 + 32 = 44$$
$$H_2O = 2 \times 1 + 16 \times 1 = 18$$

$\therefore$ the 'mass balance' is:–

$$1 \times 114 + 12.5 \times 32 = 8 \times 44 + 9 \times 18 = 514$$

i.e. 114 lb. of C_8H_{18} combines with 400 lbs. of O_2 to produce 352 lbs. of CO_2 plus 162 lb. of H_2O or:–

1 lb. of C_8H_{18} combines with 3.509 lb of O_2 to produce 3.088 lb of CO_2 and 1.421 lb. of H_2O plus 10,500 C.H.U.

But, as we have seen above, for every lb. of O_2 in the air there is 3.262 lb. of N_2, so, assuming for the moment, that N_2 plays no part in the reaction, the chemical equation may be re-written as:–

$$1.0\,C_8H_{18} + 3.509\,O_2 + 11.446\,N_2 = 3.088\,CO_2 + 1.421\,H_2O + 11.446\,N_2 + 10{,}500 \text{ C.H.U.}$$

or 1 lb. C_8H_{18} + 14.96 lb. of air yields 3.088 lbs. CO_2 + 1.421 lb. H_2O + 11.446 lb. N_2 + 10,500 C.H.U.

Thus it may be seen that, for, complete combustion, the air/fuel ratio is 15:1 approx. This is the 'stoichiometric ratio.'

The average specific heat K_p of the N_2 plus combustion products at, say, 400°K is 0.268 C.H.U./lb./°K, so, if there were no change of K_p with temp. the temp. rise of combustion would be $\frac{10{,}500}{.268 \times 14.96} = 2619°C$ (this does not allow for the latent heat of vaporisation of the liquid fuel). In practice, however the temp. rise would be substantially lower due to 1) the increase of K_p with temp. 2) the dissociation of some of the CO_2, H_2O and N_2 into C, CO, the radicals OH, O, and N, 3) the formation of oxides of nitrogen ('NOX') and ozone (O_3).

In gas turbines the air/fuel ratio is far greater than stoichiometric, being of the order of 55–70:1, nevertheless the combustion temp. rise is appreciably lower than would be calculated on the assumption of constant specific heat.

On expansion to lower temps. the heat absorbed by dissociation, etc. is recovered by recombination, especially if the air/fuel ratio is well above stoichiometric so the exhaust of gas turbines has negligible carbon monoxide (CO) O_3, etc. in contrast to reciprocating engines operating with near stoichiometric mixtures the exhaust of which often contains unburnt hydrocarbons as well as CO, etc. When operating at high turbine entry temps. however, the exhaust of a gas turbine contains NOX; sometimes as much as 18 gms. per kgm of fuel, and, if combustion chamber design leaves something to be desired, carbon (visible as a trail of smoke) and unburnt hydrocarbons. These two latter, however, though creating an impression of poor combustion efficiency, represent a minute fraction of the fuel.

Attempts are in progress to cut down the emission of oxides of nitrogen by reducing peak combustion chamber temperatures. These efforts are based on the belief that NOX has a powerful catalytic action in breaking down the 'ozone layer' high in the stratosphere and so increases the amount of certain harmful wavelengths of ultra violet light from the sun which can reach the earth's surface and cause skin cancer and other biological damage. In the writer's opinion, the 'ozone scare' is based on several dubious assumptions which support the belief, and neglect others which counter it, chief of which is that the various constituents of NOX have a strong affinity for the water vapour present in jet exhausts to form nitrous and nitric acids which have none of the catalytic properties of NOX. However, a full discussion of this subject would be lengthy and beyond the scope of this work.

The combustibility of an air-fuel mixture depends on a number of factors, the chief of which is the air/fuel ratio. Clearly, if this is less than stoichiometric, complete combustion is not possible, and even in a completely homogenous mixture—not easy to achieve in very short time intervals—there are upper and lower limits to the air/fuel ratio necessary for satisfactory combustion. If the air/fuel ratio is less than about 12:1 the mixture is too 'rich'. If greater than about 20:1 it is too 'lean'. This fact dominates gas turbine combustion chamber design in that there has to be a primary combustion zone into which only about 20% of the total air is admitted, i.e. in the primary zone the mixture is near stoichiometric. The remaining secondary air is added in a secondary mixing zone in such a manner as to mix as rapidly as possible with the extremely hot output of the primary zone.

Ignition and Flame Propagation

Unless a catalyst is present, ignition of even a completely homogenous combustible mixture requires a certain minimum temp. to initiate combustion. Except in compression ignition engines (diesels) where the air is heated by compression to a sufficiently high temp. for injected fuel to ignite, the most common means of 'triggering' combustion is by an electric spark. Sometimes 'glow plugs' or pilot flames may be used, but in gasolene piston engines and gas turbines a high tension spark plug (or plugs) are the means of initiating combustion. With the continuous combustion of gas turbines, the spark is needed only for starting (unless there is a 'flame out').

Since initial ignition is inevitably very local to the spark (or other initiating means) the flame must propagate through the rest of the mixture in a wavelike manner. Thus the speed

of propagation is very important considering that the residence time in the primary combustion zone is of the order of .001 secs. Unfortunately the rate of flame propagation in a homogenous combustible mixture at rest is very slow and it would be quite impossible to maintain combustion in a gas turbine combustion chamber primary zone if the air flow were steady—the flame would be swept downstream immediately in the high air speeds necessary to keep combustion chambers small and light. Means must therefore be provided to stabilise the flame in the primary zone. The writer first attempted to achieve this by 'upstream injection', i.e. by 'squirting' the fuel into the air stream so that the flame blew back on to the injected fuel and ignited it. This was partially successful but required about 6 ft. length of combustion chamber to achieve moderately complete combustion. Another defect of this system was that the fuel injector was located in the hottest part of the flame and suffered from overheating despite attempts to use the fuel as a cooling jacket before injection. Flame stabilisation is thus another major factor in combustion chamber design.

Fuel Injection

It is, of course, essential to achieve the speediest possible rate of mixing of fuel and primary air. With kerosene-gasolene type fuels it is possible to vaporise the fuel before injection through multiple jets, but the writer's several attempts (some thirty types of vaporisers were tried) to achieve this all failed. Though excellent primary zone combustion was often obtained, the vaporisers failed either through overheating or coke formation (due to cracking) within them. However, successful vapour injection was later achieved by others using vaporisers having air mixed with the fuel in the vaporising tubes. Nevertheless the most common form of fuel injectors are 'atomising burners' which inject a 'cone' of liquid droplets. In these the 'atomising' is achieved by admitting the fuel into the interior of the injector through tangential slots which impose an intense spin on the fuel before it emerges from the injector orifice. On leaving the orifice the rapidly spinning fuel bursts into tiny droplets under the action of centrifugal force. This procedure, of course, requires that the fuel pressure must be far higher than combustion chamber pressure to provide the necessary kinetic energy plus the surface tension energy contained in the droplets.

The behaviour of the burning droplets is a very complex matter. Their interaction with the primary air and rate of burning depends on the turbulence of the primary air the size and speed of the droplets, etc. etc. One would expect that the smaller the droplet the shorter the burning time but against this Stokes law operates to slow down relative movement and therefore the rate at which a droplet can 'engage' still unused oxygen. Further, each droplet has a 'cloak' of combustion products tending to interfere between the air and the still unburnt 'core'. Moreover, after a very short time the intense heat vaporises partially burnt droplets and this almost certainly slows down the rate of mixing for a given degree of turbulence.

Soot Formation

The carbon build up which can occur due to the cracking of the fuel in the intense heat and to locally over rich mixtures must be prevented. If it happens around the injector orifice it can distort the spray. If build up occurs on the nearby surfaces which control the motion of the primary air it alters their geometry, and therefore their intended effect on the primary air. The problem of coke formation bedevilled early combustion development. The main solution was to force some of the primary air over surfaces where coke formation tended to occur to cause it to burn off as rapidly as it was formed.

Mixing of Secondary Air

A complete combustion chamber normally has an outer casing and an inner flame tube or tubes. It is in the latter that both primary combustion and secondary air mixing takes place. As previously indicated about 20% of the total air is admitted directly to the primary combustion zone. The remainder is admitted in stages downstream of the primary zone in such a manner as to achieve as complete a mixing as possible without excessive pressure loss. This is not easily done and to obtain a satisfactory result much trial and error is usually necessary. One conflicting requirement is that the inner surface of the flame tube must be shielded from excessive temperatures by a protective 'skin' of comparatively cool air without causing a serious non-uniformity of temperature at entry to the turbine nozzle ring.

To obtain virtually complete mixing of 80% of comparatively cool air with 20% of extremely hot combustion products in a time interval of the order of .02 seconds is indeed a formidable problem and can only be done by inducing considerable turbulence over and above that created in the primary zone, so that there has to be a rapid momentum interchange only obtainable at the price of pressure loss.

It would take far too long to describe the sundry arrangements of holes, slots, perforated stub pipes, etc. by means of which the secondary air enters the flame tube.

Flame Stabilisation in the Primary Zone

This has been briefly touched upon above, but some amplification is desirable.

In brief, the most effective means in use is still that used in the first jet engine, namely to admit the primary air to the flame tube through a ring of swirl vanes surrounding the fuel injector. These vanes generate a vortex, preferably oppositely directed from that of the spin of the injected fuel spray. The success of this device was not understood until a transparent plastic model of a combustion chamber, equipped with wool tufts to indicate flow behaviour, demonstrated that there was flow reversal in the core of the vortex, i.e. the flow was towards the injector on and near its axis. Thus the initial fuel injection was upstream in effect.

At this point it should be mentioned that there was nothing novel in the use of swirl vanes surrounding a fuel injector—it had been common practice in steam boilers, etc. for some years where the volume available for combustion was far larger.

Swirl vanes are by no means the only method of flame stabilisation. Sundry devices which produce turbulence in the neighborhood of fuel injectors can be quite effective, e.g. perforated cones or plates surrounding the injector, annular V sectioned 'troughs' such as are used in after-burners of jet engines, etc.

Counter-flow Combustion Chambers

Figure 1 illustrates one of the ten counter flow type combustion chambers used in the first British jet engine. This arrangement was not a matter of choice initially; it was dictated by the need to make it conform to the rest of the engine because shortage of money proscribed the making of a completely new engine and dictated the continued use of the more expensive components—rotor assembly, compressor casing, etc. which had been designed for an entirely different (and unsuccessful) combustion chamber. Nevertheless the counter-flow arrangement had several advantages in the circumstances of the time. It was free from

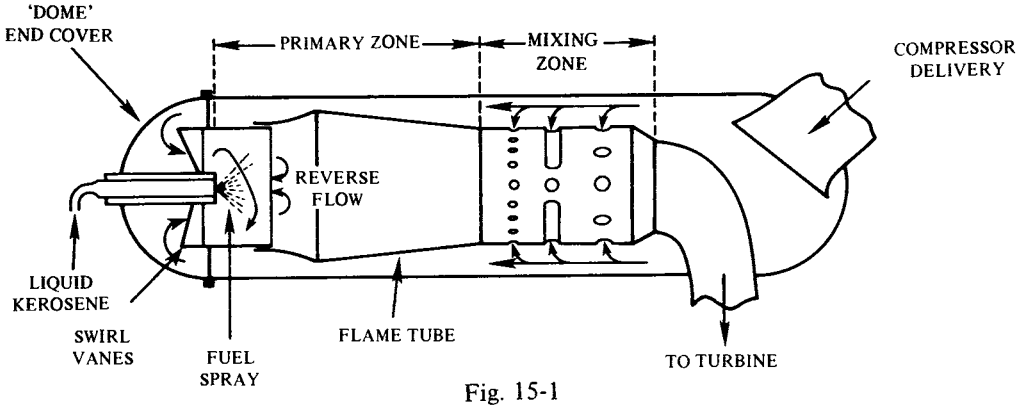

Fig. 15-1

problems of thermal expansion; it allowed the continued use of a very short shaft in the rotor assembly; the dome shaped end covers could be easily removed for inspection and modifications to the swirl vanes, flame tubes, etc. (of which there were many), and so it was retained in several later designs. It was very much a matter of "leave well alone" since experience had shown that any major change would entail another long period of development. It was, of course, eventually displaced by the 'straight through' type which, however, used the same basic principles of design in burner-flame tube arrangements.

SECTION 16
The 'Straight' Turbo Jet

The straight turbo jet is a gas turbine type gas generator in which the energy remaining at exhaust from the compressor turbine is used to provide a high velocity propelling jet by expansion through a nozzle at the rear of an aircraft fuselage or engine nacelle. It may be thought of as an 'energiser' within a duct.

Fig. 1 shows the general arrangement of the W1 engine (with combustion chamber details omitted) which powered the first successful British jet plane, the Gloster-Whittle E 28/39. Fig. 2 shows the general arrangement of the fuselage of the E. 28.

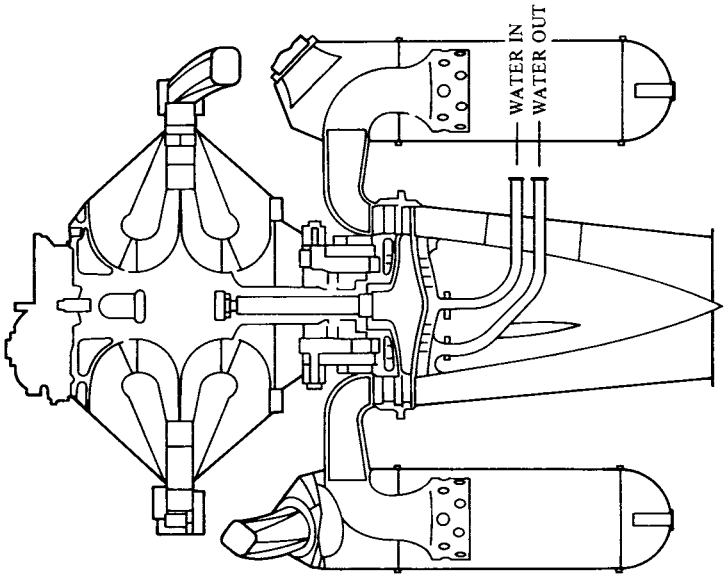

Fig. 16-1

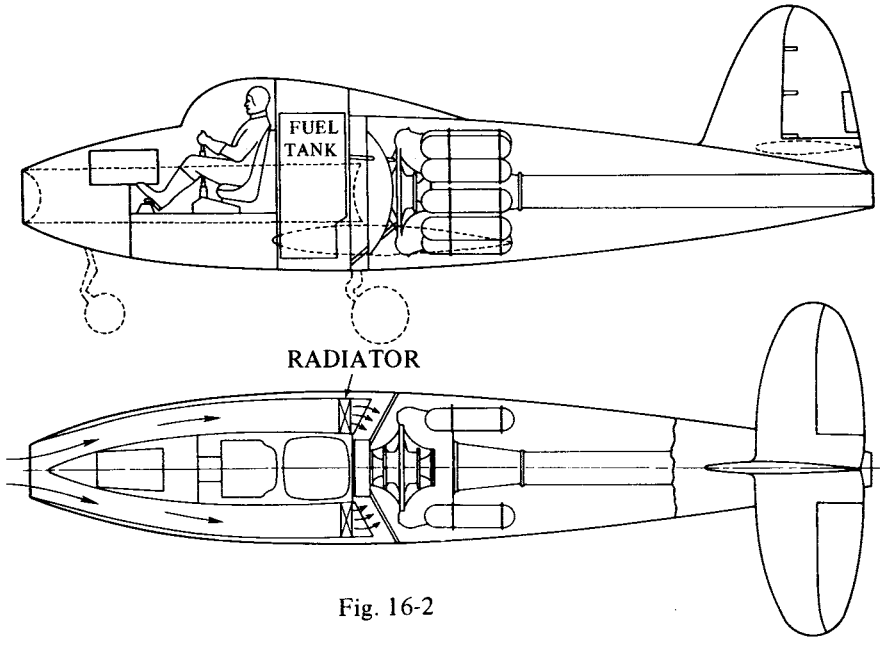

Fig. 16-2

Some facts of interest in brief are as follows:–

The W1 engine was designed for a static thrust of 1240 lbs. at 17,750 r.p.m. which it eventually produced, but for the purpose of the first flights in May 1941 it was, on Ministry insistence, derated to 16,500 r.p.m. at which the static thrust was 860 lbs. One flight was authorised at 17,000 r.p.m. and static thrust 1000 lbs. At this rating the aircraft reached a speed of 370 m.p.h. at 20,000 ft. (well below its ceiling), which was higher than expectations and slightly better than the Spitfire, then the best piston engined fighter in service.

The engine weight was 520 lbs. and the all up weight of the E. 28 was 3000 lbs. approx. The fuel tank capacity was only 80 imperial gallons which limited flight time to 50–60 minutes.

Throughout W.W. II the E. 28 was used to flight test a series of Whittle type engines of greater power–the W1A (1340 lbs. static thrust); the W2B (1400–1600 lbs. static thrust); the W2/500 (1650 lbs. static thrust) and the W2/700 (2000–2500 lbs.) The W2/700 was the last centrifugal type engine with counter flow combustion chambers. It proved too powerful to be fully opened up in level flight because the aircraft ran into compressibility troubles at about 470 m.p.h.

Meanwhile the W2B went into limited production as the Rolls-Royce Welland which powered the twin engined Gloster Meteor 1. The W2B was also the prototype of General Electric's I 14 which powered the twin engined Bell P59A, which in fact flew before the Meteor. The latter, however, was the only Allied jet fighter to go into operation during the war. (The German twin engined Me. 262 was operational a few weeks earlier than the Meteor).

There then followed a series of successful centrifugal types with 'straight through' combustion chambers–the Rolls-Royce Derwent 1; Derwent V, Nene, etc., The deHavilland Goblin and Ghost; the General Electric I.40, etc. Perhaps the most successful of these was the Derwent V (3,600 lbs. static thrust) which went into large scale production and, inter alia, powered the Meteor IV.

In parallel with the development of the centrifugal type, development of the axial flow type was in progress at the Royal Aircraft Establishment in cooperation with Metropolitan Vickers, in Germany and in the U.S.A. Eventually the early difficulties were overcome and the advantages of small frontal area increased in importance with increasing speeds to the point where, except for very small engines, the axial flow type completely displaced the centrifugal type despite the much higher cost and complication.

As previously mentioned, the jet engine as a gas generator differs from the types of gas generators already discussed in that part of the compression is provided by the ram compression in the intake at moderate and high speeds. As has been shown, the ram compression temp. rise is proportional to the square of the flight speed.

Fig. 3 is a very diagrammatic representation of an axial flow jet engine, and Fig. 4 is the corresponding Pressure-Specific Volume diagram.

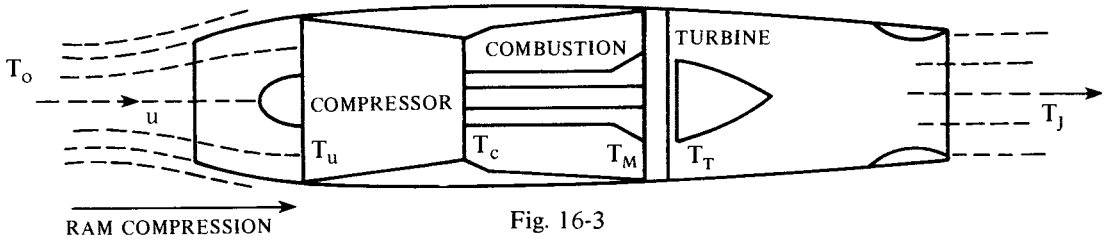

Fig. 16-3

The portion representing ram compression would, of course, be absent from the static sea level cycle.

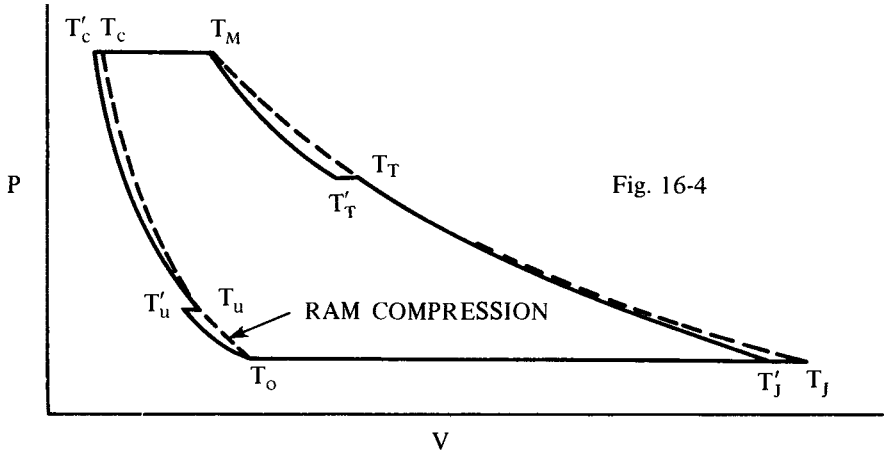

Fig. 16-4

The cycle diagrams, Figs. 5a and 5b, as used by the writer, represent sea level static and high speed flight.

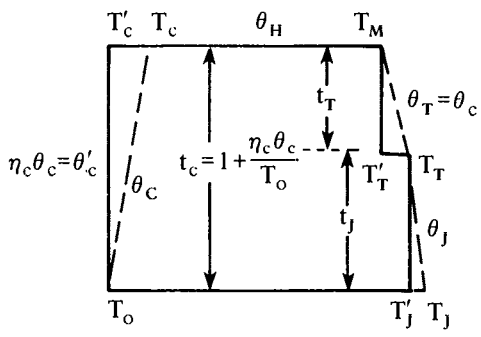

Fig. 16-5a

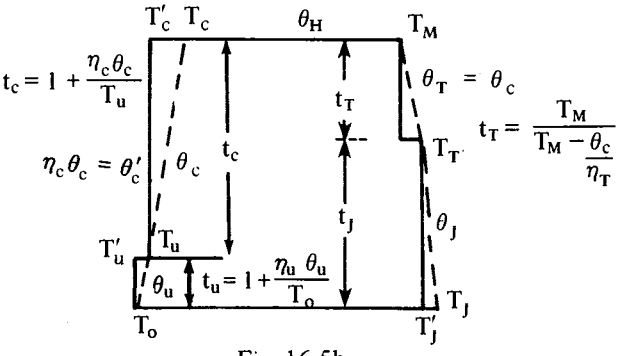

Fig. 16-5b

For sea level static, $t_J = \frac{t_c}{t_T}$; in high speed flight, $t_J = \frac{t_u t_c}{t_T}$

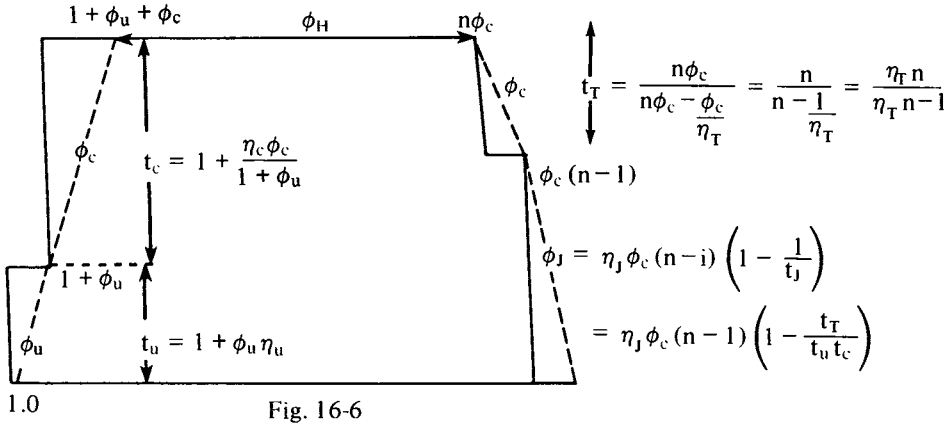

Fig. 16-6

Fig. 6 is a non-dimensional version of Fig. 5b in which all temps. and temp. differences are multiples of T_o. $\frac{T_M}{T_o}$ is shown as $n\phi_c$ because it was shown in Section 5 that over the range for which η_c and η_T may be assumed to vary little, with fixed choking nozzles in series with energy extraction between them, T_M is proportional to θ_c.

From the relationships shown in Fig. 6, one may find a number of 'doubly non-dimensional' relationships as follows:–

Since $u_j \propto \sqrt{\phi_J}$ then $\frac{u_J}{u_{JD}} = \sqrt{\frac{\phi_J}{\phi_{JD}}}$ where the suffix D implies the design condition $\therefore \quad \frac{u_J}{u_{JD}} = \sqrt{\frac{\phi_c}{\phi_{cD}} \left(1 - \frac{t_T}{t_u t_c} \Big/ 1 - \frac{t_{To}}{t_{uD}\, t_{cD}} \right)}$ (16-1)

or $$\left(\frac{u_J}{u_{JD}}\right)^2 = \frac{\phi_c}{\phi_{cD}}\left(\frac{t_{uD}\,t_{cD}}{t_u\,t_c}\right)\left(\frac{t_u\,t_c - t_T}{t_{uD}\,t_{cD} - t_{TD}}\right) \qquad (16\text{-}1a)$$

Merging the design values into a constant A

$$u_J^2 = A\phi_c\left(\frac{t_u\,t_c - t_T}{t_u\,t_c}\right) \qquad (16\text{-}1b)$$

Since spec. thrust $F_s \propto u_J - u$ $$\frac{F_s}{F_D} = \frac{u_J - u}{u_{JD} - u_D} = B\left(\sqrt{\phi_J} - \sqrt{\phi_u}\right) \qquad (16\text{-}2)$$

where $$B = \left(\sqrt{\phi_{JD}} - \sqrt{\phi_{uD}}\right)^{-1}$$

Since mass flow rate $Q \propto P_o(t_u\,t_c)^{3.5}/\sqrt{\phi_c}$

$$\frac{Q}{Q_D} = \frac{P_o}{P_{oD}}\left(\frac{t_u\,t_c}{t_{uD}\,t_{cD}}\right)^{3.5}\sqrt{\frac{\phi_{cD}\,T_{oD}}{\phi_c\,T_o}} \qquad (16\text{-}3)$$

Using (2) and (3) $$\frac{F}{F_D} = \frac{F_s Q}{F_{sD}\,Q_D} = C\frac{P_o}{\sqrt{\phi_c}}(t_u\,t_c)^{3.5}\left(\sqrt{\phi_J} - \sqrt{\phi_u}\right) \qquad (16\text{-}3)$$

where $$C = \frac{B\sqrt{\phi_{cD}}}{P_{cD}\,(t_{uD}\,t_{cD})^{3.5}}$$

In similar manner the ratios of other quantities—fuel consumption, efficiency, etc. to design values can be found.

From the foregoing it should be clear that, for a given design, the performance characteristics are functions of four variables, namely atmospheric temp. T_o, atmospheric pressure P_o, the temp. equivalent of flight speed θ_u, and the compressor temp. rise θ_c.

Many variants of several of the above equations may be obtained by substituting for t_c and t_u from $t_c = 1 + \frac{\eta_c\phi_c}{1+\phi_u}$ and $t_u = 1 + \eta_u\phi_u$.

It should be noted that none of the quantities which can be derived from the cycle diagram involve atmospheric pressure and so depend on the temp. parameters only (for given efficiencies).

The foregoing methods will now be illustrated with examples.

Example 16-1.

Fig. 7 illustrates the design cycle diagram for a Mach 2 (1950′/sec.)

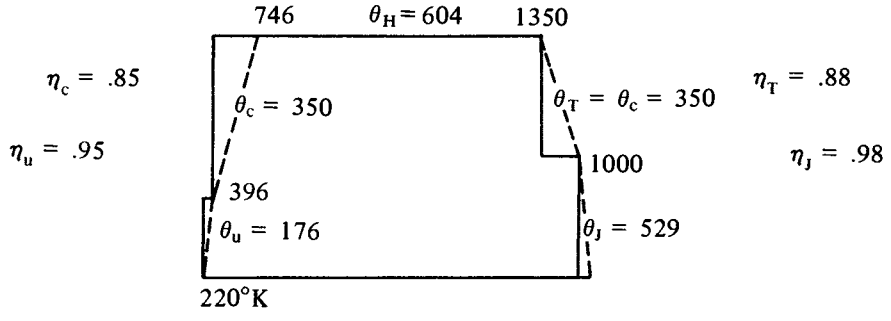

Fig. 16-7

aircraft at 40,000′. Assumptions not shown on the diagram are:– 1) the required thrust is 10,000 lbs. 2) the atmospheric pressure is 392 p.s.f.

Using the data on the diagram the following figures are obtained:–

$$t_{uD} = 1 + \frac{.95 \times 176}{220} = 1.76 \; ; \quad t_{cD} = 1 + \frac{.85 \times 350}{396} = 1.751$$

$$t_{TD} = \frac{1350}{1350 - \frac{350}{.88}} = 1.4177 \; ; \quad t_{jD} = \frac{t_{uD}\, t_{cD}}{t_{TD}} = 2.174$$

$$\theta_{JD} = .98 \times 1000 \left(\frac{t_j - 1}{t_j} \right) = 529.2°C$$

$$\therefore \quad u_{jD} = 3384'/\text{sec.} \quad \text{(i.e.} \quad 147.1\sqrt{529.2})$$

$$\therefore \quad F_{sD} = \frac{3384 - 1950}{32.2} = 44.54 \text{ lbs/lb/sec}$$

$$\therefore \quad Q_D = \frac{10{,}000}{44.54} = 224.5 \text{ lb/sec.}$$

$$f_s = \frac{\theta_H \times .24 \times 3600}{10{,}500 \times F_s} = 1.116 \text{ lb/hr/lb thrust}$$

$$\eta_o = \frac{F_s \times u}{604 \times 336} = \frac{44.54 \times 1950}{604 \times 336} = .428$$

$$\phi_{uD} = \frac{176}{220} = 0.8 \quad \phi_{cD} = \frac{350}{220} = 1.591 \quad \therefore \; n = \frac{1350}{350} = 3.857$$

$$\phi_{JD} = \frac{529}{220} = 2.405$$

$$\text{A for equation (1b)} = \frac{t_{uD}\, t_{cD}}{\phi_{cD}} \left(\frac{1}{t_{uD}\, t_{cD} - t_{TD}} \right) u_{JD}^2 =$$

$$\frac{1.76 \times 1.751}{1.591} \left(\frac{1}{1.76 \times 1.751 - 1.418} \right) u_{JD}^2 = 1.164 \times 3384^2$$

$$\text{B for equation (2)} = \frac{1}{\sqrt{2.405} - \sqrt{0.8}} = 1.523$$

$$\text{C for equation (4)} = \frac{1.523}{392\,(1.76 \times 1.751)^{3.5}} = 7.557 \times 10^{-5}$$

From the above results it is now possible to calculate the performance of the engine at other heights, flight speeds and engine speeds provided that it is assumed that there is no appreciable change in component efficiencies and that θ_c is proportional to N^2, where N is engine r.p.m.

Example 16-2.

What would be the performance characteristics of the engine of Example 1 at 20,000′ at a speed of 600 m.p.h. (880′/sec.) at the same engine speed (i.e. same θ_c and T_M) assuming $T_o = 250°K$ and $P_o = 970$ p.s.f.

For 880′/sec. $\theta_u = 36$ $\phi_u = \frac{36}{250} = 0.144$ $t_u = \frac{.95 \times 36}{250} + 1 = 1.137$. The total temp. of ram compression $= 250 + 36 = 286$ $\therefore \; t_c = 1 + \frac{.85 \times 350}{286} = 2.04$

$\phi_c = \frac{350}{250} = 1.4$ t_T is the same as for Example 1, i.e. $t_T = 1.4177$. At this point one may either use the above equations or draw the cycle diagram though equation (3) is necessary for finding Q.

Fig. 8 shows the cycle diagram with the lines omitted, and with temp. differences in boxes.

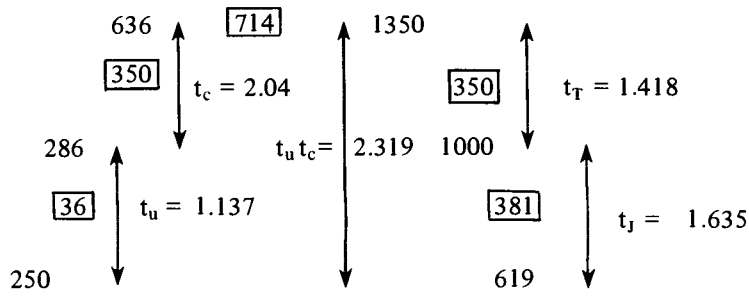

Fig. 16-8

Since θ_J is found to be 381°C $\quad u_J = 147.1\sqrt{381} = 2871'/\text{sec.}$

$$F_s = \frac{2871 - 880}{32.2} = 61.84 \text{ lbs/lb/sec.} \quad \text{(or 61.84 secs.)}$$

$$\eta_o = \frac{F_s u}{714 \times 336} = \frac{61.84 \times 880}{714 \times 336} = .227$$

Since $\dfrac{C_p \times 3600}{10{,}500} = \dfrac{.24 \times 3600}{10{,}500} = .0823$

$$f_s = \frac{.0823 \times 714}{61.84} = .95 \text{ lbs/hr/lb thrust}$$

From equation 3, since $\varphi_{cD} T_{oD} = \phi_c T_o$, (i.e. $\theta_{cD} = \theta_c$),

$$\frac{Q}{Q_D} = \frac{P_o}{P_{oD}} \left(\frac{t_u t_c}{t_{uD} t_{cD}}\right)^{3.5} \sqrt{\frac{220}{250}}$$

From Example 1 $\quad Q_D = 224.5$ lb/sec. $\quad P_{oD} = 392$ p.s.f.

and $t_{uD} t_{cD} = 1.76 \times 1.751 = 3.082$

and P_o for this example is 970 p.s.f. From Fig. 8, $t_u t_c = 2.319$

$$\therefore \frac{Q}{Q_D} = \frac{970}{392} \left(\frac{2.319}{3.082}\right)^{3.5} \sqrt{\frac{220}{250}} = .858$$

$$\therefore Q = .858 \times 224.5 = 192.7 \text{ lb/sec.}$$

$$\therefore F = QF_s = 192.7 \times 61.84 = 11{,}916 \text{ lbs.}$$

Comparison of the results of Examples 1 and 2 illustrates the extent to which high speed and low atmospheric temp. T_o can largely compensate for a much reduced air density at height. Also the striking effect of low T_o and high speed on overall efficiency.

In the case of Example 2 the thrust would be well in excess of that necessary for cruise so the aircraft would be climbing or accelerating or both.

Example 16-3.

What would be the part load performance of the same engine at 400 m.p.h. (587'/sec., θ_u = 16°C) at 10,000' if T_o = 270 and P_o = 1455 p.s.f. and N = .9N_D assuming negligible change in component efficiencies and that $\theta_c \propto N^2$.? i.e. θ_c = .81 X 350 = 283.5.

Since, as we have seen, T_M is proportional to θ_c, it is reduced to .81 X 1350 = 1093.5.

The cycle diagram now becomes as shown in Fig. 9.

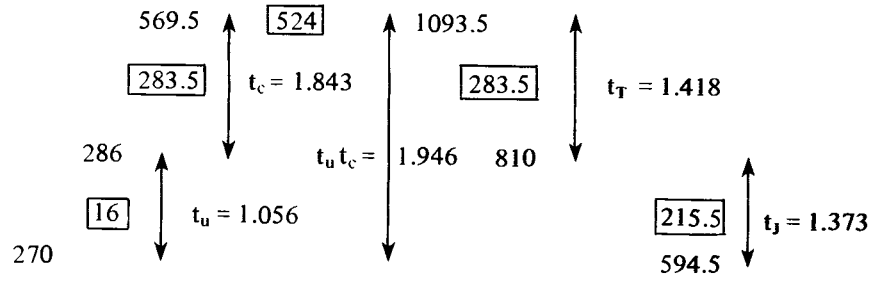

Fig. 16-9

Since θ_J = 215.5 u_J = 2160.2'/sec.

$$F_s = \frac{2160.2 - 587}{32.2} = 48.85 \text{ lbs/lb/sec}$$

$$\eta_o = \frac{48.85 \times 587}{524 \times 336} = .163$$

From equation (3) $$\frac{Q}{Q_D} = \frac{P_o}{P_{oD}} \left(\frac{t_u t_c}{t_{uD} t_{cD}}\right)^{3.5} \sqrt{\frac{1350}{1093.5}}$$

As before P_{oD} = 392 p.s.f.; $t_{uD} t_{cD}$ = 3.082 and P_o for this example is 1455 p.s.f.

From Figure 9, $t_u t_c$ = 1.946

$$\therefore \frac{Q}{Q_D} = \frac{1455}{392} \left(\frac{1.946}{3.082}\right)^{3.5} \sqrt{\frac{1350}{1093.5}} = .825 \quad \therefore \text{ since } Q_D = 224.5$$

$$Q = .825 \times 224.5 = 185.2 \text{ lbs/sec.}$$

$$\therefore \quad F = QF_s = 185.2 \times 48.85 = \underline{9,047} \text{ lbs}$$

On reviewing the reasoning leading to equation (3) it occurs to the writer that, since $t_u t_c$ is the overall temp. ratio of the cycle t_o, and since $\phi_c T_o = \theta_c$ and $\theta_c \propto N^2$, equation (3) can be simplified to

$$\frac{Q}{Q_D} = \frac{P_o}{P_{oD}} \left(\frac{t_o}{t_{oD}}\right)^{3.5} \frac{N_D}{N} \qquad (16\text{-}6)$$

Another query which may occur to the reader is why, in the above examples, the ram efficiency has been assumed to remain the same, namely 95%, when it has been previously stated that subsonic intakes are virtually 100% efficient for ram compression? There are two answers to this, namely: 1) An intake designed for supersonic flight is not equally appropriate for subsonic flight. 2) In subsonic flight, ram compression contributes far less to the total compression (as may be seen in Examples 2 and 3 above) so that (within limits) the cycle calculation is insensitive to ram efficiency assumptions.

Example 16-4.

What is the sea level static thrust of the engine of example 1 assuming that N may be increased to 1.05 N_D, that $T_o = 288°K$ and $P_o = 2116$ p.s.f.?

In this case, of course, there is no ram compression and both θ_c and T_M are increased in the ratio $(1.05)^2$ c.f. design; i.e. $\theta_c = (1.05)^2 \times 350 = 385.9$ and $T_M = (1.05)^2 \times 1350 = 1488°K$. The cycle diagram is therefore as shown in Figure 10.

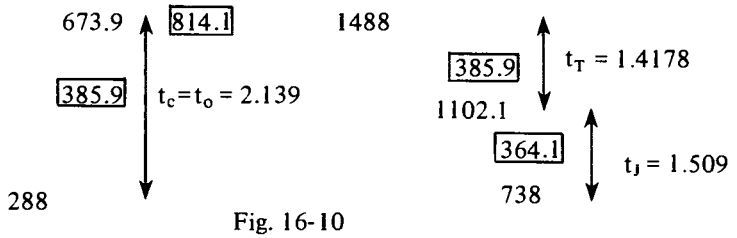

Fig. 16-10

Since $\theta_j = 364.1$ $\quad u_j = 147.1\sqrt{364.1} = 2807'/sec.$

$$\therefore \quad F_s = \frac{2807}{32.2} = 87.17 \text{ lbs/lb/sec.}$$

From equation (6) (and as before $Q_D = 224.5$, $t_{oD} = 3.082$, $P_{oD} = 392$)

$$\frac{Q}{Q_D} = \frac{2116}{392} \left(\frac{2.135}{3.092}\right)^{3.5} \times \frac{1}{1.05} = 1.406$$

$$\therefore \quad Q = 1.406 \times 224.5 = 315.7 \text{ lb/sec.}$$

$$\therefore \quad F = QF_s = 315.7 \times 87.17 = 27{,}522 \text{ lbs.}$$

$$f_s = \frac{.0823 \times \theta_H}{F_s} = \frac{.0823 \times 814.1}{87.17} = .769 \text{ lbs/hr/lb thrust.}$$

The overall efficiency is, of course, zero but the gas generator efficiency $= \frac{364.1}{814.1} = .447.$

The results of this example are probably over-optimistic in that, with the higher pressure ratio and a T_M of 1488°K both compressor and turbine efficiencies would be lower than those assumed in Example 1 especially as extra air cooling for the turbine would be necessary.

Up to this point it has been assumed that $\theta_T = \theta_c$, but, as has previously been mentioned, if the axial velocity at turbine exhaust is high then its temp. equivalent should be debited to the turbine and credited to final expansion. i.e., $\theta_T = \theta_c + \theta_a$ where θ_a is the temp. equivalent of turbine exhaust axial velocity. This means that the static pressure at turbine exhaust is lower than if $\theta_T = \theta_c$, and this, in turn, means that the partial recovery of turbine loss in final expansion is reduced since the degree of recovery depends on the final expansion static to static temp. ratio. The error due to the assumption that $\theta_T = \theta_c$ will now be examined in Example 5 below.

Example 16-5.

Taking the engine of Example 1, what is the effect of assuming that $\theta_T = \theta_c + \theta_a$ if the turbine exhaust axial velocity is 1200'/sec. for which the temp. equivalent is $\left(\frac{1200}{147.1}\right)^2 = 66.5°$, but also assuming that turbine losses are the same as in Example 1, i.e. $\frac{\theta_c}{.88} - \theta_c$

The turbine losses θ_L (converted into internal energy) are given by

$$\theta_L = \frac{\theta_c}{.88} - \theta_c = .136\,\theta_c = .136 \times 350 = 47.7°C$$

Figures 11a and 11b below indicate a method of dealing with the problem using the values

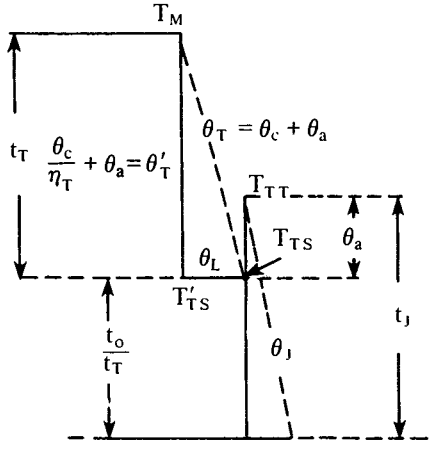

Fig. 16-11a

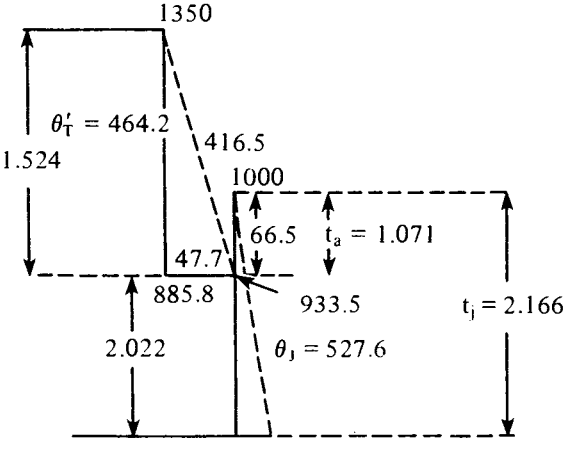

Fig. 16-11b

of Example 1 for T_M, θ_c etc., it being assumed that the isentropic heat drop in the turbine = $\frac{\theta_c}{\eta_T} + \theta_a = \frac{\theta_c}{.88} + 66.5 = \frac{350}{.88} + 66.5 = 464.2$ to give a static exhaust temp. (isentropic) of 885.8°K which is then increased by turbine losses to 933.5°K (since $.136\,\theta_c = 47.7°C$). It is then assumed that the total temp. before final expansion equals $933.5 + \theta_a =$

$933.5 + 65.5 = 1000°K$.

$t_T = \frac{1350}{885.8} = 1.524$. From Example 1, $t_o = 1.76 \times 1.751$ $(= t_u t_c) = 3.082$

$\therefore$ the static to static temp. ratio of the exhaust $= \frac{3.082}{1.524} = 2.022$. The total to static temp. ratio $t_J = 2.022 \times t_a$ (i.e. as though the exhaust axial velocity had been brought to rest isentropically to give a total temp. of 1000° and $t_a = \frac{1000}{933.5} = 1.071$)

Thus $t_j = 2.166$ (cf. 2.174 for Example 1) from which θ_J is found to be 527.6 (cf. 529.2 for Example 1).

$u_j = 3378.8'$/sec. and $F_s = \frac{3378.8 - 1950}{32.2} = 44.37$ lbs/lb/sec. (cf. 44.54 for Example 1) i.e. the error is less than ½%. With the lower final expansion ratios of Examples 2, 3 and 4 the error would be somewhat larger. The assumption of an axial velocity as high as 1200 ft/sec. is, however, somewhat extreme.

It could be argued that Example 5 exaggerates the error, small though it is, in assuming that $\theta_T = \theta_c$, because tip leakage—the main item of the turbine losses—contributes directly to the exhaust kinetic energy and the axial component of leakage at least should be added to the energy available for final expansion.

Variable Propelling Nozzles

If complete expansion in a convergent-divergent propelling nozzle is desired—as it should be—then the divergent portion needs to be variable (See Section 5). There are several mechanical arrangements for achieving this which it is not proposed to describe herein, but the amount of the variation necessary will now be briefly examined with reference to Examples 1, 2 and 3 of this section.

In these examples it was assumed that the throat section of the final nozzles was fixed otherwise the assumption that $T_{max}/\theta_c =$ const. could not have been used. But this does not carry the implication that the exit nozzle area is also fixed.

In Example 1 (the design case) the following relevant quantities were found:—
$Q_D = 224.5$ lb/sec., $T_{JD} = 1000 - 529 = 471°K$, $u_{JD} = 3384'$/sec. Since, for complete expansion, the exhaust pressure equals atmospheric pressure P_o which was given as 392 p.s.f.

$\therefore$ the exhaust density $\rho_e = \frac{P_o}{RT_J}$.

If S_{eD} is the exit area, then $Q_D = S_e \rho_e u_J$

$$\therefore\ S_{eD} = \frac{Q_D}{\rho_e u_J} \quad \text{or, substituting for } \rho_e$$

$$S_{eD} = \frac{Q_D R T_{JD}}{P_{oD} u_J} \quad \therefore \text{ from the figures from Example 1 above,}$$

$$S_{eD} = \frac{224.5 \times 96 \times 471}{392 \times 3384} = 7.652 \text{ ft.}^2$$

From Example 2, $Q = 192.7$ lb/sec.; $T_J = 619°K$; $u_J = 2871'$/sec. and $P_o = 970$ p.s.f.

$$\therefore\ S_e = \frac{192.7 \times 96 \times 619}{970 \times 2871} = 4.112 \text{ ft.}^2$$

From Example 3, $Q = 185.2$ lb/sec.; $T_J = 594.5$; $u_J = 2160'$/sec. and $P_o = 1455$ p.s.f.

$$\therefore\ S_e = \frac{185.2 \times 96 \times 594.5}{1455 \times 2160} = 3.363 \text{ ft.}^2$$

However, as may be seen, the section area of the final nozzle exit is somewhat larger than that of the entering stream (in the design condition, 224.5 lb/sec. at $T_o = 220$, $P_o = 392$ and $u = 1950'$/sec., $S_o = \frac{224.5 \times 96 \times 220}{392 \times 1950} = 6.202$ ft.^{2} i.e. $0.81\ S_{eD}$).

From the point of view of minimising external shock drag, it is obviously desirable to have a nacelle of constant section from front to rear. For the design case of Example 1 this means that S_{eD} would have to be restricted to 6.202 ft.^{2} which in turn means incomplete expansion in the final nozzle, entailing some loss of thrust. It could therefore be argued that, since effective net thrust is actual thrust less nacelle drag, it might be worth 'trading' some degree of under expansion for reduction of nacelle drag to give the optimum net thrust. Alternatively the design cycle could be altered to give $S_{eD} = S_o$, or nearly so, but the writer has not, so far, explored these alternatives.

SECTION 17

Effect on Cycle Calculations of More Accurate Methods

Introductory

Up to this point the methods used have ignored such important factors as the increase of specific heat with temperature, the fuel mass addition in combustion and the effect on the gas constant R of combustion products.

With monatomic gases the energy of atomic motion is largely kinetic energy of linear motion but with diatomic gases such as O_2 and N_2, triatomic gases such as CO_2, H_2O, etc., part of the energy is in the form of molecular rotation. The increase in this with temperature is presumed to account for the increase of C_v (R is not affected by temperature in the absence of dissociation so that the increase of C_p is the same as the increase of C_v). At very high temperatures the effective specific heat is affected by dissociation and formation of radicals. Also by the formation of oxides of nitrogen ('NOX').

It is the purpose of this section to examine the degree to which the approximations are justified for comparative purposes using the rather extreme case of a straight jet engine designed for supersonic cruise as a basis for the analysis.

More accurate methods require that enthalpy h be used instead of temperature, enthalpy differences Δh instead of temperature differences θ, pressure ratios instead of temperature ratios, etc. Also it must always be borne in mind that the expansion mass flow is greater than the compression mass flow by the amount of fuel added in combustion (usually of the order of 1.5% to a little over 2%).

For present purposes, the approximate method (i.e. the assumption of constant specific heat and neglect of fuel mass addition) will be referred to as the 'F. W. Method' and the more accurate method as 'The h–p Method'.

Symbols and Suffixes Used

Symbols

h	enthalpy
$\bar{h}$	the mean enthalpy for a process
Δh	enthalpy difference
e	enthalpy ratio
P	absolute pressure
p	pressure ratio
T	absolute temp.
ρ	density
ψ	flux density
S	section area
Q	mass flow rate
$\bar{\alpha}$	the exponent in $e^{\bar{\alpha}} = p$
δ	the numerical difference between T°K and h in kj/kg
m	fuel mass per unit compressor mass flow rate
u	velocity

Suffixes

M	the greatest value of a quantity
t	the critical value of a quantity in a choking throat (i.e. when $\psi = \psi_t$)
u	pertaining to ram compression
c	pertaining to the compressor
H	pertaining to combustion
T	pertaining to the turbine
j	pertaining to final expansion through the propelling jet
0 or 1	pertaining to an initial condition
0	is also used to denote 'overall' e.g. p_0 means overall pressure ratio
a	pertaining to the atmosphere
D	implies the design condition

As before a prime denotes an isentropic value.

Many of these have been used before but are included above for convenience.

The Cycle Diagram

The cycle diagram is now as shown in Fig. 1 in which several important relationships are indicated.

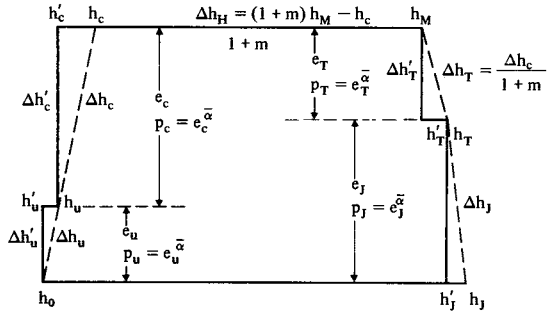

Fig. 17-1

It is now no longer possible to say that $e_u\ e_c = e_T\ e_j$ and so e_j, etc., must be calculated from the fact that $p_u p_c = p_T p_J = p_0$.

The Relationships between T, h, δ and $\bar{\alpha}$

For numerical convenience the units of h used are kJ/kg but mass flow rates remain in lb/sec. (The writer apologises for this mixture of unit systems, but it eases calculation.) To convert kJ/kgm to ft lb/lb multiply by 334.6 (cf. 336 for K_p). Using this, one finds that a calorific value of 10,500 C.H.U./lb is equivalent to 43,800 kJ/lb.

For the h–p method of dealing with problems it will frequently be necessary to refer to Fig. 2 for the value of δ and to Fig. 3 for the value of $\bar{\alpha}$ corresponding to $\bar{h}$. (It is a convenient fact that $e^{\bar{\alpha}} = p$. It is suggested that the reader verifies this by splitting an expansion from h = 1600 to h = 1000 into three or four parts and calculates the pressure ratio for each. He will find that the products of the series of pressure ratios will give the same total pressure ratio as would be obtained by taking e as 1.6 and $\bar{\alpha}$ corresponding to $\bar{h}$ = 1400.)

For the convenience of the reader who may wish to plot these curves on squared paper the necessary tabulations are given on Figs. 2 and 3.

The Calculation of Fuel Mass m

This is simple. The quantity of gas at h_M is 1 + m, ∴ the heat added

$$\Delta h_H = (1 + m)h_M - h_c, \therefore \Delta h_H = 43{,}800\,m = (1 + m)h_M - h_c \qquad (17\text{-}1)$$

from which

$$m = \frac{h_M - h_c}{43{,}800 - h_M} \qquad (17\text{-}2)$$

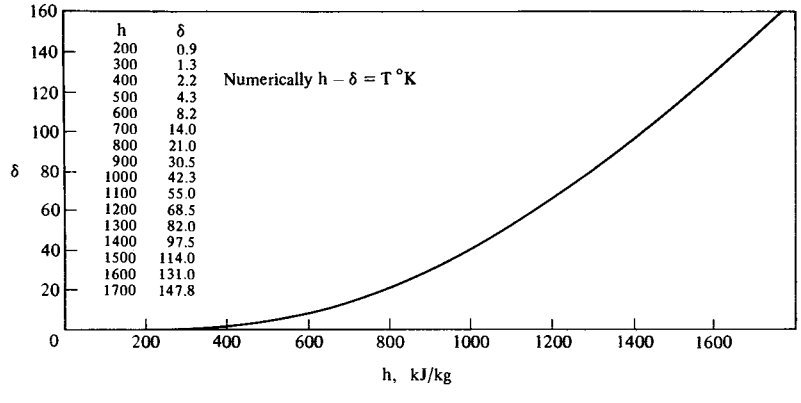

Fig. 17-2

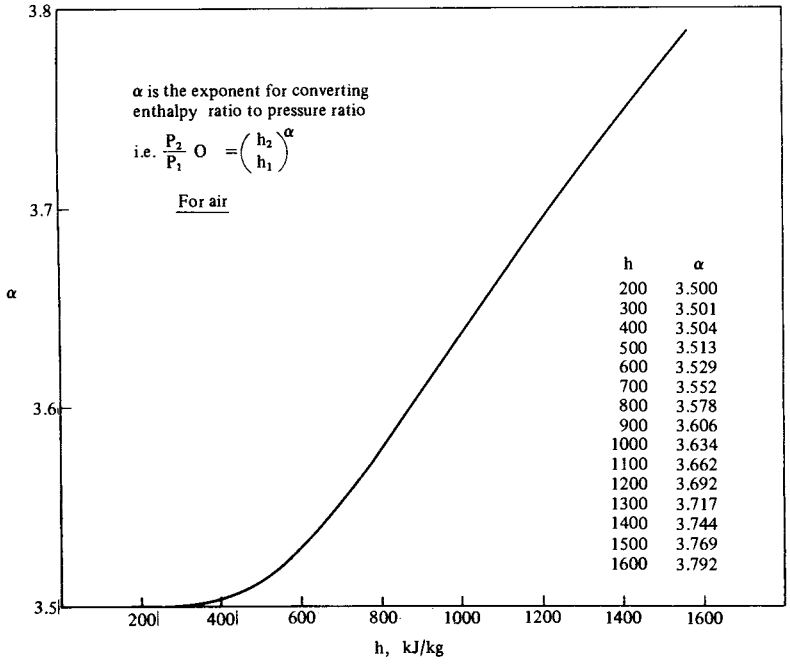

Fig. 17-3

Example 17-1

What is the value of m if $T_c = 746°K$ and $T_M = 1350°K$?

From Fig. 2, for T_c, $\delta = 18$, $\therefore h_c = 746 + 18 = 764$. For T_M, $\delta = 106$, $\therefore h_M = 1456$,

$$\therefore \quad m = \frac{1456 - 764}{43{,}800 - 1456} = .01634$$

The mass increase for expansion is 1.63% approx. It therefore seems justified to ignore the slight alteration in R due to the presence of CO_2, H_2O, etc., in the expansion part of a cycle. (In any case R cancels out as will be seen.)

Maximum Flux Density ψ_t in Isentropic Flow through a Nozzle

With the assumption of constant specific heat it was found that ψ_t corresponded to a temperature ratio of $1.2\left(= \frac{\gamma + 1}{2} \text{ when } \gamma = 1.4\right)$ but this is not so for variable specific heat. This matter will now be examined.

No simple formula can be derived so it is necessary to explore the problem numerically with the aid of Figs. 2 and 3.

In order to determine how e_t varies with h_M it is necessary to take a series of values of e and find the value of ψ for each and then to plot ψ against e to find the values of e_t and ψ_t and to repeat the procedure for a series of values of h_M. The process is best explained by an example as follows:

Example 17-2

What is the value of ψ corresponding to $h_M = 1600$ kJ/kg if $e = 1.17$?

The value of h after expansion is $\dfrac{1600}{1.17} = 1367.5$

$$\therefore \bar{h} = \frac{1600 + 1367.5}{2} = 1483.8.$$

From Fig. 3 the corresponding value of $\bar{\alpha}$ is 3.766

$\therefore$ the pressure ratio $(= e^{\bar{\alpha}})$ is $1.17^{3.766} = 1.8063$

$\therefore$ the pressure P after expansion from P_M is $\dfrac{P_M}{1.8063}$.

From Fig. 2, for $h = 1367.5$, δ is found to be 92, $\therefore$ $T = 1367.5 - 92 = 1275.5°K$.

We now have sufficient information to find ρ and u and therefore ψ.

$$\rho = \frac{P}{RT} \quad \text{and since} \quad P = \frac{P_M}{1{,}8063} \quad \text{and} \quad T = 1275.5, \rho = \frac{P_M}{1.8063 \times 1275.5R},$$

$$\Delta h = h_M \left(1 - \frac{1}{1.17}\right) = 1600 - 1367.5 = 232.5$$

for which

$$u = \sqrt{2g \times 334.6}\ \sqrt{232.5} = 146.8\ \sqrt{232.5} = 2239.4 \text{ ft/sec}$$

$$\therefore \psi \equiv \rho u = \frac{P_M}{R}\left(\frac{2239.4}{1.8063 \times 1275.5}\right) = 0.9716 \frac{P_M}{R}$$

More generally: $\rho = \dfrac{P_M}{R}\left(\dfrac{1}{e}\right)^{\bar{\alpha}} \left(\dfrac{1}{h_M/e - \delta}\right)$ and $u = 146.8 \sqrt{h_M \left(\dfrac{e-1}{e}\right)}$

$$\therefore \psi = 146.8 \frac{P_M}{R} \sqrt{h_M} \left[\left(\frac{1}{e}\right)^{\bar{\alpha}} \left(\frac{1}{h_M/e - \delta}\right) \sqrt{\frac{e-1}{e}}\right] \text{ or,}$$

Merging constants into k; $\psi = k \left(\frac{1}{e}\right)^{\bar{\alpha}} \frac{1}{\frac{h_M}{e} - \delta} \sqrt{h_M \left(\frac{e-1}{e}\right)}$

or $$\frac{\psi}{k} = \left(\frac{1}{e}\right)^{\bar{\alpha}} \left(\frac{e}{h_M - e\delta}\right) \sqrt{h_M \left(\frac{e-1}{e}\right)} \qquad (17\text{-}3)$$

from which it is fairly easy to work out tables for ψ for various values of h_M and e. This is done below for $h_M = 1600$.

e	$\frac{h_M}{e}$	$\bar{h}$	$\bar{\alpha}$	δ	$\frac{\psi}{k}$	$\frac{\psi}{\psi_t}$
1.10	1454.5	1527	3.777	105	.006235	0.9436
1.13	1415.9	1508	3.772	100	.006504	0.9831
1.15	1391.3	1496	3.769	96	.006584	0.9952
1.17	1367.5	1484	3.766	92	.006608	1.000
1.19	1344.5	1472	3.764	88	.006608	0.9988
1.21	1322.3	1461	3.760	85	.006576	0.9940
1.23	1300.8	1450	3.757	82	.006520	0.9855

The values of $\frac{\psi}{k}$ are plotted in Fig. 4 as are also similar results for $h_M = 1400$; 1200; and 1000. As may be seen, for $h_M = 1600$, $\frac{\psi}{\psi_t} = 1.0$ when $e = 1.17$, i.e. $e_t = 1.17$.

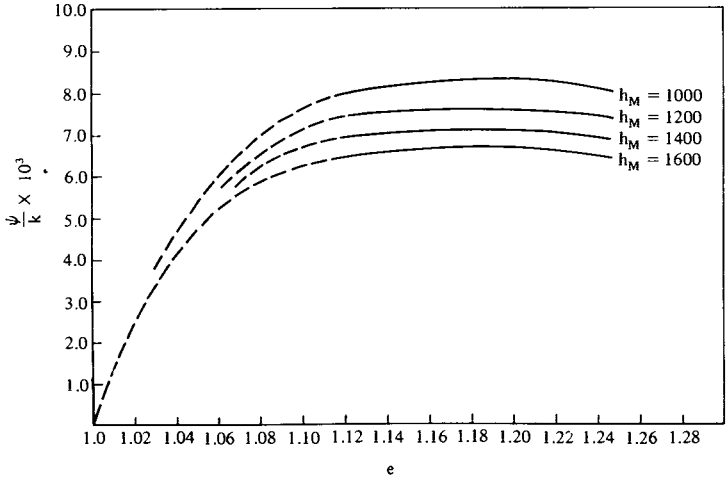

Fig. 17-4

Figure 5 shows a plot of e_t over the range $h_M = 900$ to $h_M = 1600$.

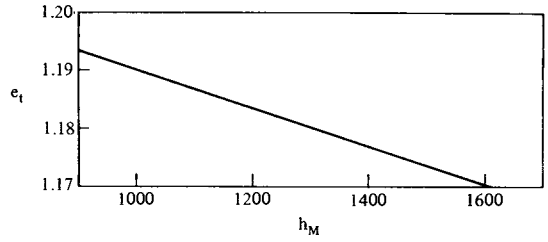

Fig. 17-5

It will be noted how extremely insensitive ψ is to e over quite a wide range of values of e. The variation is only 2% approx. over the range e = 1.13 to e = 1.23. The implication is that a nozzle designed for non-choking would become a choking nozzle in this range if there is departure from isentropic flow or there is very small nozzle distortion.

It was shown in Section 5 that, with constant specific heat, $\psi_t \frac{\sqrt{T_M}}{P_M}$ = const. for a choking nozzle. It is found that, with the h–p method it is approximately true to write $\psi_t \frac{\sqrt{h_M}}{P_M}$ = const. For the range $h_M = 1000$ to $h_M = 1600$.

$\frac{\psi_t}{k}\sqrt{h_M}$ varies as follows:

h_M	$\frac{\psi_t}{k}\sqrt{h_M}$
1000	0.2611
1200	0.2626
1400	0.2640
1600	0.2643

i.e. a variation of 1.2% over the range.

Choking Nozzles in Series with Energy Extraction between them by the h–p Method

In Section 5 it was shown that, with the FW method, if the choking throats were in fixed section ratio, the energy extraction (for a given efficiency) was proportional to T_M. Also that the temperature ratio (total to total) across the first nozzle and energy extractor (e.g. a turbine) remained constant whatever the value of T_M.

The present purpose is to examine the arrangement using the h–p method.

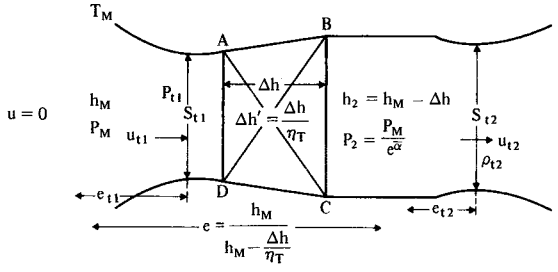

Fig. 17-6

It is represented diagrammatically in Fig. 6 which, as in the case of Fig. 5-6, is representative of a straight turbojet with the compressor turbine having choking nozzles with the final nozzle also choking.

Continuity again requires that $\rho_{t1} u_{t1} S_{t1} = \rho_{t2} u_{t2} S_{t2}$.

The calculation must be dealt with numerically using Figs. 2 and 3.

From equation (3), for the flow through S_{t1} we have

$$Q = S_{t1} \psi_{t1} = S_{t1} k \left(\frac{1}{e_{t1}}\right)^{\bar{\alpha}} \left(\frac{e_{t1}}{h_M - e_{t1}\delta}\right) \sqrt{h_M \left(\frac{e_{t1} - 1}{e_{t1}}\right)} \tag{17-4}$$

For the flow through S_{t2}, $u_{t2} = 146.8 \sqrt{(h_M - \Delta h_t)\left(\frac{e_{t2} - 1}{e_{t2}}\right)}$

$$\rho_{t2} = \frac{P_{t2}}{R(h_{t2} - \delta_{t2})} \quad \text{and} \quad P_{t2} = \frac{P_2}{e_{t2}^{\bar{\alpha}_{t2}}} = \frac{P_0}{e^{\bar{\alpha}} e_{t2}^{\bar{\alpha}_{t2}}}$$

$$\therefore \quad Q = S_{t2} \psi_{t2} = \frac{146.8}{R} S_{t2} \frac{P_0}{e^{\bar{\alpha}} e_{t2}^{\bar{\alpha}_{t2}}} \left(\frac{1}{h_{t2} - \delta_{t2}}\right) \sqrt{(h_M - \Delta h)\left(\frac{e_{t2} - 1}{e_{t2}}\right)} \tag{17-5}$$

Clearly (4) must equal (5). It is evident, however, that there is no simple formula for $\frac{S_{t2}}{S_{t1}}$ so the problem must be handled numerically as in the following example.

Example 17-3

With $h_M = 1600$ $\Delta h = 350$ and $\eta_T = 0.88$ what is the value of $\frac{S_{t2}}{S_{t1}}$?

We proceed as follows:

$\Delta h' = \dfrac{350}{0.88} = 397.7$ $\therefore$ the enthalpy ratio e across the first nozzle (which may represent a ring of choking turbine nozzles) and energy extraction ABCD is given by

$$e = \frac{1600}{1600 - 397.7} = 1.3308, h_2 = 1600 - 350 = 1250,$$

$$\therefore \bar{h} = \frac{1250 + 1600}{2} = 1425.$$

For this, from Fig. 3, $\bar{\alpha} = 3.75$ $\therefore$ the pressure ratio p is given by $p = e^{\bar{\alpha}}$, i.e.

$1.3308^{3.75} = 2.9203$, $\therefore$ $P_2 = \dfrac{P_M}{2.9203}$.

From Fig. 5, $e_{t1} = 1.175$, $\therefore$ $h_{t1} = \dfrac{1600}{1.175} = 1361.7$

$$\therefore \bar{h}_{t1} = \frac{1600 + 1361.7}{2} = 1480.9 \text{ for which } \bar{\alpha}_{t1} = 3.766$$

$$\therefore p_{t1} = 1.175^{3.766} = 1.8355, \text{ i.e. } P_{t1} = \frac{P_M}{1.8355}$$

From Fig. 2, for $h_{t1} = 1361.7$, $\delta = 91$ $\therefore$ $T_{t1} = 1361.7 - 91 = 1270.7$.

Hence $\rho_{t1} = \dfrac{P_M}{R \times 1.8355 \times 1270.7} = \dfrac{P_M}{2332.4R}$

$\Delta h_{t1} = 1600 - 1361.7 = 238.3$ from which $u_{t1} = 146.8\sqrt{238.3} = 2266$ ft/sec

$$\therefore \psi_{t1} = u_{t1}\rho_{t1} = \frac{2266.1}{2332.4}\frac{P_M}{R} = 0.9716\frac{P_M}{R}.$$

For the second nozzle with $h_2 = 1250$ and $P_2 = \dfrac{P_M}{2.9203}$ (from above)

e_{t2} from Fig. 5 is 1.183, so $h_{t2} = \dfrac{1250}{1.183} = 1056.6$

$$\therefore \bar{h}_{t2} = \frac{1250 + 1056.6}{2} = 1153.3 \text{ for which } \bar{\alpha}_{t2} = 3.678$$

$$\therefore p_{t2} = 1.183^{3.678} = 1.8554 \therefore P_{t2} = \frac{P_2}{1.8554} = \frac{P_M}{1.8554 \times 2.9203} = \frac{P_M}{5.4183}.$$

For $h_{t2} = 1056.6$, $\delta = 48$ (from Fig. 2)

$$\therefore T_{t2} = 1056.6 - 48 = 1008.6, \text{ hence } \rho_{t2} = \frac{P_{t2}}{RT_{t2}} = \frac{P_M}{R} \times \frac{1}{5.4183 \times 1008.6}$$

$$\Delta h_{t2} = 1250 - 1056.6 = 193.4 \quad \therefore u_{t2} = 146.8\sqrt{193.4} = 2041.5 \text{ ft/sec}$$

$$\therefore \psi_{t2} = \frac{P_M}{R} \times \frac{2041.5}{5.4183 \times 1008.6} = 0.3736\frac{P_M}{R}$$

It follows that $\frac{S_{t2}}{S_{t1}} = \frac{\psi_{t1}}{\psi_{t2}} = \frac{0.9716}{0.3736} = 2.6008.$

Using similar methods and making the assumption that Δh is proportional to h_M, it is found that for $h_M = 1400$ e = 1.3308 and $\frac{S_{t2}}{S_{t1}} = 2.566$ which is less than $1\frac{1}{2}\%$ smaller than for $h_M = 1600$.

For $h_M = 1200$, again e = 1.3308 and $\frac{S_{t2}}{S_{t1}} = 2.463$ which is 5.6% smaller than for $h_M = 1600$.

It should be noted that e remains constant if $\frac{\Delta h}{h_M} = \text{const.}$

We see that if S_{t2} and S_{t1} are in fixed ratio Δh is not exactly proportional to h_M but is evidently nearly so and could be made exactly so by a slight reduction of S_{t2} as h_M is reduced.

In what follows it will be assumed that Δh is in fact proportional to h_M.

A Comparison between the F.W. Method and the h–p Method for the Straight Jet

For this purpose, three widely different circumstances will be examined. It will be assumed (i) that the design is for supersonic cruise in the stratosphere at 1950 ft/sec with $T_M = 1350°K$ and $\theta_c = 350$; (2) that the efficiency of ram compression η_u is 95% at design and 98% for subsonic conditions; (3) that $\eta_c = 85\%$; (4) $\eta_T = 88\%$; (5) $\eta_j = 98\%$; (6) that for climb at 20,000 ft, gust load considerations limit the speed to 675 ft/sec (approx. 400 knots); (7) that for climb, $T_M = 1400°K$; (8) for take off, i.e. sea level static, $T_M = 1450°K$.

A. The FW Method

The design (i.e. cruise) cycle is the same as Example 16-1 but is repeated below and illustrated in Fig. 7 for ease of reference with additional figures on the diagram.

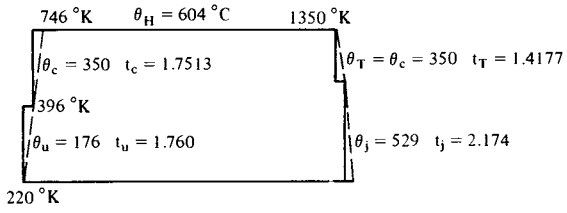

Fig. 17-7

As in Example 16-1 the design specific thrust F_{sD} = 44.54 sec. The overall temp. ratio of the cycle is 1.76 x 1.7513 = 3.0822.

∴ the overall pressure ratio is $3.0822^{3.5}$ = 51.41, i.e. the total pressure before the turbine is 51.41 P_{aD} where P_{aD} is the atmospheric pressure at design height. Therefore

$Q_D = k\dfrac{51.41}{\sqrt{1350}} P_{aD}$, so total thrust F ($\equiv F_{SD} Q_D$) is 44.54 x kP_{aD} x $\dfrac{51.41}{\sqrt{1350}}$ = 62.32 kP_{aD}.

Design Efficiency $\eta_{oD} = \dfrac{F_{SD} u_D}{\theta_{Ho} K_p} = \dfrac{44.54 \times 1950}{604 \times 336} = 0.428$ or 42.8%.

For climb at 675 ft/sec at 20,000 ft, T_0 = 272°K (I.S.A. + 4°) and P_a = 972.6 p.s.f.

θ_c, being proportional to T_M ; = $\dfrac{1400}{1350}$ x 350 = 363°C, $\theta_u = \left(\dfrac{675}{147.1}\right)^2$ = 21.1°C.

The climb cycle is shown in Fig. 8.

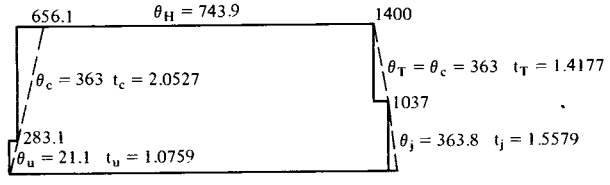

Fig. 17-8

$u_j = 147.1\sqrt{363.8}$ = 2806.2 ft/sec to give $F_S = \dfrac{2806.2 - 675}{32.2}$ = 66.19 secs

The overall temp. ratio t_0 = 1.0759 x 2.0527 = 2.2085

∴ the overall pressure ratio p_0 = $2.2085^{3.5}$ = 16.01

$\therefore Q = \dfrac{k \times 16.01 \times 972.6}{\sqrt{1400}} = 416.2\,k$

$\therefore F = QF_S = 416.2\,k \times 66.19 = 27{,}546\,k$

$\dfrac{F}{F_D} = \dfrac{Q}{Q_D} \times \dfrac{F_S}{F_{SD}} = \dfrac{27{,}546}{62.32 P_{aD}} = \dfrac{442}{P_{aD}}$

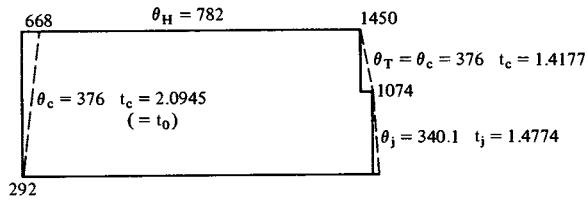

Fig. 17-9

$$\eta_0 = \frac{66.19 \times 679}{743.9 \times 336} = 0.1787 \quad \text{or} \quad 17.87\%$$

$$\therefore \frac{\eta_0}{\eta_{0D}} = \frac{17.87}{42.8} = 0.4175.$$

For sea level static, the cycle is shown in Fig. 9. $T_0 = 292°K$; $P_a = 2116$ p.s.f. θ_c for $T_M = 1450°K$ is now 376°C.

$$u_j = 147.1\sqrt{340.1} = 2712.8 \quad \therefore F_S = \frac{2712.8}{32.2} = 84.25 \text{ secs}$$

$$\therefore \frac{F_S}{F_{SD}} = \frac{84.25}{44.45} = 1.896$$

The overall pressure ratio corresponding to t_0 (or t_c since there is no ram compression) is $p_0 = 2.0945^{3.5} = 13.28$

$$\therefore P_M = 13.28 \times 2116 \quad \text{and} \quad Q = k \times \frac{13.28 \times 2116}{\sqrt{1450}} = 738k$$

$$\therefore \frac{Q}{Q_D} = \frac{13.28 \times 2116}{\sqrt{1450}} \times \frac{\sqrt{1350}}{51.41 P_{aD}} = \frac{527.3}{P_{aD}}.$$

$$\text{Hence } \frac{F}{F_D} = \frac{F_S Q}{F_{SD} Q_D} = \frac{1.8916 \times 527.3}{P_{aD}} = \frac{997.4}{P_{aD}}.$$

The overall efficiency is, of course, zero.

B. The h–p Method

The values of h corresponding to the temperatures of Fig. 7 are derived from Fig. 2 and, for the design cycle, are shown in Fig. 10.

The fuel mass (per lb) m must first be determined for fuel of calorific value of 10,500 C.H.U./lb or 43,800 kJ/lb.

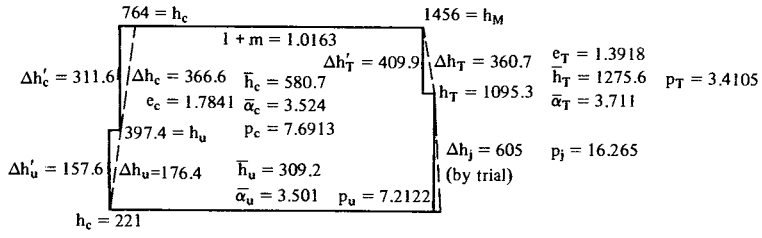

Fig. 17-10

Using equation (2)

$$m_D = \frac{1456 - 764}{43{,}800 - 1456} = .0163,$$

$$\therefore \Delta h_T = \frac{\Delta h_c}{1 + m} = \frac{366.6}{1.0163} = 360.7 \text{ (as shown in Fig. 10).}$$

The values of e, $\bar{h}$, $\bar{\alpha}$ and p for each part of the cycle are shown in Fig. 10.

The overall pressure ratio $p_{0D} = P_{UD} p_{CD} = 7.2122 \times 7.6913 = 55.47$ and since

$$p_T = 3.4105, \quad p_J = \frac{55.47}{3.4105} = 16.265.$$

(The pressure ratios are related by $p_u p_c = p_T p_j$.)

In order to find Δh_j it is necessary to resort to trial to find which value of Δh_j at $\eta_j = 0.98$ gives a pressure ratio of 16.265. Usually about three guesses will suffice though the process takes time because, for each trial value of Δh_j, $\bar{h}$, e and $\bar{\alpha}$ must be found and the value of $e^{\bar{\alpha}}$ plotted to find the required value of p_j.

Having found that $\Delta h_j = 605$, then $u_j = 146.8\sqrt{605} = 3611$ ft/sec.

$$\text{So } F_{SD} = \frac{(1 + m)u_j - u_0}{g} = \frac{1.0163 \times 3611 - 1950}{32.2} = 53.41 \text{ secs.}$$

For the h–p cycle it must be borne in mind that the mass flow Q_T in expansion is 1 + m times that in compression Q_c.

To find Q_{TD} it is necessary to find ψ_{tD} for the assumed choking turbine nozzle ring.

From Fig. 5, the value of e_t (the critical enthalpy ratio to the nozzle throats) is found to be 1.179 for $h_M = 1456$ to give $h_t = \frac{1456}{1.179} = 1234.9$, and $\bar{h}_t = \frac{1456 + 1234.9}{2} = 1345.5$,

for which $\bar{\alpha}_t$ (from Fig. 3) is 3.729.

$$\Delta h_t = \left| \begin{array}{ll} h_M = 1456 & \\ & l_t = 1.179 \\ 221.1 & \bar{h}_t = 1345.5,\ \bar{\alpha}_t = 3.729,\ p_t = 1.179^{3.729} = 1.8479 \\ & u_t = 146.8\sqrt{221.1} = 2182.8 \text{ ft/sec} \\ h_t = 1234.9,\ S = 72,\ T_t = 1234.9 - 72 = 1162.9 & \end{array} \right.$$

Fig. 17-11

The vertical line in Fig. 11 represents isentropic expansion to the throats of the turbine nozzle ring. The figures of Fig. 11 give the information necessary to calculate ψ_{tD}.

$$\rho_{tD} = \frac{P_{tD}}{RT_{tD}} \text{ and, since } P_t = \frac{P_{MD}}{P_{CD}} = \frac{P_{MD}}{1.8479} \text{ and } T_{tD} = 1162.9$$

$$\rho_{tD} = \frac{P_{MD}}{R \times 1.8479 \times 1162.9} \quad \therefore \psi_{CD} = \frac{2182.8}{1.8479 \times 1162.9} \frac{P_{MD}}{R} = 1.0158 \frac{P_{MD}}{R}$$

$$Q_{TD} = \psi_{tD} S_{t1} = 1.0158 S_{t1} \frac{P_{MD}}{R} \text{ or, since } P_{MD} = 55.47 P_{aD}$$

$$Q_{TD} = 56.35 \frac{S_{t1} P_{aD}}{R}$$

$$\text{So } Q_{CD} = \frac{Q_{TD}}{1.0163} = \frac{56.35}{1.0163} \frac{S_t P_{aD}}{R} = 55.442 \frac{S_t P_{aD}}{R}$$

$$\therefore F_D = F_{SD} Q_{CD} = 53.41 \times 55.44 S_t \frac{P_{aD}}{R} = 2961.2 S_t \frac{P_{aD}}{R}$$

$$\eta_0 = \frac{F_{SD} u_D}{[(1+m)1456 - 764]\ 334.5} = 0.435 \quad \text{or} \quad 43.5\%.$$

For the climb at $T_M = 1400$ ($h_M = 1515.8$) and $u = 675$ ft/sec, $T_0 = 272$ and $P_a = 972.6$ p.s.f. at 20,000 ft the cycle is shown in Fig. 12.

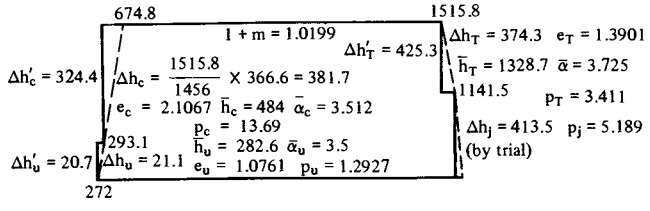

Fig. 17-12

The overall pressure ratio $p_0 = 1.2972 \times 13.693 = 17.7$,

m from (4) is given by $m = \dfrac{1515.8 - 674.8}{43{,}800 - 1515.8} = .0199.$

Most of the relevant figures are given in Fig. 12.

By trial Δh_j is found to be 413.5 $\therefore\ u_j = 146.8\sqrt{413.5} = 2985$ ft/sec

$$\therefore\ F_s = \frac{1.0199 \times 2985 - 675}{32.2} = 73.58 \text{ secs.}$$

To find Q_T we might assume that $Q_T \propto \dfrac{P_M}{\sqrt{h_M}}$ but for greater accuracy we proceed as before with the aid of Fig. 13 on which most of the relevant figures are shown for isentropic expansion to the turbine nozzle throats. From Fig. 5, for $h_M = 1515.8$, $e_t = 1.177$ to give $h_t = 1287.9$.

$h_M = 1515.8 \qquad P_M = 17.7 \times 972.6$

$\bar{h}_t = 1401.8, \bar{\alpha}_t = 3.744, \ p_t = 1.8407, \ P_t = \dfrac{17.7 \times 972.6}{1.8407} = 9352$ p.s.f.

$\Delta h_t = 227.9, u_t = 2216.1$

$h_t = 1287.9 \ \ \delta = 79 \ \ T_T = 1237.9 - 79 = 1208.9°K.$

Fig. 17-13

$$\rho_t = \frac{P_t}{RT_t} \text{ and } \psi_t = u_t\rho_t = \frac{u_t P_t}{RT_t} = \frac{2216.1 \times 9352}{1208.9\ R} = \frac{17{,}144}{R}$$

$$\therefore\ Q_T = S_t\psi_t = 17{,}144\frac{S_t}{R}$$

$$\therefore\ Q_c = \frac{17{,}144\ s_t}{1.0199\ R} = 16{,}809\frac{s_t}{R}$$

Q_{CD} was found to be $55.44\ P_{aD}\dfrac{s_t}{R}$

$$\therefore\ \frac{Q_c}{Q_{CD}} = \frac{16{,}809}{55.44\ P_{aD}} = \frac{303.2}{P_{aD}}$$

F_{SD} was found to be 53.41 sec $\therefore\ \dfrac{F_S}{F_{SD}} = \dfrac{73.58}{53.41}$

$$\therefore\ \frac{F}{F_D} = \frac{Q_c F_s}{Q_{CD} F_{SD}} = \frac{303.2}{P_{aD}} \times \frac{73.58}{53.41} = \frac{417.7}{P_{aD}}, \text{ cf. } \frac{442}{P_{aD}} \text{ for the F.W. method so}$$

the latter overestimates $\frac{F}{F_D}$ for the climb by 5.8%.

η_0 for the h–p cycle is given by

$$\eta_0 = \frac{73.58 \times 675}{(1.0199 \times 1515.8 - 674.8) \times 334.5} = .17 \quad \text{or} \quad 17\%, \text{ cf. } 17.78\%$$

for the F.W. method, the latter therefore overestimates η_c by approx. 4.6%. This, however, is of less importance than it seems in the light of the fact that fuel consumption during the subsonic phase of climb is a very small proportion of total fuel consumption because it is usual to accelerate to supersonic flight at about 30,000 ft.

The take-off (sea-level static) cycle for a T_M of 1450°K ($h_M = 1575.8$), $T_0 = 288$ ($j_0 = 289$) and $P_a = 2116$ p.s.f. is shown in Fig. 14,

m, from (4), is given by $m = \frac{1575.8 - 685.8}{43{,}800 - 1575.8} = .0211$

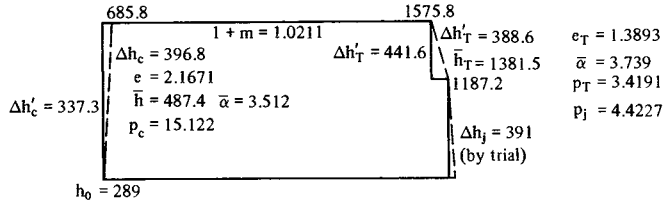

Fig. 17-14

By trial, $\Delta h_j = 391 \quad \therefore u_j = 146.8\sqrt{391} = 2902.8$ ft/sec

$\therefore \quad F_s = 90.15 \times 1.0211 = 92.05.$

To find Q_T we use Fig. 15 and the fact that from Fig. 4, for $h_M = 1575.8$, $e_t = 1.176$.

$h_M = 1575.8$

$\bar{h}_t = 1457.9 \quad \bar{\alpha} = 3.759 \quad p_t = \frac{15.12 \times 2116}{1.8393}$

$e = 1.176$ (from Fig. 4)

$\Delta h_t = 235.8 \quad \therefore u_t = 146.8\sqrt{235.8} = 2254.5$ ft/sec.

$h_t = 1346 \quad \delta = 87 \quad \therefore T_t = 1340 - 87 = 1253°K$

$$\rho_t = \frac{17{,}397}{1253R} \quad \therefore \psi_c = \frac{17{,}397 \times 22.545}{1253R} = \frac{31{,}302}{R}$$

$$\therefore Q_T = 31{,}302 \frac{S_t}{R} \text{ and } Q_c = \frac{31{,}302}{1.0211} \frac{S_t}{R} = 30{,}655 \frac{S_t}{R}.$$

Fig. 17–15

From above, $Q_{CD} = 55.44 \frac{S_t}{R} P_{aD}$,

$$\therefore \quad \frac{Q_C}{Q_{CD}} = \frac{30{,}655}{55.44\, P_{aD}} \text{ . Also from above } F_{SD} = 53.41 \text{ secs}$$

$$\therefore \quad \frac{F}{F_D} = \frac{F_s}{F_{SD}} \frac{Q_C}{Q_{CD}} = \frac{90.15}{53.41} \times \frac{30.655}{55.44\, P_{aD}} = \frac{933.3}{P_{aD}} \text{ cf. } \frac{997.4}{P_{aD}}$$

for the F.W. method. The latter therefore overestimates static thrust by 4.7%. It must be emphasised, however, that these comparisons are based on a rather extreme case. Had the design been for high subsonic cruise, agreement between the two methods would have been much closer. Moreover, for turbo fans where much of the energy interchange involves much lower temperatures, especially in the case of high bypass ratio engines, agreement would be very close indeed.

Agreement between dimensional quantities such as F_s, Q, F, etc., is *not* good, at least in the case of the foregoing comparisons. It is only in the non-dimensional ratios

$\frac{F}{F_D}$ and $\frac{\eta}{\eta_D}$ that the F.W. method approximates to the h–p method especially in less extreme cases. These ratios, however, are the most important for performance calculations; the writer therefore claims that he has justified the following procedure for such calculations for $\frac{F}{F_D}$ and $\frac{\eta}{\eta_D}$:

1) Calculate the design cycle by the h–p method.
2) Calculate the design cycle by the F.W. method using the same value of T_M as for 1).
3) Calculate the values of $\frac{F}{F_D}$ and $\frac{\eta}{\eta_D}$ for other than the design condition by the F.W. method and assume that they are the same as if calculated by the h–p method, remembering that minor discrepancies are of very little significance having regard to the fact that by far the greater part of the operational time will normally be at the design condition.

SECTION 18
Calculation of Maximum Efficiency

In the two preceding sections, the values of specific compressor energy input used in the examples were arbitrarily chosen and based on what may be achieved in a single compressor, but, as has been shown, for maximum gas generator efficiency, the greater the maximum temperature of the cycle, the greater the optimum pressure ratio.

On the assumption that practical limitations to pressure ratio do not exist, or can be overcome, the effect will now be examined.

Figure 1 shows the cycle diagram used for this purpose, and the table below illustrates the steps in the calculations to find the effect of θ_c. The assumptions used are indicated in Figure 1 for a flight speed of 1950'/sec. The approximate method is used treating enthalpy as 'pseudo' temperatures, i.e., 1460 is an actual temperature of 1354°K.

Relationships not shown in Figure 1 are: $u_J = 147.0\sqrt{\theta_J}$; $F_S = \dfrac{u_J - 1950}{g}$.

θ_c	t_c	$t_c t_u$	p_o	T_T	t_T	t_J	θ_J	u_J	F_S	θ_H	η_o	η_{GG}	η_p	$p_o F_S$
350	1.749	3.073	50.86	1110	1.374	2.236	601.3	3604	51.38	713	0.419	0.596	0.702	2613
400	1.856	3.261	62,62	1060	1.452	2.246	576.2	3529	49.03	663	0.430	0.604	0.712	3070
450	1.963	3.449	76.19	1010	1.539	2.241	548.1	3442	46.32	613	0.439	0.607	0.723	3529
500	2.071	3.6441	92.38	960	1.637	2.226	518.1	3346	43.36	563	0.447	0.608	0.736	4005
550	2.178	3.8251	109.46	910	1.748	2.188	484.1	3234	39.89	513	0.452	0.601	0.752	4366
600	2.285	4.013	129.50	860	1.876	2.139	448.8	3114	36.15	463	0.454	0.589	0.770	4681

Since maximum cycle temperature is the same for each value of θ_c, the overall pressure ratio p_o is a measure of the mass flow rate *provided that* for a given axial velocity at compressor entry, diameter is increased to accommodate the increase of mass flow based on p_o.

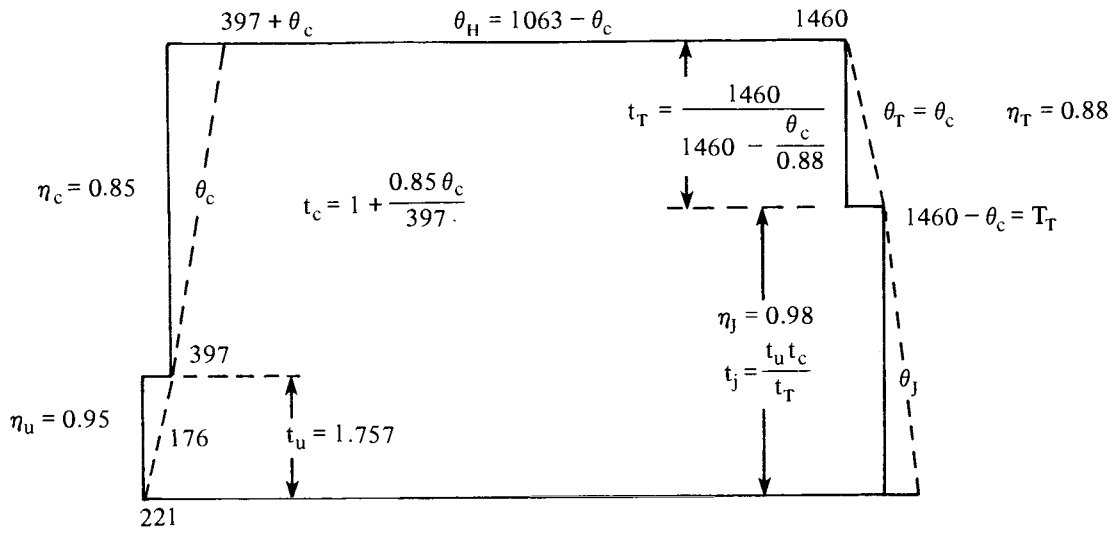

Fig. 18-1

$$\eta_o = \frac{F_S \times 1950}{335.6\,\theta_H} = \eta_{GG} \times \eta_p \quad \text{where } \eta_{GG} = \frac{\theta_J}{\theta_H} \text{ and } \eta_p = \frac{2}{\frac{u_J}{1950} + 1} \; ; \; p_o = (t_u t_c)^{3.5} ; \; p_c = t_c^{3.5}$$

For a given engine size, given flight speed, and given axial velocity, the mass flow rate would remain constant, so, since F_S falls off substantially as θ_c is increased while η_o increases this latter is at the expense of increased engine size and weight for a given total thrust. As may be seen from the table, the increase in η_o is becoming marginal at θ_c = 500 and above, while F_S is dropping off quite rapidly.

The usual criterion is the minimum value of power plant weight plus fuel weight for the design mission, which suggests that θ_c should be in the range 450–500°C for long range aircraft cruising at Mach 2.0 (1950′/sec in the stratosphere). Moreover, it is in this range that one gets a maximum value of η_{GG} which, as will be seen, is important for turbo-fan type engines.

Some of the quantities obtained from Figure 1 and its accompanying table are plotted in Figure 2, which also includes curves obtained in similar manner for a speed u of 880′/sec and T_o = 260 with the same T_{max} as Figure 1. η_u, however, was assumed to be 100% cf. 95% for the supersonic case.

As may be seen from Figure 2 η_o and F_S are very sensitive to u, the former increasing and the latter decreasing with increase of u. The effects of height and speed will be examined in greater detail later.

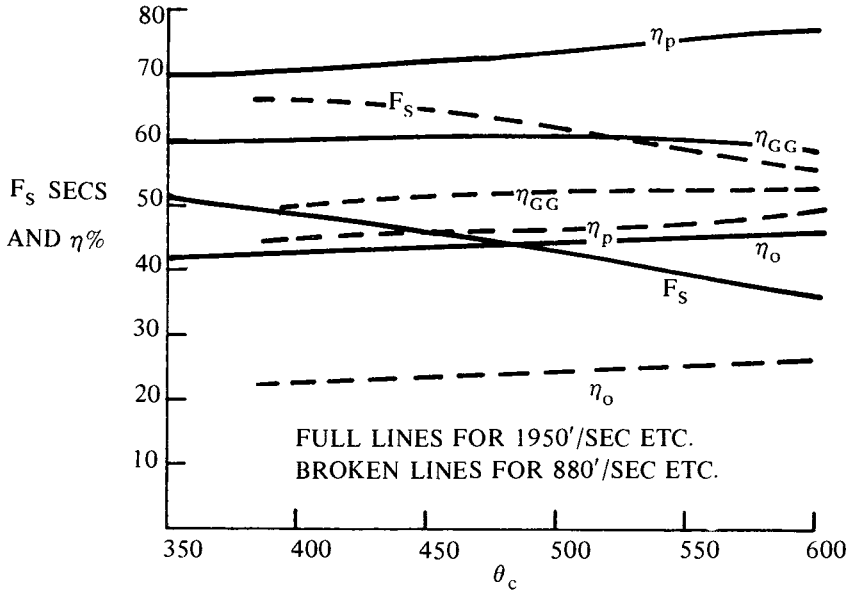
80
70
60
50
40
30
20
10
F_S SECS
AND η%
η_p
F_S
η_{GG}
η_{GG}
η_p
η_o
F_S
η_o
FULL LINES FOR 1950'/SEC ETC.
BROKEN LINES FOR 880'/SEC ETC.
350
400
450
500
550
600
θ_c

Fig. 18-2

SECTION 19
'Two Spool' Engines

Values of θ_c of the order of 500°C are beyond the capacity of single compressors unless fitted with an elaborate system of variable stators in several stages, hence the evolution of the two spool engine illustrated very diagrammatically in Figure 1. As may be seen, the first ('low pressure' or 'LP') compressor is connected to its driving turbine (the 'LP turbine') by a long shaft assembly 'threaded' through the shaft connecting the second ('HP') compressor to its driving ('HP') turbine.

In 1936 the writer attempted to design a two spool arrangement for an engine with a two stage centrifugal compressor but abandoned the scheme because of the seemingly insoluble problems of assembly and the formidable bearing and other mechanical complications. These difficulties, however, were first overcome by Rolls Royce with the Clyde turbo-prop having an axial flow LP compressor and an HP centrifugal and further developed in later engines with two axial flow compressors in series as in the Olympus 593, four of which power the Concorde.

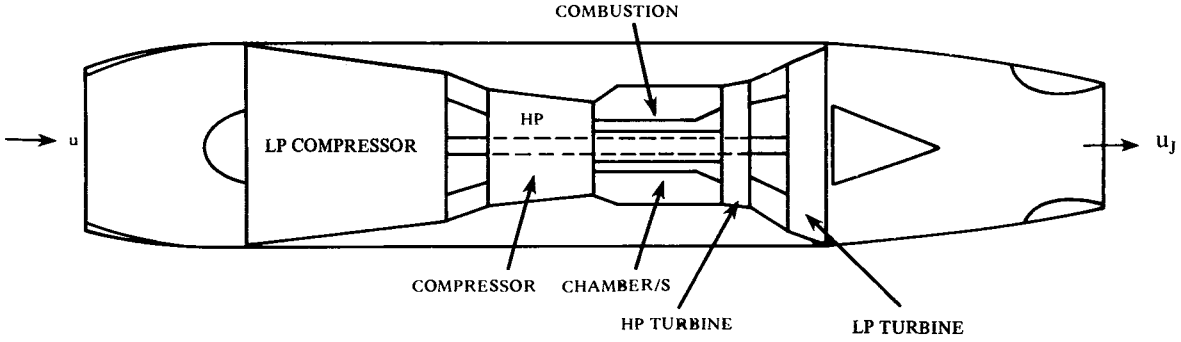

Fig. 19-1

The cycle diagram for the two spool arrangement is now as shown in Figure 2.

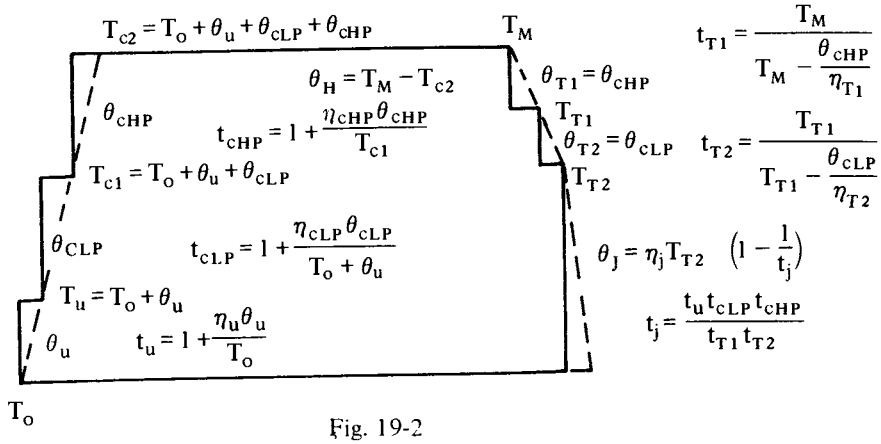

Fig. 19-2

The manner in which the total temperature rise in compression $\theta_{CLP} + \theta_{CHP}$ is distributed between the LP and HP compressors is a matter of choice for the designer and this choice is influenced by several factors which must be weighed against each other. Thus, for a given number of stages, θ_{CHP} can be substantially larger than θ_{CLP} because the entering air is much hotter. This would also mean that the LP turbine blades would be subject to a lower temperature so that, while it may be necessary to cool the HP turbine blades, this could be avoided in the LP turbine. One would also expect that by reducing θ_{CLP} the whole LP assembly – which clearly comprises the bulkiest and heaviest part of the complete assembly – would have reduced weight and bulk at the expense of some increase in weight of the HP assembly. However, such matters as shaft length, bearing and coupling arrangement, etc., must also influence the choice. The writer, however, has had no experience in the detail design of two spool axial flow engines and feels unable to comment adequately on the pros and cons involved. He does feel, however, that thermodynamic considerations point to equal temperature ratios in HP and LP compressors, i.e., that $1 + \frac{\eta_{CLP}\theta_{CLP}}{T_u}$ should equal $1 + \frac{\eta_{CHP}\theta_{CHP}}{T_{c1}}$ or $\frac{\eta_{CLP}\theta_{CLP}}{T_u} = \frac{\eta_{CHP}\theta_{CHP}}{T_u + \theta_{CLP}}$.

Example 19-1

If the surmise that t_{CHP} should equal t_{CLP} is correct, what would be the values of θ_{CLP} and θ_{CHP} if $\Sigma\theta_c = 500$ and $\eta_{CLP} = 88\%$ and $\eta_{CHP} = 86\%$ for a supersonic engine flying at a height where $T_o = 220°K$ and at a speed where $\theta_u = 176°C$.

We have two simultaneous equations, namely: $\theta_{CHP} = 500 - \theta_{CLP}$ and $\frac{0.88\,\theta_{CLP}}{396} = \frac{0.86\,\theta_{CHP}}{396 + \theta_{CLP}}$ which give a quadratic for either θ_{CLP} or θ_{CHP} the solution of which gives $\theta_{CLP} = 197$ and $\theta_{CHP} = 303$.

This distribution requires too high a heat drop in the HP turbine for a single stage which a designer might consider undesirable. There are, however, certain advantages (and disadvantages) in using a two stage HP turbine.

A feature of importance in two spool engines must now be discussed; namelv that, with a fixed throat area of the propelling nozzle, and with choking in both turbines, there is a 'thermodynamic lock' between the LP and HP assemblies. This arises from the fact that, as we have seen (Section 5) the total temperature before the first of two choking nozzles in series with energy extraction between them is a constant multiple of the energy extraction expressed as a temperature drop. Thus referring to Figure 2, and writing,

$\frac{T_m}{\theta_{T1}} = n$ and $\frac{T_{T1}}{\theta_{T2}} = m$ $\therefore$ since $T_{T1} = T_M - \theta_{T1} = n\theta_{T1} - \theta_{T1} = \theta_{T1}(n-1)$ it follows that

$\theta_{T1}(n-1) = m\theta_{T2}$ or $\frac{n-1}{m} = \frac{\theta_{T2}}{\theta_{T1}}$ or, since $\theta_{T2} = \theta_{CLP}$ and $\theta_{T1} = \theta_{CHP}$,

$\frac{n-1}{m} = \frac{\theta_{CLP}}{\theta_{CHP}} = \text{const.}$, therefore, over the speed range where it may be assumed that compressor temperature rise is proportional to the square of the rotational speed, the rpm of the HP assembly is a constant multiple of the rpm of the LP assembly.

Rotor tip speeds may, therefore, be an important factor in deciding the $\theta_{CHP}/\theta_{CLP}$ ratio. Thus, referring to Example 1 above, the shaft power of the smaller HP turbine is greater than that of the LP turbine in ratio 303/197. (Again an argument in favour of a two stage HP turbine).

This thermodynamic lock can be 'broken' in various ways, e.g., by having a variable propelling nozzle throat or by by-passing some of the LP compressor output, thereby increasing θ_{T1}. This latter would be a step in the direction of the turbo fan to be discussed later. A non-choking two stage HP turbine would also serve the purpose.

The cycle of Figure 2 can be simplified to that of Figure 1 by 'presuming' a single compressor of the same total temperature rise and same total temperature ratio and using a value of η_c to conform with this, and by 'combining' the HP and LP turbines in similar fashion (see Section 12). This procedure is useful for finding the variation of performance with height and speed.

SECTION 20
Thrust Boosting

This short section deals with thrust boosting other than by using turbo fans to be discussed later.

It is often desirable, or even necessary, to increase power temporarily at the expense of efficiency. For this there are two main methods, namely (1) coolant injection to reduce T_o 'artificially' and/or (2) after burning. The former is normally used only at take off especially in the tropics while the latter may be used at any flight condition.

Coolant Injection

For cooling the entry air, use is made of the cooling effect of evaporation of various liquids – methanol, a methanol–water mixture, etc., or just plain water.

In the writer's experience the most effective method is liquid ammonia injection. Liquid ammonia has a latent heat of evaporation (about 330 C.H.U./lb), second only to water; but for some reason this method never 'caught on' despite the sensational results in early experiments by the writer and his team in 1942. (In the experiments concerned, a large bottle of liquid ammonia outside the test house supplied a spray of the liquid into the large venturi duct used to measure the air flow into the test cell. It evaporated on injection and caused intense cooling. It was realized that ammonia is combustible so, there being no governor fitted, the operator of the control was warned that it would probably be necessary to cut back the main fuel supply to prevent overspeeding. Unfortunately, the ammonia bottle was not visible from the control room, so a system of hand signals was arranged via a test hand who could pass on a signal from the throttle operator to another test hand operating the ammonia supply valve. The signals were duly given but the operator of the ammonia valve took several seconds to release the very tight valve–or so he claimed. Another version is that he was chasing a rat. The throttle operator, being unaware of the delay, relaxed, believing that the ammonia was being injected and not producing the forecast speed increase, so that when the ammonia *did* feed in he was off guard. The result was spectacular. The tachometer, thrust measuring balance, etc., went

'off the clock' and the mercury in several manometers was blown out; the explosive bang was heard for miles. Surprisingly, the engine (the W.I.) did not disintegrate, but every turbine blade had stretched and fouled the casing. The braking effect of this probably saved the rest of the engine. In a later, more controlled, test, a 40% increase of thrust was obtained but the cooling effect was so drastic that the frost covered centrifugal compressor casing contracted to the point of causing the impellor to seize. It was also found that the ammonia corroded the bronze cages of bearings and other alloys. These problems could have been overcome, but pressure of other work resulted in the abandonment of these experiments.) A disadvantage of ammonia is its strong affinity for water and its high heat of solution therein, which, in hot humid air, can 'neutralize' the latent heat of evaporation of quite a large amount of ammonia hence the amount necessary to achieve a given cooling effect depends very much on the relative humidity. (Air at 303°K and 2110 p.s.f. with 100% relative humidity contains about 3.5% of water vapor by weight which would not only be capable of dissolving nearly its own weight of ammonia but would have a substantial warming effect due to its own condensation, the effect of which would be difficult to calculate because the latent heat of condensation into minute droplets is less than that of complete condensation to liquid by the amount of energy contained in the surface tension of the droplets. There would, of course, be a cooling effect on re-evaporation, but this would occur rather late in the compression process and so be comparatively ineffective).

After Burning

The exhaust from a jet engine contains ample oxygen for further combustion before final expansion through the jet nozzle, hence thrust can be increased considerably by after burning in the jet or 'tail' pipe at the expense of the efficiency of final expansion due to the pressure loss caused by the after burning equipment – usually two or more annular 'flame holders' of $\subset$ or $<$ section.

As we have seen, u_j is given by $u_j = 147.1\sqrt{\eta_J T_T \left(1 - \frac{1}{t_J}\right)}$ where t_J is the total to static temperature ratio of final expansion and T_T is the total temperature before expansion. By after burning, T_T can be increased by burning up to the limit of the available oxygen, but, in practice, the amount of after burning is far less than this because the penalty in reduction of jet pipe efficiency would be considerable (indeed intolerable) for long range cruise without the after burner in operation. Moreover, with after burning, a variable jet nozzle is necessary to avoid decreasing mass flow by choking and for complete or near complete expansion before final exhaust. Hence, the weight and mechanical complexity of the mechanism necessary tends to put a limit on the amount of after burning.

If the axial velocity at turbine exhaust is very high as it usually is, then to avoid high pressure loss at the point of location of the after burning flame holders, etc., it is very desirable to reduce velocity upstream of the after burner by a diffusing divergence. This, of course, also entails pressure loss so the optimum is the combination which gives the least total jet pipe pressure loss with the after burner off.

After burning is normally required, for a short line only, e.g., for take off; in combat; for transition through the 'sound barrier,' etc. Its effectiveness is obviously very dependent on the pressure ratio available for final expansion, the percentage thrust gain is therefore least at take off and greatest at maximum engine rpm and

highest air speed. Also the greater the final expansion ratio the smaller the effect on overall efficiency, i.e., the adverse effect on fuel consumption.

Example 20-1

The sea level static specific thrust without after burning is 80 secs and the temperature (static) of final exhaust is 690°K; what is the amount of after burning necessary to increase the static thrust by 20%? assuming complete mixing and also assuming that the expansion in the final nozzle is isentropic.

To give F_S = 80 secs, u_J must be 32.2 x 80 = 2576'/sec, the temperature equivalent of which θ_J is $\left(\frac{2576}{147.1}\right)^2$ = 307.1°C ∴ the total temperature T before and through the final nozzle = 307.1 + 690 = 997.1°K.

To increase the static thrust by 20% requires that u_j be increased by 20% and ∴ θ_J by $(1.2)^2$ = 1.44 ∴ with after burning θ_J = 1.44 x 307.1 = 442.2°C.

The temperature ratio t_J across the nozzle is unchanged, i.e., $t_J = \frac{997.1}{690} = 1.445$

∴ the total temperature T to give θ_J = 442.2 is found from $T\left(\frac{0.445}{1.445}\right) = 442.2$ from which T = 1436. Thus the temperature increase necessary by after burning is 1436 − 997.1 = 438.9°C.

Example 20-2

Taking the figures of Example 1, what increases in nozzle throat and exist areas would be necessary for complete expansion with the same mass flow rate Q?

(a) The throat section S_c: Without after burning the critical velocity u_c = $147.1\sqrt{\frac{997.1}{6}}$ = 1895'/sec and the static temperature $T_c = \frac{997.1}{1.2}$ = 830.9; with after burning $u_c = 147.1\sqrt{\frac{1436}{6}}$ = 2274'/sec and $T_c = \frac{1436}{1.2}$ = 1196.7.

The throat pressures will be the same with and without after burning ∴ the critical density ρ_c will be inversely proportional to T_c.

Hence, $Q = k\frac{S_{c1}\,u_{c1}}{T_{c1}} = k\frac{S_{c2}\,u_{c2}}{T_{c2}}$ where suffixes 1 and 2 denote without and with after burning.

$\therefore \frac{S_{c2}}{S_{c1}} = \frac{T_{c2}}{T_{c1}}\,\frac{u_{c1}}{u_{c2}} = \frac{1196.7 \text{ x } 1895}{830.9 \text{ x } 2274} = 1.2$, i.e., a 20% increase of throat section is necessary.

(b) The exit section S_E: Since the exit static pressure is the same, exit density ρ_E is inversely proportional to exit static temperature T_E.

$$\therefore \frac{S_{E2}}{S_{E1}} = \frac{T_{E2}}{T_{E1}} \cdot \frac{u_{j1}}{u_{j2}} = \left(\frac{1436-\theta_{J2}}{690}\right)\frac{2576}{1.2 \text{ x } 2576} \quad \text{(see Example 1)}$$

$$\therefore \frac{S_{E2}}{S_{E1}} = \frac{1436 - 442.2}{690 \times 1.2} = 1.2.$$

(This result could have been assumed from the findings of Section 5 where it was shown that S_E/S_c for a con-di nozzle is dependent only on the temperature ratio for complete isentropic expansion.)

Example 20-3

Assuming the same degree of after burning as in Example 1, what would be the effect on specific thrust and overall efficiency at a speed of 2000′/sec if, without after burning F_S = 41 secs, η_o = 0.43, and the total temperature of the jet is 1000°K?

To give F_S = 41, u_j is given by $41 = \frac{u_j - 2000}{32.2}$ from which u_j = 3520′/sec and $\theta_J = \left(\frac{3320}{147.1}\right)^2 = 510.1 \quad \therefore t_j = \frac{1000}{1000 - 510.1} = 2.041.$

If η_o = 0.43 then $\frac{F_S u}{336\theta_H} = 0.43$, i.e., $\frac{41 \times 2000}{336 \times \theta_H} = 0.43$ from which θ_H (the heat addition in the main combustion) is 567.6°C. From Example 1, the after burner increases the temperature before final expansion by 438.9°C, i.e., to 1438.9°K

$\therefore \theta_{J2}$ with after burning is given by $\theta_{J2} = 1438.9\left(1 - \frac{1}{t_J}\right) = 1438.9\left(\frac{1.041}{2.041}\right) = 733.9°C$

$\therefore u_{J2} = 147.1\sqrt{733.9} = 3982'/sec \quad \therefore F_{S2} = \frac{3982 - 2000}{32.2} = 61.56$ secs, i.e., an increase of 50.2%.

With after burning the total heat added $\Sigma\theta_H = 567.6 + 438.9 = 1006.5°C$

$$\therefore \eta_o = \frac{F_{S2} u}{336 \times 1006.5} = \frac{61.56 \times 2000}{336 \times 1006.5} = 0.364.$$

Example 20-4

Taking the figures of Example 3, what increase in nozzle section areas would be necessary for complete expansion with the same mass flow rate?

We have (as in Example 2) $\frac{S_{c2}}{S_{c1}} = \frac{T_{c2}}{T_{c1}} \frac{u_{c1}}{u_{c2}}$

$$T_{c1} = \frac{1000}{1.2} = 833.3°K \quad ; \quad u_{c1} = 147.1\sqrt{\frac{1000}{6}} = 1898'/sec$$

$$T_{c2} = \frac{1438.9}{1.2} = 1199° K \quad ; \quad u_{c2} = 147.1\sqrt{\frac{1438.9}{6}} = 2276'/sec$$

$$\therefore \frac{S_{c2}}{S_{c1}} = \frac{S_{E2}}{S_{E1}} = \frac{1199}{833.3} \times \frac{1898}{2276} = 1.2$$

(The fact that this answer is the same as for Example 2 is because the total temperatures in the two examples differ only by 2.9°.)

If, in Example 3, the after burning had increased the total temperature by 1000°C, F_S would be 83.7 secs and η_o would be 0.318, i.e., the thrust would be more than doubled. However, though there would be ample oxygen for such a large amount of after burning, the problem of nearly complete mixing before final expansion within a reasonable length would be quite acute. How serious could this be? Much less than one might suppose, as will now be demonstrated.

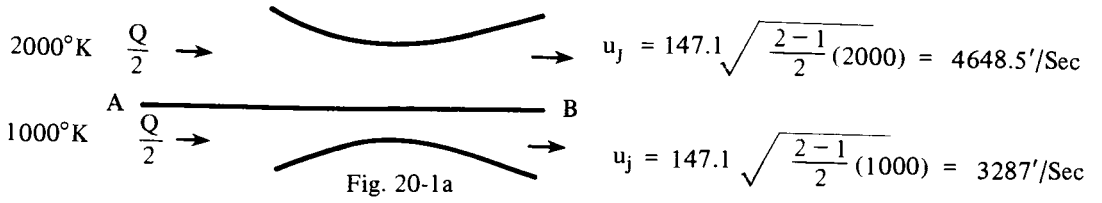

Fig. 20-1a

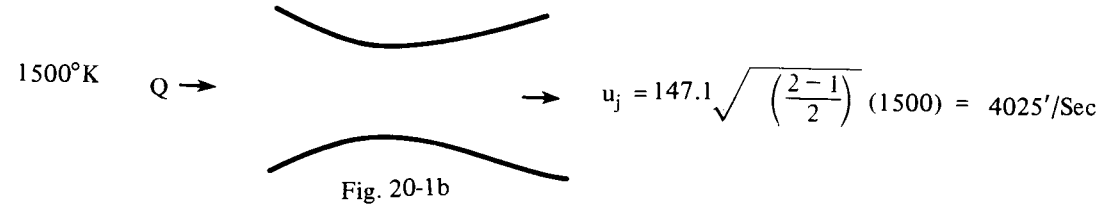

Fig. 20-1b

Figure 1a represents a con-di propelling nozzle having a total to static temperature ratio of $t_j = 2.0$ when air speed u is 2000'/sec. AB is a flexible diaphragm separating the total flow Q into two equal flows of $\frac{Q}{2}$. Above AB the total temperature is 2000°K and below AB it is 1000°K. The density of the lower flow is twice that of the upper, hence the eccentric position of AB.

Figure 1b represents a similar nozzle with a flow Q at a total temperature of 1500°K with the same temperature ratio.

In Figure 1a, the diaphragm (being flexible) ensures that the pressure along it are the same on each side.

The specific thrust of the upper flow in Figure 1a is $\frac{4648.5 - 2000}{32.2} = 82.25$ secs and for the lower flow is $\frac{3287 - 2000}{32.2} = 19.98$ secs. The total thrust, therefore, equals $\frac{Q}{2} \times 82.25 + \frac{Q}{2} \times 19.98 = 61.11\ Q$ lbs.

For Figure 1b the corresponding thrust is $Q \times \frac{4025 - 2000}{32.2} = 62.91\ Q$ lbs, i.e., about 3% greater – an astonishingly small difference for such a drastic case.

It can easily be shown that the throat and exit sections of the 'divided' nozzle would need to be about 1-1/2% larger than the undivided one for the same total flow.

The foregoing is not intended to imply that mixing is unimportant. A loss of thrust of 3% would be most undesirable. However, such an extreme case would be most improbable in practice.

If, in Figure 1a, the upper and lower total temperatures had been 1600 and 1400°K the thrust would be reduced by only 0.14%.

Where inadequate mixing is most undesirable is in the main combustion chamber otherwise the non-uniformity of velocity at exit from the turbine nozzles would seriously upset the flow pattern.

A vapor trail is visible evidence of the mixing problem. Also, experiments with stationary jet engines indicate that the axis jet flow is unaffected by mixing with the external air for some distance downstream of the exit plane. What happens is somewhat as shown in Figure 2; AB being about 6-10 diameters.

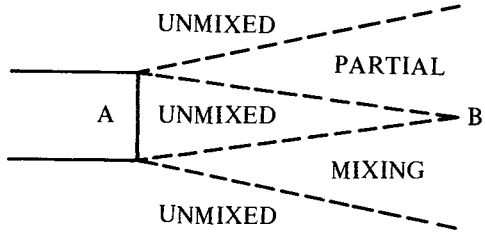

Fig. 20-2

To obtain mixing within a reasonable distance, it is necessary to use turbulence generators with their associated pressure loss, or to greatly increase the 'interface' by subdividing the flows it is desired to mix by means of fluted devices, again with pressure loss due to skin friction. The narrower the widths of the flute channels, the shorter the mixing distance needed – at the expense of increased skin friction.

The problem is obviously affected by the difference of velocity of the mixing streams. For example, two streams in contact at the same velocity and without turbulence; even with a large temperature difference, would take a very long time to mix since mixing would virtually be solely a matter of molecular diffusion.

The greater the velocity difference, the greater the mixing rate due to turbulence at the interface. But, since the mixing takes place without change of momentum, there is an inevitable conversion of kinetic energy into internal energy, part of which, however, is 'recoverable' in expansion.

It is not intended herein to go into the mixing problem at length so a simple example is used to indicate what happens.

Figure 3 illustrates a core flow of 1 lb/sec mixing with an annular flow of 1.2lb/sec, the two flows having the velocities and temperatures shown. It is assumed that the static pressure is uniform across the plane AB and that downstream of AB, the static pressure remains constant. This would; in fact, require a slight change in section (an increase):

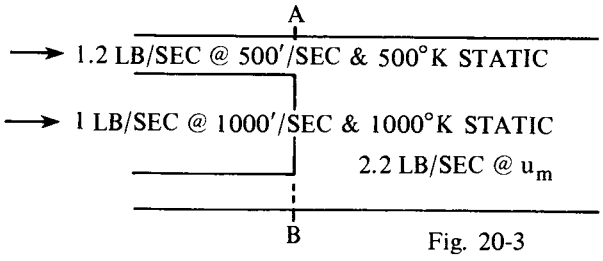

Fig. 20-3

Since there will be no change in total momentum before and after mixing

$$2.2 \times u_m = 1000 + 1.2 \times 500 \quad \therefore u_m = 727.3'/\text{sec}$$

The kinetic energy of the core stream before mixing is $\frac{1 \times 1000^2}{2g}$ and that of the annular stream is $\frac{1.2 \times 500^2}{2g}$. After mixing the total ke is $\frac{2.2}{2g} \times 727.3^2$ $\therefore$ the loss Δke is given by $\Delta ke = \frac{1}{2g}[1000^2 + 1.2 \times 500^2 - 2.2 \times 727.3^2] = 2116.1$ ft/lbs. $\therefore$ the loss per unit of total flow $= \frac{2116.1}{2.2} = 961.9$ ft/lbs, equivalent to $\frac{961.9}{336} = 2.86°$. This figure, therefore, represents the conversion of ke into internal energy per unit mass. It may be seen that there will be no great error in neglecting it in cycle calculations, as will be done later.

The pressure loss in a fluted mixing device may well be largely offset by reduced skin friction in the rear end of the jet pipe and final nozzle.

SECTION 21
Turbo Fans

Introductory

During the 1930s the writer was much concerned with the problem of increasing the propulsive efficiency of jet engines at the flight speeds which then seemed to be limited to about 500 m.p.h. owing to the high drag rise as the speed of sound was neared. It was then the general belief that the 'sound barrier' could never be passed. The writer did not share this belief and, indeed, his 1936 notebooks contained performance calculations for the straight jet up to 1500 m.p.h. which showed very clearly that efficiency could be greatly increased at supersonic speeds. (At this time the first experimental engine was under construction but had not yet been completed – its first run was not until April 12th, 1937). However, there then seemed little hope that a supersonic airplane could have a lift/drag ratio better than about 4.0 c.f. 16 or more for high/subsonic speeds. It thus seemed improbable that increase of engine efficiency could compensate for the serious drop in L/D. It would, in any event have been most unwise to have pressed the concept of jet powered supersonic aircraft in the light of the formidable wall of scepticism about the practicability of jet engines for any purpose. So the writer concentrated on the problem of improving power plant efficiency at moderate and high subsonic speeds.

It was obvious that means to 'gear down' the jet were needed, i.e. to aim for a high mass low velocity jet instead of the low mass high velocity jet of the simple jet engine.

The writer first considered the use of an ejector for the purpose but rejected this scheme when calculations showed that, though some improvement in thrust could be obtained at take off and low speed, an ejector actually reduced thrust at higher speeds. It soon became clear that mechanical means would be necessary to extract part of the energy of the jet and impart it to additional 'by-pass' air. At modest speeds the turbo-prop would have been the answer and, indeed, the Royal Aircraft Establishment was working on an axial flow gas turbine to drive a propellor in parallel with Power Jets' development of the centrifugal type jet engine. (Later, when the first experimental engine began to show real promise, the R.A.E., in co-operation with Metropolitan-Vickers, converted their turbo-prop scheme into an axial flow

jet engine—the F-2, later known as the Beryl). The writer, however, remained convinced that the propellor was not the answer for speeds of 500 m.p.h. and above, so turned his attention to the concept of using part of the gas generator output energy to drive a high mass flow low pressure compressor or 'fan'.

The primary problem was the mechanical arrangement, i.e. how to connect the fan to its driving turbine without using the two spool arrangement which, at that time, seemed to present formidable bearing, coupling and assembly problems. His first solution is shown in Figure 1 which is the principle drawing of U.K. Patent 471,368 filed in March 1936. This patent was, in fact, the master patent for all turbo fans. When it expired in 1952 it was granted the maximum allowable extension of 10 years. Even so, it expired before turbo-fans

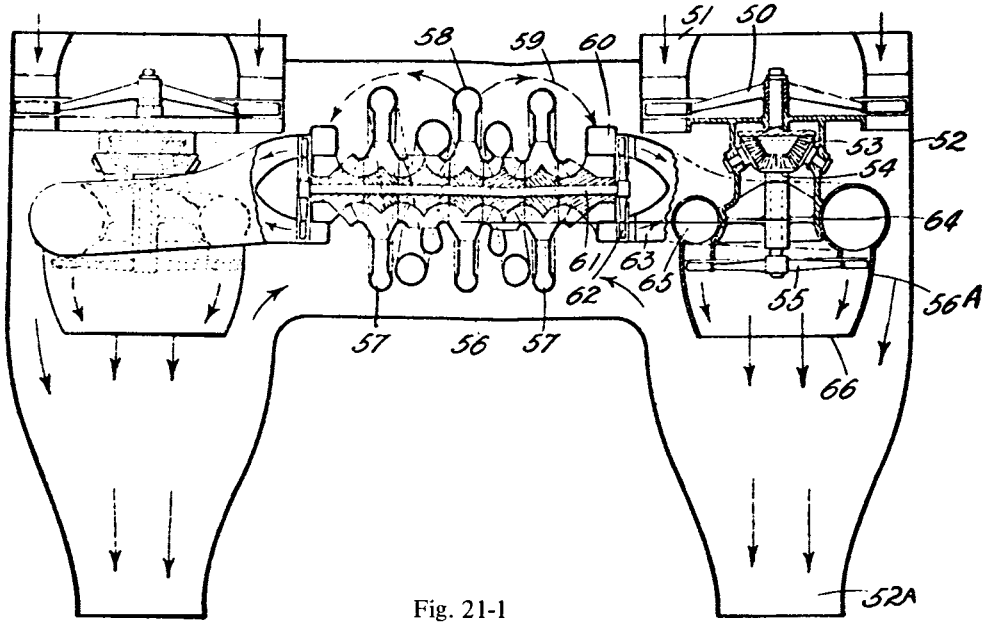

Fig. 21-1

began to supersede straight jet engines. (The Rolls-Royce Conway was going into limited production at the time but it had the very low bypass ratio of about 0.6). All modern turbo-fans fall within the first claim of this patent.

As may be seen in Figure 1, the gas generator was athwartships in a plenum chamber (56) and supplied energised gas to two turbines (55) driving fans (50) in lateral nacelles. The two fans 'supercharged' the plenum chamber as well as supplying the bypass air which rejoined the exhaust from the fan turbines before final expansion.

The gas generator is shown with two first stage centrifugal compressors (57) in parallel and a single second stage centrifugal compressor (58) all driven by two turbines (62) in parallel via combustion chambers (not shown).

No attempt was made at detail design because of pressure of work on the experimental jet engine. Moreover there was no money available for such an ambitious project.

Figure 2 shows another of the several 'tricks' proposed by the writer to circumvent threaded shafts. It is the principal drawing of U.K. Patent 593,403.

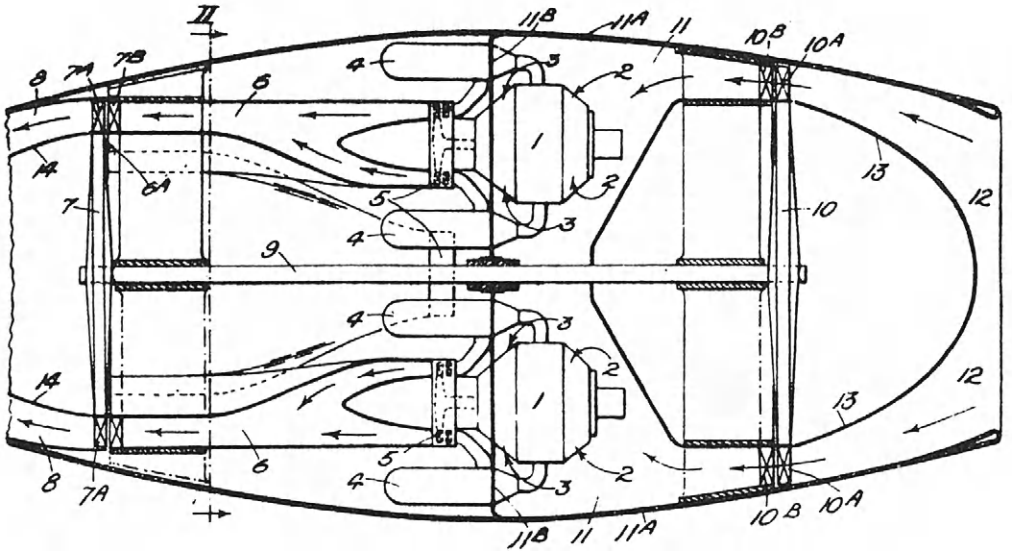

Fig. 21-2

In this arrangement three or four simple jet engines (1) were symmetrically disposed about the shaft (9) connecting the fan (10) with its driving turbine (7) driven by the energised gas from the jet engine gas generators.

This scheme also was never followed up for lack of time and money, but one might imagine that a modern form of it using axial flow type gas generators might prove interesting.

Eventually, when the simple jet had reached an advanced stage of development and was in limited production, Power Jets did start to develop a turbo-fan—the L.R.1. Unfortunately the company had been nationalised in 1944 at which time the L.R.1 was in the initial design stage. In the spring of 1946 when the L.R.1 was half built, the Company (except for a small 'rump') was merged with the R.A.E. gas turbine unit to form the National Gas Turbine Establishment. Under pressure from the aircraft industry in the U.K., which by then had been almost entirely converted to aircraft gas turbines, the Terms of Reference of the N.G.T.E precluded the design and development of engines. The functions of the N.G.T.E. were restricted to research and assisting the industry. In consequence the contracts for the L.R.1 and other projects in progress were cancelled. (This deprivation of the right to continue the work they had initiated resulted in the break-up of the greater part of the writer's very able team.)

The L.R.1, illustrated in Figure 3 very diagrammatically, also avoided the two spool arrangement. There was no mechanically independent gas generator. The power for both the main compressor (an axial flow compressor with a final centrifugal compressor stage) and the three stage fan was provided by a two stage turbine, the fan being driven through an epicyclic reduction gear.

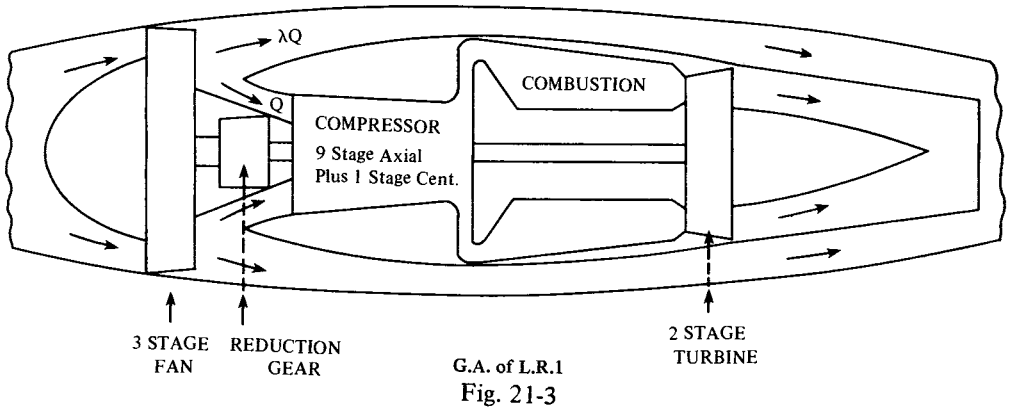

G.A. of L.R.1

Fig. 21-3

The L.R.1 was primarily intended to power a 4 engined bomber having a 4000 miles still air range with a 10,000 lb. bomb load but was also visualised as suitable for a trans-Atlantic civil aircraft. The core unit was also designed to be applicable to turbo-props and different bypass ratios by changing the gear ratio. It was, however, basically a 3.1 bypass ratio turbo fan. Its premature demise undoubtedly put back the turbo-fan era by about twenty years. (In Figures 3 and 4 λ is the bypass ratio).

Meanwhile, three years earlier, a short lived attempt was made to develop an aft fan along the lines illustrated roughly in Figure 4. At the time it was known as a 'thrust augmentor' because it was a device which could be 'tacked on' to existing jet engines without any modification to the main engine forward of the compressor turbine exhaust.

In Figure 4, (1) is the nozzle ring of the aft fan turbine (2), (3) and (4) are the rotor and stator blades of the fan. As may be seen, the fan rotor blades were formed as extension of the turbine blades but the shroud ring (5) separated the hot and cold flows.

Only one stage is shown in Figure 4, though normally two or more would be necessary—especially for the turbine component.

The first design—the No. 1 Thrust Augmentor—had no stator blading at all. It comprised a pair of contra rotating turbine-fan wheels. Seemingly the acme of simplicity, but it had to

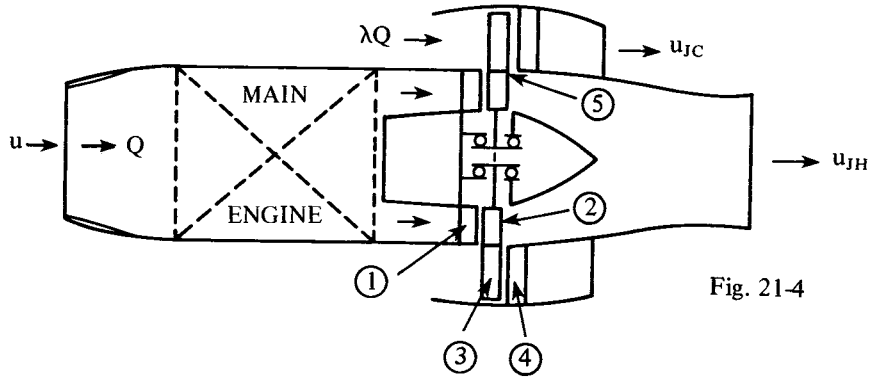

Fig. 21-4

be abandoned when detail design revealed that the necessary blade profiles and relative velocities were quite impracticable.

The second design—the No. 2 Thrust Augmentor was a more conventional two stage arrangement. It was never built by Power Jets but the drawings were shipped to the General Electric Company and became the basis of the aft fans later developed by G.E.

The aft fan, however, has several disadvantages as compared with the now conventional front fan, namely:—

1) The turbine blade speed is necessarily lower than that of the fan which is opposite from what is desirable.

2) The hot portion of the blading is the more highly stressed—again opposite from what is desirable.

3) The blades are integrally cast and so the fan blading has to be of the same material as the turbine, hence they are far heavier than they could be from the point of view of stress and temperature.

4) There is a leakage problem through the clearances. The higher pressure hot stream leaks into the fan flow thereby reducing fan efficiency.

5) There is a boundary layer 'build-up' along the core casing which also reduces fan efficiency. This can be reduced to a large extent by extending the fan inlet ducting the full length of the engine—at the expense of a substantial increase in nacelle drag.

6) The fan contributes nothing to the overall pressure ratio hence the main engine is larger than it would be if 'supercharged' by a front fan.

It would clearly be desirable to reverse the positions of the turbine and fan blades, i.e., to have the former external to the latter. This removes the first and second of the disadvantages enumerated above, but requires some very awkward ducting since the ducts carrying the hot gas supply from the main engine to the 'tip turbine' must pass through the inlet flow to the fan.

The arrangement is shown in Figure 5 which is the principal drawing of U.K. Patent 588,085.

Fig. 21-5

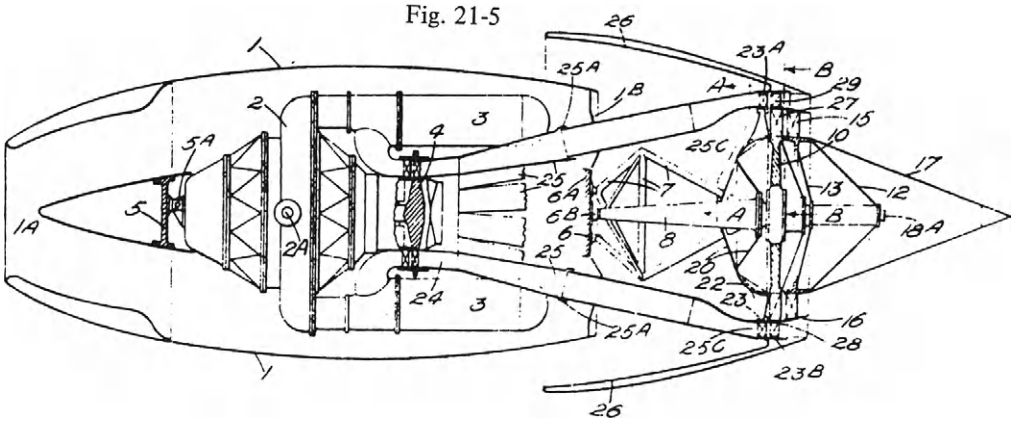

The No. 3 Thrust Augmentor designed and built by the writer and his team in 1943 was in accordance with the arrangement shown in Figure 5. On test, a 40% gain of static thrust was achieved but this was far lower than expectations because of the interference of the hot ducting with the fan inlet flow. No doubt this interference could have been greatly reduced by redesign of the gas generator ducting, but again pressure of other work ruled out further development. However, the fan with a tip turbine has shown some promise as a lift fan.

Later, as Power Jets' capacity expanded, the 'No. 4 Thrust Augmentor' was designed for addition to the Power Jets W2/700 engine. It was basically similar to the No. 2 but the scheme included after burning aft of the aft fan assembly. The purpose of the whole arrangement was to power the small Miles M52 supersonic airplane.

Again, when both power plant and aircraft were nearing completion they fell victims of the consequences of Ministry policy. The contracts were cancelled.

High Bypass Ratio Turbo-Fans

Figure 6 is a diagrammatic representation of the type of turbo-fan with high bypass ratio λ which has now largely replaced straight jet engines in subsonic aircraft.

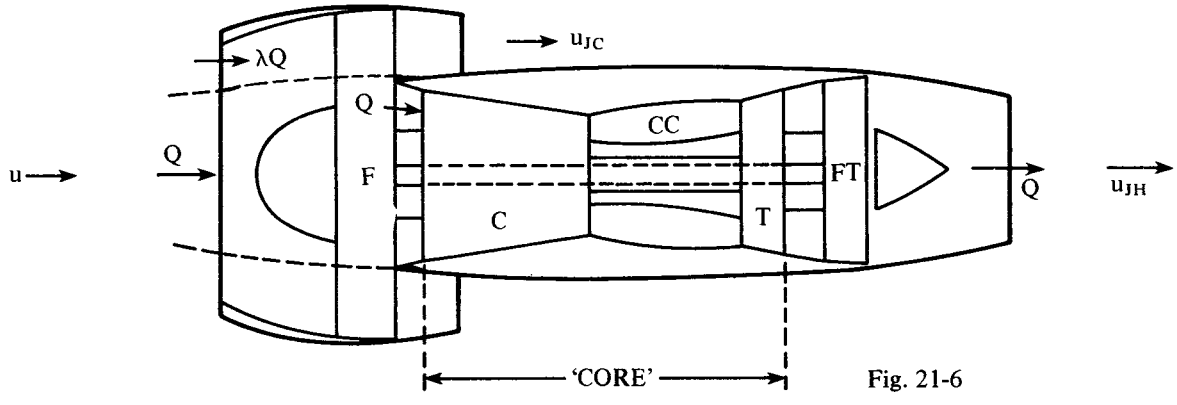

Fig. 21-6

A two spool arrangement is shown in which the shaft connecting the fan turbine FT to the fan F is threaded through the shaft of the compressor–combustion chamber–turbine unit C–CC–T which comprises the 'core engine'. The core engine itself may be a two spool assembly as in the Rolls Royce R.B. 211 which is thus a three spool engine. Another alternative arrangement is that used in the Pratt and Whitney J.T.9.D in which the core compressor has an LP section and HP section, the former being integral with the fan.

Bypass ratios have increased greatly in latter years and are now in the range 5:1 to 6:1 or more.

As indicated by the broken lines in the intake of Figure 6, part of the fan flow passes to the core compressor and thus contributes to the overall compression. Indeed, for purposes of calculation it is desirable to assume that the inner part of the fan (within the broken lines) is part of the core cycle.

If λ is the bypass ratio and the core flow is Q lb/sec. than the bypass flow is λQ and total flow is $(1 + \lambda)Q$, hence if θ_F represents the specific work done by the fan and θ_{FT} the specific work of the fan turbine, then $\theta_{FT} = (\lambda + 1)\,\theta_F$.

The specific thrust F_s is the thrust per unit core flow and is given by

$$F_s = \frac{1}{g}\,[u_{JH} - u + \lambda\,(u_{JC} - u)] \qquad (21\text{-}1)$$

u_{JC} being the 'cold jet' velocity and u_{JH} the 'hot jet' velocity.

As may be seen in Figure 6 there is no mixing of the bypass and core flows before their respective final expansions.

The bypass cycle comprises compression and expansion only. The cycle (or cycles) may be represented as in Figure 7. The displacement to the left of CE (bypass expansion) and

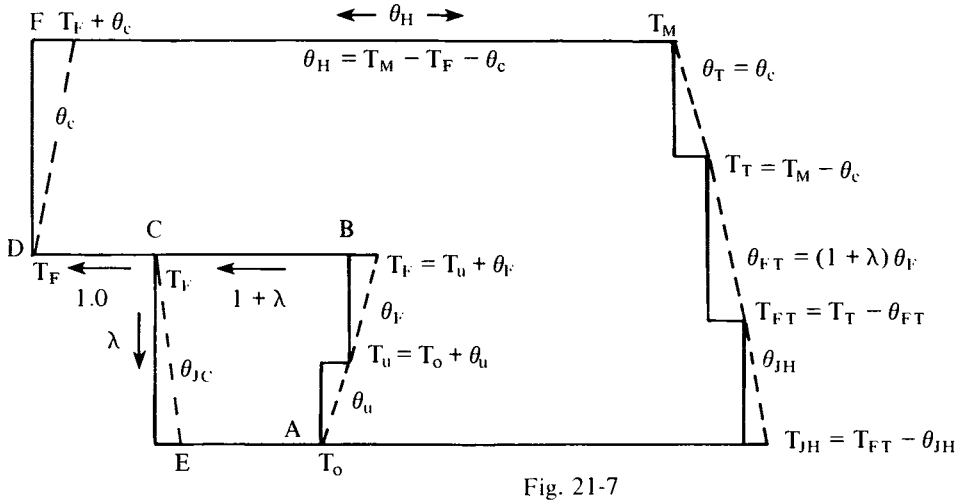

Fig. 21-7

D.F. (core compressor) as compared with A.B. (ram plus fan compression) is to indicate the different mass flows involved. T_F, the total temp. at fan discharge, is the same at B,C and D.

Alternatively the core and bypass cycles may be represented independently as in Figure 8 *as long as it is remembered that for each unit of flow in the core cycle there are* λ *units of flow in the bypass cycle.*

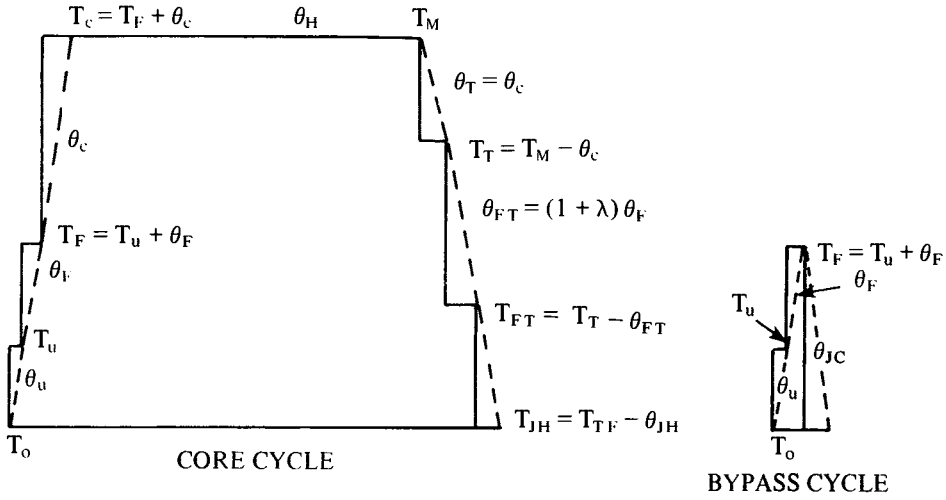

Fig. 21-8

As compared with the straight jet, the expansion efficiency is somewhat reduced, and therefore the thermal efficiency, because a much greater part of the expansion is subject to turbine losses, but this is much more than compensated for by the gain in propulsive efficiency.

Apart from the overall temp. ratio t_o there are seven temp. ratios to be taken into account, namely:—

1) Ram temp. ratio t_u given by $t_u = 1 + \dfrac{\eta_u \theta_u}{T_o}$ (21-2)

2) Fan temp. ratio t_F given by $t_F = 1 + \dfrac{\eta_F \theta_F}{T_u}$ (21-3)

3) Compressor temp. ratio t_c given by $t_c = 1 + \dfrac{\eta_c \theta_c}{T_F}$ (21-4)

4) Core Comp. Turbine temp ratio t_T given by $t_T = \dfrac{T_M}{T_M - \dfrac{\theta_c}{\eta_T}}$ (21-5)

5) Fan Turbine temp. ratio t_{TF} given by $t_{TF} = \dfrac{T_T}{T_T - \dfrac{\theta_F (1 + \lambda)}{\eta_{FT}}}$ (21-6)

6) Core Jet temp. ratio t_{JH} given by $t_{JH} = \dfrac{t_u t_F t_c}{t_T t_{TF}} \left(= \dfrac{(1) \times (2) \times (3)}{(4) \times (5)} \right)$ (21-7)

7) Bypass Jet temp. ratio t_{JC} given by $t_{JC} = t_u t_F$ $(= (1) \times (2))$ (21-8)

Other relationships between temp. ratios can be obtained by combining some of the above, thus t_T and t_c may be related by substituting for θ_c from (4) in (5) and so on.

The cold jet velocity u_{JC} is found from $u_{JC} = 147.1\sqrt{\eta_{JC} T_F \left(1 - \frac{1}{t_{JC}}\right)}$

$$\text{or} \quad u_{JC} = 147.1 \sqrt{\eta_{JC} T_F \left(1 - \frac{1}{t_u t_F}\right)} \tag{21-9}$$

and the hot jet velocity u_{JH} is found from $u_{JH} = 147.1 \sqrt{\eta_{JH} T_{TF} \left(1 - \frac{1}{t_{JH}}\right)}$

$$\text{or} \quad u_{JH} = 147.1 \sqrt{\eta_{JH} T_{TF} \left(1 - \frac{t_T t_{TF}}{t_u t_F t_c}\right)} \tag{21-10}$$

$\therefore$ Substitution for u_{JC} and u_{JH} in (1) gives

$$F_s = \frac{1}{g} \left[147.1 \left(\lambda \sqrt{\eta_{JC} T_F \left(1 - \frac{1}{t_u t_f}\right)} + \sqrt{\eta_{JH} T_{TF} \left(1 - \frac{t_T t_{FT}}{t_u t_F t_c}\right)}\right) - u(\lambda + 1)\right] \tag{21-11}$$

Though η_u, the ram efficiency, is indicated as less than unity in Figures 7 and 8 so much of the ram compression occurs ahead of the intake orifice that η_u may be taken as 1.0 with negligible error (since large bypass ratio engines are suitable only for subsonic speeds) in which case $t_u = 1 + \frac{\theta_u}{T_o}$.

The design value of the bypass ratio λ is a matter of choice for the designer. Among the factors he must take into account are:—

1) The much greater specific thrust at take-off and low speeds with high bypass ratio at the expense of a rapid fall off at high speed (of specific thrust).

2) The effect on power plant weight. The weight of the fan-fan turbine assembly is offset to some extent by the reduction in size of the core assembly but this offset is greater for low bypass ratio engines which in any case have lighter fan-fan turbine assemblies.

3) The effect on fan cowling drag.

4) The effect of the drag of the annular cold jet (which may well be supersonic) on the core casing.

Strictly speaking, the two items of drag 3) and 4) above should be deducted from engine thrust to give the true net thrust. The drag over the core casing can be much reduced by extending the length of the fan exhaust cowling but at the expense of increased drag both internally and externally of the latter. In general it pays to have a long fan exhaust duct in the case of moderate and low bypass ratios. Moreover, the higher pressure in the exhaust duct of a low bypass ratio engine makes 'duct burning' more worthwhile for thrust boosting.

Example 21-1.

Figure 9 shows the cycle for the design condition for $u = 900'$/sec. and $T_o = 221°K$ and $\lambda = 5.0$. Assumptions not shown in the diagram are:— 1) $\eta_u = 1.0$, 2) $\eta_F = .88$, 3) $\eta_c = .85$, 4) $\eta_T = .87$, 5) $\eta_{FT} = .90$, 6) $\eta_{JC} = \eta_{JH} = .98$.

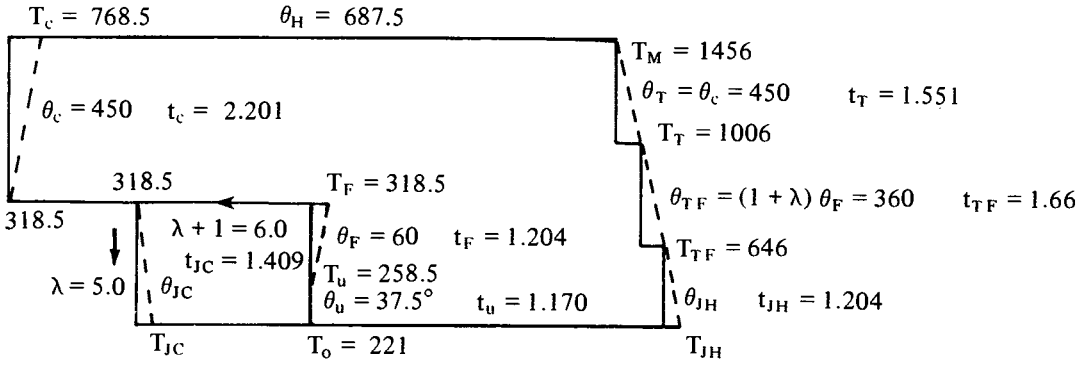

Fig. 21-9

(t_{JH} in Figure 9 from $t_{JH} = \frac{t_u t_F t_c}{t_T t_{TF}}$ and t_{JC} from $t_{JC} = t_u t_F$)

$$\theta_{JH} = 646 \times .98 \left(\frac{.204}{1.204}\right) = 107.3 \quad \therefore u_{JH} = 147.1\sqrt{107.3} = 1522.7'/\text{sec.}$$

$$\theta_{JC} = 318.5 \times .98 \left(\frac{.409}{1.409}\right) = 90.54 \quad \therefore u_{JC} = 147.1\sqrt{90.54} = 1399'/\text{sec.}$$

$$F_s = \frac{1}{g}\,(\lambda\,(1399 - 900) + 1522.7 - 900) = 96.79 \text{ secs.}$$

$$\therefore \eta_o = \frac{96.79 \times 900}{336 \times 687.5} = .377$$ (This compares with about .25 for a straight jet at the same speed).

Using the same methods and varying λ one finds the following results:–

λ	u_{JH}	u_{JH}	F_s
3	2276	1399	89.18
4	1940.2	1399	94.27
6	910.6	1399	93.27

The variation of F_s with λ for u = 900 ft/sec. is shown in Figure 10.

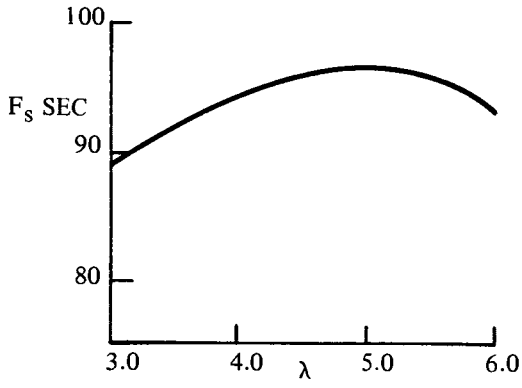

Fig. 21-10

Since the same value of θ_F was used for each value of λ it follows that u_{JC} is not affected by variation of λ though the size of the cold jet nozzle would, of course, depend very much on the choice of λ.

θ_H was also the same for each case, so peak F_s corresponds to peak overall efficiency.

As may be seen, $\lambda = 5$ is very close to the optimum and F_s is insensitive to λ in the range 4.75 – 5.25. As flight speed is reduced, the theoretical optimum value of λ increases very substantially, e.g. for a freighter designed to cruise at 400 m.p.h., it may well be of the order of 15 or more, subject to practical difficulties of weight, installation, etc.

Several years ago, the writer found a proof that the optimum value of η_o occurred when $u_{JC} = \sqrt{\eta_F \eta_{TF}}\ u_{JH}$ but the proof was very lengthy and it is not proposed to repeat it here. (It is possible that there is a much shorter proof). Thus, in Example 1, λ should have been such that $u_{JH} = \dfrac{1399}{\sqrt{.88 \times .9}} = 1572'/\text{sec.}$ whereas for $\lambda = 5$ u_{JH} was found to be 1523′/sec. approx. in Example 1, so the choice of 5 for λ was a 'very near miss'.

It may also be noted from the example that the temp. ratio across the cold jet nozzle is above the critical ratio 1.2, while the temp. ratio across the core jet nozzle is just above 1.2, so both nozzles are choking but only the cold jet justifies a con-di nozzle.

If one accepts that $u_{JH} = \dfrac{u_{JC}}{\sqrt{\eta_F \eta_{TF}}}$ then $\theta_{JH} = \dfrac{\theta_{JC}}{\eta_F \eta_{TF}}$. Using this

$$t_{JH} = \frac{T_M - \theta_c - (\lambda + 1)\,\theta_F}{T_M - \theta_c - (\lambda + 1)\,\theta_F - \dfrac{\theta_{JC}}{\eta_{JC}\eta_F\eta_T}} \qquad (21\text{-}12)$$

Using this equation in combination with equations (2), etc., and given the values of θ_u, θ_F, θ_c, T_M and the various stage efficiencies, it is possible to obtain a somewhat complicated quadratic equation for λ^*, the optimum value of λ.

Example 21-2.

What is the value of λ^* if $\theta_F = 50$ and $\theta_c = 460$ given that all other assumptions are as in Example 1?

$$t_u = 1 + \frac{37.5}{221} = 1.168 \quad \text{and} \quad T_u = 258.5$$

$$t_F = 1 + \frac{.88 \times 50}{258.5} = 1.17 \quad \text{and} \quad T_F = 308.5$$

$$t_c = 1 + \frac{.85 \times 460}{308.5} = 2.2674 \quad \therefore\ t_{JC}\,t_c = t_u\,t_F\,t_c = 3.098$$

$$t_T = \frac{1456}{1456 - \dfrac{460}{.87}} = 1.570 \quad \text{and} \quad T_T = T_M - \theta_c = 996$$

$$t_{TF} = \frac{996}{996 - \frac{(\lambda + 1)50}{.9}}$$

$$\theta_{JC} = .98 T_F \left(1 - \frac{1}{t_u t_F}\right) = .98 \times 308.5 \left(1 - \frac{1}{1.168 \times 1.17}\right) = 81.09$$

$$\therefore \text{ from (12), } \frac{3.098}{1.57\left[\frac{996}{996 - \frac{(\lambda + 1)50}{0.9}}\right]} = \frac{996 - (\lambda + 1)50}{996 - (\lambda + 1)50 - \frac{81.09}{0.98 \times 0.88 \times 0.9}}$$

which boils down to $1.862 - 0.11\lambda = \frac{946 - 50\lambda}{841.5 - 50\lambda}$ from which λ^* is found to be 6.07.

This does not, in fact, quite agree with λ^* as found from the cycle diagram which gives the following results:—

λ	u_{JC}	F_{sJC}	u_{JH}	F_{sJH}	ΣF_s	$\frac{u_{JH}}{u_{JC}}$
6.0	1326.6	79.49	1524.6	19.40	98.89	1.149
6.1	1326.6	80.81	1484	18.13	98.94	1.119
6.2	1326.6	82.13	1442	16.84	98.97	1.086
6.3	1326.6	83.46	1399	15.50	98.96	1.054

(F_{sJC} is the bypass specific thrust and F_{sJH} is the core specific thrust; each per unit core flow).

Whereas $\lambda = 6.07$ gives $\Sigma F_s = 98.93$. Clearly an insignificant difference. As the table shows, ΣF_s is very insensitive to λ and the value of $\frac{u_{JH}}{u_{JC}}$ in the neighborhood of the optimum.

As may be seen, u_{JC} is unaffected by λ for the given values of u, θ_F, η_u, η_F and η_{JC} $\therefore$ the drag over the core casing would be the same, but the fan cowling drag would, of course, increase as λ increases so that, for maximum net thrust, i.e., thrust less drag, the 'real' optimum value of λ would be somewhat less than that calculated from the cycle alone.

Example 21-3.

This example is an energy balance check on the figures of Example 1.

Referring to Figure 9, $\theta_{JC} = 90.54$ $\therefore$ $T_{JC} = 318.5 - 90.54 = 227.96$, $\therefore$ the heat rejected by the cold jet $= \lambda(227.96 - 211) = 5 \times 6.96 = 34.8$. $\theta_{JH} = 107.3$ $\therefore$ $T_{JH} = 646 - 107.3 = 538.7$ $\therefore$ the heat rejected $= 538.7 - 221 = 317.7$ $\therefore$ Total heat rejected $= 34.8 + 317.7 = 352.5$. The energy increase of the bypass flow $= \lambda(\theta_{JC} - 37.5)$ $= 5(90.54 - 37.5) = 265.2$. The energy increase of the core flow $= \theta_{JH} - 37.5 = 107.3 - 37.5$ $= 69.8$ $\therefore$ the total energy increase $= 69.8 + 265.2 = 335$. Adding this to the heat rejected we have $335 + 352.5 = 687.5$ which is equal to the heat added, which is how it should be.

Off Design Conditions

The design parameters will normally be those which are the optimum for the cruise condition, but it is necessary to examine the conditions necessary for satisfactory performance at take-off and other flight conditions, e.g., take-off, climb, 'stand off', etc.

Taking the design figures of Example 1 for θ_F, θ_c, T_M, η_F, η_c, η_T, η_{TF}, η_{JC} and η_{JH}, let us find out what the sea level static cycle/s would be. The cycle diagram is shown in Figure 11 assuming $T_o = 288°K$.

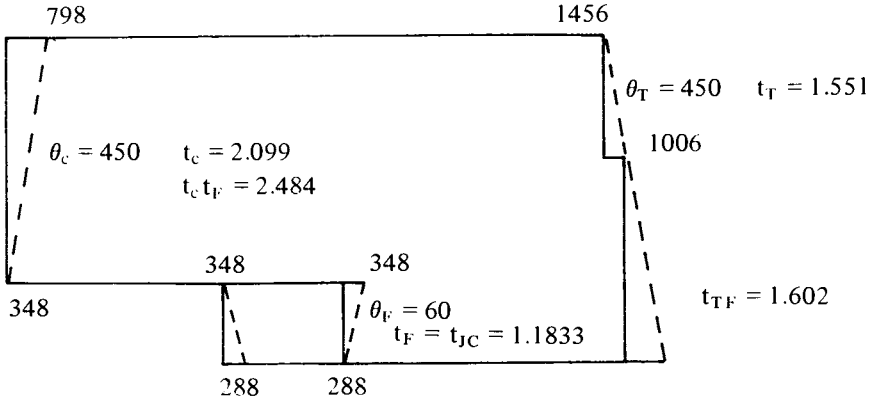

Fig. 21-11

It is found that t_{TF} cannot exceed 1.602 even if the final nozzle is opened up to the point where u_{JH} equals or is less than the axial velocity from the fan turbine.

θ_{TF} from $\dfrac{1006}{1006 - \dfrac{\theta_{TF}}{.09}} = 1.602$ is found to be 340.2°C $\therefore \lambda + 1 = \dfrac{340.2}{60} = 5.67$

$\therefore \lambda = 4.67$. Assuming that the hot exhaust energy cannot exceed 4% of θ_{TF}, $\theta_{JH} = .04 \times 340.2 = 13.6°$ which gives $u_{JH} = 147.1\sqrt{13.6} = 542.2'$/sec. which would give a thrust of 16.8 secs.

$u_{JC} = 147.1\sqrt{.98 \times 348 \times \dfrac{.1833}{1.1833}} = 1068'$/sec. to give a thrust of $33.18 \times \lambda$

i.e., $33.18 \times 4.67 = 155$, hence the total specific thrust is $155 + 16.8 = 171.8$ secs.

The cold jet velocity is nearly twice that of the hot jet which is far from the optimum ratio $\sqrt{.9 \times .88} = .89$. Moreover the reduction of λ is undesirable since it means reduced axial velocity in the fan.

For take-off, however, it is usual to allow an increase in T_M, and therefore an increase of θ_c. Let us examine the effect of increasing T_M to 1550°K for the case corresponding to the design cycle of Example 1.

As has been shown in Section 10, the condition for compressor axial velocities to match blade speeds is that the maximum cycle temp. T_M should be a constant multiple of the total temp. at core compressor entry. For the design cycle of Figure 9 (Example 1)

$\frac{T_M}{T_F} = \frac{1456}{318.5} = 4.57$ $\therefore$ T_F should be $\frac{T_M}{4.57}$ so that for $T_M = 1550°K$, $T_F = 339$

$\therefore$ θ_F (for $T_o = 288$) is reduced to $339 - 288 = 51°C$ while θ_c is increased to $\frac{1550}{1456} \times 450$ $= 479°C$. The cycle for take-off now becomes as shown in Figure 12.

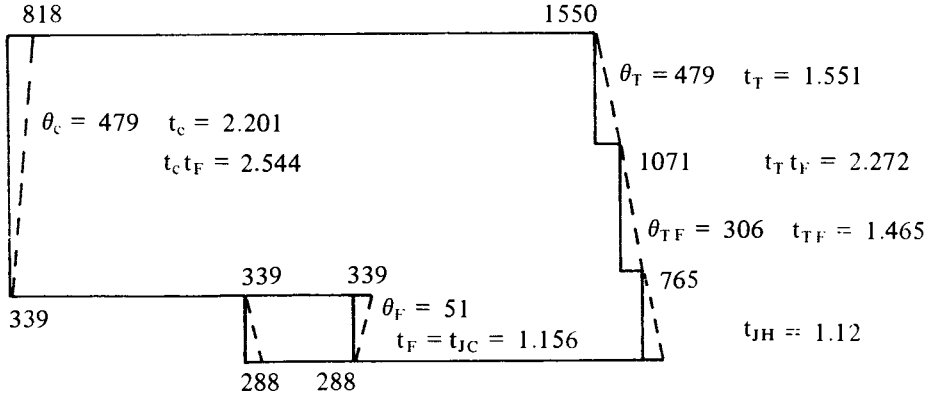

Fig. 21-12

$t_{TF} \times t_{JH} = \frac{2.544}{1.551} = 1.640$ which is still below the design value of t_{TF} (= 1.66) but if t_{JH} were to be reduced to 1.0 by opening up the final nozzle (as in the case of Figure 11) θ_{TF} would be 376.3 to give $\lambda + 1 = \frac{376.3}{51} = 7.378$ and $\lambda = 6.378$. Such a large value of λ in proportion to θ_F would be most undesirable, so let us restore λ to 5.0 to make $\theta_{TF} = 6 \times 51 = 306$ as shown in Figure 12. $t_{JH} = \frac{2.544}{2.272} = 1.12$ $\therefore$

$u_{JH} = 147.1 \sqrt{.98 \times 765 \times \frac{.12}{1.12}} = 1315.5'/\text{sec.}$ to give 40.85 secs.

For the cold jet, $u_{JC} = 147.1 \sqrt{.98 \times 339 \times \frac{156}{1.156}} = 984'/\text{sec.}$ to give

$5 \times \frac{984}{322} = 152.84$ secs. $\therefore$ Specific Thrust (per lb. of core flow) $= 152.84 + 40.85$ $= 193.7$ secs. This is a substantial increase (nearly 13%) of specific thrust as compared with the cycle of Figure 11. Moreover, on the basis that $Q \propto \frac{P_M}{\sqrt{T_M}}$, Q would be increased by 5.4% (remembering that Q is the core flow). The combined effect of the increases of specific thrust and of Q would give an overall increase of total thrust of 18.8% (for the cycle of Figure 12 as compared with that of Figure 11.)

In the discussion of axial flow compressors in Section 12 it was pointed out that an increase of axial velocity, i.e., of Q (or $1 + \lambda Q$ in the case of a bypass engine fan) reduces the work capacity but the effect was not examined. It is, in fact, quite drastic as may be seen from Figure 13 which shows the vector diagram for the exit conditions at mean radius for a design θ_F of 30°C, i.e. $\frac{u_b u_\omega}{gK_p} = 30$. As may be seen, an increase of leaving axial velocity. From 550′/sec. to 600′/sec. reduces u_ω to 186′/sec. and θ_F to $\frac{1200 \times 186}{gK_p} = 20.63°C$.

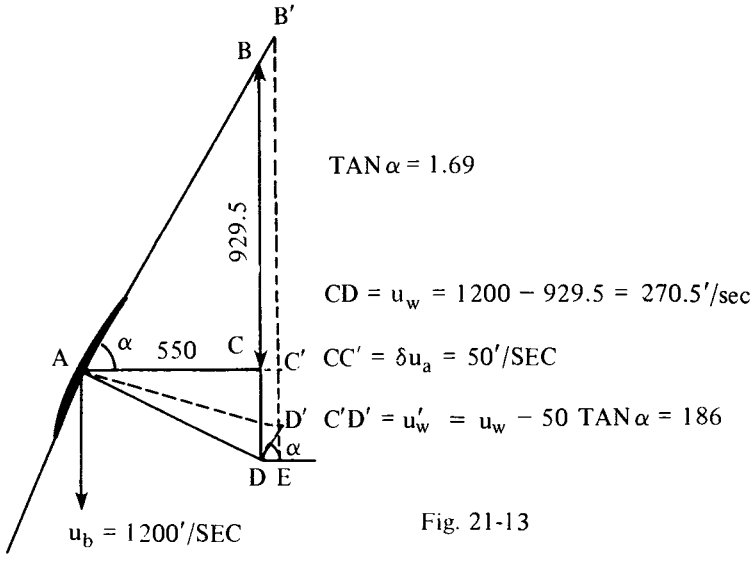

Fig. 21-13

More generally, $\delta u_\omega = -\delta u_a \tan\alpha$.

For the design condition, as has been shown in Section 12, the specific work (and therefore θ_F) can be uniform from root to tip only if the induced whirl is that of a free vortex with constant axial velocity.

Any departure from the design condition gives rise to a very complex situation. Tan α increases with r and hence the reduction of θ_F becomes greater. Indeed when $u_\omega = u_b - u_a \tan\alpha = 0$ then $\theta_F = 0$ and, since u_b also increases with r, much depends on how u_a varies with r if Q, and therefore u_a, is varied from design. The inter-relationship of u_a and u_ω in off design conditions is very complex because, as shown in Section 3, radial equilibrium requires that $2\frac{dr}{r} + \frac{d\theta_\omega}{\theta_\omega} + \frac{d\theta_a}{\theta_\omega} = 0$ (if there is no radial velocity component).

This equation may be converted to $2\frac{dr}{r} + \frac{du_\omega^2}{u_\omega^2} + \frac{du_a^2}{u_\omega^2} = 0$

$$\text{or} \quad \frac{dr}{r} + \frac{u_\omega du_\omega}{u_\omega^2} + \frac{u_a du_a}{u_\omega^2} = 0 \qquad \text{(see Equation 3-7)}$$

$$\text{or} \quad \frac{dr}{r} + \frac{du_\omega}{u_\omega} + \frac{u_a du_a}{u_\omega^2} = 0$$

By using $u_\omega = u_b - u_a \tan\alpha$ either u_ω and du_ω or u_a and du_a can be substituted to convert equation (3-7) into a differential equation connecting either r and u_ω or r and u_a. If we want to get rid of u_ω and du_ω then $du_\omega = du_b - \tan\alpha du_a - u_a d\tan\alpha$, or, since $u_b = \omega r$ and $\tan\alpha = \frac{\omega r - u_\omega}{u_a}$, with a certain amount of juggling, equation (3-7) can be converted into a complicated differential equation connecting r and u_a. It helps to note from Figure 13 that $du_a \tan\alpha = -du_\omega$.

No attempt is made here to obtain the differential equations which connect r and u_ω or r and u_a, but one can arrive at the following equation:–

$$\delta u_a = \frac{u_\omega}{u_a} \frac{(u_a \delta \tan\alpha - u_\omega \frac{\delta r}{r} - \delta u_b}{1 - \frac{u_\omega}{u_a}\tan\alpha} \qquad (21\text{-}13)$$

which, for the design blade speed, can be used to find the variation of u_a, u_ω, etc., if sufficiently small intervals of δr are chosen. Tan α, of course, is determined by design condition at each value of r.

Figure 14 illustrates the results of an iterative process applied to a case where the root

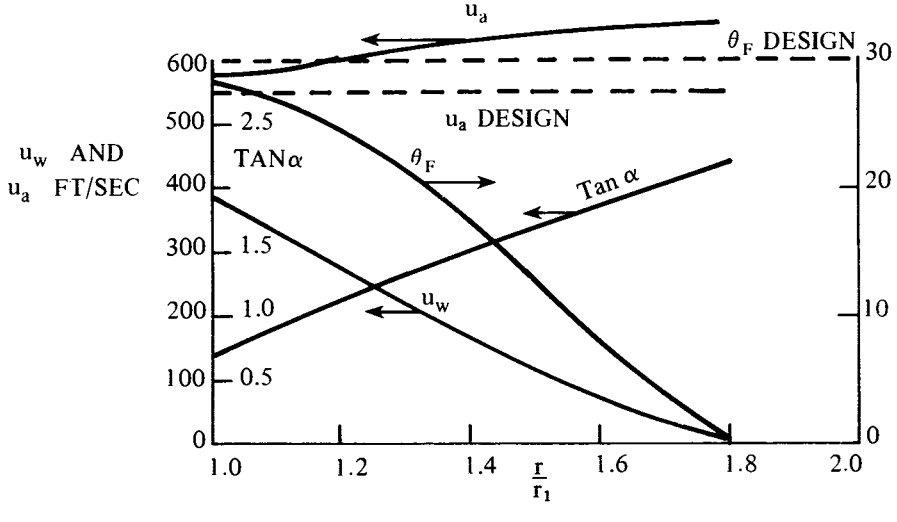

Fig. 21-14

blade speed $\left(\frac{r}{r_1} = 1.0\right)$ was 800′/sec. and the design condition was for a 30°C fan with an exhaust axial velocity of 550′/sec. at all radii; i.e. a free vortex variation of whirl velocity.

This case is somewhat extreme but possibly underestimates the effect of an increase of Q since no allowance was made for the density changes which would result from the variation of u_a and u_ω across the radius. A reduction of θ_F implies a reduction of pressure ratio and both this and the increase of u_a would reduce density, Figure 14 should therefore be regarded as very approximate, nevertheless, it illustrates the drastic effect on θ_F. As may be seen, an increase of u_a from 550′/sec. to 631′/sec. at $\frac{r}{r_1} = 1.4$ causes θ_F to fall off from 28.4° at $\frac{r}{r_1} = 1.0$ to zero at $\frac{r}{r_1} = 1.8$ approx. Beyond $\frac{r}{r_1} = 1.8$, u_ω becomes negative. i.e., the rotor would be producing torque thereby reducing the net driving torque.

Figure 14 makes no allowance for blade losses and assumes that the angle of flow at exit conforms to the blade exit angle whereas, in practice, secondary flows within the blade channel could cause some flow deviation.

An increase of u_a from 550 to 631′/sec. implies an increase of Q less than, but of the order of 14.7% which is far beyond the increase of 5.4% found for the cycle of Figure 12 as compared with that of Figure 11.

Figures 13 and 14 explain why the pressure ratio falls off so drastically with only small increase of mass flow from design, even with a single stage. The effect is 'compounded' with multi stage compressors.

In Figure 13, AD represents the angle of flow relative to the stator blade entry at design while AD′ shows the change in this which would result from increasing u_a from 550 to 600′/sec. As may be seen the change is considerable and could very well be more than enough to cause a flow breakaway within the stator blade channels and greatly reduce the pressure recovery within them.

The drastic effect of flow changes can be mitigated by using guide vanes ahead of the rotor to give a whirl in the direction of rotation at the expense of a reduction in work capacity for a given blade speed.

What about the effect of a change of speed? Fortunately, if u_a is reduced in proportion to blade speed then, neglecting the small change in density which would result, exit blade angles remain unchanged to give free vortex flow with constant axial velocity. So, if Q is closely proportional to r.p.m. the flow is compatible with design and θ_F is proportional to the square of r.p.m.

At this point it is worth pointing out that centrifugal compressors with back swept blades do not suffer from the complexities of axial flow compressors because the flow at rotor exit would be substantially uniform across the blade tips. Unfortunately their size and stress considerations prevent their use in aircraft, except, possibly, as the final stage of a compound compressor.

Reverting to the design case of Example 1 and Figure 9, and remembering that for 'correct' core compressor flow T_M should be a constant multiple of the total temp. at compressor entry ($= T_F$) then $\frac{T_M}{T_F}$ should be constant, i.e., since $T_F = T_o + \theta_u + \theta_F$, $\frac{T_M}{T_o + \theta_u + \theta_F}$ should be constant.

Thus, in Example 1, $\frac{1{,}456}{318.5} = 4.57$ $\therefore$ the core compressor would be suited to all flight conditions with $T_m = 1{,}456$ if $\frac{1{,}456}{T_o + \theta_u + \theta_F} = 4.57$. e.g., for a speed of 600'/sec. ($\theta_u = 16.7$) at a height where $T_o = 248°K$ (about 20,000') then $T_o + \theta_u + \theta_F$ should be 318.5 $\therefore$ $\theta_F = 318.5 - 16.7 - 248 = 53.8°$. This implies that the fan speed should be $\sqrt{\frac{53.8}{60}} \times$ design, i.e., 95% of design r.p.m.

Referring to the cycle of Figure 12, it will be noted that the temp. ratio across the final nozzle t_{JH} is well below the critical ratio 1.2 so there is no thermodynamic lock since the final nozzle is not choking. The same is true for moderate speeds and heights. Thus, in the immediately preceding case of $u = 600'$/sec. $T_o = 248°K$ and $\theta_F = 53.8$ and with $\lambda = 5.0$, t_{JH} works out at 1.149.

We have now reached the point where it is possible to calculate the full performance of an aircraft designed to cruise at maximum lift drag ratio in the stratosphere and powered by high bypass ratio turbo-fans. This lengthy process will not be attempted here, but a number of points which must be borne in mind are as follows:–

1) For take-off and initial climb, T_M may be allowed to be higher than for continuous climb and cruise.

2) On the climb the indicated air speed may be limited by gust load considerations (400 knots I.A.S. in the case of Concorde up to about 30,000').

3) Fuel consumed on the climb decreases the weight (as it also does for cruise).

4) The height gained on climb is a gain of potential energy which will be partially recovered on descent. ("partially" because of weight reduction by the fuel consumed).

5) The form drag is proportional to I.A.S. and the induced drag (or 'lift drag') is inversely proportional to I.A.S. for subsonic aircraft.

6) The optimum rate of climb (subject to the above mentioned gust load limitations) is that which yields the best m.p.g. taking into account that the potential energy gained on the climb is partially recoverable on descent.

7) The fuel required for stand off and/or diversion, i.e., reserve fuel, depends to a large extent on air traffic control requirements which are rarely of the kind best suited to the aircraft.

8) Fuel must be allowed for taxiing and awaiting clearance for take-off (which can be quite lengthy if, due to weather and other things, there is a large number in line at and near the runway threshold. On more than one occasion the writer has been a passenger when the airplane had to return to take on more fuel after an excessively long delay. One would expect

that this sort of thing may one day be a thing of the past with improvements in airport layouts and ground control).

9) The slow climb during cruise as fuel is consumed, needed for optimum range, may not be allowed by air traffic control regulations. (Fortunately this restriction–so far– does not apply to S.S.T.s flying well above the main traffic lanes).

10) Headwinds and/or the longer flight path of 'weather pattern' flying must be allowed for. (Again S.S.T.s are less 'vulnerable' to these sources of extra fuel consumption).

For the engine to be consistent with design at flight speeds and heights other than those on which the design is based and operating at design T_M, the following rules apply:–

1) θ_c = constant = that for design *if the compressor turbine is choking.*

2) t_T = constant = that for design (which follows from 1).

3) $\frac{T_M}{T_F}$ = constant *if the cold nozzle is choking.*

4) $(\lambda + 1)\frac{Q}{N_F}$ = constant (where N_F = fan r.p.m.)

5) Subject to 4) λ should be such that $u_{JC} = \sqrt{\eta_F \eta_c}$ approx.

As has been shown there are conditions where rules 1–5 cannot simultaneously apply, e.g., take-off and initial climb where it is desirable to increase T_M. If T_M is different from design then the following additional rules apply:–

6) $\frac{T_M}{\theta_c}$ = constant = that for design *if the compressor turbine is choking.*

7) t_T = constant = that for design (which follows from 6).

Though it is not proposed to attempt a full set of performance calculations, it seems desirable to illustrate the application of the foregoing rules. For this purpose the design cycle of Example 1 will be taken for an engine to produce 10,000 lbs. thrust for an aircraft cruising at a lift/drag ratio of 18 (i.e., the weight per engine = 180,000 lbs.) at a height where the atmospheric pressure is 392 p.s.f. (about 40,000′).

To avoid reference back, the following figures from the example are repeated as follows:–
u = 900′/sec. (θ_u = 37.5°C); T_o = 221°K;

For the ram compression η_u = 1.0, t_u = 1.170 and T_u = 258.5

For the fan:– θ_F = 60°, t_f = 1.204, T_F = 318.5, η_F = .88 and $\lambda + 1$ = 6.0

For the core compressor:– θ_c = 450, t_c = 2.201, T_c = 768.5 and η_c = .85

For the core compressor turbine:– T_M = 1456 θ_T = 450°C, t_T = 1.551 and η_T = .87

For the fan turbine:– T_T = 1006, θ_{TF} = 360°C t_{TF} = 1.66 and η_{TF} = .9

For the hot jet:– T_{TF} = 646°K, θ_{JH} = 107.3, t_{JH} = 1.204, u_{JH} = 1522.7′/sec. and η_{JH} = .98

For the cold jet:– $T_F = 318.5$, $\theta_{JC} = 90.5$, $t_{JC} = 1.409$, $u_{JC} = 1399'$/sec. and $\eta_{JC} = .98$

These figures gave $F_s = 96.79$ secs. (per unit core flow).

For the purpose of the following examples some further assumptions are necessary, namely 1) at entry to the fan the axial velocity $u_a = 550'$/sec.

2) after descent to 5000′ (after the end of cruise) the aircraft weight is 70% of that at beginning of cruise, i.e., $.7 \times 180{,}000 = 126{,}000$ lb/engine

3) at 5000′, $T_o = 278°K$ and atmospheric pressure = 1,761 p.s.f.

We also need to know:– 4) Q for the design condition, 5) the annulus area S at fan entry, 6) the overall pressure ratio for the design condition.

For 4) $Q = \frac{10{,}000}{96.79} = 103.1$ $\therefore$ the fan flow $= 6 \times 103.1 = 618.7$ lb/sec.

For 5) the atmospheric density $\rho_o = \frac{392}{96 \times 221} = .01848$; the temp. equivalent of 550′/sec. = 14°C $\therefore$ density ρ_a at fan entry $= \left(\frac{T_u - 14}{T_u}\right)^{2.5} \times .01848 \times \left(\frac{T_u}{T_o}\right)^{2.5}$

$\therefore \rho_a = \left(\frac{258.5 - 14}{221}\right)^{2.5} \times .01848 = .0238$ $\therefore S = \frac{(\lambda+1)Q}{u_a \rho_a} = \frac{618.7}{.0238 \times 550} = 47.3 \text{ ft}^2$

For 6) the overall pressure-ratio $p = (t_u t_F t_c)^{3.5} = (1.17 \times 1.204 \times 2.201)^{3.5} = 52.48$

For the calculation of drag we assume that maximum lift/drag-ratio occurs when form drag equals induced (i.e. lift) drag and that form drag is proportional to ρu^2 and induced drag is inversely proportional to ρu^2 (neglecting high Mach No. increase of form drag)

i.e. $D = k_1 \rho u^2 + \frac{k_2}{\rho u_2}$. For the design condition assumed, $k_1 \rho u_2 = \frac{k_2}{\rho u^2} = 5000$ lb

and $\rho u^2 = .01848 \times 900^2 = 14{,}969$, $\therefore k_1 = \frac{5{,}000}{14{,}969} = .334$ and $k_2 = 5{,}000 \times 14{,}969 =$

74.845×10^6 $\therefore D = .334 \rho u^2 + \frac{74.845 \times 10^6}{\rho u^2}$ (flight at speeds less than max L/D is 'unstable' in the sense that any drop in speed results in increased drag which causes a further drop in speed. This difficulty, however, can be avoided when necessary by the use of spoilers, wing flaps, etc.).

Example 21.4.

What should be the engine cycle conditions for steady cruise at 500′/sec. air speed at a height of 5000′, using the assumptions, etc. from above?

The answer to this could be dealt with by tabulation, but the writer feels that the reader will find it easier to follow by cycle diagrams.

At 5000′, $\rho = \frac{1761}{96 \times 278} = .066$ and at 500′/sec. $\rho u^2 = 16{,}500$

$\therefore D = .334 \times 16{,}500 + \frac{78.845 \times 10^6}{16{,}500} = 5{,}511 + 4{,}778 = 10{,}289$ lbs. (thus, as the induced drag component is the smaller, 500′/sec. is higher than minimum drag speed).

Case 1. $T_M = 1456$. This being the same as design, T_F should also be the same, i.e., $T_F = 318.5$. $\theta_u = \left(\frac{500}{147}\right)^2 = 11.6°C$ $\therefore T_u = 278 + 11.6 = 289.6°K$ so $\theta_F = T_F - T_u = 318.5 - 289.6 = 28.9°C$.

The cycle becomes as shown in Fig. 15.

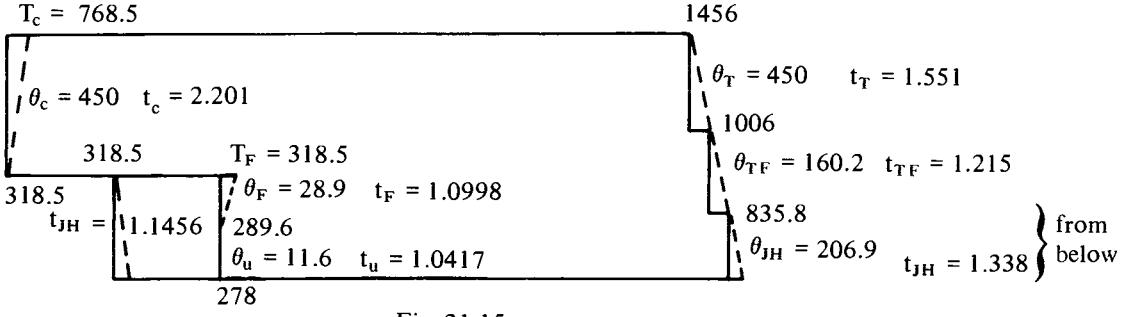

Fig. 21-15

The overall temp. ratio = 1.0417 × 1.0998 × 2.201 = 2.5214 ∴ pressure ratio = 25.45

∴ since T_M is unchanged, $Q = \frac{p_o}{p_{oD}} \times \frac{25.45}{52.48} \times Q_D$. At 5,000′, p_o = 1,761 p.s.f.

$\therefore Q = \frac{1761}{392} \times \frac{25.45}{52.48} \times 103.1 = 224.6$ lb/sec.

θ_F having dropped from 60° to 28.9°, the fan speed should reduced in the ratio $\sqrt{\frac{28.9}{60}} = .694$ ∴ the axial velocity u_a should be .694 × 550 = 382′/sec. for which $\theta_{ua} = \left(\frac{382}{147}\right)^2 = 6.74°C$ ∴ $\rho_a = \left(\frac{289.6 - 6.74}{278}\right)^{2.5} \times \rho_o = 1.0443\,\rho_o$

At 5,000′, $\rho_o = \frac{1{,}761}{96 \times 278} = .066$ ∴ $\rho_a = .069$ ∴ $(\lambda + 1)Q = \rho_a u_a S = .069 \times 382 \times 47.3 = 1{,}245$ and, since Q = 224.6, $\lambda + 1 = \frac{1{,}245}{224.6} = 5.54$. Hence $\theta_{TF} = 5.54 \times 28.9 = 160.2$

and $t_{TF} = \dfrac{1{,}006}{1{,}006 - \dfrac{160.2}{9}} = 1.215 \quad \therefore \quad t_{JH} = \dfrac{t_u t_F t_c}{t_T t_{FT}} = \dfrac{1.0417 \times 1.0998 \times 2.201}{1.551 \times 1.215} = 1.338$

from which $\theta_{JH} = .98 \times 835.8 \left(\dfrac{.338}{1.338}\right) = 206.9°\,C, \quad \therefore \quad u_{JH} = 147\sqrt{206.9} = 2{,}114.5'/sec$

$$\theta_{JC} = 318.5 \times .98 \left(\frac{.1456}{1.1456}\right) = 39.7°C, \quad \therefore$$

$u_{JC} = 147\sqrt{39.7} = 925.9'/sec.$

$F_s = \dfrac{1}{g}\,[\lambda \times (925.9 - 500) + 2114.5 - 500]$ which, since $\lambda = 4.54$, gives $F_s = 110.2$ secs.

$\therefore$ Thrust $= QF_s = 224.6 \times 110.2 = 24{,}748$ lbs.

This is well over twice the drag (= 10,289) so the aircraft would climb or accelerate or both.

As may be seen, the ratio $\dfrac{u_{JC}}{u_{JH}} = \dfrac{925.9}{2114.5} = .438$ is well below the optimum $\sqrt{.9 \times .88} = .89$. Moreover the hot jet nozzle is choking which means that θ_{TF} should be the same as design which isn't possible (inter alia, the products of the turbine temp. ratios would exceed the overall temp. ratio of 2.521). The cycle of Figure 15 just doesn't 'fit'. The difficulty is much as for the take-off cycle.

Obviously the matching becomes more difficult if T_M is reduced in order to reduce thrust, since, for satisfactory core compressor operation, T_F must be reduced in proportion to T_M if the core compressor turbine is choking which in turn means a further reduction of θ_F.

What are the alternatives, or combination of alternatives, by means of which one may 'escape' the obstacles to level and steady cruise at 500'/sec. at 5,000'?

They are one or more of the following:–

1) Spoilers and/or flaps may be used to increase the drag.

2) Core compressor efficiency can be reduced by operating well down the pressure ratio–mass flow parameter characteristic thus reducing overall pressure ratio and therefore Q.

3) λ may be increased by opening up the final nozzle–at the expense of fan efficiency.

4) The link between T_M and T_F may be broken by using a core compressor turbine which is non-choking, i.e., has two or more stages in which there is no choking in either nozzle or rotor blades.

5) Ditto for the fan turbine.

6) The use of variable intake guide vanes (i.e. stator blades) ahead of the fan first stage rotor to reduce the work capacity of the fan without seriously affecting its efficiency.

7) The use of a two spool core compressor with the first stage coupled to the fan (as in the J.T. 9D).

8) The use of a two spool core compressor mechanically independent of the fan, i.e., a three spool engine (as in the R–R R.B.211).

9) The bypassing of a portion of the core compressor delivery so that the mass flow rate in expansion is less than Q. i.e. using a high pressure bypass in addition to the low pressure bypass. ('Bleeding' the core compressor to provide turbine blade cooling is a step in this direction, but becomes less necessary for reduced T_M).

Of these alternatives, 1), 2), and 3) are very undesirable on the grounds of excessive fuel consumption. 9) is also undesirable for the same reason plus the considerable mechanical complication it would entail.

Of the remaining five, various combinations need to be considered. In the writer's opinion, 6) i.e., the use of variable intake guide vanes, is the best single method whether or not one or more of 4), 5), 7) and 8) are also used.

Intake guide vanes (again in the writer's opinion) are desirable as at least a partial protection against bird strikes—one of the most common hazards, especially at take-off and landing. Their use is often opposed on the grounds of fan noise due to the 'siren effect' as rotor blades pass through their wakes, and the need for anti-icing means.

Strictly speaking, for the energy increase to be uniform from root to tip, the intake guide vanes should be shaped for free vortex flow in the direction of rotor rotation so as to give a constant value of $u_b \times \Delta u_\omega$ but this refinement is scarcely necessary. Variable intake guide vanes are so potent in reducing work capacity that the deflection needed is very small. For example, a 30° fan with a mean u_b of 1200'/sec. must produce a whirl of

$\frac{30 \times 336 \times 32.2}{1200} = 270.5'/\text{sec.}$ at mean radius without inlet guide vanes. If it is desired to reduce θ_F to 20° then $\frac{\Delta u_\omega \times 1{,}200}{32.2 \times 336} = 20$ from which $\Delta u_\omega = 189.3'/\text{sec.}$ Thus, the inlet guide vanes must generate a pre-whirl of $270.5 - 180.3 = 90.2'/\text{sec.}$ at mean radius. With an axial velocity of, say, 550'/sec. the exit angle (of the guide vanes) is $\tan^{-1} \frac{90.2}{550} = 9.3°$. At this small angle a constant angle produces a whirl very little different from a free vortex. It is found that over a radius range of 1 to 2 (root to tip) the variation in θ_F is about from 20.1° at the root to 19.96 at the tip.

The writer has not examined the matter but there *might* be a case for having guide vane exit angles which would generate a whirl greater than that of a free vortex at the root and less at the tip so that the fall off of θ_F from root to tip with increase of Q, i.e., of axial velocity would be far less drastic than the sort of thing illustrated in Figure 14. On the other hand, any variation in θ_F must take the form of a variation in axial velocity with axial discharge from the first stage stators. Thus the increased axial velocity, at the root at entry to a second stage, would reduce θ_F at the root of the second stage so that the distribution of θ_F in the second stage would tend, to some extent at least, to compensate for the distribution of θ_F for the first stage.

Case 2. Having got nowhere in Case 1 in meeting the requirements for steady cruise at 500'/sec. at 5000', beyond demonstrating that the result is unsatisfactory if the design cycle of Example 1 has the built-in 'locks' between T_M and T_F, between T_F and T_u, etc., it is now necessary to look at the problem with those locks avoided by one or more of the methods discussed in Case 1.

Referring to the design cycle of Example 1 and the cycle of Figure 9 it may be seen that choking in the compressor turbine is unavoidable in a single stage turbine with an energy drop equivalent to 450°C. A single stage turbine *could* be designed for this having a large residual whirl after the rotor which contributed to the power of the fan turbine, but only at the expense of choking in the rotor blading, whether or not there was choking in the nozzle blading. It is therefore clearly desirable to use a multi-stage core compressor turbine, in which there is no choking either in nozzle or rotor blading. The same applies even more to the fan turbine with its design temp. ratio of 1.66 which is, in fact, greater than that of the core compressor turbine (t_T = 1.551). Having regard to the fact that the choking velocity is proportional to the square root of the total temperature relative to the blading, even a two stage turbine would probably be marginal from the choking point of view for a specific energy drop equivalent to 450°C. Without examining the matter in detail, the writer suspects that the blade speed necessary to avoid choking would be excessive and the blading and rotor disc would be overstressed.

With three stage core compressor and fan turbines, choking can be avoided in all stators and rotors and the design becomes much more 'flexible', especially as there are no serious problems in providing variable jet nozzles for both the core and bypass jets.

After two quick 'tryouts' it is found that the cycle of Figure 16 meets the requirement specified, namely a thrust of 10,290 lbs. at 500'/sec. at 5000'.

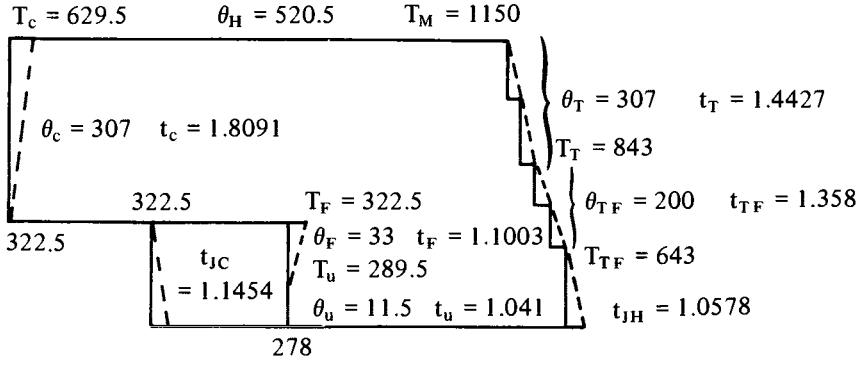

Fig. 21-16

For the cycle of Figure 16 the same component efficiencies as those in Example 1 were used, namely:— η_u 1.00, η_F = .88, η_c = .85, η_T (for the two stages) = .87, η_{TF} (for the two stages) = .9, $\eta_{JH} = \eta_{JC}$ = .98.

$\lambda + 1 = \frac{\theta_{TF}}{\theta_F}$ so λ is seen to be 5.061

From θ_{JH} = .98 X 643 $\left(\frac{.0578}{1.0578}\right)$, θ_{JH} = 34.4 $\therefore$ u_{JH} = 147.1 $\sqrt{34.4}$ = 863'/sec.

From θ_{JC} = .98 X 322.5 $\left(\frac{.1454}{1.1454}\right)$, θ_{JC} = 40.1 $\therefore$ u_{JC} = 147.1 $\sqrt{40.1}$ = 931.7'/sec.

$$\therefore\ F_s = \frac{1}{g}\ [\lambda(931.7 - 500) + 863 - 500] \text{ and, for } \lambda = 5.061,\ F_s = 79 \text{ secs.}$$

The pressure ratio of the design cycle was 52.48; the pressure ratio for the cycle of Figure 16 is given by $p = (t_u t_F t_c)^{3.5} = (1.041 \times 1.1003 \times 1.8091)^{3.5} = 12.81$.

The atmospheric pressure for the design cycle (P_{oD}) was 392 p.s.f. and P_o for 5,000′ is 1,761 p.s.f. $\therefore \frac{p P_o}{p_D P_{oD}} = \frac{P_{max}}{P_{maxD}} = \frac{12.81}{52.48} \times \frac{1761}{392} = 1.0966$, i.e. the cycle of Figure 16 at 5,000′ has virtually the same maximum pressure as the design cycle at 40,000′.

If one may assume that one of the temp. ratios in expansion is sufficiently near the choking value of 1.2 so that $Q \propto \frac{P_{max}}{\sqrt{T_M}}$ then $\frac{Q}{Q_D} = \frac{P_{max}}{P_{maxD}} \sqrt{\frac{T_{MD}}{T_M}} = 1.0966 \sqrt{\frac{1,456}{1,150}} = 1.234$

Q_D for the design cycle was found to be 103.1 lb/sec/lb of core flow $\therefore$ for this case $Q = 1.234 \times 103.1 = 127.2$ lb/sec. $\therefore$ Thrust $= QF_s = 127.2 \times 79 = 10{,}050$ lbs.

This is a little short of the required 10,290 but is near enough considering the element of uncertainty in the assumptions, especially in the case of Q which, in practice, would be somewhat greater with the temperature ratios indicated in Figure 16 for two 2 stage turbines in series.

The cycle of Figure 16 is not necessarily the optimum for the conditions. For example, the hot jet velocity u_{JH} is lower than the cold jet velocity u_{JC} whereas it should be higher.

The overall efficiency η_o is given by $\frac{F_s u}{K_p \theta_H}$ $\therefore \eta_o = \frac{79 \times 500}{336 \times 520.5} = .226$, which is very reasonable for the low speed and height. It could probably be improved by juggling with θ_F, θ_c, λ and T_M but not by any significant amount. In any event the flight condition corresponds to flight in a holding pattern pending landing clearance. For diversion to an alternate airfield it would pay (subject to air traffic control) to open up and climb for approximately half the distance.

A further look at Figure 16 indicates that fan speed would be 74% of design and core assembly speed about 83% of design (N being approx. proportional to $\sqrt{\theta}$) while the reduction of volumetric flow is greater. Variable stators for both fan and core compressor would assist in obtaining better matching between blade speeds and mass flow rate. A full investigation into this would require a knowledge of fan and core compressor characteristics for which testing would be necessary. In all probability it would be found necessary to run at points on the characteristics well below those for optimum efficiency of fan and core compressor. To that extent the cycle of Figure 16 is altogether too optimistic.

Low Bypass Turbo Fans with Exhaust Mixing

This type of engine, illustrated diagrammatically in Figure 17, is likely to become of great importance for S.S.T.s and other supersonic aircraft flying at Mach Nos. up to about 2.5 (above which 'straight' jets and even ram jets begin to be competitive except for take-off, acceleration and climb).

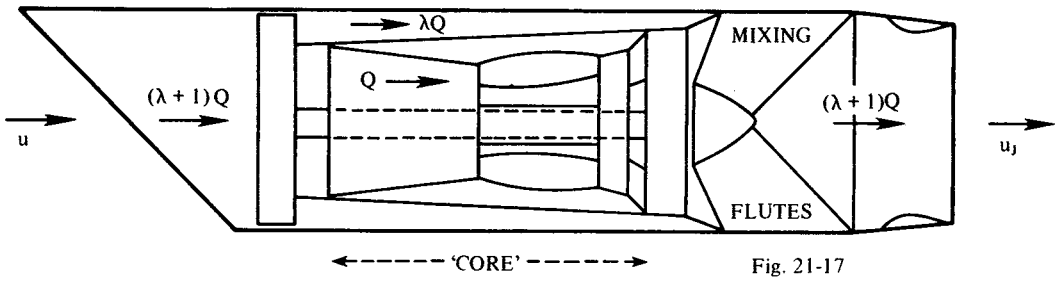

Fig. 21-17

The core engine is much the same as for the high bypass engine, but the bypass flow λQ rejoins and mixes with the core flow immediately aft of the fan turbine instead of discharging through an independent 'cold' nozzle.

It follows that the static pressures of the bypass and core flows must be equal, or very nearly equal, at exhaust from the fan turbine.

In deciding on the value of λ, the designer must weigh the 'pros and cons' of several factors including:–

1) effect on wave drag
2) effect on nacelle skin friction
3) effect on power plant weight
4) the effectiveness of mixing.

In theory, neglecting nacelle drag, etc., the efficiency of any turbo-fan engine would benefit by mixing the core and bypass flows before final expansion, but, in practice, adequate mixing becomes increasingly difficult with increase of λ.

The cycle diagram for this type of engine is shown in Figure 18.

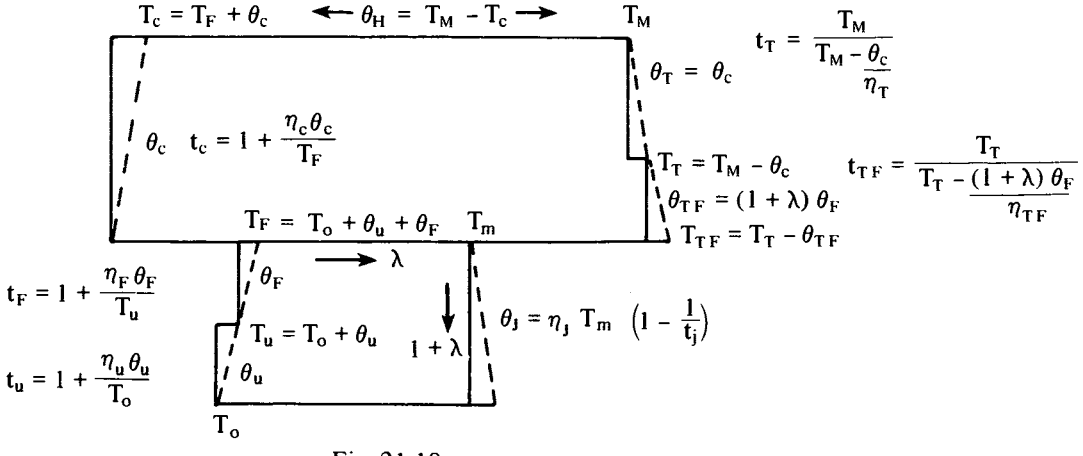

Fig. 21-18

The constant pressure line through T_F to T_{TF} is a total pressure line. More accurately it should be a static pressure line, but the final temp. ratio t_j is so high at supersonic speeds that any error due to this inaccuracy is found to be negligible in relation to other assumptions.

In this compound cycle, as before, λ is the bypass ratio and T_m (not to be confused with T_M) is the total temp. after mixing of the bypass and core flows.

In addition to the relationships shown in the diagram, several others may readily be seen, e.g.:–

$$T_m = \frac{\lambda T_F + T_{TF}}{\lambda + 1} \tag{21-14}$$

$$t_j = t_u t_F \tag{21-15}$$

$$t_c = t_T t_{TF} \quad \text{or} \quad t_{TF} = \frac{t_c}{t_T} \tag{21-16}$$

From Equation (16) and Figure 18 it may be seen that

$$\frac{T_T}{T_T - \frac{(1+\lambda)\theta_F}{\eta_F}} = \left(\frac{T_M - \frac{\theta_c}{\eta_T}}{T_M}\right)\left(1 + \frac{\eta_c \theta_c}{T_u + \theta_F}\right)$$

or

$$\frac{1}{1 - \frac{(1+\lambda)\theta_F}{\eta_F T_T}} = \left(1 - \frac{\theta_c}{\eta_T T_M}\right)\left(1 + \frac{\eta_c \theta_c}{T_u + \theta_F}\right) \tag{21-17}$$

From (17), if T_u (i.e. $T_o + \theta_u$), θ_c, T_M and the various efficiencies are known, θ_F may be found if λ is predetermined and vice versa. If λ is given, θ_F can be found as the solution of a somewhat untidy quadratic, but if θ_F is given, λ is readily calculated as indicated in the table below for u = 2,200'/sec. (i.e. θ_u = 223.7) T_o = 220°K; T_M = 1650°K; θ_c = 450°C; η_u = .95; η_F = .88; η_c = .85; η_T = .87 and η_{FT} = .89.

From this data $\frac{1}{t_T}$ = 0.687; T_T = 1200°K and T_u = 443.7°K.

θ_F	T_F	t_c	t_{TF}	θ_{FT}	$\lambda+1$	λ
60	503.7	1.759	1.209	184.4	3.07	2.07
70	513.7	1.745	1.199	176.9	2.53	1.53
80	523.7	1.730	1.189	169.6	2.12	1.12
90	533.7	1.717	1.179	162.4	1.80	0.80

As may be seen, λ drops very rapidly with increase of θ_F. (It is desirable to obtain a relationship between θ_F and λ in any case).

An example of a cycle for θ_F = 83°C using the values of u, θ_c, T_M, etc. given above is shown in Figure 19.

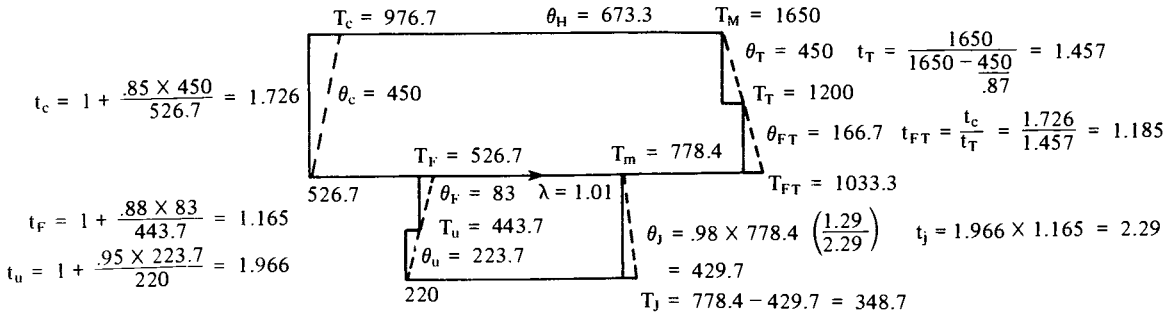

Fig. 21-19

It will be noted that Figure 19 includes the additional assumption that $\eta_J = .98$.

$\lambda = 1.01$ is obtained from $\theta_{FT} = (\lambda + 1)\,\theta_F$ i.e. $\lambda + 1 = \frac{166.7}{83} = 2.01$

T_m is obtained from $\frac{1.01 \times 526.7 + 1{,}033.3}{2.01} = 778.4$

t_J is obtained from $t_j = t_u t_F = 1.966 \times 1.165 = 2.290$

Heat balance check:– The jet energy equivalent $= \theta_J \times 2.01 = 863.7$
The ram energy equivalent $= \theta_u \times 2.01 = 449.6$

$\therefore$ the equivalent of the energy increase is $863.7 - 449.6 = 414.1$

The equivalent of the heat rejected is $2.01\,(348.7 - 220) = 258.7$

$414.1 + 258.7 = 672.8$ c.f. $\theta_H = 673.3$. The agreement would have been exact if a greater number of significant figures had been used.

The jet velocity $u_J = 147.1\sqrt{429.7} = 3{,}049'$/sec. $\therefore$ the specific thrust (per lb/sec of core flow) $F_s = \frac{2.01}{g}(3{,}049 - 220) = 53$ secs.

Overall efficiency $\eta_o = \frac{F_s u}{K_p \theta_H} = \frac{53 \times 2{,}200}{336 \times 673.3} = .515$

This type of engine is thus seen to be very efficient at flight Mach Nos. of about 2.2.

The thermal efficiency $\eta_{th} = \frac{(\lambda + 1)(\theta_J - \theta_u)}{\theta_H} = \frac{2.01(429.7 - 223.7)}{673.3} = .612$

The propulsive (or Froude) efficiency $\eta_F = \frac{2}{\frac{u_J}{u} + 1} = \frac{2}{\frac{3049}{2200} + 1} = .838.$

$\eta_{th} \times \eta_P = \eta_o = .838 \times .612 = .513$ which substantially agrees with the figure found from $\eta_o = \frac{F_s u}{K_p \theta_H}$.

The improvement in overall efficiency obtained by mixing before final expansion is in the range 4 - 5 %. This may not seem impressive but it could mean a possible increase in payload (for a given range) of the order of 30%.

Clearly such high efficiencies go a long way to offsetting the low lift/drag ratios of supersonic aircraft.

In Figure 19, t_j is seen to have the high figure of 2.29 so one might expect that it would pay to increase T_m by additional heating in the bypass ('duct burning') or by after burning but, though F_s could be increased very substantially it can easily be shown that overall efficiency would be reduced. For example, if, in the cycle of Figure 19, T_m is increased to 1000°K, the equivalent of the extra heat addition is $2.01\ (1000 - 778.4) = 445.4$ to give a total heat energy addition of $445.4 + 673.3 = 1118.7$. θ_J would be $.98 \times 1000 \left(\frac{1.29}{2.29}\right) = 552°C.$

$u_j = 147.1 \sqrt{552} = 3456'/\text{sec.}$ and $F_s = \frac{3456 - 2200}{32.2} \times 2.01 = 78.42$ secs.

$\therefore \eta_o = \frac{78.42 \times 2200}{336 \times 1118.7} = .459.$ So F_s is increased from 53 to 78.42 secs. at the expense of a drop in η_o from .515 to .459. Nevertheless, for comparatively short range missions, it may be worthwhile to sacrifice overall efficiency to gain such a large increase in thrust, especially if the increase is needed for temporary boost only. The above reduction in efficiency does not take into account any pressure loss which would result from the additional combustion apparatus, and which would cost some loss in efficiency even when not in use. This loss, however, would be very small.

SECTION 22
Effect of Height and Speed on Performance

For a preliminary look at this question the supersonic engine cycle of Figure 18 of Section 21 will be used for a height where $T_o = 221°K$ since it seems likely that straight jets are a thing of the past for other than high supersonic speeds.

In calculations on this basis, the writer found himself up against an aspect of the subject which was new to him and which must now be explained. It was found that for design speeds of the order of 2000′/sec. where the ram pressure ratio is a high proportion of the total pressure ratio, the axial velocity at compressor entry would become a limiting factor.

As has been stressed earlier, the axial flow u_a at the compressor face should not differ appreciably from a constant proportion of blade speed, i.e. $\frac{\theta_a}{\theta_c}$ should be approximately constant. To satisfy this condition it was found that reduced flight speeds meant reduced engine r.p.m. below flight speeds of the order of 1600′/sec., otherwise u_a became much too high to conform with the condition that the mass flow rate Q is proportional to the maximum pressure of the cycle and inversely proportional to the square root of the maximum cycle temp.

Let it be assumed that θ_a, the temp. equivalent of axial velocity u_a at compressor entry, is given by $\theta_a = x\theta_c$. It is, of course, desirable that x should be constant but unfortunately this is not possible for varying flight conditions if θ_c is constant especially for supersonic engines operating at subsonic speeds, as may be seen from the following reasoning:

Considering first the flow at compressor entry; $Q \propto \rho_a u_a$ or, since $u_a = 147.1\sqrt{\theta_a}$ and $\theta_a = x\theta_c$, $Q \propto \rho_a \sqrt{x\theta_c}$ (22-1)

If ram efficiency is less than 100% then ρ_a, the density at compressor entry, is found as shown in Figure 1.

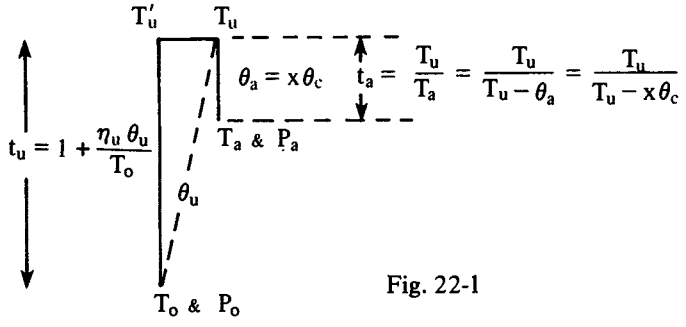

Fig. 22-1

The total to static pressure-ratio $p_u = t_u^{3.5}$. The total to static pressure ratio to give u_a ($= 147.1\sqrt{x\theta_c}$) is $t_a^{3.5}$ $\therefore$ the static pressure at compressor entry $P_a = P_o\left(\frac{t_u}{t_a}\right)^{3.5}$

$$\therefore \rho_a = \frac{P_a}{RT_a} = \frac{P_o}{RT_a}\left(\frac{t_u}{t_a}\right)^{3.5} \quad \text{or, since } T_a = T_u - x\theta_c,\ \rho_a \propto \frac{1}{T_u - x\theta_c}\left(\frac{t_u}{t_a}\right)^{3.5} \tag{22-2}$$

Substituting for ρ_a in (1) one may write

$$Q = k_1 \frac{1}{T_u - x\theta_c}\left(\frac{t_u}{t_a}\right)^{3.5}\sqrt{x\theta_c} \tag{22-3}$$

Now considering Q as governed by the expansion:—as has been shown, $Q \propto \frac{P_{max}}{\sqrt{T_{max}}}$

and $T_{max} \propto \theta_c$, $\therefore$ since $P_{max} \propto (t_u t_c)^{3.5}$, $Q = k_2 \frac{(t_u t_c)^{3.5}}{\sqrt{\theta_c}}$ (22-4)

It follows from (3) and (4) that $k_1\left(\frac{1}{T_u - x\theta_c}\right)\left(\frac{t_u}{t_a}\right)^{3.5}\sqrt{x\theta_c} = k_2 \frac{(t_u t_c)^{3.5}}{\sqrt{\theta_c}}$

$$\text{or} \quad \frac{\theta_c\sqrt{x}}{(T_u - x\theta_c)(t_a t_c)^{3.5}} = \text{const.} \tag{22-5}$$

$$\text{using } t_a = \frac{T_u}{T_u - x\theta_c} \quad (5) \text{ becomes } \frac{\theta_c\sqrt{x}\,(T_u - x\theta_c)^{2.5}}{(T_u t_c)^{3.5}} = \text{const.} \tag{22-5a}$$

Example 22-1.

The value of the constant in (5a) can be found by using the design values for the quantities in the equation. Assuming that θ_a is equivalent to Mach 0.6 then $\theta_a = x\theta_c = 0.6\ \frac{T_u}{6} = 0.1\ T_u$. If other assumptions for the design condition are 1) $T_o = 221$, 2) $u = 2100'/\text{sec.}$; 3) $\eta_u = .95$; 4) $\theta_c = 500$ and 5) $\eta_c = .84$ what is the value of the constant in equation (5a)?

$$T_u = T_o + \theta_u = 221 + \left(\frac{2100}{147}\right)^2 = 425.1°\text{K} \quad (\theta_u = 204.1)$$

$$500\,x = 0.1\,T_u = 42.51 \quad \therefore \quad x = .085$$

$$t_u = 1 + \frac{\eta_u \theta_u}{T_o} = 1 + .95 \times \frac{204.1}{221} = 1.877$$

$$t_c = 1 + .84\,\frac{\eta_c \theta_c}{T_u} = 1 + \frac{.84 \times 500}{425.1} = 1.988$$

$$\therefore \quad \frac{\theta_c \sqrt{x}\,(T_u - x\theta_c)^{2.5}}{(T_u t_c)^{3.5}} = \frac{500\sqrt{.085}\,(425.1 - .085 \times 500)^{2.5}}{(425.1 \times 1.988)^{3.5}} = .0238$$

It is clearly undesirable that $x = \frac{\theta_a}{\theta_c}$ should vary much from the design value with axial flow compressors. If it is too small there is a risk that the angle of attack will be reduced to the stalling point and surging of the compressor will occur. It it is too large then the characteristics of an axial flow compressor are such that there is a rapid fall off in pressure ratio and efficiency, i.e. θ_c and η_c are reduced. A reduction in θ_c means a proportionate reduction in T_{max}; which all adds up to reduction in thrust and overall efficiency.

In fact it is impossible to calculate overall performance unless the effect of x on θ_c, η_c, etc. are known. But if x is assumed constant then it is reasonable to calculate the way θ_c etc. vary with height and speed.

Example 22-2.

If the flight speed is 900′/sec. ($\theta_u = 37.5°$) and $T_o = 250°K$ (about 20,000′) and $\frac{\theta_a}{\theta_c} = x = .085$ (as in Example 1) what is the corresponding value of θ_c from equation (5a) assuming that η_u and η_c are the same as in Example 1?

Since $t_c = 1 + \frac{\eta_c \theta_c}{T_u}$, θ_c must be found from $\frac{\theta_c \sqrt{.085}\,(250 + 37.5 - .085\,\theta_c)^{2.5}}{(T_u t_c)^{3.5}} = .0238$

$$T_u = 287.5 \quad \therefore \quad \frac{.292\;\theta_c\,(287.5 - .085\,\theta_c)^{2.5}}{\left[287.5\left(1 + \frac{.84\,\theta_c}{287.5}\right)\right]^{3.5}} = .0238$$

By trial θ_c is found to be 338°C.

On completing Example 2, the writer made a discovery which was novel to him but which is probably a blinding glimpse of the obvious to a competent mathematician. He was struck by the fact that the value of $\frac{\theta_c}{T_u}$ was the same in both Examples 1 and 2. This proved to be no fluke as will now be shown.

Writing a (a constant) instead of x, equation (5a) may be rewritten

$$\frac{T_u \frac{\theta_c}{T_u} \sqrt{a}\,\left[T_u\left(1 - a\frac{\theta_c}{T_u}\right)\right]^{2.5}}{\left[T_u\left(1 + \frac{\eta_c \theta_c}{T_u}\right)\right]^{3.5}} = \text{Const.}$$

which reduces to $$\sqrt{a}\ \frac{\frac{\theta_c}{T_u}\left(1-a\frac{\theta_c}{T_u}\right)^{2.5}}{\left(1+\eta_c\frac{\theta_c}{T_u}\right)^{3.5}} = \text{Const.} \qquad (22\text{-}5b)$$

from which it is clear that if η_c is constant $\frac{\theta_c}{T_u}$ must be constant and the same as the design value.

Therefore for constant axial velocity Mach number at compressor intake θ_c *is a constant multiple of* T_u.

Since it has been shown that T_M is a constant multiple of θ_c it follows that T_M *is also a constant multiple of* T_u.

Another curious result is obtained as follows:– Figure 2 illustrates a method of finding how the axial velocity at compressor exit varies.

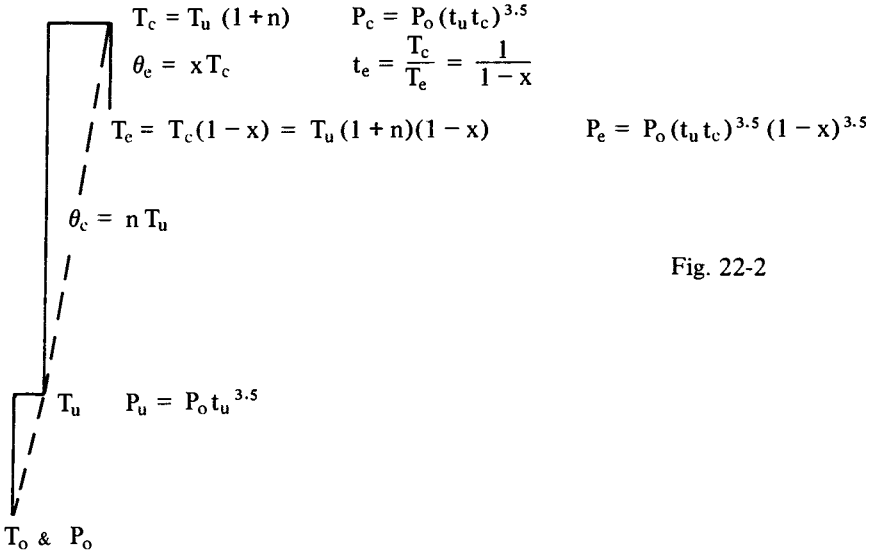

Fig. 22-2

The density ρ_e at T_e is given by $\rho_e = \frac{P_e}{RT_e}$ and the axial velocity u_e is

$$u_e = 147\sqrt{x\,T_u\,(1+n)} \quad \therefore \quad Q = k_1\,\rho_e\,u_e = k_2\,\frac{P_e}{T_e}\,\sqrt{xT_u}$$

Substituting for P_e and T_e from the diagram and merging constants

$$Q = k_3\,\frac{P_o(t_u t_c)^{3.5}(1-x)^{3.5}\,\sqrt{xT_u}}{T_u(1-x)}$$

$$\text{or} \quad Q = \frac{k_3 P_o (t_u t_c)^{3.5} (1-x)^{2.5} \sqrt{x}}{\sqrt{T_u}} \tag{22-6}$$

$$\text{For expansion,} \quad Q = k_4 \frac{P_o (t_u t_c)^{3.5}}{\sqrt{m T_u}} \tag{22-7}$$

(since it has been shown that T_M is multiple of T_u for constant Mach No. for axial velocity at compressor entry and assuming constant η_c)

Equating (6) and (7) gives:–

$$\frac{k_3 P_o (t_u t_c)^{3.5} (1-x)^{2.5} \sqrt{x}}{\sqrt{T_u}} = \frac{k_4 P_o (t_u t_c)^{3.5}}{\sqrt{m T_u}}$$

which reduces to $(1-x)^{2.5} \sqrt{x}$ = const. from which x *must be constant*, i.e. over the range of operation for which the assumptions are valid, *the axial velocity at compressor discharge is a constant multiple of* $\sqrt{T_c}$ *and therefore of* $\sqrt{T_u}$. Thus axial velocities at both entry and exit remain 'in step' with rotational speed. It is a reasonable presumption that axial velocities throughout the compressor are proportional to rotational speed over the range where mass flow rate Q may be assumed $\propto \frac{P_{max}}{\sqrt{T_{max}}}$, i.e. over the range where the turbine nozzles are choking or near choking.

Considering Examples 1 and 2, a change of T_u from 425.1 to 287.5°K means a change of θ_C from 500°C to 338°C. The corresponding variation in rotational speed would be in the ratio $\sqrt{\frac{338}{500}} = .822$ – not drastic for the large change in flight conditions.

Evidently the variation in T_u would be far smaller (and hence the variation in θ_c, T_M, etc.) if the design condition had been for high subsonic speed. Thus, for example, if the design condition had been for 900'/sec. at a height where $T_o = 221°K$ then T_u would have been 258.5°K which implies that at sea level static ($T_u = T_o = 288°K$) the speed of rotation should be about 5½% *greater* than design.

Having determined the proportionality of θ_c and T_M to T_u it is now possible to revise the non-dimensional diagram for the straight jet engine as shown in Figure 3, which is valid only for the range where η_c, η_T and η_u may be assumed constants (η_j is normally so near 1.0 that it may be presumed constant). This, however, is a reasonably safe assumption over the normal operating range other than take off.

It will be noted that $1 + \phi_u$, i.e. $\frac{T_u}{T_o}$, occurs in nearly every quantity and one might be tempted to base a non-dimensional diagram on $\frac{T_u}{T_o}$ but, since $T_u = T_o + \theta_u$ it is a very variable quantity. So is T_o but it is determined by I.S.A., i.e. by the height up to the tropopause above which it is constant.

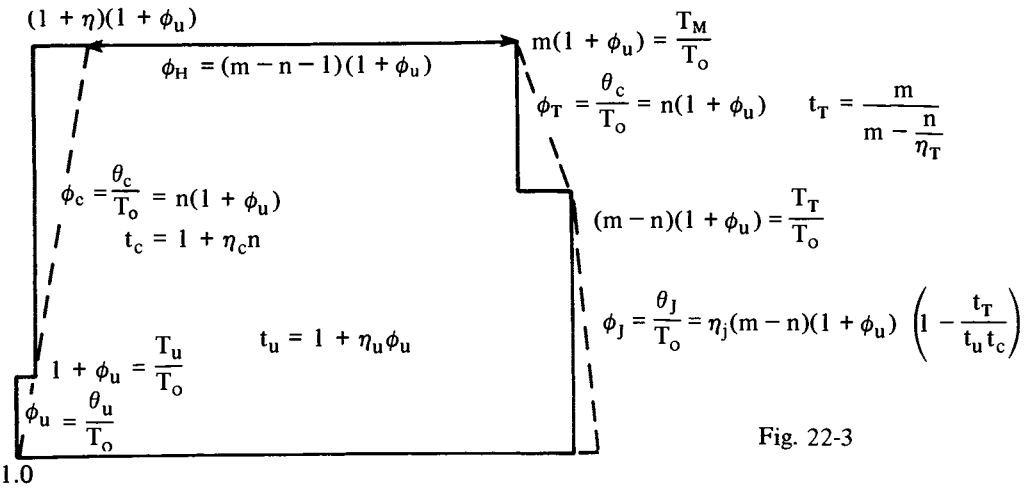

Fig. 22-3

It will be noted that the temperature ratios t_c and t_T are constants, but t_u and t_j depend upon flight speed.

Figure 3 gives all the information necessary to find the effect of speed and height on performance for a given design cycle, though it is perhaps less confusing to work in temps. and temp. differences.

We have information as follows:—

$F_s \propto \sqrt{\phi_J} - \sqrt{\phi_u}$ and $F_{sD} \propto \sqrt{\phi_{JD}} - \sqrt{\phi_{uD}}$ where the suffix D implies the design condition $\therefore \frac{F_s}{F_{sD}} = \frac{\sqrt{\phi_J} - \sqrt{\phi_u}}{\sqrt{\phi_{JD}} - \sqrt{\phi_{uD}}}$ or $\frac{\sqrt{\theta_J} - \sqrt{\theta_u}}{\sqrt{\theta_{JD}} - \sqrt{\theta_{uD}}}$ (22-8)

$Q \propto \frac{(t_u t_c)^{3.5}}{\sqrt{m(1+\phi_u)}} P_o$ and $Q_D \propto \frac{(t_{uD} t_c)^{3.5}}{\sqrt{m(1+\phi_{uD})}} P_{oD} \therefore \frac{Q}{Q_D} = \sqrt{\frac{1+\phi_{uD}}{1+\phi_u}} \left(\frac{t_u}{t_{uD}}\right)^{3.5} \frac{P_o}{P_{oD}}$ (22-9)

or $\frac{Q}{Q_D} = \sqrt{\frac{T_{oD} + \theta_{uD}}{T_o + \theta_u}} \left(\frac{t_u}{t_{uD}}\right)^{3.5} \frac{P_o}{P_{oD}}$ (22-10)

$\frac{F}{F_D} = \frac{QF_s}{Q_D F_{sD}}$ $\therefore$ from (8) and (10) $\frac{F}{F_D} = \frac{\sqrt{\theta_J} - \sqrt{\theta_u}}{\sqrt{\theta_{JD}} - \sqrt{\theta_{uD}}} \sqrt{\frac{T_{oD} + \theta_{uD}}{T_o + \theta_u}} \left(\frac{t_u}{t_{uD}}\right)^{3.5} \frac{P_o}{P_{oD}}$ (22-11)

or $\frac{F}{F_D} = \frac{\sqrt{\theta_J} - \sqrt{\theta_u}}{\sqrt{\theta_{JD}} - \sqrt{\theta_{uD}}} \sqrt{\frac{T_{uD}}{T_u}} \left(\frac{t_u}{t_{uD}}\right)^{3.5} \frac{P_o}{P_{oD}}$ (22-12)

$\eta_o \propto \frac{F_s \sqrt{\theta_u}}{\theta_H}$ and $\eta_{oD} \propto \frac{F_{sD} \sqrt{\theta_{uD}}}{\theta_{HD}}$ $\therefore$ using (8)

$$\therefore \frac{\eta_o}{\eta_{oD}} = \frac{F_s}{F_{sD}} \sqrt{\frac{\theta_u}{\theta_{uD}}} \frac{\theta_{HD}}{\theta_H} = \frac{\sqrt{\theta_J} - \sqrt{\theta_u}}{\sqrt{\theta_{JD}} - \sqrt{\theta_{uD}}} \sqrt{\frac{\theta_u}{\theta_{uD}}} \frac{\theta_{HD}}{\theta_H} \tag{22-13}$$

but, as may be seen from Figure 3, $\frac{\theta_{HD}}{\theta_H} = \frac{\phi_{uD}}{\phi_H} = \frac{1+\phi_{uD}}{1+\phi_u} = \frac{T_{oD}+\theta_{uD}}{T_o+\theta_u}$

$$\therefore \frac{\eta_o}{\eta_{oD}} = \frac{\sqrt{\theta_J} - \sqrt{\theta_u}}{\sqrt{\theta_{JD}} - \sqrt{\theta_{uD}}} \sqrt{\frac{\theta_u}{\theta_{uD}}} \frac{T_{oD}+\theta_{uD}}{T_o+\theta_u} \tag{22-13}$$

It is obviously desirable to find an expression for θ_J as follows:–

From Figure 3, $\phi_J = \frac{\theta_J}{T_o} = \eta_j (m-n)(1+\phi_u) \frac{(t_u t_c - t_T)}{t_u t_c}$ (22-14)

$$\phi_{JD} = \frac{\theta_{JD}}{T_{oD}} = \eta_j (m-n)(1+\phi_{uD}) \left(\frac{t_{uD} t_c - t_T}{t_{uD} t_c}\right) \tag{22-14a}$$

remembering that t_T and t_c have been found to be constants.

Dividing (14) by (14a) gives

$$\frac{\theta_J}{\theta_{JD}} = \frac{T_o}{T_{oD}} \left(\frac{1+\phi_u}{1+\phi_{uD}}\right)\left(\frac{t_{uD}}{t_u}\right)\left(\frac{t_u t_c - t_T}{t_{uD} t_c - t_T}\right)$$

$$\text{or} \quad \theta_J = \theta_{JD} \frac{T_u}{T_{uD}} \frac{t_{uD}}{t_u} \left(\frac{t_u t_c - t_T}{t_{uD} t_c - t_T}\right)$$

$$\text{or} \quad \theta_J = \theta_{JD} \frac{T_u}{T_{uD}} \frac{t_{uD}}{t_u} \left(\frac{\frac{t_u t_c}{t_T} - 1}{t_{uD} \frac{t_c}{t_T} - 1}\right) \tag{22-15}$$

Example 22-3.

Using the design cycle shown in Figure 4 and assuming that $F_D = 10{,}000$ lbs. at $u_D = 2{,}100'$/sec. How does thrust F and overall efficiency η_o vary with speed near sea level where $T_o = 290$, over the speed range $0 - 900'$/sec.? Assume $P_o = 2100$ p.s.f.

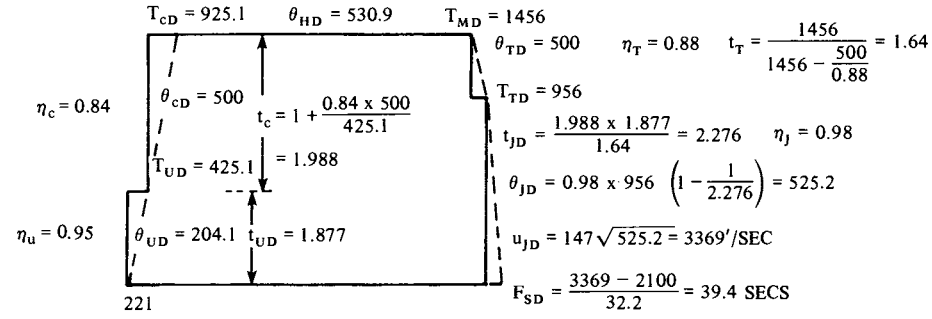

Fig. 22-4

$$Q_D = \frac{10{,}000}{39.4} = 253.8 \text{ lb/sec.}$$

$$\eta_{oD} = \frac{39.4 \times 2100}{530.9 \times 336} = .464$$

The following tabulation results:—

u'/sec	θ_u°C	T_u°K	t_u	θ_j°C	u_j'/sec	F_s secs	Q lb/sec	QF_s lb	θ_H°C	η_o
0	0	290	1.0	111.8	1554	48.27	296.8	14,326	362.2	0
200	1.8	291.8	1.006	115.7	1581	42.89	302.1	12,958	363.2	.07
400	7.4	297.4	1.024	127.4	1659	39.10	318.4	12,451	371.5	.125
600	16.16	306.2	1.055	147.1	1783	36.74	348.4	12,788	383.1	.171
800	29.6	319.6	1.097	174.7	1943	35.49	390.9	13,873	399.2	.212
900	37.5	327.5	1.123	191.4	2034	35.21	419.1	14,758	409	.231

To obtain θ_J equation (15) was used but F_s was found from $\frac{147\sqrt{\theta_j} - u}{g}$.

Equation (10) in the form $Q = Q_D \sqrt{\frac{T_{uD}}{T_u}} \left(\frac{t_u}{t_{uD}}\right)^{3.5} \frac{P_o}{P_{oD}}$ was used for Q. For θ_H we have

$T_M = \frac{T_u}{T_{uD}} \times 1456$ and $\theta_c = \frac{T_u}{T_D} \times 500$ and

$$\theta_H = T_M - T_u - \theta_c = \frac{T_u}{425.1}(1456 - 500) - T_u = T_u \left(\frac{956}{425.1} - 1\right).$$

For η_o we have $\eta_o = \frac{F_s u}{336\,\theta_H}$

Thus, for the purpose of the example, equations (8), (10) and (13), etc. are not really necessary.

The values of F (= QF_s) and η_o are plotted in Figure 5.

Example 22-4.

Using the same design cycle as Example 3, find the variation of F and η_o for the speed range 900 - 2100'/sec. at a height where $T_o = 221°K$ and $P_o = 390$ p.s.f. (about 40,000').

The tabulation is as follows:–

u	θ_u	T_u	t_u	θ_J	u_j	F_s	Q	QF_s	θ_H	η_o
900	37.5	258.5	1.161	164.8	1887	30.66	98.37	3016	322.7	.254
1200	66.6	287.6	1.286	227.2	2216	31.55	133.38	4208	359.2	.314
1500	104.1	325.1	1.447	308.1	2580	33.54	189.80	6366	406.0	.369
1800	149.9	370.9	1.644	402.5	2949	35.69	277.70	9909	463.3	.413
2100	204.1	425.1	1.877	525.2	3369	39.40	412.40	16,248	530.9	.464

The values of F and η_o are also plotted in Figure 5.

The foregoing discussion and Examples 3 and 4 bring out some very important points. Perhaps the chief of these is that the designer is faced with something of a dilemma if the design cycle of a high supersonic engine is based on its design cruising height and speed–

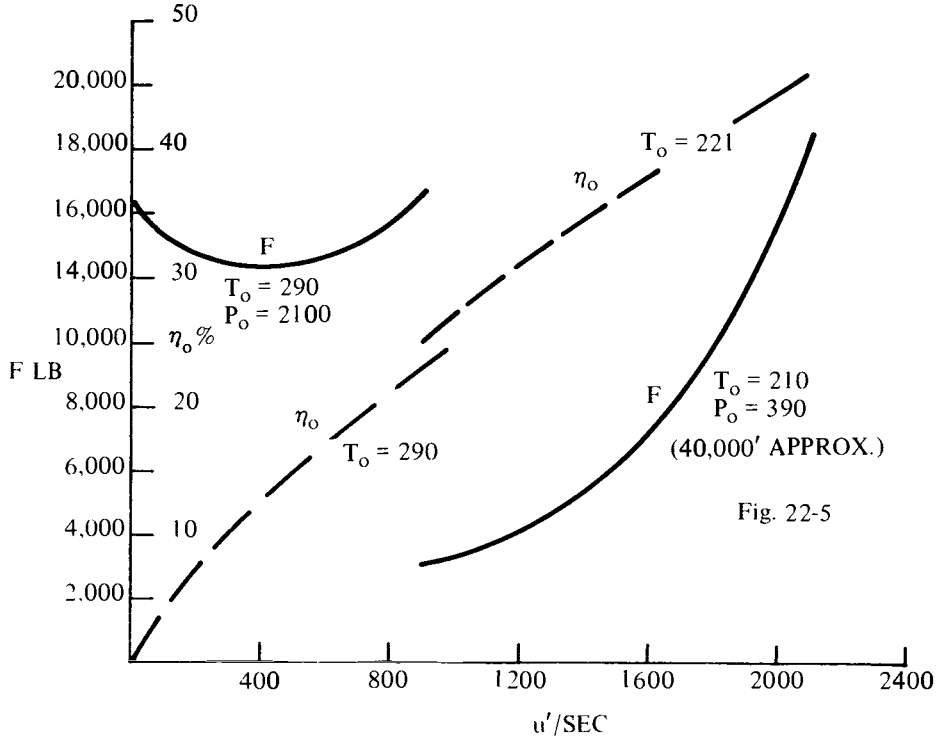

Fig. 22-5

as it should be for long cruising range—in that at take-off and low heights and speeds the thrust is far too low if the conditions that T_{max} and θ_c are multiples of T_u are to be observed. The reason for this is that if T_u, the total temp. at compressor entry is low, so are the appropriate values of θ_c and T_{max}. Thus, in Example 3, at $u = 0$ $T_u = T_o = 290°C$ and θ_c would be $\frac{290}{T_{uD}} \times \theta_{cD}$ i.e. $\frac{290}{425.1} \times 500 = 341.1°C$, and T_{max} would be $\frac{290}{425.1} \times 1456 = 993.3°$ and the rotational speed N would be $\sqrt{\frac{290}{425.1}}\ N_D = .83\ N_D$ approximately.

For θ_c and T_M to be the same for the design condition and for take-off then the design condition would need to be based on the same T_u (for fixed compressor and turbine geometry), thus, if for sea level $T_o = 290°K$, and $u = 0$, the appropriate design condition would require that $T_u = T_o + \theta_u = 290°K$. Thus for a height at which $T_o = 221°K$ the matching value of $\theta_u = 290 - 221 = 69°C$ which corresponds to a speed of $147\sqrt{69} = 1221'$/sec.

Clearly a very much greater thrust for take off, etc. could be obtained by increasing N to N_D or more but at the expense of departing from optimum flow conditions in the compressor. A rough calculation shows that an increase of T_{max} to 1500°K should increase F_s from 48.27 secs. to 73.71 secs. and N from .83 N_D to N_D approx. but, with a vertical pressure ratio v mass flow parameter characteristic for the compressor, the working point would drop so far down the characteristic that Q would only increase by 22%, i.e. in proportion to N approx., hence the initial take-off thrust would be $1.22 \times \frac{73.71}{48.27} \times 14{,}326 = 26{,}700$ lbs. approx. The compressor efficiency would drop to about 71%. The assumptions on which this calculation was based were rather pessimistic; a static thrust of 30,000 lbs. is probably nearer the mark.

It should be re-emphasised that θ_c and T_M are constant multiples of T_u only for *fixed* compressor and turbine geometry; i.e. no variable compressor stator blades, etc. If the com-

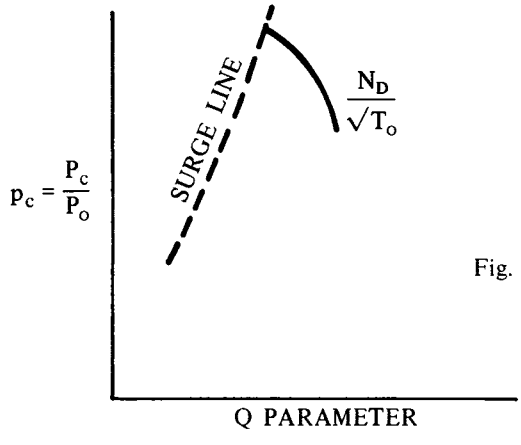

Fig. 22-6

pressor characteristic could be made to be more in accordance with Figure 6 then a much better performance could be obtained when T_u is much lower than the design condition because the working point would not drop so far down the characteristic.

Variable compressor stators help to obtain the kind of characteristics shown in Figure 6. So would rotor blades designed for whirl velocity equal to blade speed at mean radius at rotor exit (i.e. the relative leaving velocity at mean radius would be axial)—if one could 'get away' with the large deflection this would entail both in rotors and stators. This might prove possible if the blade pitch could be sufficiently small. This, however, even if aerodynamically possible, would almost certainly be structurally impossible except for very short blading.

SECTION 23
A Super-Thrust Engine

By way of conclusion of this work it may be of interest to take a look at what might be possible if the requirement was for a very large thrust regardless of fuel consumption. Such an engine would, of course, be for very specialised purposes, e.g. for boosting a space shuttle vehicle to speeds where rockets could take over with reasonable efficiency and thus save the large amount of rocket fuel needed for launch and acceleration to speeds of the order of 3,000 m.p.h. After rocket takeover the air breathing engines would become 'dead weight' for the remaining ascent into orbit, but would at least be available for use on return and so alleviate the great accuracy needed at present to bring the engineless vehicle to a safe landing.

Super-thrust engines could also be of use for single mission very high performance missiles.

As we have seen, in all engines discussed herein, the fuel necessary is far below that corresponding to the stoichiometric air fuel ratio of about 15:1. It follows that the means for obtaining great thrust would be to have additional combustion wherever this is possible, e.g. between the core compressor turbine and the fan turbine in the case of a low bypass ratio engine, combined with after burning before final expansion.

A low bypass ratio engine is indicated as being the most suitable for the purpose in order to obtain a high final expansion ratio and thus increase the effectiveness of after burning.

Figure 1 shows the take-off cycle for a super thrust engine based on the following assumptions: $T_o = 288°K$, $\theta_T = 200°C$ (i.e. the 'fan' is a multi-stage L.P. compressor); that T_{max} can be as high as 1850°K for short periods with considerable blade cooling; that the fan turbine can also operate with a turbine entry temp. of 1850°K; that after burning is permissible up to 2500°K; that the L.P. turbine is spaced sufficiently far from the core compressor turbine for supplementary combustion chambers to be installed between them; that $\theta_c = 500°C$; and that component efficiencies are as follows:– $\eta_F = .86$, $\eta_c = .84$; $\eta_T = .86$; $\eta_{FT} = .86$; $\eta_J = .96$.

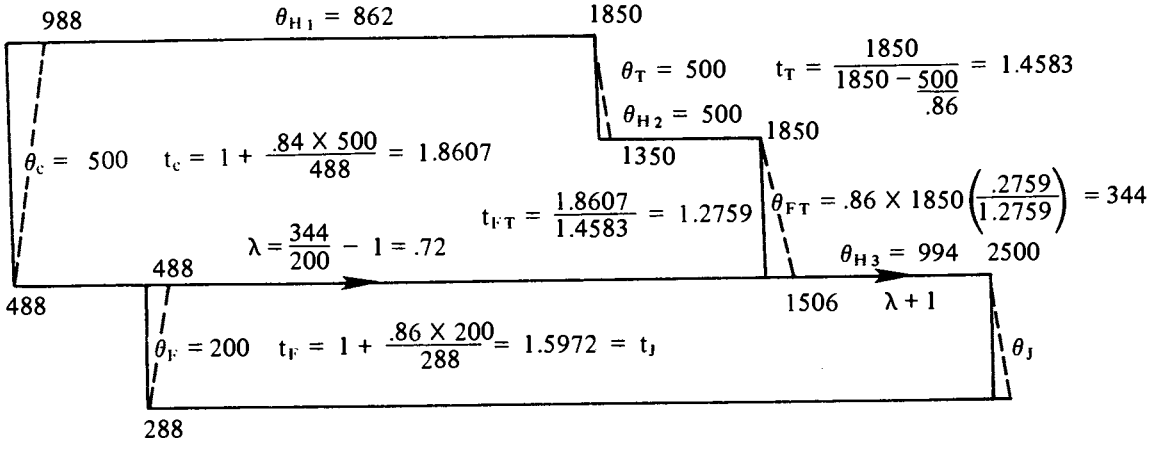

Fig. 23-1

$$\theta_J = .96 \times 2500 \left(\frac{.5972}{1.5972}\right) = 897.4 \quad \therefore \; u_J = 147.1\sqrt{897.4} = 4406.5'/\text{sec.}$$

$F_s = \frac{1+\lambda}{g} \times 4406.5 = 235.4$ secs., i.e. of the order of 3 times that of a straight jet and comparable with the specific thrust of a rocket. The total heat energy added $\propto$ $862 + 500 + 994 + .72\,(2500 - 488) = 3805$. The equivalent of the exhaust energy = $1.72\,\theta_J = 1.72 \times 897.4 = 1543.5$ $\therefore \; \eta_{th} = \frac{1543.5}{3805} = .406$ which is surprisingly high considering that such a large proportion of the heat is added at quite a modest temp. ratio.

The specific fuel consumption in lbs/sec. for a calorific value of 10,500 C.H.U/lb. would be $\frac{3805 \times .24}{10{,}500} = .087$ lb/sec. for 1.72 lb/sec. of air $\therefore$ the air/fuel ratio $= \frac{1.72}{.087} = 19.8$ approx., i.e. appreciably weaker (or 'leaner') than stoichiometric.

In the above example no attempt was made to determine the optimum value of λ.

Unfortunately there is a serious 'matching problem' as between low speeds at low heights and very high speeds in the stratosphere—hence the several attempts to solve the problem of variable bypass ratio.

At very high speeds there is little or no advantage in using any bypass at all. Indeed, even with the straight jet, the higher the speed the lower the compressor temp. rise should be (otherwise, *in the limit*, the ram temp. rise plus the compressor temp. rise would approach the max cycle temp. to the point of eliminating the heat addition in the main combustion).

The cycle of Figure 2 illustrates the point for a speed of 3000 m.p.h. ($u = 4400'/\text{sec.}$ and $\theta_u = 896°C$) with a straight jet plus after burning with component efficiencies as indicated in the diagram.

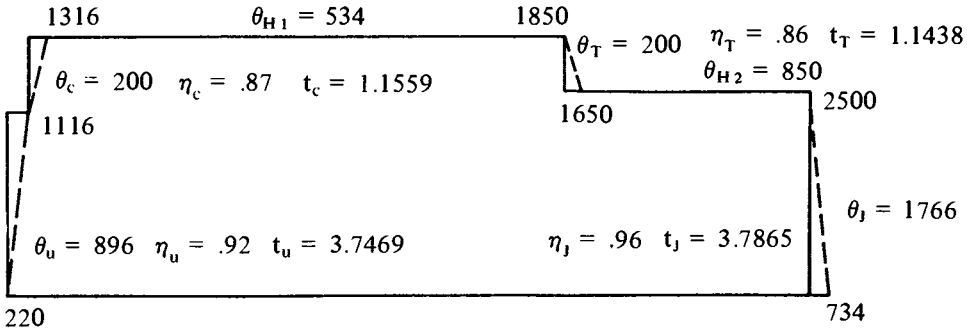

Fig. 23-2

For $\theta_J = 1766$ $u_J = 6182'$/sec. and $F_s = \frac{6182 - 4400}{32.2} = 55.34$ secs.

$\theta_{H1} + \theta_{H2} = 534 + 850 = 1384$ $\therefore$ $\eta_o = \frac{55.34 \times 4400}{336 \times 1384} = .524$

In this example, complete expansion in the jet nozzle would require that $\frac{S_E}{S_o} = 2.375$ which would obviously be very undesirable. For $S_E = S_o$ the under expansion would be such that the pressure at the nozzle exit would be a little over 3 atmospheres. The same difficulty occurs with the ramjet case below.

A ramjet at the same speed and same ram and jet efficiencies and $T_{max} = 2500$ would have $F_s = 54.98$ and $\eta_o = .520$. So under such conditions the turbojet is merely a 'super-charged ramjet'. It is evident that the utility of a turbojet ends at about 3000 m.p.h. and possibly below, having regard to power plant weight.

It would clearly be desirable to convert from the cycle of Figure 1 to that of Figure 2 and then switch to ramjets if air breathing engines are to be used for speeds greater than 3000 m.p.h.

For take off, initial acceleration and climb, a further substantial increase of thrust could be obtained by coolant injection. As mentioned earlier in this work, liquid ammonia is the most potent agent for this purpose. Coolant injection, by reason of its effect on initial cycle temp. T_o, could also greatly alleviate the problem of matching as between sea level static and high speed in the stratosphere.

An engine with a core mass flow of 500 lb/sec. operating with the cycle of Figure 1 would have a take-off thrust of 117,700 lbs. With ammonia injection this might be increased to 160,000 lbs. or more by virtue of the double effect of increasing F_s and increasing mass flow rate.